Targeting Scleraxis Combats Cardiac Fibrosis and Preserves Myocardial Function in Pressure-overloaded Myocardium

A Thesis Submitted to the Faculty of Graduate Studies of
The University of Manitoba
In Partial Fulfillment of the Requirements of the Degree of

DOCTOR OF PHILOSOPHY

By

Raghu Sundaresan Nagalingam

Department of Physiology and Pathophysiology,
Max Rady College of Medicine,
Rady Faculty of Health Sciences,
University of Manitoba,
Winnipeg,
Canada.

ACKNOWLEDGEMENTS

I would like to thank all those who helped me with my PhD and who made achieving this milestone in my life possible. First and foremost, I would like to express my sincere gratitude to my mentor and supervisor, Dr Michael Czubryt. I thank him from the bottom of my heart for his patience, motivation, and unconditional moral support throughout this program. He is one of the essential pillars of my life, who has helped me realize the bigger picture of my research. He has always guided me to find the positives in my failures and has taught me work ethic, integrity, and valuable life lessons.

I want to extend my heartfelt regards to my committee members, Dr Ian Dixon, Dr Thomas Netticadan, and Dr Jeffrey Wigle, for their tremendous support, constructive feedback, valuable guidance, and encouragement throughout my graduate studies. Each of them contributed by helping me understand the different perspectives of my research and by helping to shape this thesis. I would also like to thank them for their invaluable provision of technical expertise and reagents, which I have used in my study.

I thank my past and present lab members, Hamza Safi, Dr Nina Aroutiounova, Matthew Stecy, Leah Schwartz, Dr Rushita Bagchi, Sikta Chattopadhyaya, Danah Al-Hattab, Patricia Roche, Allison Ledingham, Teri Moffatt and Jayden Borley. They have all been wonderful colleagues and have always supported me throughout the program. I want to extend my gratitude to Dr Natalie Landry, Dr Gauri Akolkar, Krista Filameno, Dr Navid Koleini, Dr Abhay Srivastava, Dr Weiang Yan and Dr Mark Hnatowich for their valuable problem-solving ideas and sharing regents during critical times.

I owe a big hug to David Cheung for being my lifeline with animal ECHOs and the second-biggest contributor to the experiments in my thesis. He worked with me for several weekends solely performing murine ECHOs. He is completely selfless and values the importance of such a challenging study.

I am grateful to my best friends, Dr Pema Raj, Dr Saravanan Sekaran, Ariff Iqbal, and Dr Nawab Dar for taking care of me during my struggles and challenges. They

offered me moral support and valuable feedback about my research, all while we shared a space.

I acknowledge all the R.O. Burrell lab members, especially Rob Mazur and Sheri Bage. I would also like to thank Gail McIndless, Judy Olfert, Mary Brown, and Kairee Ryplanski for their administrative help. I also want to extend my gratitude to all the ICS members and Department of Physiology and Pathophysiology members who helped me and supported me during this program.

I am deeply grateful to the following institutions for their generous funding, scholarships, and fellowships during my program: St. Boniface Hospital Research Foundation, Institute of Cardiovascular Sciences, University of Manitoba, Canadian Institute of Health Research, Research Manitoba, Heart and Stroke Research Foundation of Canada, and Bank of Montreal Fellowship.

I am forever indebted to my loving parents, Dr S. Nagalingam and N. Meenachi for providing their unconditional love and support. Also, I would like to offer my sincere regards to my in-laws, Muralidharan Balasundharam and Usharani Muralidharan, for their understanding and support. Thanks to all my family members, especially Dr N. Ravi Sundaresan, Dr B. Senthil Kannan, N. Uma Chandra, Vishnu Prabha Rajendran, S. Madhumitha, and P. T. Saravanan, who stood by me when I needed them the most.

Finally, I am extremely blessed and thankful to the love of my life, Padmapriya Muralidharan, for being a diligent friend and providing unconditional love and endless support to help me achieve my dream. Without all of these people and their support, this degree wouldn’t have been possible. A big thank-you to everyone!

DEDICATION

I dedicate this thesis

to

Prof. Michael Paul Czubryt

for his faith and utmost trust in me. He is an inspirational mentor, who has taught me so much, and without whom completing this degree would not have been possible.

கற்க கசடறக் கற்பவை கற்றபின்
நிற்க அதற்குத் தக.
-திருவள்ளுவர்

Texts worthy of learning must be learned flawlessly; After learning, one should act according to the qualifications of the learned.
-Thiruvalluvar.

Table of Contents

List of Abbreviations

2-D TTE	Two-dimensional transthoracic echocardiography
AAV	Adeno associated virus
ACE	Angiotensin converting enzyme
ACEi	Angiotensin converting enzyme inhibitor
ADAMTS2	A disintegrin and metalloproteinase with thrombospondin motifs 2
AGE	Advanced glycation end products
Ang II	Angiotensin II
ANOVA	Analysis of variance
ARB	Angiotensin receptor blocker
AT_1 receptor	Angiotensin II receptor type 1
α-SMA	α-Smooth muscle actin
bHLH	Basic helix-loop-helix
BMP	Bone morphogenetic protein
bp	Base pairs
BSA	Bovine serum albumin
cAMP	Cyclic adenosine monophosphate
cDNA	Complementary deoxyribonucleic acid
ChIP	Chromatin immunoprecipitation
CREB	cAMP response element-binding protein
C-Terminal	Carboxyl-terminal
CTGF	Connective tissue growth factor
Col-1α1	Collagen type 1α1
Col-1α2	Collagen type 1α2
Col-3α1	Collagen type 3α1
Col-5α1	Collagen type 5α1
CTGF	Connective tissue growth factor
DAPI	4′,6-diamidino-2-phenylindole
DCM	Dilated cardiomyopathy

DDR2	Discoidin domain receptor 2
DMEM	Dulbecco's modified eagle medium
DMSO	Dimethyl sulfoxide
DNA	Deoxyribonucleic acid
E/A	Ratio of mitral valve early (E) and late (A) filling velocities
ECM	Extracellular matrix
ECV	Extracellular volume fraction
ED-A-Fn	Extra domain-A fibronectin
EF	Ejection fraction
EMSA	Electrophoretic mobility shift assay
EMT	Epithelial-to-mesenchymal transition
EndoMT	Endothelial-to-mesenchymal transition
ET-1	Endothelin1
FBS	Fetal bovine serum
FS	Fractional shortening
FSP-1	Fibroblast-specific protein 1
GAPDH	Glyceraldehyde-3-phosphate dehydrogenase
GFP	Green fluorescent protein
HCM	Hypertrophic cardiomyopathy
HFpEF	Heart failure with preserved ejection fraction
HFrEF	Heart failure with reduced ejection fraction
HHD	Hypertensive heart disease
hnRNP	Heterogeneous nuclear ribonucleoproteins
ICD	Implantable cardioverter defibrillator
Id-1	Inhibitor of DNA binding 1
IL	Interleukin
IPF	Idiopathic pulmonary fibrosis
IVRT	Isovolumic relaxation time
kDa	Kilodaltons
KO	Knock-out
LL	Look-locker version of MRI

LGE	Late gadolinium enhancement
LV	Left Ventricle
LVEF	Left ventricular ejection fraction
LVIDd	Left ventricular internal diameter during diastole
LVIDs	Left ventricular internal diameter during systole
LVPWd	Left ventricular posterior wall thickness
MAPK	Mitogen activated protein kinase
MCFs	Mouse cardiac fibroblasts
MI	Myocardial infarction
miRNA	MicroRNA
MMP	Matrix metalloproteinase
MOI	Multiplicity of Infection
MOLLI	Modified look-locker inversion
MRI	Magnetic resonance imaging
mRNA	Messenger Ribonucleic Acid
MRTF	Myocardin related transcription factor
NFATc	Nuclear factor of activated T-cells
NFκB	Nuclear factor kappa B
N-terminal	Amine terminal
PBS	Phosphate buffered saline
PCR	Polymerase chain reaction
PDGF	Platelet derived growth factor
POSTN	Periostin
PPAR-γ	Peroxisome proliferator activated receptor-γ
PPCI	Primary percutaneous coronary intervention
PVDF	Polyvinylidene difluoride
qPCR	Quantitative polymerase chain reaction
RAAS	Renin-Angiotensin-Aldosterone system
RCFs	Rat cardiac fibroblasts
RIPA	Radioimmunoprecipitation assay buffer
RNA	Ribonucleic acid

ROS	Reactive Oxygen Species
SAVR	Surgical aortic valve replacement
Scx	Scleraxis
Scx-fKO	Scleraxis fibroblast specific knock-out
$Scx^{fl/fl}$	Scleraxis-floxed allele
SDS-PAGE	Sodium dodecyl sulfate polyacrylamide gel electrophoresis
SEM	Standard error mean
shMOLLI	Shortened modified look-locker inversion
Smad	Sma and Mad (mothers against decapentaplegic) related protein
Snai 1	Snail Family Transcriptional Repressor 1
STAT-3	Signal transducer and activator of transcription 3
STE	Speckle tracking echocardiography
STEMI	ST-elevation myocardial infarction
TAC	Transverse aortic constriction
TBST	Tris-buffered saline and tween-20
TCF21	Transcription factor 21
TGFβ	Transforming Growth Factor β
TIMP	Tissue inhibitor of matrix metalloproteinase
TNFα	Tumor necrosis factor α
TUNEL	Terminal deoxynucleotidyl transferase-mediated dUTP nick-end labeling
TWIST-1	Twist-related protein 1
WT	Wild Type

List of Figures

List of Tables

List of Copyrighted Material Used

1. Raghu S Nagalingam, Danah S Al-Hattab, and Michael P Czubryt, **What's in a name? On fibroblast phenotype and nomenclature**, Canadian journal of physiology and pharmacology 97(6): 493-497© 2019, Canadian Science Publishing. https://cdnsciencepub.com/doi/abs/10.1139/cjpp-2018-0555

2. Hamza A Safi, Raghu S Nagalingam, and Michael P Czubryt, **Scleraxis: a force-responsive cell phenotype regulator**, Current Opinion in Physiology 01: 104-110 © 2018, Elsevier. https://www.sciencedirect.com/science/article/pii/S2468867317300081

3. Raghu S. Nagalingam, Hamza A. Safi, Danah S. Al-Hattab, Rushita A. Bagchi, Natalie M. Landry, Ian M.C. Dixon, Jeffrey T. Wigle, and Michael P. Czubryt, **Regulation of cardiac fibroblast MMP2 gene expression by scleraxis**, Journal of Molecular and Cellular Cardiology. 120: 64-73 © 2018, Elsevier. https://www.jmcc-online.com/article/S0022-2828(18)30151-2/fulltext

4. R J Everett, C G Stirrat, S I R Semple, D E Newby, M R Dweck, and S Mirsadraee, **Assessment of myocardial fibrosis with T1 mapping MRI**, Clinical Radiology, 71(8), 768-78, © 2016, Elsevier. https://www.clinicalradiologyonline.net/article/S0009-9260(16)00089-1/fulltext
(Figure 4)

5. Ramón Querejeta, Begoña López, Arantxa González, Eloy Sánchez, Mariano Larman, José L. Martínez Ubago, and Javier Díez, **Increased**

collagen type I synthesis in patients with heart failure of hypertensive origin, Circulation, 110(10), 1263-1268, © 2004, Circulation, Wolters Kluwer Health, Inc. https://www.ahajournals.org/doi/10.1161/01.cir.0000140973.60992.9a (Figure 3)

6. Rudolf A. de Boer, Gilles De Keulenaer, Johann Bauersachs, Dirk Brutsaert, John G. Cleland, Javier Diez, Xiao-Jun Du, Paul Ford, Frank R. Heinzel, Kenneth E. Lipson, Theresa McDonagh, Natalia Lopez-Andres, Ida G. Lunde, Alexander R. Lyon, Piero Pollesello, Sanjay K. Prasad, Carlo G. Tocchetti, Manuel Mayr, Joost P.G. Sluijter, Thomas Thum, Carsten Tschöpe, Faiez Zannad, Wolfram-Hubertus Zimmermann, Frank Ruschitzka, Gerasimos Filippatos, Merry L. Lindsey, Christoph Maack, and Stephane Heymans, **Towards better definition, quantification and treatment of fibrosis in heart failure. A scientific roadmap by the Committee of Translational Research of the Heart Failure Association (HFA) of the European Society of Cardiology**, European journal of heart failure, 21(3), 272-285, © 2019, John Wiley & Sons Ltd, reproduced with permission of Licensed Content from Creative Commons Attribution-Non-Commercials. https://onlinelibrary.wiley.com/doi/full/10.1002/ejhf.1406 (Figure 4)

7. Ilaria Russo, and Nikolaos G Frangogiannis, **Diabetes-associated cardiac fibrosis: cellular effectors, molecular mechanisms and therapeutic opportunities**, Journal of Molecular and Cellular Cardiology, 90, 84-93, © 2016, Elsevier. https://doi.org/10.1016/j.yjmcc.2015.12.011 (Figure 5)

8. The images of heart, fibroblast, and myofibroblast were adopted and used in **Figure 1** and **48** from the Smart Medical Servier Art and copyright obtained from Creative Commons Attribution 3.0 Unported License. https://smart.servier.com/

AUTHOR CONTRIBUTIONS

This dissertation includes multiple authored manuscripts and their contributions for each manuscript are listed below:

Manuscript 1: What's in a name? On fibroblast phenotype and nomenclature.
(Review article Published in Canadian journal of physiology and pharmacology).
Authors' List: **Raghu S Nagalingam**, Danah S Al-Hattab, and Michael P Czubryt.

Authors' contribution:

1). **Raghu S Nagalingam:** Conceptualized the idea for the manuscript, designed the schematic diagram, and drafted the manuscript.

2). **Danah S Al-Hattab:** Conceptualized the idea for the manuscript and drafted the manuscript.

3). **Dr. Michael P Czubryt:** Conceived and conceptualized the idea for the manuscript, corrected the drafted manuscript along with schematic diagram, and approved the final version of the manuscript.

Manuscript 2: Scleraxis: a force-responsive cell phenotype regulator.
(Review article Published in Current Opinion in Physiology).
Authors' List: Hamza A Safi, **Raghu S Nagalingam**, and Michael P Czubryt.

Authors' contribution:

1). **Hamza A Safi:** Conceptualized the idea for the manuscript and drafted the manuscript.

2). **Raghu S Nagalingam:** Conceptualized the idea for the manuscript and drafted the manuscript.

3). **Dr. Michael P Czubryt:** Conceived and conceptualized the idea for the manuscript, designed the schematic diagram, corrected the drafted manuscript, and approved the final version of the manuscript.

Manuscript 3: Regulation of cardiac fibroblast MMP2 gene expression by scleraxis, Journal of Molecular and Cellular Cardiology.

(Research article Published in Journal of Molecular and Cellular Cardiology).
Authors' List: **Raghu S. Nagalingam**, Hamza A. Safi, Danah S. Al-Hattab, Rushita A. Bagchi, Natalie M. Landry, Ian M.C. Dixon, Jeffrey T. Wigle, and Michael P. Czubryt.

Authors' contribution:

1). **Raghu S. Nagalingam:** Conceptualized the study, designed the experiments; performed majority of the experiments, interpreted the data, and drafted the manuscript.

2). **Hamza A. Safi:** Helped to perform experiments and acquired the data.

3). **Danah S. Al-Hattab:** Performed EMSA.

4). **Rushita A. Bagchi:** Helped in experiments and acquired the data.

5). **Natalie M. Landry:** Performed experiments and acquired the data.

6). **Ian M.C. Dixon:** Critically reviewed and edited the manuscript.

7). **Jeffrey T. Wigle:** Blind observer for imaging experiments, critically reviewed and edited the manuscript.

8). **Dr. Michael P Czubryt:** Conceived and conceptualized the study, helped to design the experiments, performed statistical analyses, designed the schematic diagram, corrected the drafted manuscript, and approved the final version of the manuscript.

ABSTRACT

Cardiac fibrosis is a major cause of arrhythmia and sudden death. Fibrotic myocardium loses its ability to contract and relax due to increased tissue stiffness, which leads to heart failure. The severity of heart failure is determined by the amount of fibrosis and its association with other cardiac pathogeneses. Inadequate understanding of the mechanisms and lack of specific therapeutic targets makes cardiac fibrosis a lethal disease. Mechanical stress or injury induces fibroblast-to-myofibroblast activation, which promotes uncontrolled matrix turnover and pathological remodelling. Therefore, limiting fibroblast activation may reduce fibrosis and its associated adverse outcomes. The transcription factor scleraxis is up-regulated in failing human hearts and various heart failure models. Furthermore, scleraxis directly transactivates genes that collectively define the myofibroblast phenotype, including collagens, α-smooth muscle actin, and fibronectin. Thus, we hypothesize that scleraxis gene deletion will attenuate fibrosis and improve cardiac function in pressure-overloaded myocardium, and scleraxis transcriptionally regulates matrix proteins periostin and MMP-2. Tamoxifen-induced fibroblast-specific scleraxis knockout (Scx-fKO) attenuated pressure-overload-induced cardiac fibrosis, and significantly improved cardiac function compared to wild-type (WT) transverse aortic constriction (TAC) animals. Wild-type TAC myocardium showed a marked increase in periostin-positive myofibroblasts, which were not present in Scx-fKO TAC mice; knockout cells demonstrated a failure of fibroblast activation and a reduction in fibrosis in response to pressure overload. After 4 weeks of TAC, scleraxis deletion in established cardiac fibrosis prevented the further decline in cardiac function, and cells showed loss of periostin expression concomitant with an improvement in fibrosis. In long-term pre-existing pressure-overloaded hearts, Scx-fKO animals exhibited significant improvement in systolic function and reduction in heart failure-induced mortality than WT controls. Furthermore, scleraxis directly binds and transactivates periostin and MMP-2 gene promoters and regulates their expression in cardiac myofibroblasts. Scleraxis-mediated transactivation was validated using luciferase, electrophoretic mobility shift, and chromatin immunoprecipitation assays. Scleraxis is sufficient and essential for TGFβ1-mediated induction of periostin and MMP-2 gene expression in cardiac

myofibroblasts. Collectively, these results indicate that scleraxis governs fibroblast activation during heart failure, that arresting fibrosis improves cardiac function, that scleraxis transcriptionally regulates profibrotic-responsive genes, such as periostin and MMP-2, and that scleraxis is a viable antifibrotic treatment target.

CHAPTER I: INTRODUCTION

1. Cardiac fibrosis

Cardiac fibrosis is the extensive pathological remodelling of the extracellular matrix (ECM) that occurs after injury or persistent stress. Fibroblast-to-myofibroblast activation is the primary cause of the excess buildup of matrix proteins inside the myocardium, and an altered process of ECM degradation by these myofibroblasts leads to fibrotic scars. These fibrotic scars, comprised of both collagen type I and III fibers, and the collagen frameworks themselves, are physiologically abnormal [1]; fibrotic scars display uneven crosslinking of thick and thin filaments of collagen fibers, which makes it difficult for proteases or collagenases to break them down [2]. These fibrotic scars elevate the stiffness of the myocardium thereby impairing myocardial elasticity and disturbing cardiac contractility, which interferes with electrical conduction, and leads to arrhythmia and sudden death [3]. Furthermore, reduction in myocardial compliance impairs contractility and drives the myocardium to heart failure with reduced ejection fraction (HFrEF) [4]. Elevated cardiac stiffness also impairs ventricular filling, leading to heart failure with preserved ejection fraction (HFpEF) [5-8].

Extracellular matrix proteins, consisting of a dense collagen framework, encapsulate the myocardial cells (including myocytes, fibroblasts, and perivascular cells) and ensure the structural and functional integrity of the myocardium. Fibroblasts secrete the following: ECM proteins, such as collagen, fibronectin, elastin, fibrillin, laminin, glycoproteins, proteoglycans; critical regulatory proteins of the ECM, including matrix metalloproteinases (MMPs) and tissue inhibitors of matrix metalloproteinases (TIMPs); and also several other cytokines and growth factors. Fibroblasts play a unique role in maintaining homeostasis by responding to the paracrine signals from neighbouring cells, where the synthesis and breakdown of ECM proteins are tightly regulated.

The myocardium responds to stress stimuli such as Transforming Growth Factor β (TGFβ), cytokines, various growth factors, and mechanical stress or injury by initiating the fibroblast-to-myofibroblast activation, which in turn promotes the pathological matrix remodelling process. Myofibroblasts are found only in injured or failing myocardium, not

in healthy hearts. These myofibroblasts are highly contractile and motile, and combined with the significant synthetic potential of matrix proteins to relieve the myocardium's stress, provide an adaptive response to damage. The long-term persistence of myofibroblasts at the injury site alters the ECM turnover and shifts the balance because of uncontrolled synthesis and reduced degradation of matrix proteins inside the myocardium. Excessive accumulation of these fibrotic lesions can lead to interrupted cell-to-cell and cell-to-ECM signalling and elevates myocardial stiffness; ultimately, the myocardium fails (Fig. 1).

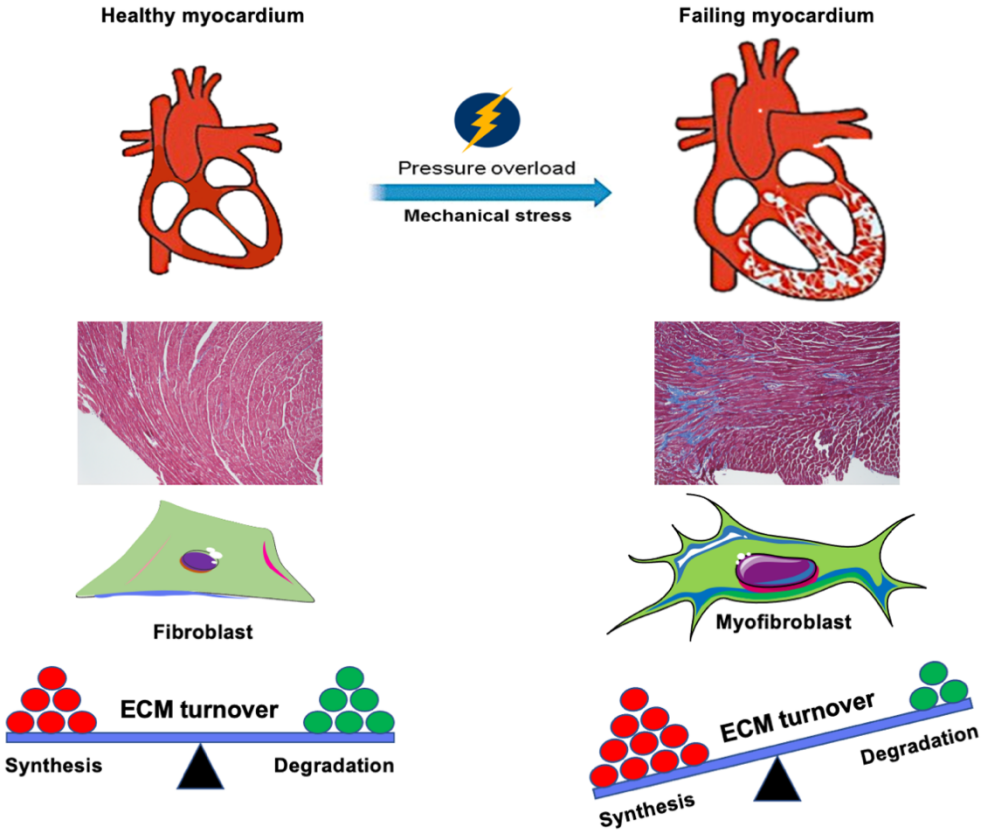

Figure 1: Physiological comparison between normal and failing myocardium. Healthy myocardium responds to pressure overload (mechanical stress) or other pathological stimuli leading to adverse cardiac remodelling. Fibrotic lesions inside the myocardium increase myocardial stiffness and interfere with cellular interactions. Fibroblast-to-myofibroblast activation is crucial in driving the uncontrolled ECM turnover, which promotes cardiac fibrosis-associated heart failure. Fibroblast and

myofibroblast images were adopted and used from the Smart Medical Servier Art and copyright obtained from Creative Commons Attribution 3.0 Unported License. https://smart.servier.com/

1.1: Prevalence and epidemiology

Myocardial fibrosis is an independent risk factor for heart failure and is caused by various cardiac pathogeneses [9]. The severity of cardiac fibrosis is based on its association with other cardiac disorders like myocardial infarction, hypertension, valvular defects, cardiomyopathies, and diabetes. Treatments for cardiac fibrosis are extremely limited so elucidating the signalling mechanisms involved in cardiac fibrosis could be crucial for patient management.

1.2: Classification of cardiac fibrosis

Myocardial fibrosis is classified by its pathological nature and its cause. Most fibrosis occurs in several forms—focal, diffuse, mid-wall, and perivascular—during the ECM remodelling process. Fibrosis is majorly classified into 2 types: reactive interstitial fibrosis and replacement fibrosis.

1.2.1: Reactive interstitial fibrosis

Cardiac reactive interstitial fibrosis is characterized by the widespread or diffuse distribution of extracellular collagen across the myocardium and the absence of myocyte necrosis. Reactive fibrosis is a well-known adaptation process triggered by renin-angiotensin-aldosterone activation, β-adrenergic signalling, oxidative stress, and hyperglycemia [10, 11]. Pressure overload, cardiomyopathies, diabetes, aortic valve stenosis, valvular regurgitation, and aging are major causes of reactive fibrosis [12-18]. This process is reversible, so timely intervention is essential to prevent the transition to irreversible replacement fibrosis [12].

1.2.2: Replacement fibrosis

Cardiac replacement fibrosis is determined by its underlying etiology, localizes to areas of cell death by necrosis, and displays a diffuse pattern. Myocardial infarction (MI)

is its primary cause, which forms irreversible scars after cardiac cell damage. These scars are predominantly collagen type I and III fibers, which initially prevent myocardial rupture after infarction [1, 19, 20]. End-stage reactive fibrosis can become irreversible replacement fibrosis because of cell damage by apoptosis or necrosis. Myocarditis, ischemic cardiomyopathy, hypertrophic cardiomyopathy (HCM), toxic cardiomyopathies, and inflammatory disease can also contribute to replacement fibrosis.

1.3: Clinical diagnosis and management for cardiac fibrosis

Patients with cardiac fibrosis show an increased risk of heart failure-related adverse outcomes. Cardiac pathologies display a diverse pattern of fibrosis, which determine the severity of heart failure. Cardiac fibrosis is always associated with other cardiac pathogeneses such as hypertension, MI, and diabetes. Several diagnostic tools are available to diagnose myocardial fibrosis clinically; when applied early, they help limit cardiovascular-associated adverse outcomes and can optimize patient care.

1.3.1: Biopsy or autopsy specimens and limitations

In older studies, autopsy tissues were stained with Masson's trichrome to determine a fibrosis-related cause of death. Later, the identification of cardiac fibrosis became limited to heart explant tissues from patients. These endomyocardial tissues were collected during valve replacement surgery, implantable cardioverter-defibrillator implantation, myectomy, and catheter-based surgeries. Histopathological tissue biopsies were stained with appropriate stains or underwent hydroxyproline assay to determine their collagen content; the severity of cardiac fibrosis was determined based on the amount of collagen present in the sample. These techniques were limited by their invasiveness and by procedure-related risks, therefore assessment of fibrosis was highly dependent on tissue availability, and early detection of fibrosis was nearly impossible.

1.3.2: Biomarkers for cardiac fibrosis

Recently, biomarker research is paving a new path for detecting cardiac fibrosis via blood sampling. Biomarker analysis is a minimally invasive technique that identifies

metabolic and cellular changes in the blood, which help determine the degree of cardiac fibrosis. To date, the strongest clinical biomarker candidates are C-terminal cleaved collagen I propeptides and N-terminal cleaved collagen III propeptides. Concentrations of these biomarkers are highly elevated in serum samples of patients with hypertensive heart failure [21-23]. Serum collagen propeptide concentrations and severity of fibrosis were cross-validated with endomyocardial tissue biopsies. Levels of other predicted biomarkers, like Galectin-3, scleraxis, TIMP-1, connective tissue growth factor (CTGF), and IL-4, 6, and 10, were all increased in the serum or plasma of patients with heart failure [24-30], and lower concentrations of MMP-1, 2, and 9 were found in the plasma of hypertensive patients [31, 32]. The cardiac specificity of these biomarkers, however, is debated since increases in their concentrations is also correlated with pulmonary, liver, and renal fibrosis. Complete validation of these biomarkers is critical to begin to specifically identify cardiac fibrosis with a simple blood test.

1.3.3: Echocardiography for cardiac fibrosis

Echocardiography is a non-invasive, cost-effective, and readily available tool to assess collagenous scar tissues inside the myocardium. This technique is used to assess systolic and diastolic dysfunction in patients with heart failure, as well as HCM in the pediatric population [33]. Trans-mitral Doppler echocardiography is used to calculate the change in the mitral valve blood inflow during left ventricular (LV) diastole in patients with myocardial fibrosis. Trans-mitral Doppler also measures diastolic functional parameters such as isovolumic relaxation time and E/A ratio, which provide data about impaired diastolic relaxation in advanced heart failure patients with and without fibrosis. M-mode Doppler echocardiography measures blood flow velocities from the mitral valve to the apex, which provides LV relaxation measurement. Factors such as age, rapid heart rate, increased venous return, and hypertension affect trans-mitral and M-mode Doppler measurements.

Speckle tracking echocardiography (STE) is a powerful, modern imaging tool that provides segmental and global views of myocardial deformation. This deformation signifies local pathological changes in the ECM due to interstitial fibrosis, hypertrophy, and other cellular complications. Speckle tracking echocardiography detects the

longitudinal systolic and early diastolic strain rate to quantify myocardial segmental deformation in HCM patients [34]. Several studies report a strong link between STE imaging and local histopathological deformations, providing new insights into this modality for the diagnosis of early cardiac complications [35-37]. High-resolution images and skilful operators are required for optimal STE.

1.3.4: Magnetic resonance imaging for cardiac fibrosis

Magnetic resonance imaging (MRI) is the gold standard diagnostic tool for myocardial fibrosis. It provides excellent temporal and spatial images non-invasively, which assess myocardial structure and function. Late gadolinium enhancement (LGE) and T1 mapping are the most widely used MRI methods for imaging myocardial fibrosis.

Late gadolinium enhancement identifies irreversible replacement fibrosis and provides reproducible, accurate results with excellent quality images. While LGE offers qualitative images, it fails to detect diffuse myocardial fibrosis. Therefore, T1 mapping—a well-established technique that provides 3-dimensional images without ionizing radiation—is used to quantify the amount of diffuse myocardial fibrosis. The severity of myocardial fibrosis is based on signal intensity and T1 relaxation time using a colour scheme. High T1 signal intensity represents protein accumulation related to fibrosis and fluid retention (edema); low T1 signal intensity represents lipid deposition [38]. The Look-Locker version of T1 mapping could previously acquire multiple image sampling with T1 relaxation curves at various timepoints. However, cardiac movement hindered the image acquisition and resolution of T1 mapping. Later, modified Look-Locker inversion (MOLLI), provided new options, including selective acquisition of images at any given point during the cardiac cycle with a single breath hold. However, T1 mapping values were determined to be very low in patients with tachycardia, and in some cases, MOLLI required breath holding of longer than 15 seconds, which cannot be safely done in patients with bradycardia, advanced age, and pulmonary disorders [39]. These challenges were addressed in shortened MOLLI (ShMOLLI) imaging, which requires only 7-8 seconds of breath-holding time, enough to get accurate and reproducible T1 mapping.

T1 mapping values are heartbeat independent [40]. Later studies made some changes to T1 mapping by using pre- (native T1) and post-gadolinium-based infusion (post-contrast T1), providing a new dimension to cardiac MRI. Native T1 to post-contrast T1 imaging shows a clear difference between infarcted and non-infarcted myocardium and detects infiltrative interstitial fibrosis and amyloid deposition in Anderson–Fabry disease patients, validated by histological sections. T1 mapping cannot directly describe the ECM area, but the extracellular volume (ECV) fraction can serve as a surrogate to measure ECM space. Extracellular volume values are highly reproducible, and T1 mapping distinguishes between extracellular space and blood volume using a gadolinium-based contrast medium. Patients with heart failure have abnormal ECV values, which correlate with histopathological sections stained for fibrosis. T1 mapping detects disease, describes its progression, and provides information about its prognosis, which is essential to determine the best treatment plan for patients with fibrosis-associated heart failure.

1.3.5: Clinical application of cardiac MRI in different cardiac pathologies

Myocardial infarction produces replacement fibrosis inside the myocardium; these infarcts progress from sub-endocardium to epicardium transmurally that leaves the myocardium less functional (Fig. 2). LGE assessment showed that the reduction in LV ejection fraction is directly correlated with infarct size after myocardial infarction [41, 42]. The mid-wall fibrosis pattern, detected using LGE, is found in 30% of patients with dilated cardiomyopathy (DCM), and is directly associated with arrhythmias and sudden death. In HFpEF patients, post-contrast T1 measurements were inversely correlated with diastolic function [43].

Patients with aortic stenosis and hypertension presenting with diffuse fibrosis, which then progressed to irreversible replacement fibrosis, displayed a mid-wall pattern on LGE imaging (Fig. 2). There was also a marked increase in ECV in hypertensive patients with ventricular hypertrophy compared to those without hypertrophy [44]. In addition, hypertensive patients with LV hypertrophy displayed increased native T1 values compared to control myocardium.

In patients with HCM, elevated myocardial stiffness from myocardial fibrosis led to systolic and diastolic failure, cardiac arrhythmia, and sudden death. Late gadolinium enhancement identified the focal pattern of replacement fibrosis in most HCM patients (Fig. 2), and also determined disease progression and severity [45].

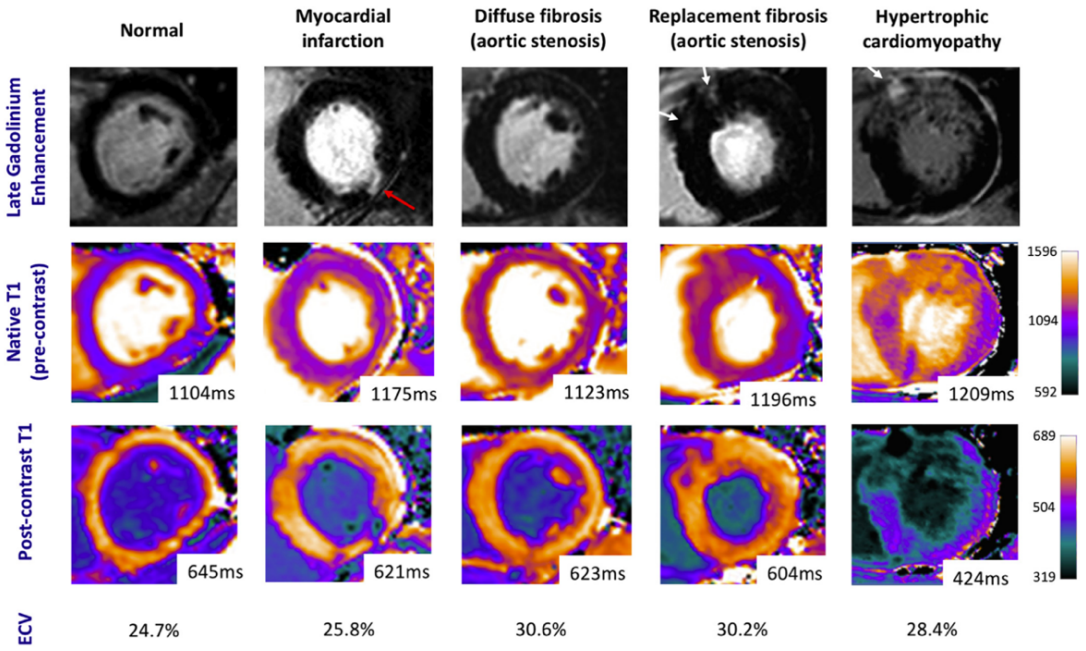

Figure 2: Cardiac magnetic resonance short axis images with LGE and T1 mapping in different cardiac conditions.

Areas of subendocardial (myocardial infarction, red arrow) and mid-wall (AS and HCM, white arrows) LGE are also identified with pre- and post-contrast T1 maps. There is an increase in diffuse fibrosis in the AS patients as represented by higher ECV values. There is significant overlap between native T1 values in healthy controls and disease states. Reprinted from R J Everett, C G Stirrat, S I R Semple, D E Newby, M R Dweck, and S Mirsadraee, Assessment of myocardial fibrosis with T1 mapping MRI, 71(8), 768-78, © 2016, by Clinical Radiology reproduced with permission of ELSEVIER INC. https://www.clinicalradiologyonline.net/article/S0009-9260(16)00089-1/fulltext

1.3.6: Treatment and strategies for cardiac fibrosis

Cardiac fibrosis is an important player in wound healing after injury; it is an early adaptation that includes fibroblast activation and scar formation. Illustrating the detailed

mechanism involved in pathological remodelling will help design new strategies and therapeutic options to target cardiac fibrosis. Clinically, patients are currently treated for their underlying pathology, such as heart failure and hypertension, rather than being treated for fibrosis directly. Indeed, fibrosis is a secondary outcome of many cardiac pathologies and is an independent cause of arrhythmias and sudden death [46]. The most commonly prescribed drugs to treat heart failure in patients with cardiac fibrosis are angiotensin-converting enzyme inhibitors (ACEI), angiotensin receptor blockers (ARBs), β-blockers, diuretics, and statins [47]. These drugs can delay the advancement of heart failure and, in some cases, pleiotropically impact fibrosis progression. Eplerenone is used as an antifibrotic, which blocks either the aldosterone pathway [48] or inhibits $K_v1.3$ potassium channels, suppressing regulatory T-lymphocytes [49], and resulting in decreased myocardial fibrosis. Nintedanib and Pirfenidone, used to treat idiopathic pulmonary fibrosis (IPF), reduce fibrosis and limit the progression of the disease [50, 51]. However, IPF patients treated with Nintedanib showed an increased prevalence of MI compared to placebo, signifying increased cardiovascular risk for this therapy [52]. Pirfenidone treatment reduced arrhythmogenic atrial remodelling and fibrosis in the congestive heart failure canine model, thereby limiting atrial fibrillation [53]. It also reduced Angiotensin II (AngII)-induced LV hypertrophy and fibrosis-related remodelling [54]. *In vitro* treatment with Pirfenidone reduced fibroblast proliferation, migration, myofibroblast contractility, and cellular α-smooth muscle actin (α-SMA) expression [55]. Metformin treatment ameliorated fibrosis in murine pressure overload model, thereby improving diastolic function. Additionally, in isolated adult murine cardiac fibroblasts metformin treatment inhibited collagen synthesis via targeting TGFβ/Smad3 signalling [56]. Bleomycin induced lung fibrosis model, metformin treatment resolved established fibrosis via promoting AMPK activity [57]. Peroxisome proliferator activated receptor-γ (PPAR-γ) agonist piperine attenuated cardiac fibrosis in murine pressure overload or isoprenaline model [58]. Pioglitazone, a PPAR-γ agonist treatment reduces cardiac fibrosis in murine pressure overload model. *In vitro* treatment with pioglitazone limited EndMT and TGFβ/Smad3 signalling and promoted PPAR-γ activation [59]. TGFβ/Smad3 and renin-angiotensin-aldosterone signalling pathways are the most influential triggers for cardiac fibrosis progression, determining potential therapeutic

targets in these signalling pathways will provide significant insights into clinical management and patient care. However, several unanswered questions in targeting or blocking these cellular mediators of cardiac fibrosis exist, which if ignored, may lead to adverse effects in the cardiac repair process.

2. Cardiac fibrosis in association with diverse pathological conditions

Myocardial fibrosis is an independent contributor to arrhythmias and sudden death [60, 61]. It is associated with, or a secondary outcome of, several other cardiac pathogeneses such as hypertension, MI, valvular disorders, and diabetic cardiomyopathy. Mostly, the etiology and pattern of cardiac fibrosis differ according to the underlying cause, and myocardial fibrosis predicts the severity of the disease that leads to heart failure. For example, dilated cardiomyopathy patients with fibrosis showed a nearly 17-fold increased mortality rate as compared to dilated cardiomyopathy patients without fibrosis [46]. Thus, limiting fibrosis inside the myocardium is predicted to lower the risk of heart failure-associated co-morbidities. Several preclinical animal studies that target fibrosis to improve cardiac function are explained hereafter.

2.1: Hypertension and fibrosis

Hypertension is the most prevalent cardiovascular disorder. Persistent high blood pressure elevates cardiac afterload, thereby promoting LV hypertrophy and myocardial fibrosis—a process termed hypertensive heart disease (HHD) [62-64]. In the hypertensive patient population, cardiac fibrosis is a major predictor of adverse cardiovascular outcomes. This is due to pathological remodelling, which includes fibroblast activation causing accumulation of fibrillar collagen and matrix proteins inside the myocardium-encompassing microvasculature (Fig. 3) [65]. These systemic changes in the patient's myocardium are initially an adaptive response to hypertension; eventually, they disrupt the myocardial architecture, triggering increased stiffness and conduction abnormalities leading to diastolic and systolic dysfunction [65, 66]. In hypertensive patients, the pattern of myocardial fibrosis is mostly diffuse interstitial reactive fibrosis, and in some cases replacement fibrosis. Accumulation of collagen fibers combined with perivascular and

interstitial fibrosis result in structural and functional abnormalities in coronary microcirculation in the hypertensive myocardium [67].

Myocardial fibrosis is the outcome of pathological signalling of several cellular and non-cellular factors in HHD. In the rat myocardium, aortic banding or norepinephrine infusion led to up-regulation of TGFβ, fibronectin, and collagen expression, which was directly related to elevated cardiac fibrosis and LV hypertrophy [68, 69]. In hypertensive patients, peripheral blood monocytes showed increased TGFβ production, correlating with pathological cardiovascular remodelling [70]. In adult rat cardiac fibroblasts, AngII and aldosterone interaction promoted collagen turnover [71]. The salt-induced rat hypertension model showed increased expression of angiotensinogen and AngII-AT1 receptors, causing elevated cardiac perivascular and interstitial fibrosis along with cardiomyocyte hypertrophy [72]. Angiotensin II and aldosterone can trigger type I collagen synthesis in hypertensive human hearts, which leads to increased deposition of collagen fibers inside the myocardium [73].

Myocardial tissue biopsies from patients with HHD had increased accumulation of collagen type I fibers in the myocardial interstitial space. The accumulation of collagen is strongly associated with cardiac functional deterioration, and along with serum levels of propeptide of procollagen type I (PIP), serves as a marker of myocardial fibrosis (Fig. 3) [74, 75]. In hypertensive patients, echocardiography reveals a strong correlation between elevated collagen content and LV chamber stiffness [75]. Hypertensive patients exhibited a higher degree of diffuse fibrosis in their myocardium compared to normotensive patients; cardiac MRI with T1 mapping and ECV quantification described the area of fibrosis and its severity [76, 77].

In terms of HHD treatment, spontaneously hypertensive rats who received high-dose lisinopril (an ACEI) treatment showed decreased arterial pressure and significantly reduced collagen volume fraction and LV hypertrophy compared to the normotensive controls [78]. Further extension of the study with aged hypertensive rats (76 weeks old) subjected to long-term (8-month) lisinopril treatment showed partial recovery in myocardial stiffness and reduction in fibrosis compared to age-matched Wistar Kyoto

(WKY) control rats [79]. In patients with HHD who underwent lisinopril treatment for 6 months, endomyocardial biopsy and Doppler echocardiography showed a reduction in myocardial fibrosis and improved diastolic function without affecting LV hypertrophy [64]. In hypertensive patients, adding spironolactone (a potassium-sparing diuretic) to the treatment regimen of ACEIs and ARBs increased survival [73]. Losartan (an ARB) treatment for 12 months in hypertensive patients showed a remarkable reduction in the cardiac fibrosis-associated collagen volume fraction and ventricular chamber stiffness [75]. A meta-analysis of hypertension treatments showed that ACEIs improve LV mass index more than beta-blockers and diuretics, while calcium channel blockers provide partial benefits [80]. In hypertensive patients, eplerenone (a mineralocorticoid receptor antagonist) or enalapril (an ACEI) treatment effectively reduced LV hypertrophy and blood pressure. The combination of eplerenone and enalapril decreased systolic blood pressure and LV mass more than eplerenone treatment alone [81].

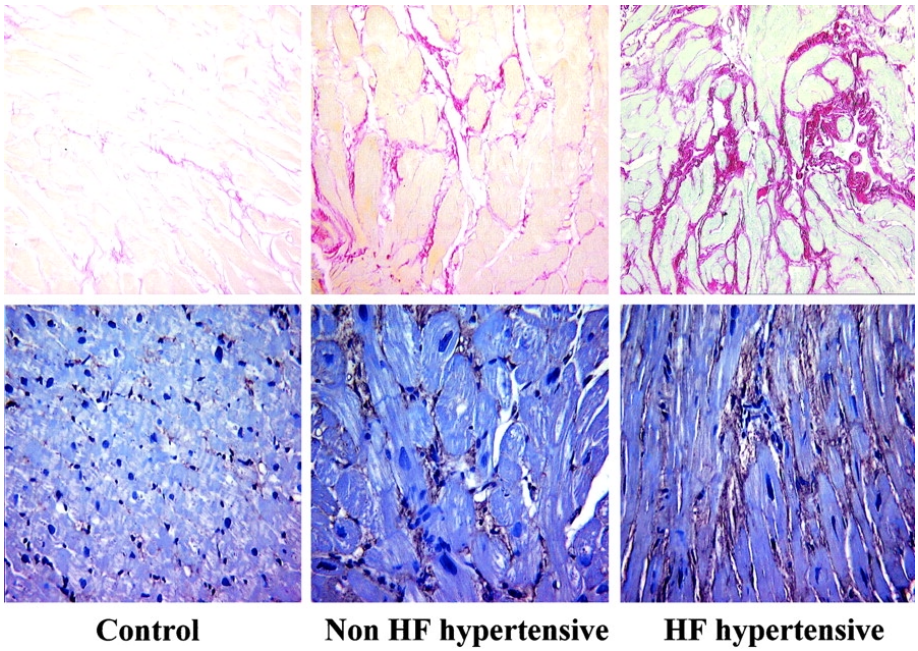

Figure 3: Collagen staining of endomyocardial tissues sections.

Endomyocardial tissues from 1 subject from each group. Top, Sections were stained with Picrosirius red, and interstitial and perivascular collagen tissue was identified in red (×20). Bottom, Sections were immunostained with an antibody anticollagen type I, and collagen type I fibers were identified in brown (×40). Reprinted from Ramón Querejeta,

Begoña López, Arantxa González, Eloy Sánchez, Mariano Larman, José L. Martínez Ubago, and Javier Díez, Increased collagen type I synthesis in patients with heart failure of hypertensive origin, 110(10), 1263-1268, © 2004, Circulation, reproduced with permission of Licensed Content Publisher Wolters Kluwer Health, Inc. https://www.ahajournals.org/doi/10.1161/01.cir.0000140973.60992.9a

2.2: Myocardial infarction and fibrosis

Myocardial infarction refers to irreversible cardiac muscle damage. It typically results from obstructed blood flow with the loss of cardiomyocytes by necrosis after 30 minutes of ischemia, and is predominantly caused by coronary artery disease. After MI, wound healing plays a vital role in stabilizing the myocardial structure and function. Wound healing is classified by 3 phases: acute or inflammatory, proliferation or post-inflammatory, and chronic or scar maturation. The acute or inflammatory phase begins 1 to 7 days after infarction in humans (Fig. 4), but the duration for other species may differ.

Initially, the damage signals attract the proinflammatory M1 macrophages, neutrophils, monocytes, and leukocytes to clear the dead cells and debris at the injury site by phagocytosis [82]. Next, the proliferation phase occurs within 7 days to 6 months after infarction (Fig. 4); anti-inflammatory M2 macrophages promote fibroblasts to migrate toward the injury site, followed by fibroblast proliferation and activation to myofibroblasts, which initiates the granulation process. The myofibroblast population is increased near the injury site, which increases collagen production and other matrix proteins to help build the scar. Participation of cells other than resident fibroblasts in scar formation has been a long-standing debate; however, genetic lineage tracking in mice of fibroblasts revealed that only resident fibroblasts significantly contributed to the myofibroblast population in both MI and pressure-overload models [83]. Single-cell sequencing of Pdgfrα-expressing fibroblasts after ischemic injury revealed four specific subsets of myofibroblast population after injury. Gene expression profile for these myofibroblast subsets are uniquely different from one another and contributing to tissue repair process [84]. Single-cell RNA-seq analysis revealed that IL-11 expression is highly enriched in cardiac myofibroblasts after injury, also showed distinct subsets of

myofibroblast population [85]. Studies on diverse cardiac fibroblasts population after injury has been published recently [86, 87].

The chronic or scar maturation phase, starts approximately 6 months after MI (Fig. 4). In this phase, collagen crosslinking helps to mature the infarct scar and determines the mechanical properties of the myocardium. After scar maturation, myofibroblasts will undergo apoptosis or become quiescent matrifibrocytes in humans [88]. Most of the myofibroblasts becomes senescent to evade the apoptosis and continuously remodel even after mature scar formation leading to chronic inflammation and tissue fibrosis [89]. The mature scar can act as non-excitable insulation to the myocardium. Failure in myofibroblast removal after scar maturation results in excessive fibrosis; this process is called pathological remodelling of the myocardium [90]. This pathological remodelling affects myocardial compliance, which leads to impairment in cardiac function [91].

Several proinflammatory and profibrotic factors help rebuild the myocardium after ischemic injury, leading to ventricular remodelling [92, 93]. Replacement fibrosis, mediated by myofibroblasts and fibroblasts, plays a vital role during scar formation to prevent cardiac rupture [19, 20]. In post-MI hearts, matrix protein remodelling is initiated by proinflammatory factors, which differ entirely from the end-stage matrix protein remodelling mediated by profibrotic factors during scar formation [94, 95]. These changes in the ECM remodelling interfere with cell-ECM communication, which is essential for normal cell function and survival [96, 97]. Thus, a proper balance in these factors contributes to the healthy rebuilding of the ECM at the injury site and prevents pathological remodelling.

In post-MI patients after the first acute clinical event, nearly 22% of males and 46% of females developed heart failure within 6 years. This indicates that heart failure frequency and MI-associated adverse remodelling is higher in females [98]. Infarct size is a critical determining factor for adverse cardiac remodelling. Additionally, rat hearts underwent progressive ventricular dilation when the infarct size was more than 20-40%,

whereas they did not develop dilation in the non-infarcted area when infarct size was smaller than 20% [99, 100].

ST-elevation MI (STEMI) patients and MI patients with LV dysfunction are treated with ACEIs as an early and long-term therapy [101]. Captopril (an ACEI) treatment in post-MI rats significantly improved long-term survival rates and limited adverse ventricular remodelling when compared to control animals [100]. Long-term administration of captopril and other drugs, including Aspirin, beta-blockers, and fibrinolytic therapy, significantly improved survival rate and lowered all-cause morbidity and mortality compared to placebo in post-MI patients with systolic dysfunction [102]. Hemodynamically stable patients who undergo primary percutaneous coronary intervention (PPCI) are treated with beta-blockers as early and long-term drug therapy [101, 103]. Fibrinolytic therapy is recommended for post-STEMI patients who cannot undergo PPCI in time. Aspirin, P2Y12 inhibitors, or dual antiplatelet therapy as well as statins or other lipid-lowering therapies are recommended for post-MI patients depending on the etiology [101].

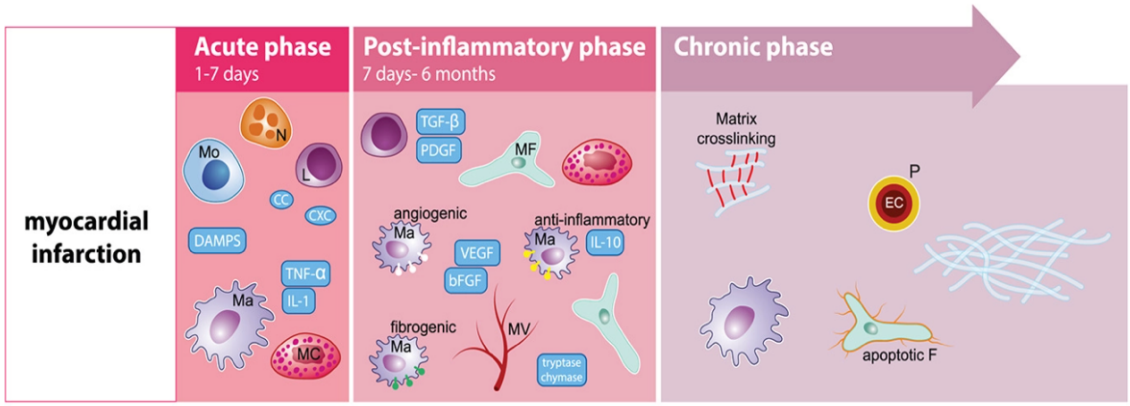

Figure 4: Timeline for myocardial infarction and wound healing.
Myocardial wound healing is a complex process that involves proinflammatory cytokines, profibrotic factors, and several cellular components of the myocardial tissue. Fibroblasts and myofibroblasts play a central role in this unique wound healing process, as well as other cell types like macrophages, monocytes, neutrophils, and lymphocytes. Increased collagen and other ECM protein turnover provides structural support to the

myocardium after injury. Reprinted from Rudolf A. de Boer, Gilles De Keulenaer, Johann Bauersachs, Dirk Brutsaert, John G. Cleland, Javier Diez, Xiao-Jun Du, Paul Ford, Frank R. Heinzel, Kenneth E. Lipson, Theresa McDonagh, Natalia Lopez-Andres, Ida G. Lunde, Alexander R. Lyon, Piero Pollesello, Sanjay K. Prasad, Carlo G. Tocchetti, Manuel Mayr, Joost P.G. Sluijter, Thomas Thum, Carsten Tschöpe, Faiez Zannad, Wolfram-Hubertus Zimmermann, Frank Ruschitzka, Gerasimos Filippatos, Merry L. Lindsey, Christoph Maack, and Stephane Heymans, Towards better definition, quantification and treatment of fibrosis in heart failure. A scientific roadmap by the Committee of Translational Research of the Heart Failure Association (HFA) of the European Society of Cardiology, 21(3), 272-285, © 2019, European journal of heart failure, Published in John Wiley & Sons Ltd, reproduced with permission of Licensed Content from Creative Commons Attribution-Non-Commercials. https://onlinelibrary.wiley.com/doi/full/10.1002/ejhf.1406

2.3: Valvular heart disease and fibrosis

Mitral valve prolapse and aortic stenosis are the primary causes of valvular heart disease. They are linked to life-threatening complications and increased mortality rates, especially in older, symptomatic patients [104-109]. Mitral valve prolapse is the most prevalent valvular disorder and is caused by thickening of the valvular leaflet, abnormal valve stretching, and chordal rupture. It often leads to atrial and ventricular arrhythmias and can cause sudden cardiac death. In some cases, mitral valve prolapse causes congestive heart failure [110-115]. Patients with chronic mitral valve prolapse display fibrosis of the papillary muscles, proteoglycan accumulation on the leaflets, and persistent mitral valve regurgitation. Regurgitation causes volume overload, which leads to ventricular remodelling characterized by increased chamber dimension and eccentric hypertrophy, and eventual heart failure [110, 111, 116]. Aortic stenosis is the progressive obstruction of valvular blood flow, which also contributes to ventricular remodelling, cardiac hypertrophy, and heart failure [117].

Normal heart valves have 3 layers of fibroblast-like valvular interstitial cells. These interstitial valve cells are vimentin-positive, which is essential for maintaining homeostasis [118]. Increased mechanical stress can damage valvular endothelial cells,

resulting in infiltration of lipids and inflammatory cells. Further lipid oxidation promotes proinflammatory and profibrotic cytokines, resulting in the activation of valvular interstitial cells to adopt a myofibroblast-like phenotype. This process increases contraction and formation of prominent stress fibers. Collagen secretion is driven by the activated valvular interstitial cells under the influence of AngII and TGFβ, which leads to the buildup of fibrous tissues inside the valve. This fibrous tissue promotes thickening of the valve and elevates its stiffness, eventually resulting in stenotic valve disorders [117, 118].

Angiotensin II and angiotensin-converting enzymes are highly elevated in the stenotic valve, and they bind to the AngII receptors in myofibroblast-like cells, which then participate in pathological remodelling [119]. BMP-4 (bone morphogenic protein-4) is shown to activate valvular interstitial cells to promote pathological remodelling during mitral valve prolapse [120]. Cardiac MRI and two-dimensional echocardiography are the gold standard diagnostic tools for mitral valve prolapse and aortic stenosis [106, 121].

In end-stage severe aortic stenosis, cardiac fibrosis significantly drives the phenotype from adaptive ventricular remodelling with HFpEF to maladaptive remodelling with HFrEF [122, 123]. Histopathological and contrast-enhanced MRI examination of tissue from surgical aortic valve replacement patients showed that cardiac fibrosis is directly linked to poor post-operative clinical outcomes and a reduction in long-term survival [122, 124, 125].

In patients with mitral valve prolapse, cardiac MRI and autopsy revealed that fibrosis of the papillary muscles and the inferobasal segment of the LV wall leads to valve leaflet prolapse. This replacement fibrosis is directly correlated with ventricular arrhythmias [110, 111]. Reduction in post-contrast T1 during cardiac MRI demonstrated that mitral valve prolapse is directly associated with diffuse LV fibrosis. In the mouse model [108], increased TGFβ levels promoted mitral valve prolapse while attenuating TGFβ using a neutralizing antibody resulted in reduced valve thickness and leaflet length [126]. Valvular replacement surgery is the only effective and available treatment for

chronic and severe aortic stenosis or mitral valve prolapse, while cardiac MRI plays an indispensable role in early diagnosis [116, 127].

2.4: Diabetes and fibrosis

Diabetes is a metabolic disorder that promotes pathological alterations in the myocardium. Diabetic cardiomyopathy is characterized by interstitial and perivascular fibrosis not caused by atherosclerosis or high blood pressure [128]. In some cases, myocardial scars related to replacement fibrosis were noted in diabetic patients without a prior MI [129, 130]. In diabetic patients, cardiac MRI helps to identify cardiac fibrosis, which is associated with heart failure-related hospitalization and mortality [131]. This unique phenotype is influenced by various factors such as hyperglycemia, increased reactive oxygen species (ROS), advanced glycation end-products (AGEs), and neurohormonal factors. In the diabetic myocardium, increased AGEs can crosslink with ECM proteins, which transduces profibrotic signals through the RAGE signalling pathway, and can also trigger TGFβ/Smad signalling to promote cardiac fibrosis. *In vitro* studies demonstrate that high glucose can promote fibroblast proliferation and activation to myofibroblast initiate excess production of ECM proteins (Fig. 5) [132, 133].

Streptozotocin-induced type 1 diabetes in rat and mouse models showed induction of profibrotic genes and reduced microvascular capillary density followed by myocyte hypertrophy and cardiac interstitial fibrosis [134-137]. Preclinical type-1 diabetic large animal models exhibited profibrotic phenotypes inside the myocardium, and alloxan administration promoted cardiac fibrosis in mongrel dogs [138]. Similarly, rhesus monkeys fed with alloxan developed insulin-dependent type-1 diabetes, which resulted in a near 2-fold elevation of collagen in the left ventricle without the presence of cardiac hypertrophy [139].

Type 2 diabetic ob/ob mice developed cardiac perivascular fibrosis and collagen deposition along with increased TGFβ and plasminogen activator inhibitor expression [140]. Leptin receptor truncation led to severe obesity in db/db animals within 2 months along with increased cardiac fibrosis and diastolic dysfunction [141-144].

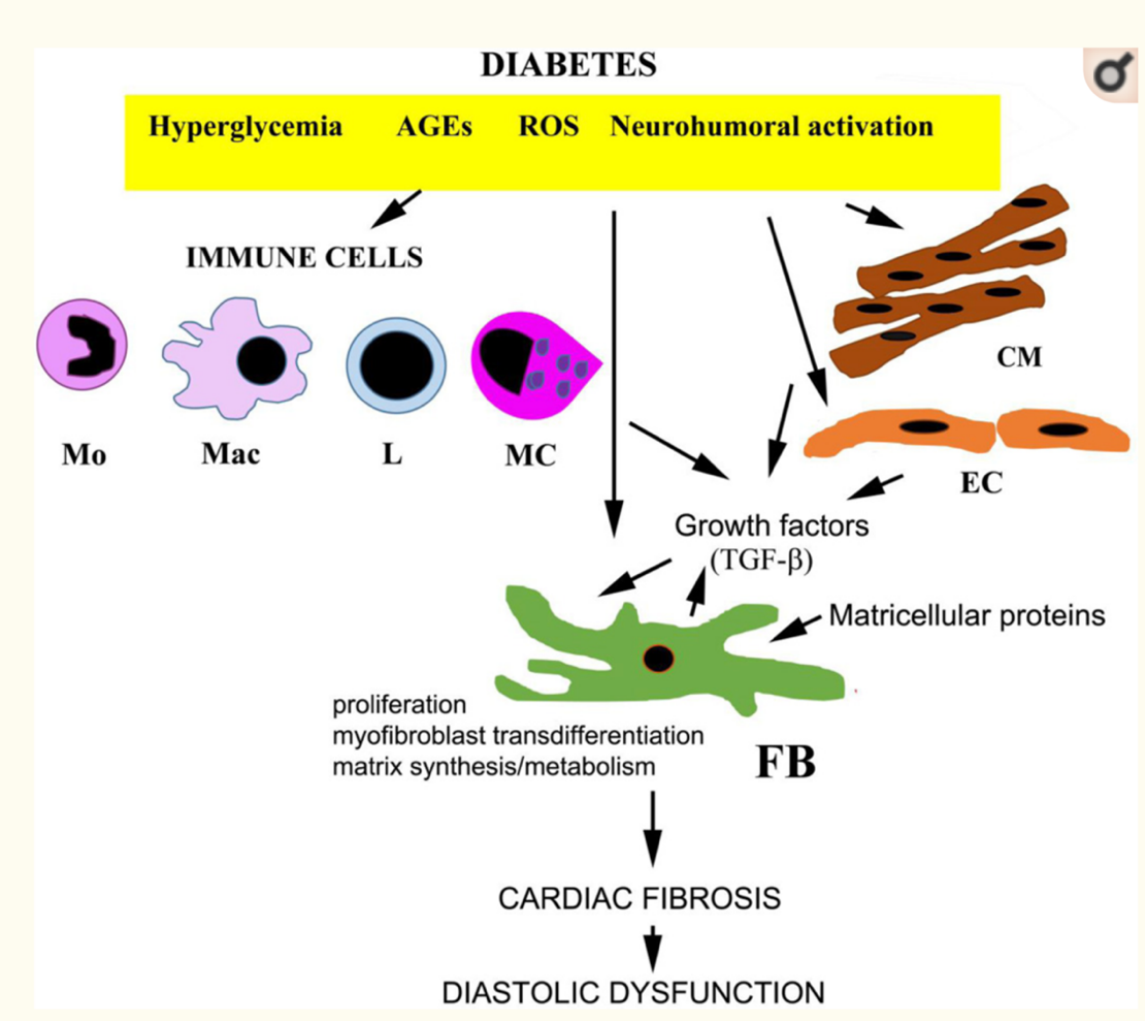

Figure 5: The cell biology of diabetes-associated cardiac fibrosis.

Diabetes-associated hyperglycemia, generation of advanced glycation end-products (AGEs) and reactive oxygen species (ROS), and neurohumoral activation directly activate resident cardiac fibroblasts and may induce a proliferative response and a matrix-synthetic phenotype. Induction and activation of fibrogenic growth factors (such as TGFβ) may play an important role in fibroblast stimulation. Immune cells (monocytes/Mo, macrophages/Mac, lymphocytes/L and mast cells/MC) may contribute to the fibrotic response by secreting profibrotic mediators. Cardiomyocytes (CM) and endothelial cells (EC) may also secrete growth factors and modulate fibroblast phenotype. Endothelial cells and pericytes may transdifferentiate into fibroblasts contributing to the expansion of the fibroblast population in diabetic hearts. Deposition of

matricellular proteins (such as thrombospondin-1) in the diabetic myocardium may promote a profibrotic phenotype in interstitial cells. Reprinted from Ilaria Russo, and Nikolaos G Frangogiannis, Diabetes-associated cardiac fibrosis: cellular effectors, molecular mechanisms and therapeutic opportunities, 84-93, © 2016, Journal of Molecular and Cellular Cardiology reproduced with permission of ELSEVIER INC. https://doi.org/10.1016/j.yjmcc.2015.12.011

3. The extracellular matrix remodelling and matricellular proteins

The cardiac ECM is a complex three-dimensional framework that provides structural support and strength to the myocardium as well as the cells within it. The ECM is comprised of both fibrous (collagenous) and non-fibrous (proteoglycans, glycoproteins, and glucosaminoglycans) proteins [145]. Additionally, the ECM can serve as a reservoir for cytokines, growth factors, MMPs, TIMPs, and miRNAs to participate with and mediate signals to the cells [146-148]. In response to stress or injury, the ECM undergoes remodelling, which includes alteration in the proliferation and activation of cardiac fibroblasts that normally maintain the balance of the myocardium. During this remodelling process, synthesis, integration, and degradation of matrix proteins are affected, which alters the ECM architecture and leads to cardiac fibrosis. There are few essential ECM proteins such as collagen, fibronectin, periostin, α-SMA, and MMPs, which take part in the pathological remodelling process and play a vital role in cardiac fibrosis. Their potential role in cardiac fibrosis-associated remodelling is discussed below.

3.1: Collagen and matrix remodelling

The collagen framework provides support for cell attachment and helps release growth factors and signalling molecules, such as TGFβ, which are essential for the homeostasis of the myocardium. In healthy myocardium, the ECM is comprised of both fibrillar and non-fibrillar collagen. It is comprised of 85% collagen type I, 11% collagen type III, and the remaining <5% is made up of various fibrillar and non-fibrillar collagens such as type IV, V, and VI [1]. Collagen type I fibrils are thick, whereas collagen type III

fibrils are thin and reticular, and link together to surround the muscle cells, thereby providing integrity to the myocardium.

Myocardial fibroblasts are the primary source of collagen production and control the collagen turnover process (synthesis and degradation) inside the myocardium. The estimated half-life of a collagen fibre is 80 to 120 days. Procollagen molecules are synthesized and secreted into the myocardial extracellular space, followed by systemic enzymatic cleavage of both amino (N) and carboxyl (C) terminal domains to become mature collagen. Mature collagen molecules then assemble and crosslink together to form a strong triple helix collagen fibril. The cleavage of collagen type I N-terminal propeptide is mediated by ADAMTS2 (a disintegrin and metalloproteinase with thrombospondin motifs-2) [149], whereas collagen type I C-terminal propeptide is cleaved by BMP-1 (bone morphogenetic protein-1) [150]. The cleaved procollagen N- and C-terminal propeptides are released into the bloodstream. Concentrations of these propeptides in plasma and serum serve as a tool for indirect measurement of collagen synthesis and are also used as a biomarker for disease pathogenesis [151, 152]. The serological concentration of C-terminal collagen type 1 propeptide is directly correlated with diastolic dysfunction [7]. Previous studies have shown that type III collagen propeptide concentration in serum is directly associated with increased heart failure risk and morbidity [153].

Cardiac hypertrophy and fibrosis-associated pathological remodelling have altered collagen composition, which impacts ventricular and vascular stiffness and distensibility [1]. Cardiac myofibroblasts are the primary source of pathological collagen synthesis, which can lead to fibrosis and heart failure [10, 154]. Upon responding to pressure-overload-related stress, type III collagen expression increases in early stages of remodelling, and in late stages of tissue repair, a substantial increase in type I collagen content occurs. In human and preclinical models, collagen secretion into the interstitial space during the matrix remodelling process is influenced by AngII, TGFβ, endothelin-1 (ET-1), platelet-derived growth factor, CTGF, and insulin growth factor [10, 71, 155-160]. Canonical TGFβ is a well-established mechanism for collagen synthesis. TGFβ1-mediated intracellular signalling proteins called Smads act as transcriptional regulators of

myofibroblast activation and collagen synthesis [161]. After injury, cardiac AngII levels are highly elevated, promoting fibroblast proliferation and collagen synthesis. AngII-mediated collagen synthesis requires both TGFβ1/ Smad-3 and MAPK signalling in cardiac fibroblasts [162, 163]. In cardiac myofibroblasts, scleraxis transcriptionally regulates collagen Iα2 expression [164]. Scleraxis and Smad-3 synergistically regulate the expression of collagen Iα2, and scleraxis is also essential for TGFβ1-mediated collagen synthesis [165]. In human cardiac fibroblasts, Col-1a1, 1a2, and 3a1 genes are post-transcriptionally regulated by heterogeneous nuclear ribonucleoproteins (hnRNP) A1, E1, and K [166].

Collagen synthesis is essential for scar formation in post-MI hearts to avoid myocardial slippage and cardiac rupture [1, 19, 20]. However, the excess collagen deposition after scar maturation can be detrimental and eventually can lead to cardiac arrhythmia and heart failure [3]. ET-1 promoted collagen synthesis in rat infarct scar regions, whereas ET-A receptor blocker (LU 135252) promoted MMP activity and collagen degradation resulted in the expansion of infarct scar leading to deleterious effects [167]. Canine myocardium 6 weeks post-MI revealed a 5-fold increase in collagen content at the infarct region, whereas border and remote regions showed unchanged collagen content [168].

In hypertensive patients, increased type I collagen synthesis and deposition is positively correlated with propeptide of procollagen type I concentration in serum, which enhances myocardial fibrosis and heart failure progression [169]. In chronic heart failure patients, mineralocorticoid receptor antagonist (spironolactone) treatment resulted in reduced fibrosis and circulating collagen propeptides, indicating decreased collagen synthesis compared to placebo treatment [73]. In overt heart failure animal models, ACEI (temocapril hydrochloride) treatment reduced the mRNA expression of type I collagen, while ARB (candesartan cilexetil) treatment stimulated gelatinase activity to initiate the degradation of collagen, which resulted in the reduction of myocardial fibrosis [170].

3.2: Fibronectin and matrix remodelling

Fibronectin is an adhesive dimeric glycoprotein synthesized by fibroblasts, endothelial cells, and others. It also can be secreted in both plasma and the ECM [171, 172]. In normal physiology, fibronectin is present in basement membranes and different ECM tissues. Germline knockout of fibronectin is embryonically lethal due to resulting mesodermal and vascular defects [173, 174]. Fibronectin is essential in the developmental and wound healing process. It acts as a bridge between interstitial collagen and cells, thereby promoting cell adhesion and migration [175]. Fibronectin influences the structure and mechanics of the ECM by binding to other matrix proteins such as collagen, heparin sulphate, integrin, and fibrin [176].

TGFβ1, AngII, and dexamethasone induce total fibronectin expression, whereas TGFβ1 preferentially elevates extra domain A-containing fibronectin (EDA-Fn) accumulation in human fibroblasts [177, 178]. EDA-Fn and TGFβ play a collaborative role in promoting cardiac fibroblast-to-myofibroblast activation, which is essential in cardiac remodelling [179]. EDA-Fn can induce collagen deposition and elevate the levels of MMP-2 and 9, leading to adverse cardiac remodelling. Fibronectin polymerization is critical in collagen deposition to the ECM, while fibronectin and collagen together promote cell contractility. In cardiac myofibroblasts, internal microfilaments fuse with extracellular domains of fibronectin via a fibronexus. This unique process allows myofibroblasts to apply contractile forces to the ECM [180].

Tissue injury increases fibronectin concentration, which preferentially elevates the splice variant of EDA-Fn expression in interstitial tissues of ischemic hearts, failing hearts, pressure-overloaded myocardium, and atherosclerotic lesions [181-186]. Fibronectin knockout animals subjected to pressure overload showed reduced cardiomyocyte hypertrophy and improved cardiac function compared to controls [187].

EDA-Fn levels are highly elevated in atherosclerotic arteries and are associated with stable plaque formation in asymptomatic patients and animal models [185, 188]. Notably, EDA-Fn plays a varying role by contributing to early or late atherosclerotic

plaque formation, depending on whether it is derived from endothelial or smooth muscle cells [189].

Fibronectin expression is highly elevated after MI, which promotes scar formation and remodelling in human and animal models [190-192]. EDA-Fn promotes adverse cardiac remodelling after MI, whereas EDA-Fn-null animals show improved survival and cardiac function after infarction [177]. Inhibition of fibronectin accumulation reduced cardiac fibrosis and improved cardiac function in ischemic heart failure animals [181]. Thus, intervening to limit EDA-Fn could prevent cardiac fibrosis and failure.

3.3: Periostin and matrix remodelling

Periostin, part of the fasciclin family, is a 90 kDa matricellular secretory protein highly expressed in the early developmental stages of mouse embryos. It is localized to the mature cardiac valves and endocardial cushions of the embryonic myocardium [193]. Periostin plays a vital role in promoting collagen fibrogenesis and is involved in atrioventricular valve maturation during cardiogenesis [194]. Periostin expression is absent in the adult heart until injury, although it is essential in maintaining the biomechanical properties of the adult myocardium. Periostin is highly expressed in other matrix-rich tissues like tendons and promotes tendon healing [195-197].

Periostin potentially binds to several ECM proteins including collagen I, collagen V, fibronectin tenascin-C, and heparin, thereby mediating profibrotic signalling mechanisms [195, 198-200]. Periostin promotes the proteolytic activity of lysyl oxidase (LOX) by recruiting BMP-1 onto the fibronectin matrix, which enhances collagen crosslinking [201]. Periostin facilitates cardiac fibroblast migration and also acts as a ligand for the integrins αvβ3 and αvβ5 by promoting the phosphorylation of FAK [202].

After MI and adeno associated virus (AAV)-mediated systemic injection of periostin, promoter-driven reporter gene expression was found in cardiac myofibroblast-like cells in the scar region, whereas this reporter gene expression was not found in non-infarcted hearts [203]. Periostin expression is high in myofibroblasts and is also broadly employed as a cellular marker for myofibroblasts. In contrast, fibroblasts do not appear

to express periostin [83, 204]. Previously, Twist, Id1, c-jun, STAT-3, and NFkB were shown to regulate periostin expression transcriptionally by binding directly to its promoter [205-207].

Previous studies showed that periostin-null mice were smaller in overall body weight, displayed early pre-weaning loss (~14%), and exhibited significant valve and leaflet abnormalities [208, 209]. Periostin-null mice developed a periodontal disease-like phenotype that could be alleviated by reducing strain on the periodontal ligaments and craniofacial ECM anomalies [209].

Periostin expression is remarkably elevated in the myocardium due to aging and pathologies such as MI, hypertension, cardiac hypertrophy, dilated cardiomyopathy, and diabetic cardiomyopathy [202, 204, 210-214]. Profibrotic factors, including AngII and TGFβ, up-regulate periostin expression in rat cardiac fibroblasts [215]. Oxidative stress induces periostin expression in the rat hypertension model, contributing to myocardial fibrosis and hypertension [216]. Periostin overexpression via gene transfer in rat myocardium promoted LV dilation and cardiac dysfunction, whereas inhibition of periostin gene using antisense strategy in heart failure rats showed significant improvement in cardiac function and survival rate [213]. In long-term pressure-overloaded animals, periostin deficiency resulted in a significant decrease in cardiac fibrosis and hypertrophy. At the same time, periostin-null animals were prone to cardiac rupture after MI, indicating poor scar formation, although mice that survived exhibited reduced fibrosis [211]. Overall, this evidence suggests that periostin is an essential and integral part of wound healing and the matrix remodelling process after injury.

In failing human hearts, periostin expression is up-regulated and positively correlated with LV diastolic dimension and myocardial fibrosis [204, 217]. In periodontal ligament cells, mechanical stretch can elevate periostin expression, which is essential for maintaining periodontal ligaments' structural integrity and function [218, 219]. Mechanical stretch-induced periostin expression in cardiomyocytes and residential fibroblasts. Periostin expression is markedly reduced in LV assist device-implanted

patients compared to pre-implantation tissue samples, indicating clinical unloading of mechanical stress inside the myocardium [220].

3.4: Matrix metalloproteinases and matrix remodelling

Matrix metalloproteinases (MMPs) are active players in normal and pathological ventricular ECM remodelling. They promote the enzymatic degradation of fibrillar collagens and other ECM proteins [221-223]. Myocardial fibroblasts are the major source of MMPs in the myocardium, but MMPs are also secreted by other cardiac cell types, including cardiomyocytes, endothelial cells, immune cells and smooth muscle cells [224-226]. There are 25 MMPs cloned and characterized, out of which MMP-1, 2, 3, 8, 9, 12, 13, 28, and membrane-type MMPs are known to participate in the cardiac remodelling process [227, 228].

MMPs are classified based on substrate specificity. The collagenases MMP-1, 8, and 13 are capable of degrading collagen types I, II, III, versican aggrecan, and proteoglycans. The stromelysins include MMP-3 and 7, which act on collagen type I, III, IV, proteoglycans, and fibronectin. MMP-2 and 9 are the gelatinases that work on fibronectin, laminin, denatured fibrillar collagens, collagen type IV, and proteoglycans. The membrane-type MMPs include MMP-14 targets—fibrillar collagens, perlecan, and versican. Usually, these MMPs are secreted as inactive proenzymes or zymogens, and upon proteolytic cleavage of an N-terminal propeptide yield the active MMPs. The C-terminal region of each MMP species is structurally unique, which helps in binding to their respective ECM substrates [221-223].

Several factors influence the activity of MMPs inside the myocardium: mechanical stretch, oxidative stress, brain natriuretic peptide (BNP), and proinflammatory cytokines [229-235]. In cardiac fibroblasts, MMP-2 secretion is up-regulated by mechanical stretch, oxidative stress, TGFβ, TNFα, IL-1β, and BNP [236, 237]. Proinflammatory cytokines and oxidative stress can significantly elevate MMP-9 expression in cardiac fibroblasts [235, 236, 238].

In the healthy myocardium, the proteolytic activity of MMPs is modulated by TIMPs, which serve as the major inhibitors of MMPs in the myocardium. Cardiac fibroblasts are the principal secretory source of TIMPs; TIMP-1, 2, 3, and 4 are expressed in the heart [239]. The myocardial expression of TIMPs varies: TIMP-1 is minimally expressed in healthy hearts compared to TIMP-2, 3, and 4 [226]. In chronic pressure-overloaded human hearts, TIMP-1 and 2 are highly expressed in cardiac interstitial fibrosis [240]. MMP and TIMP expression is tightly regulated to maintain the homeostasis in the healthy myocardium, whereas changes in their proteolytic activity could result in adverse pathological remodelling and heart failure [241].

During heart failure, both animal and human myocardium show increased MMP activity and reduced TIMP expression, stimulating ventricular remodelling. These progressive changes promote pathological ventricular remodelling and dilation, leading to heart failure [242-244]. MMP-2 and MMP-9 can help free latent TGFβ peptide from the ECM, which accelerates collagen synthesis via canonical and non-canonical TGFβ signalling pathways, and leads to myocardial fibrosis [245]. In post-MI patients, MMP-1 levels are elevated in serum after day 4 of reperfusion and reach a maximum at day 14, with a nearly 50% reduction by day 28. Similarly, TIMP-1 concentration starts to rise on day 5 and peaks at day 14. Additionally, MMP-1 serum concentration is positively correlated with LVEF and inversely correlated with LV systolic volume index [246].

In patients with DCM, myocardial MMPs showed a disparity in their expression pattern; MMP-9 and MMP-3 levels are elevated, while MMP-1 levels are low, and MMP-2 levels are similar to those in non-heart failure patients [244]. In heart failure patients, explant tissues showed a 4-fold increase in MMP-2 activity compared to control hearts [204]. In acute MI patients, baseline MMP-8 serum concentration is an independent predictor of LV remodelling leading to adverse clinical outcomes and hospitalization [247]. In patients with coronary artery disease, MMP-9 plasma concentration serves as a prognostic marker for cardiovascular-related mortality [248]. T Thus, understanding the specific role of MMPs will provide better insights into the adverse cardiovascular remodelling process, which will help improve patient care.

4. Cardiac fibroblast to myofibroblast [1]

When tissues undergo physical stress or damage, fibroblasts become activated and undergo a series of phenotype changes, initially increasing their ability to proliferate and migrate, and then eventually converting fully to myofibroblasts, which greatly reduce their migration and proliferation while simultaneously increasing their synthesis of ECM dramatically [249-251]. Upon resolution of the stress or damage, myofibroblasts may undergo apoptosis, returning the tissue more or less to its original state; however, if resolution is delayed or impeded, myofibroblasts may persist for years, such as may occur after myocardial infarction [20, 252]. Furthermore, the phenotype of these persistent myofibroblasts may be different from that which arises during the initial response to injury [90, 253]. The conversion of fibroblasts to myofibroblasts can thus be either highly beneficial, as in the case of normal wound healing or after myocardial infarction where stable scar body display distinct formation is required, or detrimental when persistent myofibroblasts lead to long-term scarring and fibrosis, which in the myocardium can contribute to arrhythmogenesis [90, 254]. The complex nature of fibroblast to myofibroblast conversion, coupled with the varied developmental origins of fibroblasts, has led to confusion in the literature around the use of the term "myofibroblast" as well as the description of the phenotype change itself -which has been variously described as activation, conversion, or even differentiation. An intermediate phenotype, the proto-myofibroblast, has also been described as an activated fibroblast not yet expressing α-smooth muscle actin (α-SMA), a hallmark of the myofibroblast phenotype [255]. Without doubt, the fact that myofibroblasts may arise from other cell types, including pericytes, hepatic stellate cells, epithelial cells, and endothelial cells, has further added to the confusion around naming conventions. Here we discuss the terminology and nomenclature of both the cells involved and the conversion process itself, with a focus on the myocardium, to prompt discussion by the scientific community

[1] Reprinted from Raghu S Nagalingam, Danah S Al-Hattab and Michael P Czubryt, What's in a name? On fibroblast phenotype and nomenclature, Canadian journal of physiology and pharmacology 97(6): 493-497© 2019, with permission from Canadian Science Publishing. https://cdnsciencepub.com/doi/abs/10.1139/cjpp-2018-0555

on the importance of developing unified language for the discussion, study, and analysis of these important cells.

4.1: Fibroblast origins and phenotypes

Given the significant burden of fibrotic diseases on human clinical outcomes, the past decade has seen a dramatic resurgence of interest in fibroblast and myofibroblast biology [256]. The conversion of fibroblasts to myofibroblasts is a critical step in the development of fibrosis and thus represents an important potential point of attack for therapeutic development [257]. However, it is important for researchers to employ well-defined terminology for describing fibroblasts, myofibroblasts, and their interconversion to avoid sowing confusion, drawing inaccurate conclusions, or making unwarranted assumptions. A reasonable starting point is to consider the heterogeneity of fibroblasts both between and within tissues and to examine the universal use of the term “fibroblast” itself.

Multiple lineage tracing studies have investigated the developmental origins of fibroblasts within different anatomical sites. Fibroblasts from different tissues within the and characteristic transcriptional patterns of gene expression, indicating that fibroblast differentiation varies across tissue types [258]. Furthermore, even within a single tissue type, heterogeneity of fibroblasts has been reported, likely owing to differing embryonic origins coupled with clonal selection and expansion of fibroblast subsets, which may alter response to disease [259]. For example, in the case of dermal fibroblasts, those in facial skin originate from the neural crest, those in the anterior body are derived from the lateral plate mesoderm, and those in the posterior compartment arise from the dermomyotome [260]. Thus, the functional heterogeneity of skin fibroblasts reflects, in part, the existence of different fibroblast lineages, resulting in fibroblasts that may respond differently to environmental stimuli or signals. Following dermal injury, the initial wave of repair that involves collagen deposition and scarring is mediated by a deeply located fibroblast lineage, which when activated expresses myofibroblast markers such as α-SMA [261]. Conversely, a superficial fibroblast lineage is recruited in the re-epithelialization that

forms hair follicles. The variable contribution of these lineages during healing provides insight into why scars that are rich in ECM may be devoid of hair follicles [261].

The primary cellular source for the cardiac fibroblast population is epithelium-derived. During embryonic cardiac development, cells from the proepicardial organ migrate to constitute the epicardium, a subset of which undergoes epithelial-to-mesenchymal transition (EMT), invades the myocardium, and subsequently differentiates into fibroblasts [262, 263]. In contrast, fibroblasts in the atrioventricular valve leaflets and tendinous cords of the mitral and tricuspid valves are primarily derived from the endocardium, through endothelial-to-mesenchymal transition (EndMT) [264, 265]. There is evidence that ventricular and atrial fibroblasts, despite apparently common embryonic origins, exhibit key phenotypic differences. Atrial fibroblasts are present in higher density, have higher basal rates of ECM production, and show a greater propensity to activation than ventricular fibroblasts - differences that are maintained in the failing heart [266]. This same study reported over 200 differences in gene expression between atrial and ventricular fibroblasts. Thus, while embryonic origin can contribute to fibroblast heterogeneity, it is likely that other factors, such as the specific cellular milieu, also have important roles to play.

Although no specific protein marker exclusive to fibroblasts has been identified to date, several distinctive markers when considered together can be helpful in identifying organ-specific fibroblasts. In human cardiac tissue, ECM protein markers such as collagen and fibronectin have been used to label and identify fibroblasts. However, these proteins can be also expressed by valve interstitial cells, vascular smooth muscle cells, and pericytes [267]. The intermediate filament-associated calcium-binding protein fibroblast-specific protein 1 (FSP-1) was originally thought to be expressed primarily in cardiac fibroblasts, but further studies have revealed a much broader range of expression, including hematopoietic cells, vascular smooth muscle cells, and endothelial cells both in the unstressed heart and following pressure overload or myocardial infarction [268]. Further studies are thus needed to reevaluate currently used fibroblast markers and to evaluate novel putative markers through individual cell transcriptomic and proteomic analysis. The identification of a highly specific fibroblast marker - whether for fibroblasts

in general or for those specifically in tissues such as the heart remains a critical priority for the field. However, it is possible that such a specific marker simply does not exist; this problem is compounded by the fact that other cell types such as pericytes and hepatic stellate cells may fulfill fibroblast-like functions while clearly being non-fibroblast in nature and despite the fact that these cells can contribute to the population of myofibroblasts in pathology [269].

Ultimately, the relative physiological impact of fibroblast heterogeneity remains unclear, particularly as this heterogeneity may (or may not) impact the transition of fibroblasts to myofibroblasts during stress or damage. The phenotype of an individual fibroblast stems from many interrelated factors, including developmental origin, tissue type, and likely many stochastic variables such as dynamic and steady-state physical forces acting on the cell, the specific cellular composition of the milieu within which the fibroblast exists, and the identity and concentration of growth factors, cytokines, and substrates that impinge upon the cell. An important question is thus whether there is anything to be gained by further subdividing fibroblasts into subtypes based on, for example, marker expression. It may also be important to consider the role played by the cell rather than or in addition to the presence of specific markers as well as the fate of the cell during pathological stress or damage, i.e., whether the cell converts to a myofibroblast fate. In the heart, an important question is whether all cardiac fibroblasts possess equal potential for converting to myofibroblasts or even if there are subpopulations differentiable by whether or not they can become myofibroblasts. A related question is whether the same specific population(s) of fibroblasts is activated in different pathologies such as pressure overload versus myocardial infarction.

4.2: Fibroblast phenotype switching

Early studies had noted that, following tissue injury, myofibroblasts arising during tissue granulation exhibited distinct morphological characteristics from fibroblasts, such as prominent stress fibers that were hypothesized to contribute to wound contraction [270]. In the intervening years, many studies have described the physical and functional characteristics of myofibroblasts in various tissue types and in particular their central role

in wound healing and fibrosis. The phenotypic switch from fibroblasts to myofibroblasts represents a major change in cell function brought about by significant changes in gene expression to facilitate the dramatic increase in the synthesis of ECM and related remodeling enzymes such as matrix metalloproteinases (MMPs). Recent work in the field has, however, made it clear that the definition of what constitutes a myofibroblast may need to be revisited or at a minimum, consideration is needed as to whether additional terms are required to describe what has turned out to be a highly heterogeneous cell population [250].

Traditionally, it was believed that fibroblasts are activated to undergo conversion to myofibroblasts; thus, cells were either fibroblasts or myofibroblasts. It was soon realized, however, that other cell states exist. As noted above, the term "proto-myofibroblast" was proposed to describe fibroblasts that had become activated to begin the process of conversion to myofibroblasts but did not yet express α-SMA, a hallmark indicator that fibroblasts had become proper myofibroblasts since stromal fibroblasts do not normally express α-SMA [255]. While it remains unclear whether proto-myofibroblasts actually arise during injury responses *in vivo*, this work has helped to usher in an important discussion on myofibroblast heterogeneity, a discussion that is complicated by variability in wound healing across tissue types.

During skin wound healing, fibroblasts in the vicinity of the injury become activated, resulting in a phenotype that is proliferative and motile; these cells migrate to the site of injury, complete their conversion to myofibroblasts, and robustly synthesize ECM to aid in wound closure and repair [271]. Once the tissue has been repaired, ideally to its original pre-injury state, these myofibroblasts undergo apoptosis or in some cases adopt a quiescent phenotype; however, it remains unclear exactly how these processes are controlled or what the role of these quiescent cells actually may be [249]. In some situations, such as diabetes, the cellular and molecular mechanisms governing wound healing may go awry, resulting in wounds that fail to heal, possibly due to a failure of fibroblasts to be fully activated to myofibroblasts [272]. Conversely, the persistence of active myofibroblasts at the site of injury may lead to abnormal scarring, including hypertrophic scars or dermal keloids [273].

Following cardiac injury, quiescent cardiac fibroblasts may be triggered by growth factors, inflammatory cytokines, or physical stress to become activated and undergo phenotype conversion into myofibroblasts [250, 251]. Earlier studies had implicated a host of contributory cell types in the genesis of myofibroblasts, including EndMT or EMT of various cell types such as hematopoietic bone marrow cells or pericytes [274-278]. However, recent lineage-tracing studies have shown that 80%–85% of myofibroblasts derive from resident cardiac fibroblasts within the left ventricle of the adult mouse heart after pressure overload [83, 279]. Similarly, resident fibroblasts are the primary contributors to cardiac remodeling after myocardial infarction [88]. Resident cardiac fibroblasts are thus the primary source of myofibroblasts during cardiac injury and healing, regardless of the nature of the underlying insult.

Recent studies of post-myocardial infarction healing have led to the recognition of novel phenotypic stages during the conversion of fibroblasts to myofibroblasts and beyond (Fig. 6). Upon tissue injury, fibroblasts mediate inflammatory and immune responses as part of the repair process. Within the first day post-infarction, resident cardiac fibroblasts appear to take on a pro-inflammatory phenotype, releasing several MMPs and inflammatory cytokines and growth factors including IL-1β, IL-6, and TNFα [250]. Additional secreted factors include pro-fibrotic TGF-β1 and fibroblast growth factors that stimulate further fibroblast migration and activation [250]. The renin–angiotensin system is also important in fibroblast activation. Not only can angiotensin II stimulate fibroblast activation and collagen synthesis via AT1 receptors, fibroblasts themselves can generate angiotensin-converting enzyme and angiotensin II [280, 281].

By the third day, fibroblasts appear to become anti-inflammatory, assisting in the tissue granulation process by secreting pro-angiogenic and anti-inflammatory factors. During these early days, fibroblasts are proliferative and motile, resembling the proto-myofibroblast state [88]. Cell phenotype then progresses over days and weeks to that of a more traditional myofibroblast: proliferation and migration decreases, while ECM synthesis is sharply increased concomitant with expression of α-SMA as well as periostin another marker known to be expressed in myofibroblasts but not fibroblasts [83] leading

to formation and eventual maturation of the infarct scar. By approximately 4 weeks, the majority of periostin-labeled cells undergo apoptosis as evidenced in the presence of TUNEL-positive nuclei [88]. It has long been known that myofibroblast-like cells remain within the scar years or decades after the initial insult [252, 282]. Fu et al. suggested that the cells persisting longer than 10 days post-infarction are an altered myofibroblast that has lost α-SMA expression and shows reduced proliferation, which they have termed the "matrifibrocyte" [88]. Interestingly, these cells showed gene expression patterns reminiscent of chondrocytes and osteoblasts, although distinct from both cell types and from myofibroblasts. It remains unclear if these are the same cells noted in humans years after infarction. It also remains unclear if these cells play specific roles, such as stabilization or maintenance of the scar, or if they are simply remnants that escaped apoptosis.

Another intriguing question is whether matrifibrocytes also appear in other disease processes marked by cardiac fibrosis such as pressure overload. Studies employing genetic lineage tracking of fibroblasts using a periostin-Cre reporter mouse revealed that periostin expressing myofibroblasts are induced by pressure overload following transverse aortic constriction primarily in the left ventricle free wall and septum, whereas induction of fibrosis by angiotensin II and phenylephrine resulted in fibroblast activation throughout the heart [83]. However, the question of whether the myofibroblasts arising in this latter study are the same as those arising post-infarction remains to be determined. It also is important to determine how myofibroblasts arise and whether they exhibit a similar life cycle in other tissue types, including those in which myofibroblasts are derived from nonfibroblast populations such as hepatic stellate cells or pericytes.

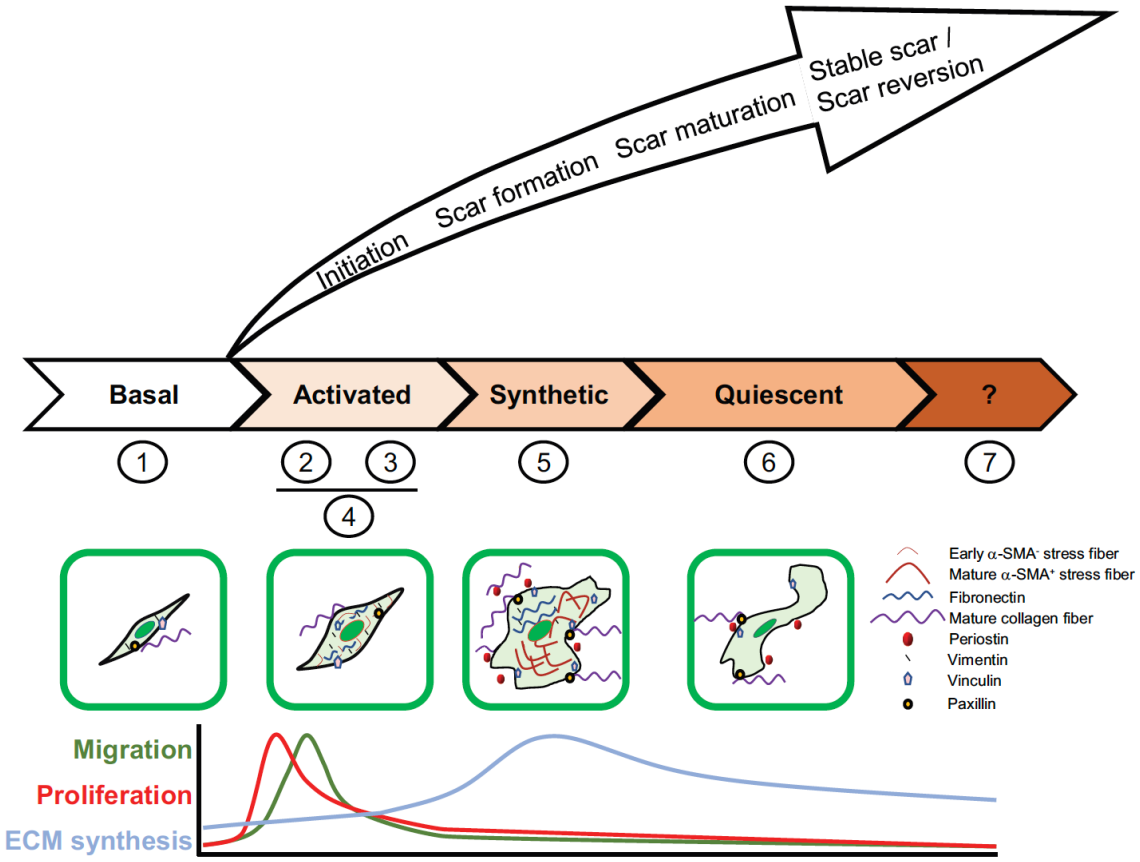

Figure 6: Putative schema of fibroblast to myofibroblast phenotype conversion. Basal fibroblasts (1) exhibit relatively low rates of migration, proliferation, and synthesis of extracellular matrix (ECM). Upon activation signals such as may occur during tissue damage, e.g., cytokines, growth factors, or mechanical stress, fibroblasts initially adopt a pro-inflammatory phenotype (2), increasing their rates of proliferation and migration; this stage is followed shortly by an anti-inflammatory phenotype (3). These early phenotypes, prior to induction of α-smooth muscle actin (α-SMA) expression, may represent the proto-myofibroblast stage (4). Activated fibroblasts decrease their proliferation and migration rates concomitant with a marked increase in ECM synthesis, adopting the synthetic myofibroblast phenotype indicated by expression of markers such as α-SMA and periostin (5). Over time, myofibroblasts reduce ECM production, then either undergo apoptosis or enter a quiescent phase (matrifibrocyte (6)) marked by reduced α-SMA expression. It remains unclear what is the exact long-term phenotype of myofibroblasts

that persist (7), including whether they maintain the matrifibrocyte phenotype. The long-term persistence of myofibroblasts at the site of injury may determine whether stable scars are formed or whether the injured tissue fully heals with scar reversion. Reprinted from Raghu S Nagalingam, Danah S Al-Hattab, and Michael P Czubryt, What's in a name? On fibroblast phenotype and nomenclature, Canadian journal of physiology and pharmacology 97(6): 493-497© 2019, with permission from Canadian Science Publishing. https://cdnsciencepub.com/doi/abs/10.1139/cjpp-2018-0555

5. Scleraxis: a force-responsive cell phenotype regulator [2]

Scleraxis is a basic helix-loop-helix (bHLH) transcription factor that appears to be most highly expressed in tissues that are routinely subjected to large physical forces, including tendons, ligaments, and cardiac valves [283, 284]. Scleraxis is also highly expressed in regions rich in connective tissue such as the tongue, limbs, diaphragm and bronchial cartilage [285]. This curious expression pattern suggests that scleraxis may be involved in the response of cells and tissues to mechanical stress.

From a yeast 2-hybrid screen of an embryonic mouse cDNA library, scleraxis was first identified as an interacting partner of the ubiquitous E-box binding transcription factor E12 [285]. Similar to other class I bHLH proteins, scleraxis possesses a basic amino acid-rich DNA- binding site which allows binding to the E-box consensus sequence (CANNTG, N = any nucleotide) within target gene promoters. Scleraxis also possesses a helix-loop-helix protein interaction domain, which facilitates its binding to transcriptional regulatory partners such as E12, E47, CREB and Smad3 [165, 286-288]. This ability to physically interact with other transcriptional regulators may provide the mechanism by which scleraxis can control expression of different subsets of interaction may also explain why scleraxis appears to bind to only a subset of E-box sequences,

[2] Reprinted from Hamza A Safi, Raghu S Nagalingam, and Michael P Czubryt, Scleraxis: a force-responsive cell phenotype regulator, Current Opinion in Physiology 01: 104-110 © 2018, with permission from Elsevier.
https://www.sciencedirect.com/science/article/pii/S2468867317300081

which are fairly common cis regulatory elements throughout the genome. Much of the current body of research on scleraxis has focused on its role in the development and function of tendons, and its expression pattern confirms the critical role that scleraxis plays in this tissue. Scleraxis was reported to be expressed as early as 9.5 days post-coitus in the developing mouse embryo, particularly within the somites and mesenchymal precursors of the axial and appendicular skeleton of the embryo [285]. By embryonic day 12, scleraxis can be detected in small tendon fibers, and its expression is present throughout embryonic development in virtually all differentiating tendon cells [289, 290]. Scleraxis gene knockout studies demonstrate its requirement for normal tendon differentiation and formation, as scleraxis null mice exhibit severe limits on the mobility of the legs, back and tail stemming from the formation of a disorganized tendon matrix and a failure of tendon precursors to appropriately differentiate during development [284, 291].

An increase in scleraxis expression has been noted in healing tendons: following injury of the adult patella, paratenon cells surrounding the tendon proliferate, migrate to the site of injury and begin to express scleraxis and extracellular matrix (ECM) proteins to repair the injury [292]. Several reports have noted that forced over-expression of scleraxis in human embryonic stem cell-derived mesenchymal stem cells or in tendon pro-genitors enhances tendon repair via cell reprogramming [293, 294]. These results provide important clues that scleraxis can independently alter cell differentiation and phenotype.

5.1: Regulation of epithelial-to-mesenchymal transition

Epithelial-to-mesenchymal transition (EMT) is a biological process in which differentiated epithelial cells lose their epithelial characteristics and acquire a mesenchymal phenotype, which includes an elevated resistance to apoptosis, enhanced migratory capacity and invasiveness, and significantly increased production of ECM components [295]. EMT plays critical roles in the formation of the body plan and in the differentiation of numerous tissues and organs, including heart development, where EMT

of epicardial cells gives rise to the majority of cardiac fibroblasts [296, 297]. Our laboratory was the first to study the regulation of EMT in the myocardium by scleraxis.

We noted that hearts from scleraxis null mice exhibited a significant loss of cardiac fibroblasts, concomitant with reduced mesenchymal marker gene expression and increased epithelial marker expression [288]. We therefore hypothesized that scleraxis may be involved in the EMT process that underlies cardiac fibroblast development, and found that scleraxis activated the gene promoters of the mesenchymal markers Snail 1 and Twist 1, although it was unclear whether this was a direct or indirect effect. Moreover, scleraxis over-expression in A549 human epithelial cells resulted in up-regulation of mesenchymal and fibroblast markers, and down-regulation of epithelial markers, suggesting that scleraxis alone is sufficient to induce EMT. TGFβ is a potent inducer of EMT in many precursor cell types, and we found that TGFβ induced EMT of A549 cells and concomitantly resulted in an increase in scleraxis expression. Notably, scleraxis knock-down attenuated the ability of TGFβ to induce EMT, revealing a clear requirement for scleraxis in this process. Scleraxis thus appears to be a transcriptional inducer of EMT, however the precise mechanism underlying its mode of action remains to be defined, and further studies are needed to determine whether regulation of EMT by scleraxis is a common phenomenon in other tissues.

5.2: Phenotypic regulation of cardiac fibroblasts

The finding that scleraxis can regulate EMT begs the question of whether scleraxis exerts general effects on cell phenotype, and if so, in which cells it operates. Recent work from our laboratory and others indicates that scleraxis does, in fact, play the role of a cell phenotype regulator in tendons and in the heart. Scleraxis has been shown to be a crucial transcription factor in promoting the proliferation of fibroblasts and the synthesis of matrix proteins during embryonic tendon development, although it is unclear whether this reflects a role for scleraxis in EMT as noted above, or in general phenotype modulation. Scleraxis gene deletion in mice negatively impacts the development and differentiation of force-conducting tendons due to impaired conversion of tendon progenitors to discrete tendons, resulting in severe tendon defects [284].

Fibrocartilaginous tendon enthesis maturation is also mediated by scleraxis: conditional deletion of scleraxis attenuated the formation of tendon entheses during embryonic development, leading to negative functional consequences [298].

Recently it was shown that, in response to scleraxis over-expression, bone marrow-derived mesenchymal stem cells displayed reduced proliferation and clonogenicity, and underwent phenotype conversion to cells that highly resembled tendon progenitors, with a marked up-regulation of the tendon marker tenomodulin [299]. Conversely, knockdown of scleraxis in embryonic stem cells or in fetal tenocytes blocked their ability to build artificial tendons in a 3D matrix an effect that could be rescued by scleraxis over-expression [291]. These results implicate scleraxis as a regulator of tendon cell phenotype during development. Interestingly, scleraxis knockdown in adult tenocytes failed to impact their ability to remodel a 3D matrix, suggesting that in tendons, the importance of scleraxis changes over time, although this observation may also reflect a difference in plasticity between fetal and adult tenocytes [291]. In the heart, genetic deletion of scleraxis decreased the structural formation of valves mediated by tendon-like connective tissues linked with reduced expression of collagen type XIV. Additionally, loss of scleraxis drives heart valve precursor cells to a chondrogenic differentiation pathway, leaving smaller sets of heart valve precursor cells undifferentiated and expressing mesenchymal markers [283].

As noted above, we found that scleraxis null mice lost approximately 50% of their complement of cardiac fibroblasts, which may be due to altered EMT. These mice also exhibited significant downregulation of ECM genes including those encoding type I collagen, fibronectin, vimentin and the collagen receptor DDR2, and the bulk ECM was significantly reduced [288]. While this loss might be attributed to the reduced number of fibroblasts, isolation of the remaining knockout fibroblasts revealed a deficit in matrix gene expression that could be rescued by scleraxis over-expression. Similarly, knockdown of scleraxis in isolated primary cardiac proto-myofibroblasts had virtually identical effects on the same target genes as *in vivo* knockout, and furthermore completely attenuated TGFβ-induced cell contraction - a hallmark of the myofibroblast phenotype. Over-expression of scleraxis in isolated primary cardiac proto-myofibroblasts

induced full conversion to myofibroblasts, including upregulation of matrix gene expression, increased a-smooth muscle actin expression and an increase in cell contractility. Collectively, these results indicate that scleraxis is required and sufficient to drive the conversion of cardiac fibroblasts toward the myofibroblast phenotype, a finding that has significant implications for the pathophysiological induction of fibroblast to myofibroblast transition that occurs with pressure overload or following myocardial infarction.

Mechanical stretch promoted the phenotypic conversion of isolated primary cardiac fibroblasts to myofibroblasts in a process that required the presence of scleraxis [300]. Overexpression of scleraxis alone mimicked the effect of mechanical stretch on fibroblast to myofibroblast conversion, including reducing motility and proliferation, providing further support for our finding that scleraxis is a key player in this process. It thus appears that scleraxis, at least in tendons and cardiac fibroblasts, can impact both EMT and cell phenotype conversion.

5.3: Scleraxis-mediated intracellular signaling pathways

An important avenue of investigation is the analysis of intracellular signaling pathways involving scleraxis, that is those upstream signals that alter scleraxis expression or activity, as well as the gene network whose expression is governed by scleraxis. Surprisingly, and despite a twenty-year body of literature on scleraxis, relatively little is known in this regard. While several reports have demonstrated changes in scleraxis expression in response to growth factors, for example, in most cases it is unclear how scleraxis expression changes. Similarly, the expression of many genes has been reported to change following manipulation of scleraxis expression, yet very few studies have actually tested whether this is a direct effect of scleraxis acting on a target gene promoter, or an indirect effect (Table 1, Table 2). Several recent studies have begun to shed light on these areas.

To date, almost nothing is known of the *cis*-regulatory elements present within the scleraxis promoter. An early report indicated that the bHLH transcription factor paraxis binds to an E-box within the scleraxis promoter to increase scleraxis expression [301].

Another bHLH transcription factor, TCF21, has been found via chromatin immunoprecipitation to bind to the scleraxis promoter - a noteworthy finding, since TCF21 is required for cardiac fibroblast specification, and since our data has revealed a partial phenocopy of this effect in scleraxis null mice, that is loss of 50% of cardiac fibroblasts [288, 297, 302]. More recently it was shown that dexamethasone caused the glucocorticoid receptor to bind to a regulatory sequence in the scleraxis promoter, reducing scleraxis expression and inhibiting the differentiation of tendon stem cells to tenocytes [303, 304]. This finding has clinical relevance, since glucocorticoids have been reported to induce tendon rupture through a poorly-defined mechanism. The response of scleraxis expression to glucocorticoids may be further altered by glutamate or N-methyl-D-aspartate, however the mechanism involved is unclear [305]. It has been reported that factors secreted from myoblasts can up-regulate scleraxis expression in human hamstring tendon-derived cells, but neither the specific identity of these factors nor their mechanism of action have been identified, although the myokine myostatin has been shown to induce scleraxis expression in tenocyte formation [306-308]. It is unknown whether cardiomyocytes may similarly secrete factors to alter scleraxis expression in cardiac fibroblasts.

TGFβ is a potent activator of fibrosis in many tissues, and several laboratories have noted that it induces scleraxis expression. We have reported that TGFβ and its down-stream, canonical effector Smad3 are able to up-regulate scleraxis expression, while inhibitory Smad7 had the opposite effect, however the precise location of a Smad-binding element within the scleraxis promoter remains elusive [165]. TGFβ may also regulate scleraxis expression via a Smad-independent mechanism involving c-Jun, but again the precise mechanism is unclear [309]. Stretch has similarly been reported to induce scleraxis expression in primary human rotator cuff fibroblasts, although the mechanism was not determined [310]. In our studies of mechanical stretch, we noted that stretch activated a scleraxis promoter luciferase reporter, indicating the presence of a yet-to-be-identified stretch-responsive regulatory element [300]. In this regard, it is intriguing that scleraxis knockout adversely affects the development of force-transmitting tendons throughout the body, yet has minimal effect on other classes of tendons, such as those

that anchor muscles to the skeleton [284]. The cystic fibrosis transmembrane conductance regulator is activated by stretch, and DF508 mice bearing a dysfunctional form of this channel exhibit impaired tendon structure and function with a reduction in matrix production and a significant loss of expression of scleraxis [311]. Mechanical force and stretch may thus represent key drivers of scleraxis expression and function, which in turn would be expected to stimulate the production of an ECM capable of withstanding increases in such forces (Figure 7).

If little is known of the promoter elements governing scleraxis expression, even less is known about post-translational modifications that alter scleraxis activity. We recently reported the first such modification: phosphorylation of scleraxis on two highly-conserved serine residues is vital for its transcriptional activity, and we identified casein kinase 2 as the likely regulator [312]. This finding may help explain previous reports that casein kinase 2 inhibition can attenuate fibrosis. It has also been reported that, in avian heart valve precursor cells, TGFβ2 mediates scleraxis gene expression via a mechanism that can be repressed by the MAPK signaling pathway, however it is unclear whether this is a direct effect of MAPK-mediated phosphorylation of scleraxis [313]. Intriguingly, it was reported that scleraxis physically interacts with the deacetylase SIRT1, which appeared to be important for the ability of scleraxis to induce tenogenic differentiation, suggesting that scleraxis may be negatively regulated by acetylation [314].

Several downstream gene targets of scleraxis have been identified with sufficient depth of analysis to demonstrate a direct interaction of scleraxis with their promoters. Scleraxis has been widely reported to regulate tenomodulin expression, and using C3H10T1/2 cells, it was reported that scleraxis induces a tenocyte-like phenotype and directly binds to the tenomodulin gene promoter [315]. Scleraxis directly regulates Col1a1 expression in conjunction with NFATc in tendon fibroblasts by binding to a cis response element [316]. Similarly, in cardiac fibroblasts we have reported that scleraxis directly trans-activates the expression of the major ECM proteins Col1a2 and fibronectin by binding to E-boxes within their promoter regions [164, 165, 317].

We also found that scleraxis up-regulates expression of α-smooth muscle actin in cardiac fibroblasts by binding to two E-boxes in the gene promoter [288]. This is consistent with a report that activated paratenon cells involved in tendon healing express increased levels of scleraxis and a-smooth muscle actin 7 days after injury, although it was unclear whether scleraxis directly regulates actin expression in these cells [292]. In contrast, in kidney mesangial cells, α-smooth muscle actin expression was negatively regulated by scleraxis binding to only one of these two E-boxes [318]. Thus, gene regulation by scleraxis appears to be tightly regulated in a cell type-dependent manner. For this reason, high-throughput approaches such as ChIP-seq will be required to accurately identify scleraxis target genes in different tissues.

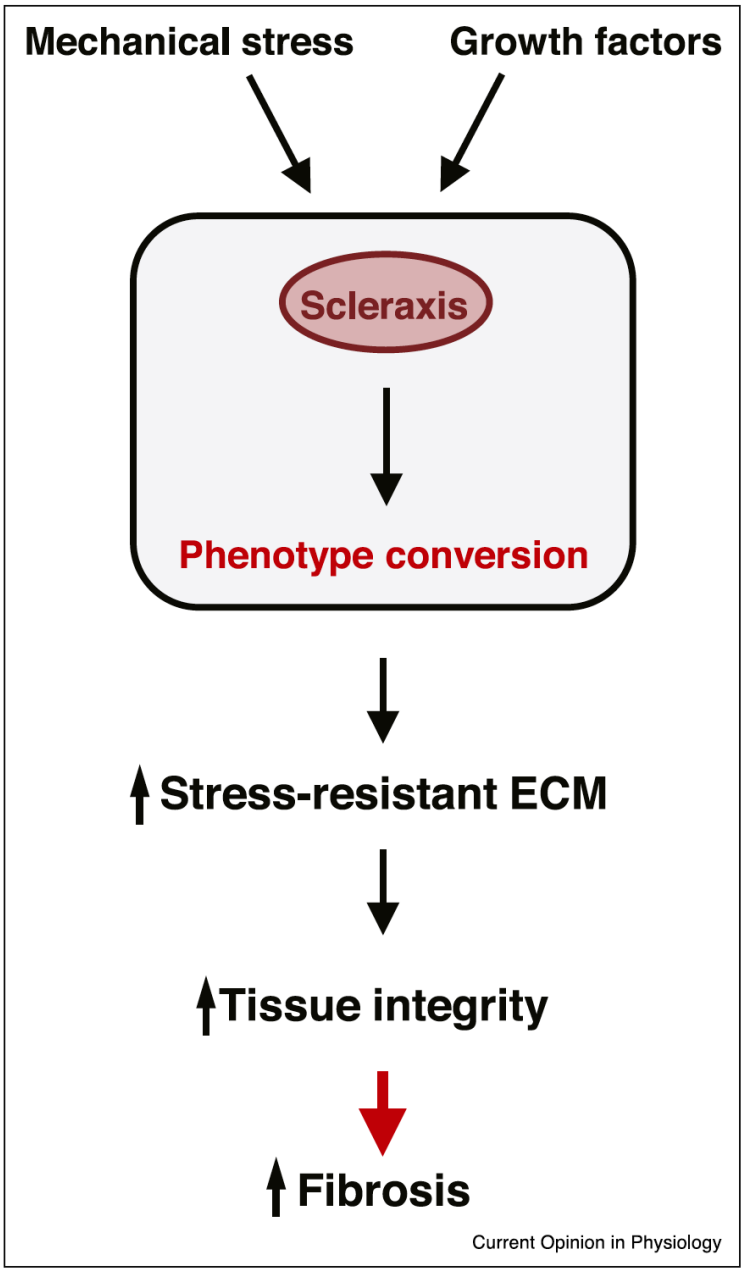

Figure 7: Scleraxis-mediated production of extracellular matrix via cell phenotype regulation.

Studies to date in tenocytes and cardiac fibroblasts support a model in which scleraxis expression increases in response to increased mechanical stress (e.g. stretch) acting upon the cell. External stress may also act via the release of matrix-entrapped growth factors, such as TGFβ which is maintained in a latent complex within the extracellular matrix

(ECM) and is released by mechanical force, and which in turn up-regulates scleraxis expression. Scleraxis induces cell phenotype conversion via the concerted regulation of a host of downstream target genes, including those encoding ECM components. As a result, additional matrix is synthesized to provide greater resistance to stress and mechanical force, increasing tissue integrity. However, if the upstream signals (e.g. mechanical force or growth factor release) remain active, or if a stop signal fails to be induced, the progressive increase in ECM production may lead to fibrosis and compromised tissue function. Reprinted from Hamza A Safi, Raghu S Nagalingam, and Michael P Czubryt, Scleraxis: a force-responsive cell phenotype regulator, Current Opinion in Physiology 01: 104-110 © 2018, with permission from Elsevier. https://www.sciencedirect.com/science/article/pii/S2468867317300081

Table 1. Known target genes of scleraxis.

While a number of genes show evidence of being regulated by scleraxis, relatively few have undergone detailed promoter analysis. The listed genes have published evidence for direct transcriptional regulation by scleraxis.

Target gene	Cell type	Reference
Tenomodulin	C3H10T1/2	[315]
Collagen 1α1	Tendon fibroblasts	[316]
Collagen 1α2	Cardiac fibroblasts	[165]
Fibronectin	Cardiac fibroblasts	[317]
α-Smooth muscle actin	Cardiac fibroblasts	[288]
α-Smooth muscle actin	Kidney mesangial cells	[318]

Table 2. Putative target genes of scleraxis.

Several extracellular matrix or matricellular genes have been noted to show expression that parallels that of scleraxis, but have not been rigorously tested as to whether or not they are direct gene targets of scleraxis.

Target gene	Cell type	Reference
Snail1	Cardiac fibroblasts	[288]
Twist1	Cardiac fibroblasts	[288]
Collagen 3α1	Cardiac fibroblasts	[288]
Vimentin	Cardiac fibroblasts	[288]
Periostin	Cardiac fibroblasts	[288]
MMP2	Cardiac fibroblasts	[288]
Fibromodulin	Cardiac fibroblasts, atrioventricular valve canal	[288, 313]
Decorin	Cardiac fibroblasts, atrioventricular valve canal	[288, 313]
Lumican	Cardiac fibroblasts, atrioventricular valve canal	[288, 313]
Brevican	Atrioventricular valve canal	[313]
Neurocan	Atrioventricular valve canal	[313]
Collagen 2α1	Mitral valve interstitial cells	[313]
Aggrecan	ROS17/2.8 osteosarcoma cells	[319]
BMP4	Kidney mesangial cells	[318]

CHAPTER II: RATIONALE, HYPOTHESIS & OBJECTIVES

Previously, we have reported that the transcription factor scleraxis has been found in fibroblasts and myofibroblasts; it drives fibroblast activation and ECM protein expression and serves as a critical effector of TGFβ1/Smad signalling [164, 288]. Mechanical stretch induces scleraxis expression; scleraxis-null cells failed to display stretch-mediated fibroblast-to-myofibroblast activation [300]. Scleraxis overexpression induces fibrosis-responsive genes Col-1α1, Col-1α2, Col-3α1, Col5α1, EDA-Fn, MMP-2, vimentin, α-SMA, and periostin in cardiac myofibroblasts. Simultaneously, the knockdown of scleraxis negatively impacts the profibrotic genes in cardiac myofibroblasts [288]. During pathological remodelling, scleraxis expression is elevated in the infarct scar tissue of rat myocardium [164]. In HCM patients, increased scleraxis serum concentration positively correlates with cardiac fibrosis [27]. The role of scleraxis in pathological remodelling is largely unknown; however, blocking scleraxis expression could limit myofibroblast conversion and profibrotic genes responsible for cardiac fibrosis. Therefore, we have decided to study the impact of scleraxis in pressure-overload-induced cardiac fibrosis.

Hypothesis

Conditional gene deletion of scleraxis will attenuate fibrosis and improve cardiac function in pressure-overloaded myocardium, and scleraxis transcriptionally regulates matrix proteins periostin and MMP-2.

Aim 1: Scleraxis regulates pressure overload-induced cardiac fibrosis

Objective: 1

To compare the expression levels of scleraxis in control and pressure-overloaded myocardium.

Objective: 2

To evaluate the impact of scleraxis gene deletion in the development of pressure-overload-mediated cardiac fibrosis.

Objective: 3

To study the effect of scleraxis gene deletion in pre-existing pressure-overload-mediated cardiac fibrosis.

Objective: 4

To understand the long-term effects of scleraxis gene deletion on cardiac fibrosis in a pre-existing pressure-overload condition.

Aim 2: Scleraxis transcriptionally regulates matrix proteins periostin and MMP2

Objective: 1

To examine the transcriptional regulatory role of scleraxis in periostin gene expression.

Objective: 2

To evaluate scleraxis-mediated transcriptional control of MMP2 expression in cardiac fibroblasts and myofibroblasts.

CHAPTER III: MATERIALS & METHODS

1. Methods for Role of scleraxis in pressure overload-induced cardiac fibrosis

1.1: Animal husbandry

Mice and rats used for the study were maintained on a 12:12 day:night cycle, provided standard chow and water *ad libitum*, and treated in accordance with the guidelines of the Canadian Council on Animal Care and the University of Manitoba Animal Care Committee.

1.2: Mouse models used in the study

For scleraxis conditional gene deletion studies, we crossed the established $Scx^{flox/flox}$ [284] and $TCF21^{iCre}$ ($Tcf21^{tm3.1(cre/Esr1*)\ Eno}$) mouse lines to obtain $Scx^{flox/flox}$;$TCF21^{iCre}$ mice [297]. For scleraxis reporter studies, Scx-GFP mice were employed as previously described [320]. Scleraxis knock-out experiments were carried out using cardiac fibroblasts isolated from germline knockout $Scx^{-/-}$ mice [284].

1.3: Pressure overload surgery and tamoxifen mediated gene deletion

Thoracic aorta constriction (TAC) surgery was employed to induce pressure overload as a well-established model of cardiac fibrosis [321]. Animals were anesthetized and intubated prior to opening the thoracic cavity. The aortic arch was constricted using 7-0 silk sutures with a 27-gauge guide, then the thoracic cavity was closed, and animals allowed to recover [322]. Sham-operated animals underwent surgery, but without suture placement around the aorta. Gene deletion was initiated by once-daily gavage of tamoxifen in corn oil (186 mg/kg) for five consecutive days to induce fibroblast-specific scleraxis knockout (Scx-fKO), with scleraxis-intact controls ($Scx^{+/+}$) maintained by provision of corn oil vehicle alone. Following tamoxifen administration, the efficacy of scleraxis gene deletion was assessed in isolated cardiac fibroblasts.

1.4: Echocardiography

Non-invasive two-dimensional transthoracic echocardiography (2-D TTE) was performed on awake mice to assess both systolic and diastolic cardiac function. For assessment of systolic function, cardiac images were acquired using the Vivid 7 ultrasound machine (GE Medical Systems) with a 13-MHz linear array ultrasound probe. Three different frames of parasternal short axis view images were collected under M-mode echocardiography and measured various systolic parameters such as fractional shortening (FS), left ventricular end-diastolic diameter (LVEDd), left ventricular end-systolic diameter (LVEDs), interventricular septal thickness (IVS) and left ventricular posterior wall thickness (LVPWd). Left ventricular ejection fraction (LVEF) was calculated using the modified biplane method and images acquired from the parasternal long axis view. For assessment of diastolic function, cardiac images were acquired using the Vevo 2100 ultrasound machine (VisualSonics) with a 18-38 MHz linear array ultrasound probe (MS400). Diastolic parameters including E, A and E/A ratio were determined using Doppler flow imaging in the parasternal long axis view. Post-acquisition analyses were performed offline using EchoPAC software (Vivid 7, version 11.2, GE Medical Systems) and the Vevo Lab software version 3.2.0 for systolic and diastolic parameters respectively. Both data collection and analyses were performed by two blinded observers (DYCC and DSJ).

1.5: Isolation and maintenance of cell cultures

Primary adult rat cardiac fibroblasts (RCFs) were isolated from male Sprague Dawley rat hearts (>225 g body weight) by enzymatic digestion as described previously [323]. Cells were grown in DMEM/F12 (1:1) medium supplemented with 10% fetal bovine serum, 1% penicillin-streptomycin and 100 μM ascorbic acid. Primary adult mouse cardiac fibroblasts (MCFs) were isolated from 8-week old wild type (WT) or scleraxis knockout (KO) mice using Liberase TH Research Grade (Roche, USA) as described [288, 323]. Cells were maintained in DMEM/F12 (1:1) medium supplemented with 10% fetal bovine serum and 1% penicillin-streptomycin. NIH3T3 fibroblasts (ATCC, USA) were cultured in DMEM containing 10% fetal bovine serum and 1% penicillin-streptomycin. Adult human cardiac myofibroblasts (Cell Applications, USA)

were cultured in DMEM/F12 (1:1) medium supplemented with 20% fetal bovine serum and 1% penicillin-streptomycin.

RCFs were used 6 h after isolation (zero passage, P0), or were passaged once at 48 h after initial plating (P1; activated fibroblasts) or a second time at 96-120 h after initial plating (P2; myofibroblasts) as performed previously [288, 317, 323]. For $TGF\beta_1$ treatment, P1 cells were plated on 35 mm cell culture dishes and maintained in 10% serum-containing medium for 16 h to reach 70% confluence, then serum starved for 6 h prior to treatment with $TGF\beta_1$ (10 ng/ml) or vehicle (PBS). After 24 h treatment, cells were harvested for processing. For adenoviral infection experiments, both RCFs and MCFs at P1 were grown to 70% confluence and infected with adenoviruses encoding either scleraxis (AdScx) or Green Fluorescent Protein (AdGFP) at a multiplicity of infection of 10 in serum free medium for 48 h. For luciferase assays, NIH3T3 fibroblasts were grown in 6 well plates to reach 60-70% confluence and maintained in low serum (0.5%) for 2 h prior to transfection. For chromatin immunoprecipitation assays, adult human cardiac myofibroblasts were grown in 150 mm dishes, and serum starved 6 h prior to treatment with $TGF\beta_1$ (10 ng/ml) or vehicle. Cells were fixed and harvested 24 h later.

1.6: Protein Extraction and Western Blotting

Murine ventricular tissues were flash-frozen and dissolved in protein extraction reagent type-4 (Sigma-Aldrich, USA) along with Halt protease and phosphatase inhibitor cocktail (ThermoFisher Scientific, Canada). For collagen immunoblots, 60 μg protein samples were resolved on 6% SDS-PAGE gels; for other immunoblots, 40 μg protein lysates were resolved on 10% SDS-PAGE gels. For assessment of secreted proteins, equal volumes of culture media were collected along with Halt protease and phosphatase inhibitor cocktail across different treatment or culture conditions as required. Proteins were concentrated from media samples using Amicon Ultra-15 centrifugal filters (Millipore Sigma, USA). Equal volumes of concentrated protein samples were resolved on 10% SDS-PAGE gels. For whole-cell lysates, primary cells were dissolved in RIPA cell lysis buffer (ThermoFisher Scientific, Canada) containing Halt protease and phosphatase inhibitor cocktail and transferred to 0.2 μm immune-Blot PVDF membranes

(Bio-Rad, Canada). The PVDF membranes were blocked in 3% BSA or 5% milk in TBST for 1 hour at room temperature. For primary antibody detection, blots were probed with 1% nonfat milk in TBST at 4^{o}C overnight, followed by washing and incubation with secondary antibody in TBST with 1% nonfat milk for 1 h at room temperature. Protein bands were visualized using Pierce ECL western blotting chemiluminescent substrate (ThermoFisher Scientific, Canada) and exposed to CL-XPosure film (Mandel Scientific, Canada). Protein quantification was conducted using Image J (NIH, USA), with normalization to Ponceau S staining of membranes or internal controls as required [324]. For whole-cell lysates, samples were normalized to horseradish peroxidase-conjugated β-actin (Santa Cruz Biotechnology Inc., USA). Scleraxis detection was performed as previously described [288].

1.7: Immunofluorescence imaging of cardiac myofibroblasts

Primary mouse cardiac P1 myofibroblasts (10,000 to 20,000 cells) from WT or KO mice were plated on glass coverslips; in addition, some cells were serum starved for 6 hours and infected with AdLacZ or AdScx for 48 hours as described above. Cells were fixed in 4% paraformaldehyde in PBS and permeabilized with 0.1% Triton X-100, then blocked with 10% donkey serum and probed with anti-MMP2 antibody (Novus Biosciences, USA). Secondary antibodies conjugated to Texas Red (Molecular Probes, USA) were used for visualization, with DAPI as a nuclear counterstain. Images were obtained on a Zeiss AxioImage M1 epifluorescence microscope using appropriate filters with a 20X objective.

1.8: Immunofluorescence staining of myocardial tissues

Paraffin-embedded murine cardiac tissue sections underwent deparaffinization followed by rehydration and antigen retrieval using citrate buffer at 90°C for 20 min. Sections were blocked using 10% donkey serum (ThermoFisher Scientific, Canada) for 1 h at room temperature. Slides were then incubated with 1:250 dilution of periostin antibody (Abcam) at 4°C overnight. Tissue sections were washed thrice for 5 mins with PBS and then incubated with secondary antibody Alexa Fluor 647-conjugated goat anti-rabbit (ThermoFisher Scientific, Canada) for 1 h at room temperature. Slides were

washed thrice for 5 mins with PBS and mounted with ProLong Diamond Antifade with DAPI (ThermoFisher Scientific, Canada). Tissue sections were imaged using a Nikon-NIS-Elements AR Ver5.20.00 microscope.

1.9: Histological analysis

Murine hearts were washed in ice cold PBS and fixed in 10% buffered formalin, then embedded into paraffin blocks. Paraffin-embedded tissues were sectioned at 0.5 μm thickness, then sections were stained either with Masson's Tri-Chrome or Picrosirius red for the detection of cardiac fibrosis.

1.10: Quantitative real-time PCR

Murine ventricular tissues were processed using TRIZOL reagent (ThermoFisher Scientific, Canada) for RNA isolation following manufacturer's instructions. Adult primary cardiac fibroblasts from rats or mice were harvested using RNA lysis buffer followed by RNA isolation using Monarch Total RNA Miniprep kit (NEB, USA) according to the manufacturer's instructions. cDNA was generated from 1 μg RNA samples using iScript cDNA Synthesis kit (Bio-Rad, USA). qPCR reactions were prepared using 5 μl SsoAdvanced Universal SYBR Green Supermix (Bio-Rad, USA) and 4 μl 1:6 diluted cDNA template along with 200 nM forward and reverse primers in a total volume of 10 μl per reaction. PCR amplification was performed in duplicate for each reaction on a CFX384 Touch Real-Time PCR (Bio-Rad, USA). The cycling conditions were 95°C (3 min), followed by 40 cycles of denaturation at 95°C (15 s) and extension at 62°C (30 s). After amplification, a continuous melt curve was generated from 60 to 95°C to confirm amplification of single amplicons. Relative gene expression was calculated using the $2^{-\Delta\Delta Ct}$ method with normalization to Gapdh (Table 3). Amplicon identity was confirmed by sequencing.

1.11: Plasmid DNA constructs and luciferase reporter assay for periostin promoter

NIH3T3 fibroblasts were co-transfected with pGL4.10-POSTN-L, pGL4.10-POSTN-S or mutants with either a scleraxis expression vector (pcDNA-Scx) or empty vector control (pcDNA; both vector backbones were pcDNA3.1, ThermoFisher

Scientific, Canada) using TransIT-2020 transfection reagent for 24 h (Mirus-Bio, USA) in low serum condition. A co-transfected Renilla luciferase vector (pRL) was used as an internal transfection control. According to the manufacturer, the Dual-Luciferase Reporter Assay System kit was used to measure the luciferase activity on a Glomax-Multi+ Multimode Plate Reader (Promega, USA) 's directions. Two different sequences of the human periostin gene proximal promoter (Long: -886 to +93 bp relative to the transcription start site; Short: -504 to +93 bp) were PCR amplified from the pEZX-PG02.1 vector (GeneCopoeia, USA) using primers (Table 4) incorporating Xho I and Hind III restriction sites, and sub-cloned into the pGL4.10-luc2 luciferase reporter vector (Promega, USA) to generate pGL4.10-POSTN-L and pGL4.10-POSTN-S, respectively. Two potential scleraxis-binding E-box sequences (CANNTG) in pGL4.10-POSTN-S were subjected to site-directed mutagenesis (QuikChange II XL; Agilent Technologies, USA) using specific primers (Table 6), and mutants were verified by sequencing.

1.12: Plasmid DNA constructs and Luciferase reporter assay for MMP-2 promoter

The human MMP2 gene promoter (-1659 to +57 bp) was PCR amplified from pGL2- MMP-2-luc (a kind gift from Dr. Etty Benveniste) using primers incorporating Bgl II and Hind III restriction sites, and sub-cloned into pGL4.10-luc2 (Table 5). Site-specific mutations were introduced individually or in combination into the six putative E-box sequences (CANNTG) of the 1.6 kb MMP2 promoter construct by site-directed mutagenesis (QuikChange II XL; Agilent Technologies, USA) (Table 7) and mutant clones verified by sequencing. An MMP2 promoter mutant truncated immediately upstream of E-box 6 was generated by PCR and cloned into pGL4.10-luc2, with or without site-directed mutation of the E-box. NIH3T3 fibroblasts were co-transfected with a luciferase reporter vector containing the human MMP2 gene promoter (pGL4-MMP2), and pECE (empty vector control) or pECE-HAFLAG- Scx (scleraxis expression vector) for 24 h along with a Renilla luciferase expression vector (pRL) as an internal transfection control. Alternatively, isolated cardiac P1 myofibroblasts from WT or scleraxis KO mice were transfected with the truncated E6 reporter vector (as above) for 24 h, then treated with TGFβ1 (10 ng/ml) or vehicle for a further 24 h prior to luciferase

assay. Luciferase activity was analyzed using the Dual Luciferase Reporter Assay System on a Glomax-Multi+ Multimode Plate Reader (Promega, USA).

1.13: Electrophoretic mobility shift assay for periostin promoter

HEK293 cells were used as a source of scleraxis-enriched or control nuclear extracts as previously described [165]. Oligonucleotides spanning the human periostin gene promoter region encompassing E-boxes E1 and E2, or identical oligonucleotides with the E-boxes mutated to attenuate scleraxis binding, were either labeled with biotin or used as unlabeled cold probes (Integrated DNA Technologies, USA) (Table 8). Probes were incubated with the scleraxis-enriched or control nuclear extracts to form DNA-protein complexes. In some samples, DNA-protein complexes were incubated with anti-scleraxis or control IgG antibodies. For cold competition samples, a 250-fold excess of unlabeled probes was used. The LightShift Chemiluminescent EMSA kit (ThermoFisher Scientific, Canada) was used for DNA-protein complex cross-linking and detection. Samples were separated on a 6% polyacrylamide gel, transferred to nitrocellulose membranes (Bio-Rad, USA) and detected using ECL on CL-Xposure blue X-ray film (Mandel Scientific, Canada).

1.14: Electrophoretic mobility shift assay for MMP-2 Promoter

Scleraxis-enriched nuclear extracts isolated from HEK293 cells were used for gel mobility shift assays as described previously [288]. Biotin-labeled oligonucleotides (bearing wild type or mutant E-boxes within the human MMP2 gene promoter) and non-labeled “cold” probes were synthesized (Table 8; Integrated DNA Technologies, USA) and incubated with the nuclear extracts. DNA-protein complexes were separated on a 6% polyacrylamide gel and transferred to nitrocellulose membranes (Bio-Rad, Canada). The DNA complexes were crosslinked using a LightShift Chemiluminescent EMSA Kit (Thermo Fisher Scientific, Canada), and complexes detected using ECL on CL-Xposure blue X-ray film (Thermo Fisher Scientific, Canada).

1.15: Chromatin immunoprecipitation assay for periostin promoter

Frozen murine heart tissues were processed using EZ-Magna ChIP HiSens Chromatin Immunoprecipitation Kit (Millipore Sigma, USA) and the experiment was carried out based on manufacturer's instructions. Adult human cardiac myofibroblasts were treated with TGFβ_1 or vehicle for 24 h in serum-free medium. Cells were cross-linked with 4% paraformaldehyde, then chromatin was sheared into 300-500 base pair fragments by sonication. After sonication, cell lysates were pre-cleared with 25 µl protein G-coupled magnetic beads (Cell Signaling Technology, USA) for 30 min at 4°C to reduce non-specific binding. 10% of total chromatin was collected as input control. Chromatin was incubated with either 10 µg anti-scleraxis antibody or pre-immune serum overnight. DNA-protein immune complexes were precipitated using protein G-coupled magnetic beads. The DNA-protein complexes were reverse cross-linked using 5 M NaCl. DNA fragments were precipitated and purified for qPCR analysis. Specific primers were used to amplify the region of the scleraxis-bound E-boxes (E1 and E2) in the proximal human periostin gene promoter (Supplemental Table 9).

1.16: Chromatin immunoprecipitation assay for MMP-2 Promoter

Adult human cardiac myofibroblasts were cross-linked with 4% paraformaldehyde and DNA fragmented by sonication. To reduce the non-specific background, cell lysates were precleared after sonication using 75 µl herring sperm DNA (200 µg/ml)/Magna ChIP Protein A+G Magnetic Beads mixture (EMD Millipore, Canada). Soluble chromatin was incubated with 10 µg anti-scleraxis antibody, or pre-immune serum as a negative control; for some experiments, an antibody to acetylated histone 3 lysine 9 (H3K9-Ac; Cell Signaling Technology, USA) or nonspecific IgG was used for immunoprecipitation. The DNA-protein immune complexes were precipitated using Magna ChIP protein A+G Magnetic Beads. Addition of 5 M NaCl reversed cross-links in the DNA-protein complexes. The DNA fragments were purified using GeneJET DNA Cleanup Kit (Thermo Fisher Scientific, Canada) followed by qPCR using specific primers for the scleraxis-binding E-box site (E6) in the human MMP2 gene promoter (Table 9). Genomic DNA was used as a positive (input) control.

1.17: Statistical analysis

Data are reported as mean ± standard deviation or mean ± standard error of a minimum of three independent biological replicates. For animal studies, each 'n' represents individual animals distributed blindly between groups for different treatments. To reduce variability, all cells including control and treatment groups were isolated and cultured on the same day. Results were analyzed by two-tailed Student's t-test or one-way analysis of variance with Student-Newman-Keuls post-hoc analysis or two-way analysis of variance with Tukey's post-hoc analysis as appropriate, with $P<0.05$ considered to be statistically significant.

Table 3. Primers used for quantitative real-time PCR

Forward (F) and reverse (R) primers are shown. Amplicon size is given in base pairs (bp).

Scx-F (rat/mouse)	5'- ACAGATCTGCACCTTCTG -3'	
Scx-R (rat/mouse)	5'- GCTCAGATCAGGTCCAA -3'	177 bp
Postn-F (rat)	5'- TCGTGGAACCAAAAATTAAAGTC -3'	
Postn-R (rat)	5'- CTTCGTCATTGCAGGTCCTT -3'	77 bp
Gapdh-F (rat)	5'- GCAAGTTCAACGGCACAG -3'	
Gapdh-R (rat)	5'- GCCAGTAGACTCCACGACAT -3'	140 bp
Postn-F (mouse)	5'- TGCTGCCCTGGCTATATGAG -3'	
Postn-R (mouse)	5'- GTAGTGGCTCCCACAATGCC -3'	101 bp
MMP-2-F (Rat/Mouse)	5'- CCCATGAAGCCTTGTTTACCA -3'	
MMP-2-R (Rat/Mouse)	5'- TGGAAGCGGAACGGAAACT -3'	70 bp
Col-1α1-F (mouse)	5'- GCTCCTCTTAGGGGCCACT -3'	
Col-1α1-R (mouse)	5'- CCACGTCTCACCATTGGG -3'	103 bp
Col-1α2-F (mouse)	5'- GTCCCCGAGGCAGAGAT -3'	
Col-1α2-R (mouse)	5'- CCTTTGTCAGAATACTGAGCAGC -3'	130bp

Col-3α1-F (mouse)	5’- GGTTTCTTCTCACCCTGCTTCA -3’	121 bp
Col-3α1-R (mouse)	5’- GGTTCTGGCTTCCAGACATC -3’	
EDA-Fn-F (rat/mouse)	5’ - ACTGCAGTGACCAACATTGACC - 3’	114 bp
EDA-Fn-R (rat/mouse)	5’ - CACCCTGTACCTGGAAACTTGC - 3’	
Gapdh-F (mouse)	5’- TCACCACCATGGAGAAGGC -3’	169 bp
Gapdh-R (mouse)	5’- GCTAAGCAGTTGGTGGTGCA -3’	

Table 4. Primers used for cloning the periostin promoter

Forward and reverse primers for the long (979 bp) and short (597 bp) promoter sequences are shown.

Long forward	5’- ATTCCTCGAGTGGAGTAGTAAGAACGCACA -3’
Long reverse	5’- TACCAAGCTTTCCCCGAAGAGAACTGGCAG -3’
Short forward	5’- ATTCCTCGAGTTGTACGATAGCAAGGAAAA -3’
Short reverse	5’- TACCAAGCTTTCCCCGAAGAGAACTGGCAG -3’

Table 5. Primers used for cloning the MMP-2 promoter

Forward and reverse primers for the human MMP-2 promoter sequences are shown.

Forward	5’- CGAGATCTAAACTGACTCTGGAAAGTCAGAG -3’
Reverse	5’- AGAAGCTTCCACCGCCTGAGGAAGTCTGGAT -3’

Table 6. Primers used for mutagenesis of E-boxes within the short periostin promoter

E-box sequences are in boldface; mutated nucleotides are underlined.

ΔE1-POSTN-F	5' - AGTGAGTCAATTGTT**C<u>CGCG</u>G**ATTAAAAATAAGTAC -3'
ΔE1-POSTN-R	5'- CTCTCTCAGGAAAGA**C<u>GCCC</u>G**AGAGATAAGCTGTGA -3'
ΔE2-POSTN-F	5'- AAACATGCAGTGAGT**C<u>CAGC</u>G**TTCATATGATTAAAA -3'

ΔE2-POSTN-R	5'- TTTTAATCATATGAA**C<u>GCTG</u>G**ACTCACTGCATGTTT -3'

Table 7. Primers used for mutagenesis of E-boxes within the MMP-2 promoter

E-box sequences are in boldface; mutated nucleotides are underlined.

ΔE1-MMP-2-F	5'- TCACAGCTTATCTCT **C<u>GGGC</u>G**TCTTTCCTGAGAGAG -3'
ΔE1-MMP-2-R	5'- CTCTCTCAGGAAAGA**C<u>GCCC</u>G**AGAGATAAGCTGTGA -3'
ΔE2-MMP-2-F	5'- AAACATGCAGTGAGT**C<u>CAGC</u>G**TTCATATGATTAAAA -3'
ΔE2-MMP-2-R	5'- TTTTAATCATATGAA**C<u>GCTG</u>G**ACTCACTGCATGTTT -3'
ΔE3-MMP-2-F	5'- AAGTTAAGGCTTACA**C<u>TGGC</u>G**CAGAAGGAAAGAGGT -3'
ΔE3-MMP-2-R	5'- ACCTCTTTCCTTCTG**C<u>GCCA</u>G**TGTAAGCCTTAACTT -3'
ΔE4-MMP-2-F	5'- ATCATTGTGGCTGAT**C<u>GTGC</u>G**TTTCTGACCATTCCT -3'
ΔE4-MMP-2-R	5'- AGGAATGGTCAGAAA**C<u>GCAC</u>G**ATCAGCCACAATGAT -3'
ΔE5-MMP-2-F	5'- AAGGGCCTAGAGCGA**C<u>TAAA</u>G**TTTCCCAGCAGGGGG -3'
ΔE5-MMP-2-R	5'- CCCCCTGCTGGGAAA**C<u>TTTA</u>G**TCGCTCTAGGCCCTT -3'
ΔE6-MMP-2-F	5'- AGATCGCGAGAGAGG**C<u>TTTA</u>G**GGGTGACGAGGTCGT -3'
ΔE6-MMP-2-R	5'- ACGACCTCGTCACCC**C<u>TAAA</u>G**CCTCTCTCGCGATCT -3'

Table 8. Oligonucleotide probes used for electrophoretic mobility shift assay

E-box sequences are in boldface; mutated nucleotides (ΔE) are underlined.

E1/2-POSTN-F	5'- CATGCAGTGAGT**CAATTG**TT**CATATG**ATTAAAAATAAG -3'
E1/2-POSTN-R	5'- CTTATTTTTAAT**CATATG**AA**CAATTG**ACTCACTGCATG -3'
ΔE1/2-POSTN-F	5'- CATGCAGTGAGT**C<u>CAGC</u>G**TTC**<u>CGCG</u>G**ATTAAAAATAAG -3'
ΔE1/2-POSTN-R	5'- CTTATTTTTAAT**C<u>CGCG</u>G**AA**C<u>GCTG</u>G**ACTCACTGCATG -3'
E5-MMP-2-F	5'- AAGGGCCTAGAGCGA**CAGATG**TTTCCCAGCAGGGGG -3'
E5-MMP-2-R	5'- CCCCCTGCTGGGAAA**CATCTG**TCGCTCTAGGCCCTT -3'

ΔE5-MMP-2-F	5'- AAGGGCCTAGAGCGA**C<u>TAAA</u>G**TTTCCCAGCAGGGGG -3'
ΔE5-MMP-2-R	5'- CCCCCTGCTGGGAAA**C<u>TTTA</u>G**TCGCTCTAGGCCCTT -3'
E6-MMP-2-F	5'- AGATCGCGAGAGAGG**CAAGTG**GGGTGACGAGGTCGT -3'
E6-MMP-2-R	5'- ACGACCTCGTCACCC**CACTTG**CCTCTCTCGCGATCT -3'
ΔE6-MMP-2-F	5'- AGATCGCGAGAGAGG**C<u>TTTA</u>G**GGGTGACGAGGTCGT -3'
ΔE6-MMP-2-R	5'- ACGACCTCGTCACCC**C<u>TAAA</u>G**CCTCTCTCGCGATCT -3'

Table 9. Primers used for qPCR following chromatin immunoprecipitation assay

Forward (F) and reverse (R) primers used for ChIP and product size is given in base pairs (bp).

POSTN-ChIP-F (human)	5'- AACATGCAGTGAGTCAATTGTT -3'	142 bp
POSTN-ChIP-R (human)	5'- AGGAAGCATCGGCAACTTCA -3'	
MMP-2-ChIP-F (human)	5'- CTGACCCCAGGGAGTGCAGGGTGT -3'	265 bp
MMP-2-ChIP-R (human)	5'- CTCGCCCTCCTCCACTTTTCTCCTC -3'	
POSTN-ChIP-F (mouse)	5'- GGCCCCAGTTTCATAGGACT -3'	114 bp
POSTN-ChIP-R (mouse)	5'- TCACAGGGGCATTTAACCCAA -3'	
Col-1α2-ChIP-F (mouse)	5'- TGGGGAAATTAGGGGGCAGG -3'	288 bp
Col-1α2-ChIP-R (mouse)	5'- GACACCTACGTGGGCTCTTTA -3'	

Table 10. Antibodies used for immunoblotting

Primary and secondary antibodies with specific dilutions used for western blotting and immunostaining.

Antibodies	Dilution/Use	Cat. No	Company
Collagen type I	1:1000 (WB)	CL50151AP-1	Cedarlane
Fibronectin	1:2000 (WB)	Ab2413	Abcam

Periostin	1:2000 (WB) 1:500 (IF)	Ab14041	Abcam
GAPDH	1:5000 (WB)	2118S	Cell Signaling
Scleraxis	1:1000 (WB)	-	QED Bioscience Inc
MMP2	1:2000 (WB) 1:500 (IF)	NB200-193	Novus Biosciences
β-actin	1:1000 (WB)	4967S	Cell Signaling
α-tubulin	1:10000 (WB)	12G10	Developmental Studies Hybridoma Bank
β-actin-HRP	1:65000 (WB)	SC-47778	Santa Cruz Biotechnology
Goat α-rabbit-HRP	1:10000 (WB)	111-035-003	Jackson Immuno Research
Goat α-mouse-HRP	1:10000	115-035-003	Jackson Immuno Research
α-rabbit HRP	1:5000	7074S	Cell Signaling

CHAPTER IV: RESULTS

1. Scleraxis regulates pressure overload-induced cardiac fibrosis

1.1: Pressure overload induces scleraxis expression in murine hearts

1.1.1: Study design

Scleraxis promoter-driven green fluorescent protein (GFP) transgene-expressing animals (WT GFP) underwent pressure overload via TAC or sham surgery for 4 weeks. The sham surgery cohort served as a control (Fig. 8).

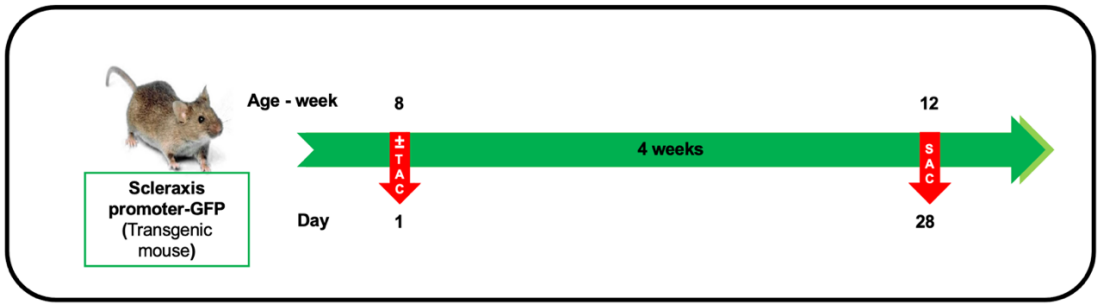

Figure 8: Experimental design for induction of pressure overload in scleraxis promoter harbouring GFP transgenic mice.
This study design includes a timeline for the induction of pressure overload (TAC) or sham surgery and its duration.

1.1.2: Pressure overload promotes cardiac hypertrophy in the murine myocardium

Transverse aortic constriction-induced pressure overload is a widely accepted model for promoting cardiac hypertrophy and myocardial fibrosis. In our present study, WT GFP animals who underwent TAC surgery displayed myocardial hypertrophy after 4 weeks, while the sham animals did not. Myocardial hypertrophy was quantified using the ratio of heart weight to body weight (HW/BW), heart weight to tibia length (HW/Tibia), or lung weight to body weight (LW/BW). Overall, we observed nearly a 40% enhancement in heart size due to pressure overload (Fig. 9).

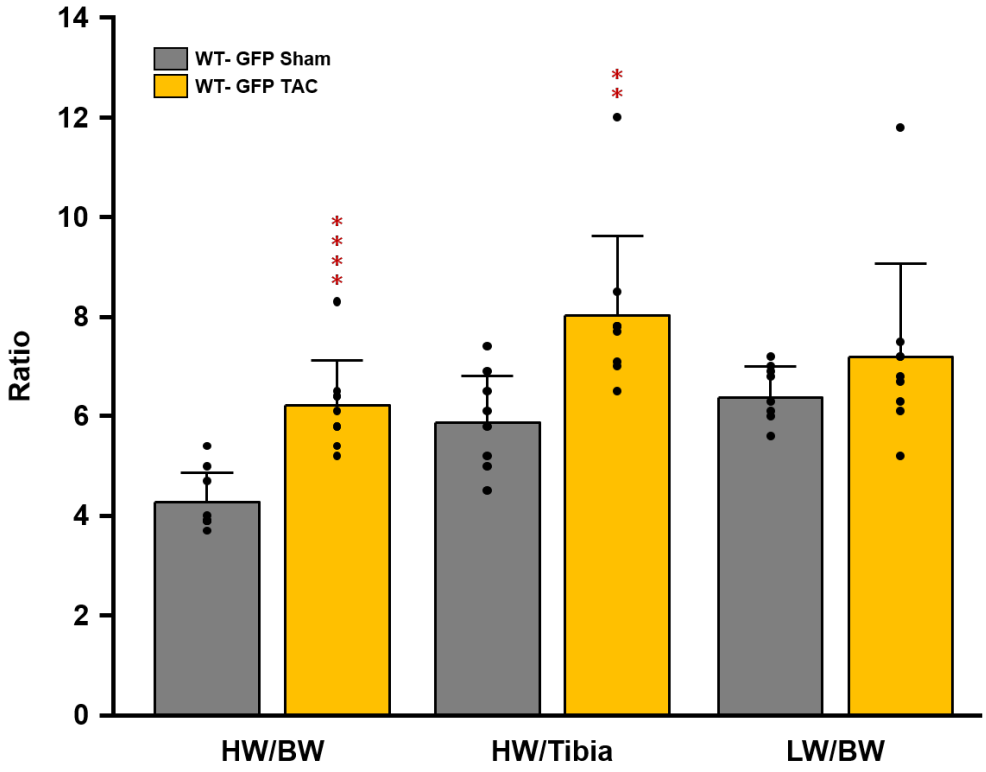

Figure 9: Pressure overload induces cardiac hypertrophy in scleraxis promoter-harbouring GFP transgenic mice after 4 weeks.

Following 4 weeks of TAC, HW/BW, and HW/Tibia were significantly enhanced in WT GFP animals compared to sham, but no differences were observed in LW/BW between WT GFP TAC and sham animals; n=9, two-tailed unpaired t-test, mean ± standard deviation; ****p<0.0001, **p<0.01 vs WT GFP sham.

1.1.3: Pressure overload elevates scleraxis and periostin expression in the murine myocardium

Our laboratory's previous studies showed that scleraxis expression was elevated in cyclically stretched cardiac proto-myofibroblasts and infarcted rat hearts [164, 300]. Scleraxis also serves as a cardiac fibrosis diagnostic marker in patients with HCM [27]. However, the expression of scleraxis in pressure-overload-induced cardiac fibrosis is unclear. In our current study, we report that in transgenic mice harbouring scleraxis promoter-driven GFP reporter, GFP protein expression is elevated nearly 8-fold and periostin protein expression is also elevated in pressure-overloaded myocardium as

compared to sham (Fig. 10). The scleraxis promoter is activated due to pressure overload, thereby increasing GFP expression, which is an indirect measure of scleraxis expression inside the pressure-overloaded myocardium. At the same time, periostin expression is elevated in TAC hearts compared to sham. Periostin expression directly translates to increased fibroblast-to-myofibroblast activation in pressure-overloaded myocardium [211]. Overall, a parallel pattern of expression of scleraxis and periostin was observed in the pressure-overloaded myocardium (Fig. 10).

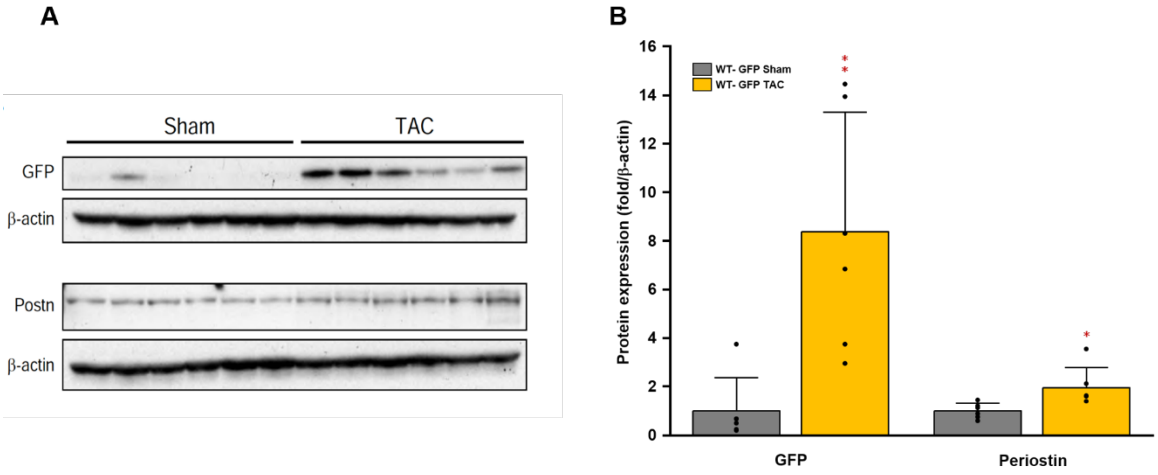

Figure 10: Pressure overload induces scleraxis and periostin expression in scleraxis-promoter harbouring GFP transgenic mice.

Pressure overload promotes scleraxis promoter-harbouring GFP protein expression and periostin expression after 4 weeks of TAC in comparison to sham animals (**A**), and quantification was performed using ImageJ (**B**); n=6, two-tailed unpaired t-test, mean ± standard deviation; **p<0.01, *p<0.05 vs WT GFP sham.

1.2: The impact of scleraxis gene deletion in pressure-overload-mediated cardiac fibrosis

1.2.1: Study design

Scleraxis-floxed ($Scx^{fl/fl}$) mice were crossbred with the Tcf21-iCre (fibroblast-specific Cre)-expressing line to generate $Scx^{fl/fl}$-Tcf21-iCre animals. At 8 weeks of age, scleraxis gene deletion was achieved via gavage of 186 mg/kg of tamoxifen once a day

for 5 days to Scx$^{fl/fl}$-Tcf21-iCre animals to achieve fibroblast-specific scleraxis knockout animals (Scx-fKO). Corn oil gavage served as a control (WT). One week after initial tamoxifen or corn oil gavage, pressure overload was surgically induced via TAC in both WT and Scx-fKO mice (n=10 per group), while sham-operated animals served as the control (n=10 per group). All the animals underwent echocardiographic assessment to measure cardiac function 1 day before TAC (Baseline) and 1 day before animal sacrifice (Endpoint). Eight weeks after TAC or sham surgery, animals were sacrificed and tissues were harvested for biochemical analysis (Fig. 11).

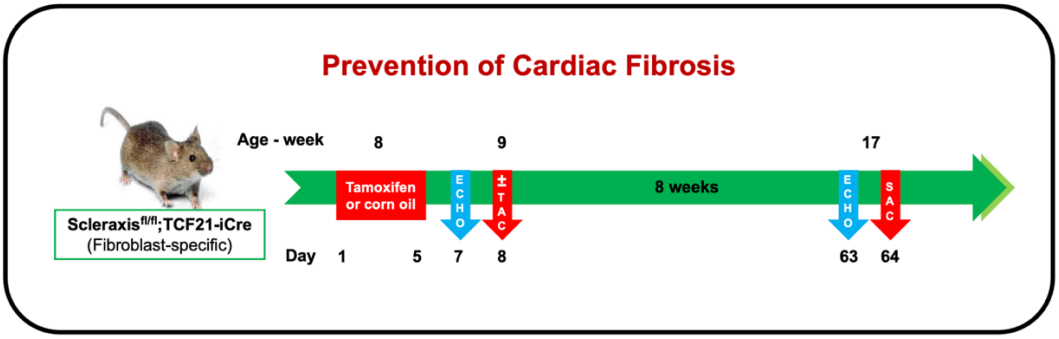

Figure 11: Experimental design for prevention of pressure-overload-mediated myocardial fibrosis.

Schematic representation of the study design includes scleraxis gene deletion using tamoxifen or corn oil, pressure overload via TAC or sham surgery, echocardiographic (ECHO) assessments, and study duration.

1.2.2: Scleraxis gene deletion has no effect on pressure-overload-mediated cardiac hypertrophy

Following 8 weeks of pressure overload, both WT TAC and Scx-fKO TAC animals developed myocardial hypertrophy; however, we noted no changes between WT TAC and Scx-fKO TAC animals compared to WT sham animals. For the hypertrophic measurements, we used either HW/BW or HW/Tibia or LW/BW (Fig. 12). Therefore, scleraxis gene deletion does not affect pressure-overload-induced cardiac hypertrophy.

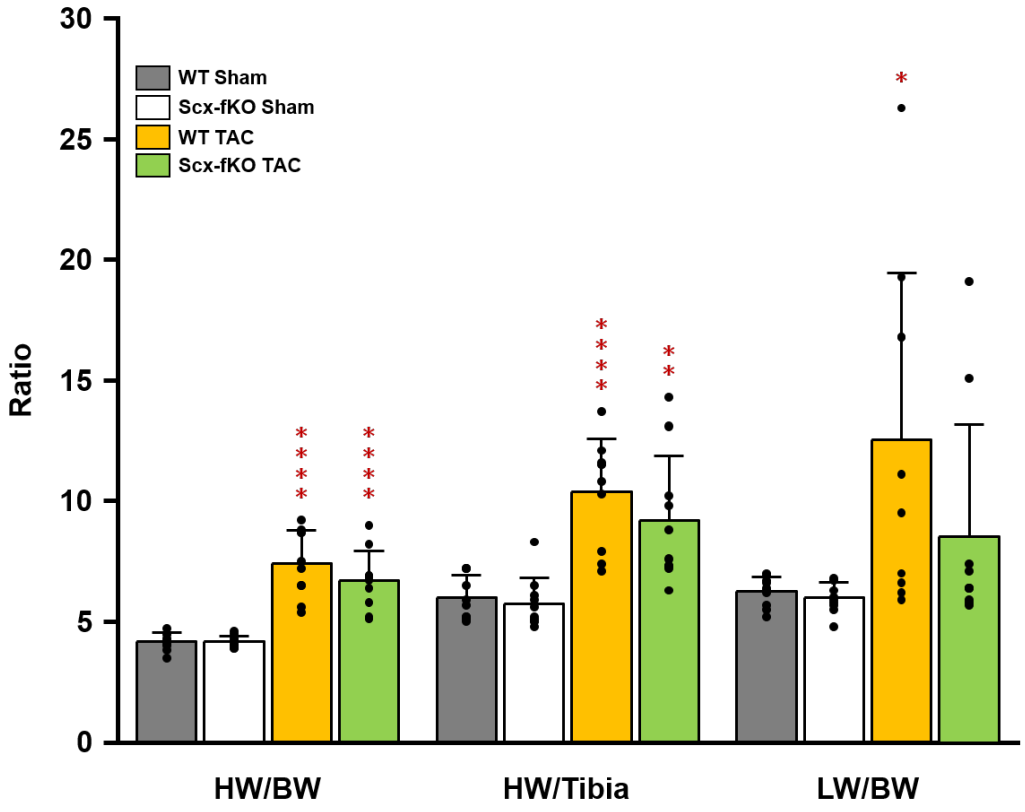

Figure 12: Scleraxis deletion does not alter cardiac hypertrophy after 8 weeks of pressure overload.

Pressure-overload-induced hypertrophy was similar between WT and Scx-fKO TAC animals after 8 weeks. Data represented as HW/BW, HW/Tibia, or LW/BW; n=10, two-way ANOVA, mean ± standard deviation; ****p<0.0001, **p<0.01, *p ≤ 0.05 vs WT sham.

1.2.3: Scleraxis gene deletion attenuates cardiac fibrosis in 8 weeks of pressure-overloaded myocardium

After 8 weeks of pressure overload, trichrome and Picrosirius red (PSR)-stained histopathological sections revealed increased fibrosis in WT TAC animals. In contrast, fibrosis was attenuated in Scx-fKO TAC animals (Fig. 13A)**.** The areas of fibrosis in these sections were quantified (Fig. 13B). These findings show that the absence of scleraxis expression during pressure overload limits myocardial fibrosis.

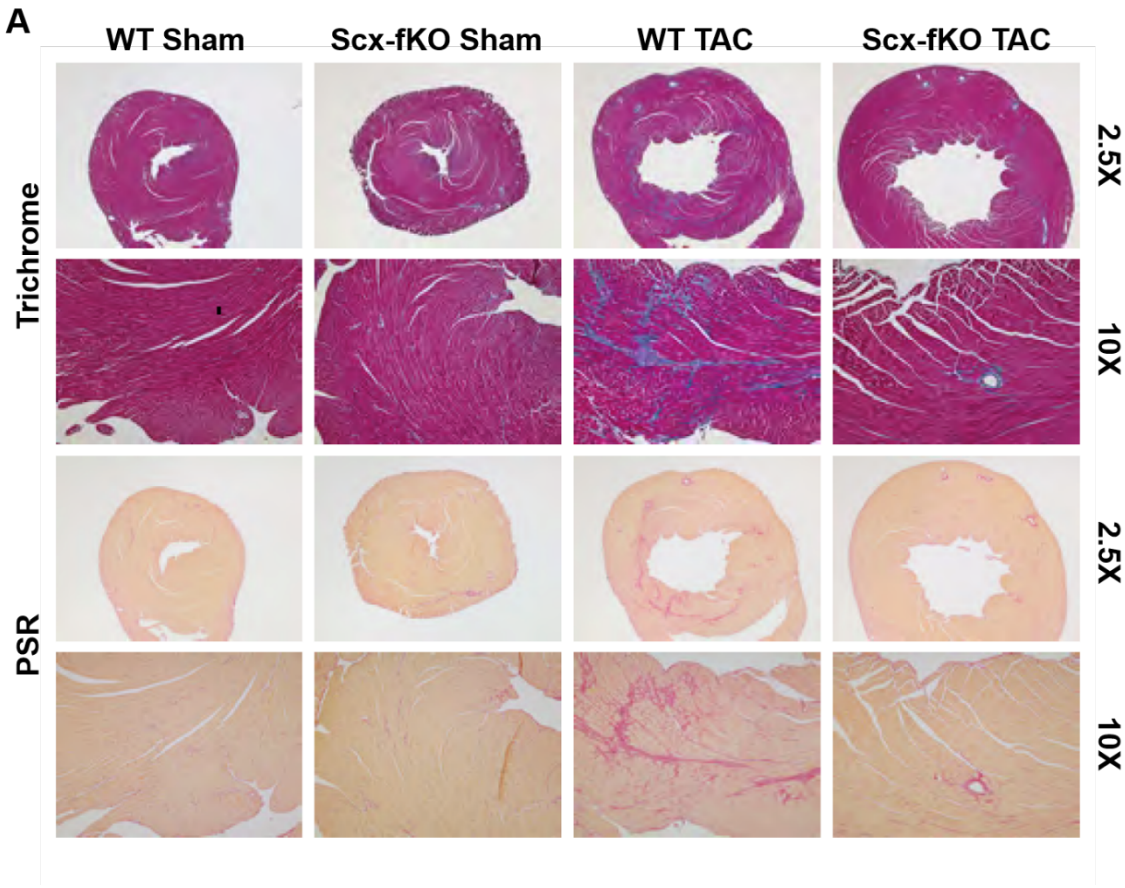
A
WT Sham
Scx-fKO Sham
WT TAC
Scx-fKO TAC
Trichrome
PSR
2.5X
10X
2.5X
10X

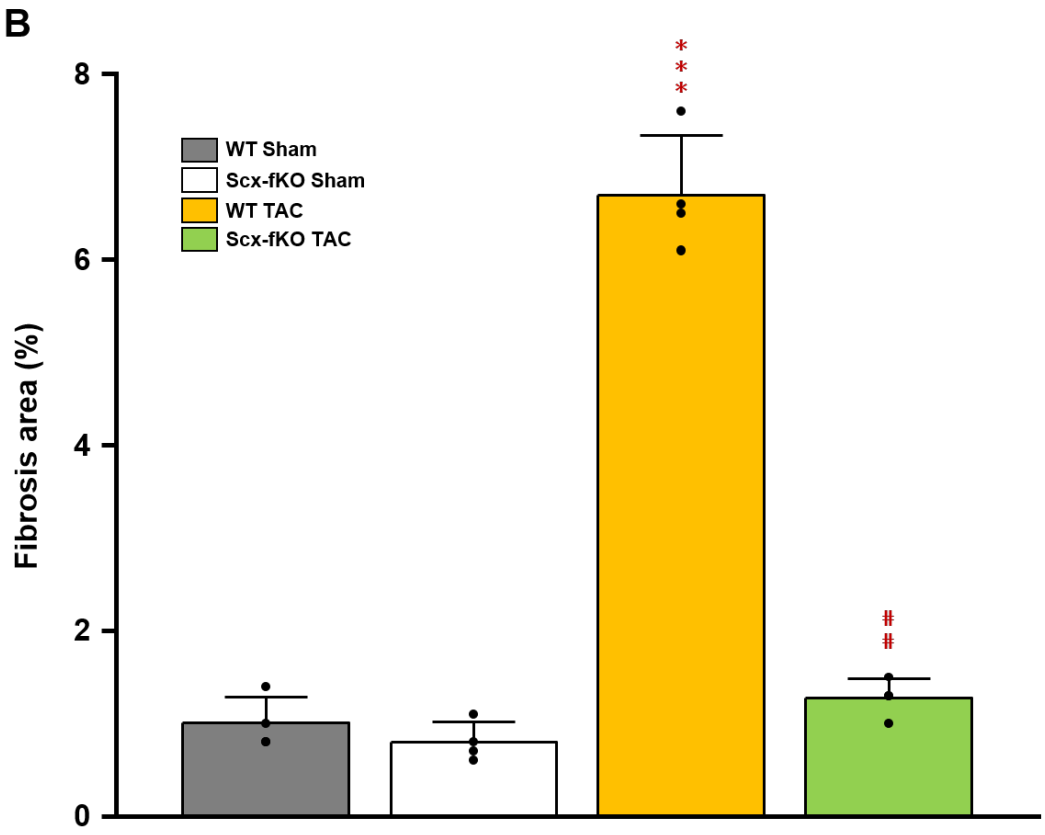

Figure 13: Histopathological staining and quantification of fibrosis area in the myocardium after 8 weeks of pressure overload.

Fibrosis is demonstrated by trichrome (blue) and PSR (red) in these myocardial sections. Trichrome and PSR staining revealed increased fibrosis in WT TAC compared to WT sham animals, but not in Scx-fKO TAC animals (**A**). Area of fibrosis quantification was performed in histopathological sections using ImageJ (**B**); n=4, two-way ANOVA, mean ± standard deviation; ***p<0.001 vs WT sham; ##p<0.01 vs WT TAC.

1.2.4: Scleraxis gene deletion reduces fibrosis-responsive gene expression in the myocardium after 8 weeks of pressure overload

Our laboratory's previous in vitro experiments showed that gain and loss of function of scleraxis in cardiac myofibroblasts potentially impacted major cardiac collagen isoforms Col-1α1, 1α2, 3α1, 5α1, and fibroblast/myofibroblast marker genes DDR2, EDA-Fn, vimentin, and periostin [288]. In the present study, mRNA expression of marker genes of cardiac fibrosis such as Col-1α1, 1α2, 3α1, and EDA-Fn were highly

elevated at the mRNA level after 8 weeks of pressure overload in WT TAC animals (Fig. 14). In contrast, Scx-fKO TAC animals displayed a dramatic reduction in these genes' expression, with levels similar to that of WT sham animals. Several previous studies reported that pressure-overloaded myocardium showed increased fibroblast-to-myofibroblast activation, which resulted in elevated collagen and periostin protein levels. In our current study, WT animals post-8 weeks of pressure overload displayed augmented collagen, EDA-Fn, and periostin protein expression compared to WT sham. Simultaneously, Scx-fKO hearts showed a reduction in collagen, periostin, and EDA-Fn protein expression in an existing pressure-overload condition (Fig. 15). Therefore, the reduction in fibrotic gene expression in Scx-fKO TAC myocardium leads to a significant reduction in myocardial fibrosis.

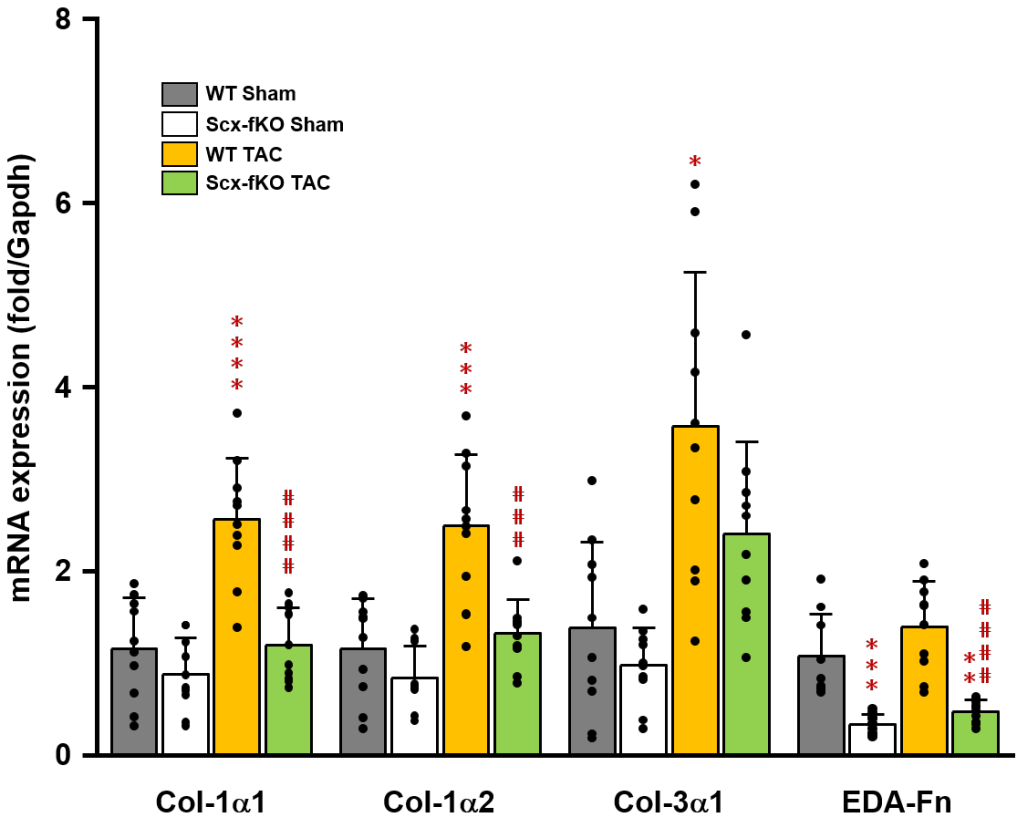

Figure 14: Scleraxis gene deletion reduces fibrotic gene mRNA expression following 8 weeks of pressure overload.

Scx-fKO TAC animals displayed a significant attenuation of major collagen isoforms and EDA-Fn expression at the mRNA level compared to WT TAC animals, with WT sham as a control; n=10, two-way ANOVA, mean ± standard deviation; ****p<0.0001, ***p<0.001, **p<0.01, *p<0.05 vs WT sham; ####p<0.0001, ###p<0.001 vs WT TAC.

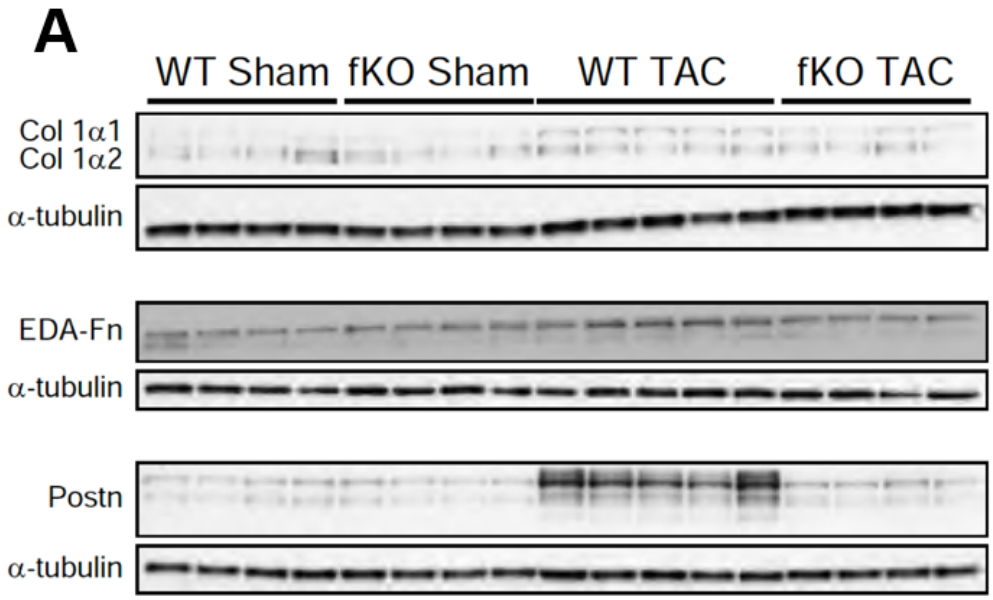

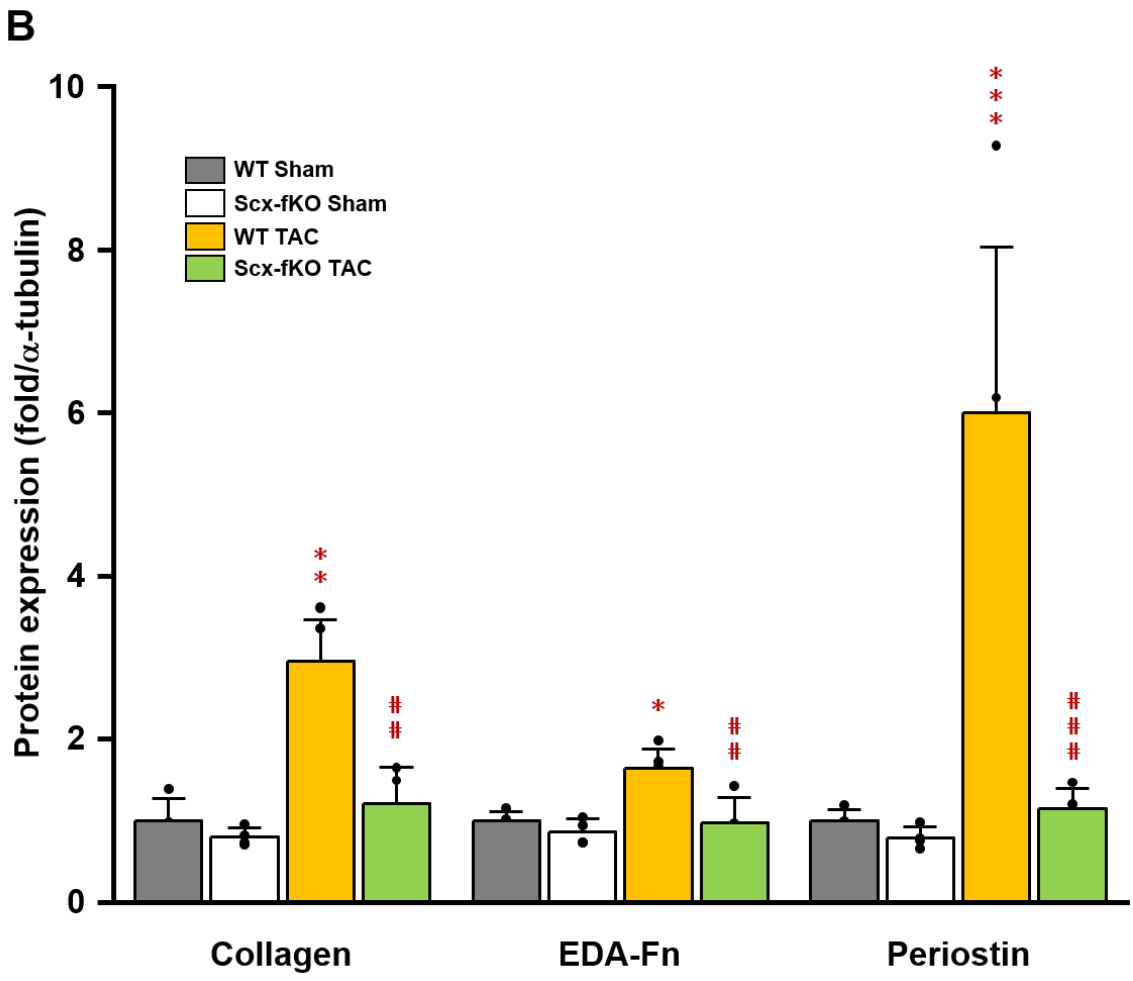

Figure 15: Scleraxis gene deletion attenuates fibrotic protein expression following 8 weeks of pressure overload.

Scx-fKO TAC animals displayed a significant attenuation of type I collagen, EDA-Fn, and periostin protein expression compared to WT TAC animals (**A**), and quantification was performed using ImageJ (**B**); n=4-5, two-way ANOVA, mean ± standard deviation; **p ≤ 0.01, *p ≤ 0.05 vs WT sham; ##p ≤ 0.01, ###p ≤ 0.001 vs WT TAC.

1.2.5: Scleraxis knockout limits periostin-positive cells inside pressure-overloaded myocardium

Periostin expression is elevated inside the myocardium after injury or stress. It also serves as a critical marker for myofibroblasts and is associated with cardiac fibrosis [83, 204, 325]. Immuno-labelled periostin-positive cell numbers were limited in Scx-fKO

TAC hearts, while WT TAC hearts displayed higher periostin-positive cell numbers than WT sham (Fig. 16A). The periostin-positive cells were also quantified (Fig. 16B). Thus in Scx-fKO TAC hearts, a reduced myofibroblast presence results in a reduction of myocardial fibrosis.

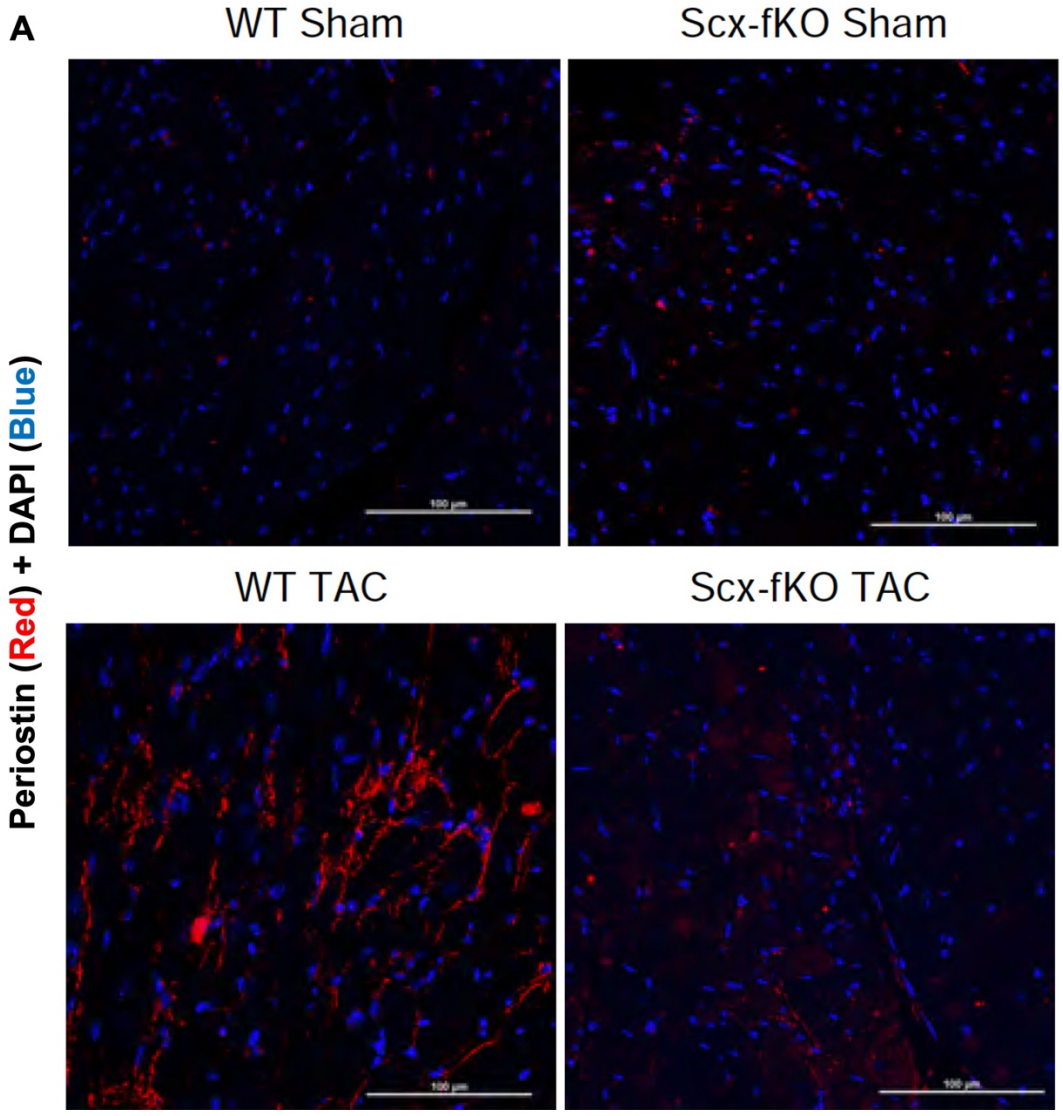

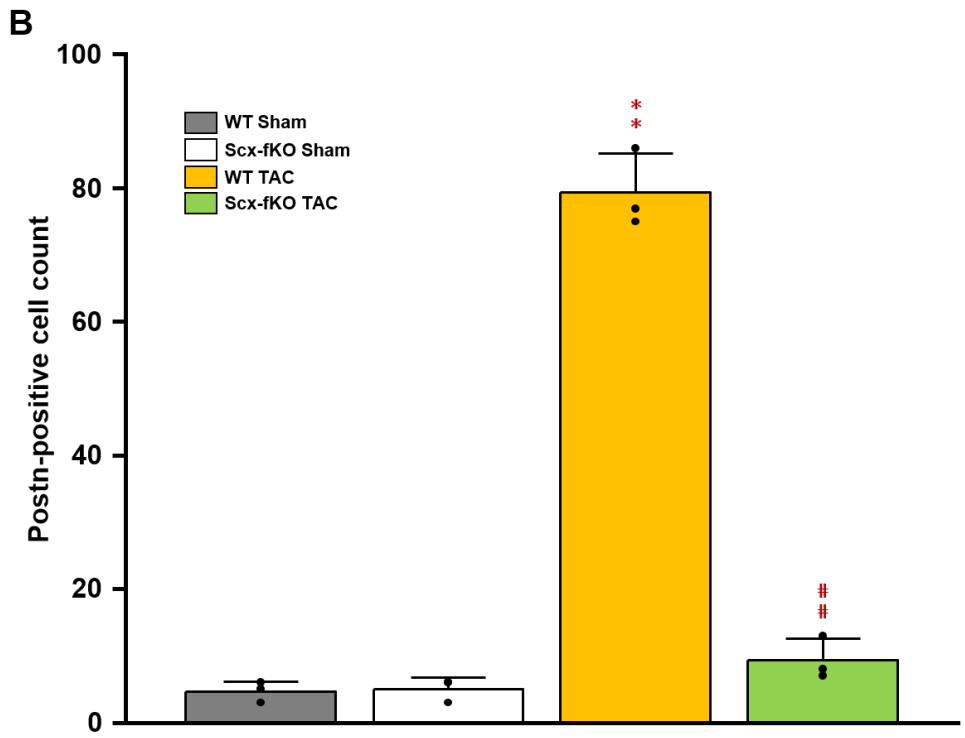

Figure 16: Immunostaining and quantification of periostin-positive cells in pressure-overloaded myocardium.

Histopathological sections were stained with periostin (red) and DAPI (blue) (**A**). Immunostained periostin-positive cells were quantified (**B**). Scleraxis gene deletion limits periostin-positive cells in pressure-overloaded myocardium, indicated by a lower myofibroblast population compared to WT TAC hearts, with WT sham as a control; n=3, two-way ANOVA, mean ± standard deviation; **p ≤ 0.01 vs WT sham; ##p ≤ 0.01 vs WT TAC.

1.2.6: Scleraxis is essential in regulating periostin and collagen 1α2 gene expression at the chromatin level

Previously, our laboratory reported that scleraxis and Smad3 synergistically regulate Col-1α2 gene expression [165]. Also, scleraxis plays a crucial role in recruiting Smad3 to the Col-1α2 promoter-bound transcription complex at the chromatin level. In scleraxis-null mouse hearts, Smad3 cannot participate in the assembly of transcription complex at the Col-1α2 promoter due to lack of scleraxis [288]. In the present study, 8

weeks of pressure overload elevated RNA Pol II-bound periostin promoter or Col-1α2 promoter in WT TAC hearts at the chromatin level. On the other hand, the Scx-fKO TAC hearts showed attenuation of periostin or Col-1α2 promoter recruitment to the RNA Pol II-bound transcription complex compared to WT sham. These results are demonstrated in a chromatin immunoprecipitation (ChIP) assay (Fig. 17). Therefore, scleraxis is critically important in regulating profibrotic genes such as periostin and Col-1α2 at the chromatin level in pressure-overloaded myocardium.

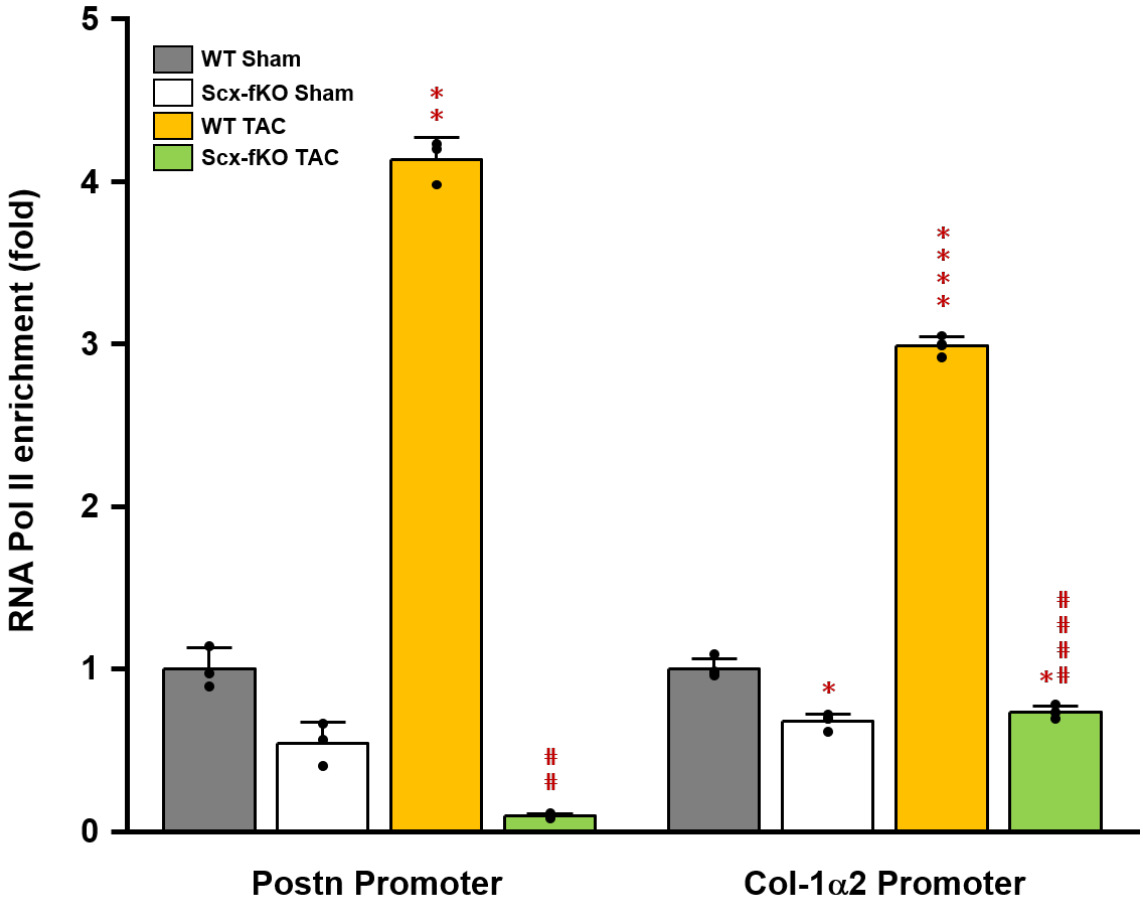

Figure 17: Scleraxis gene deletion attenuates RNA Pol II-bound fibrotic gene promoters at the chromatin level in pressure-overloaded myocardium.
Chromatin pulldown of RNA Pol II-bound periostin (Postn) promoter or Col-1a2 promoter was increased in WT TAC compared to WT sham, but reduced in Scx-fKO TAC, in a chromatin immunoprecipitation (ChIP) assay; n=3, two-way ANOVA, mean ±

standard deviation; ****p<0.0001, ***p<0.001, **p<0.01 vs WT sham; ####p<0.0001 vs WT TAC.

1.2.7: Scleraxis deletion improves systolic and diastolic function after 8 weeks of pressure overload

Other labs have reported that both systolic and diastolic function are affected by fibrosis in the pressure-overloaded myocardium [326, 327]. In our study, two-dimensional echocardiography revealed that WT TAC animals after 8 weeks of pressure overload had worsened systolic parameters such as LVEF and fractional shortening (FS) (Fig. 18), as well as diastolic parameters such as early (E) and late (A) ventricular filling (Fig. 19A), compared to WT sham animals. Scx-fKO TAC hearts showed improved systolic and diastolic function compared to WT TAC animals even in the presence of cardiac hypertrophy. In addition, the E/A ratio was unchanged in all cohorts (Fig. 19B). We believe that WT TAC animals undergo pseudo-normalization of the E/A ratio prior to heart failure.

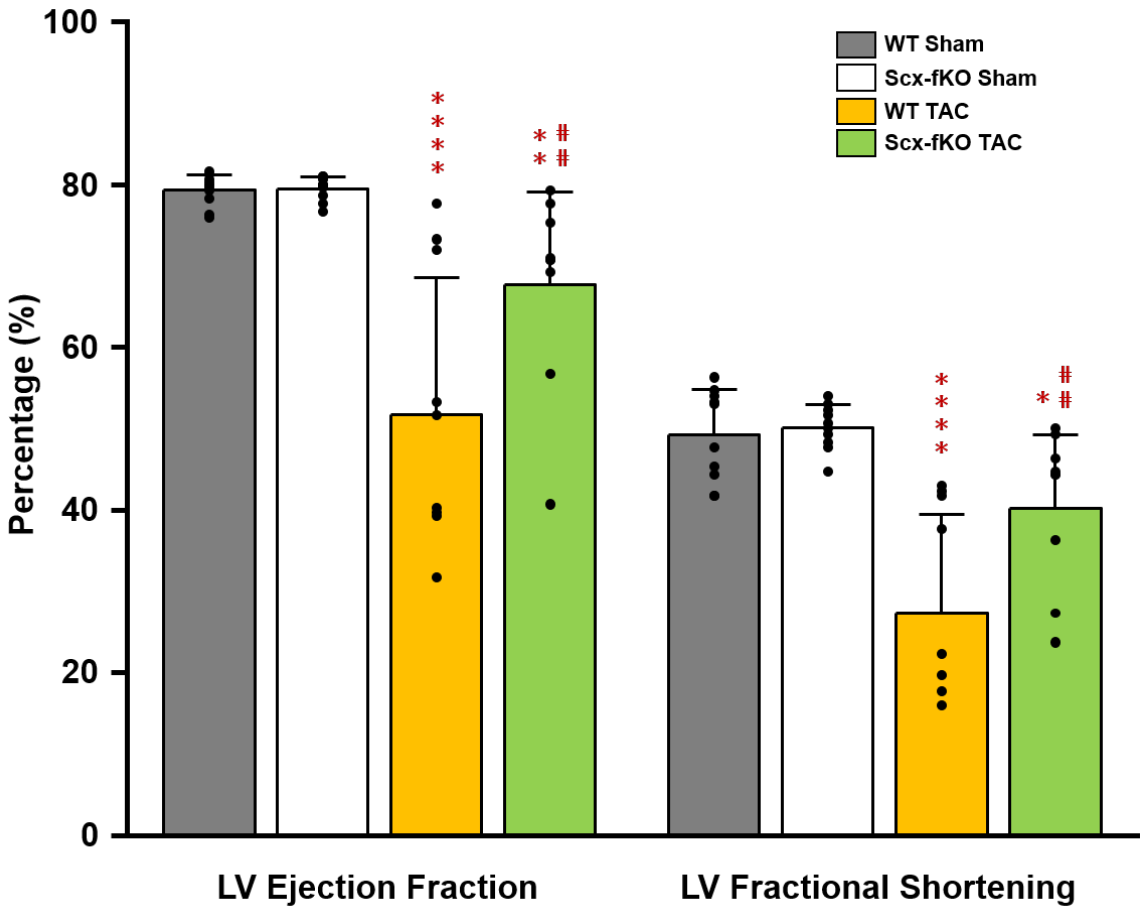

Figure 18: Scleraxis gene deletion improves systolic function in pressure-overloaded myocardium.

Echocardiography revealed improved systolic function (LV ejection fraction and fractional shortening) in Scx-fKO TAC compared to WT TAC after 8 weeks of pressure overload, with WT sham as a control; n=10, two-way ANOVA, mean ± standard deviation; ****p<0.0001, **p<0.01, *p<0.05 vs WT sham; ##p<0.01 vs WT TAC.

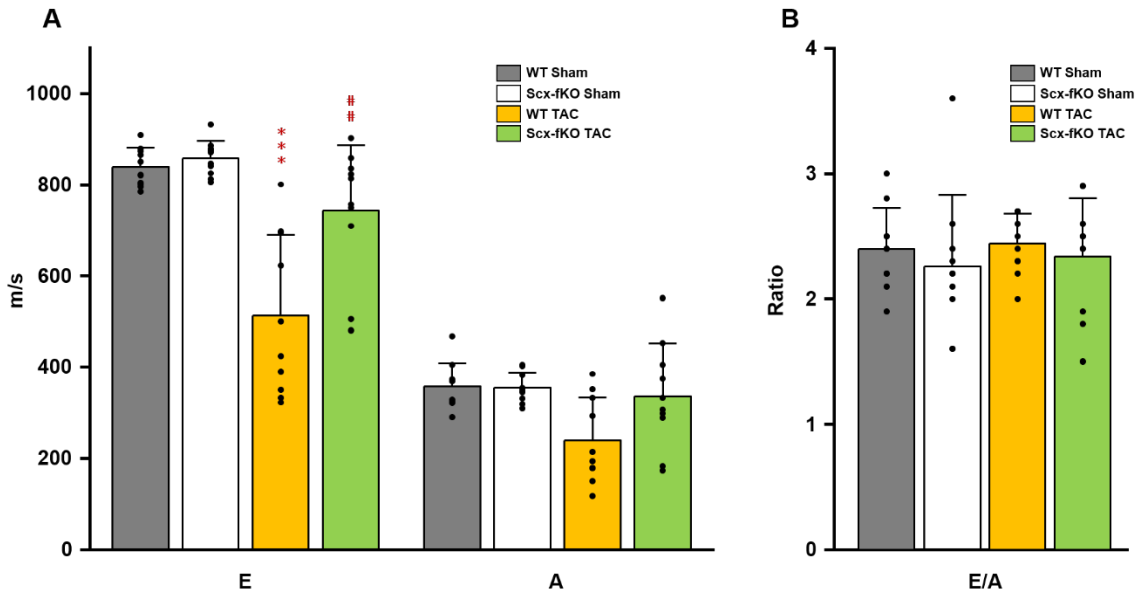

Figure 19: Scleraxis gene deletion improves diastolic function in pressure-overloaded myocardium.

Echocardiographic measures of early (E) and late (A) diastolic function were improved in Scx-fKO TAC compared to WT TAC, with WT sham as a control (**A**), but no differences were observed in E/A ratio in all cohorts after 8 weeks of pressure overload (**B**); n=10, two-way ANOVA, mean ± standard deviation; ***p<0.001 vs WT sham; ##p<0.01 vs WT TAC.

1.2.8: Scleraxis deletion preserves cardiac morphology after 8 weeks of pressure overload

In our present study, Scx-fKO TAC animals displayed a significant improvement in LV internal diameter during systole (LVIDs) after 8 weeks of pressure overload compared to WT TAC animals. Whereas LV internal diameter during diastole (LVIDd) showed no difference between Scx-fKO TAC and WT TAC animals (Fig. 20). Furthermore, after 8 weeks of pressure overload, Scx-fKO TAC animals displayed elevated LV posterior wall thickness during diastole (LVPWd) compared to WT TAC. However, no significant differences were noted in LV septal wall thickness during diastole (LVSd) between WT TAC and Scx-fKO TAC (Fig. 21). We believe that increased septal wall thickness could relieve myocardial stress from pressure overload in

Scx-fKO TAC animals. Corroborating these results, in Scx-fKO TAC animals there was a significant reduction in the myofibroblast population and profibrotic protein expression, which attenuated myocardial fibrosis and improved cardiac function.

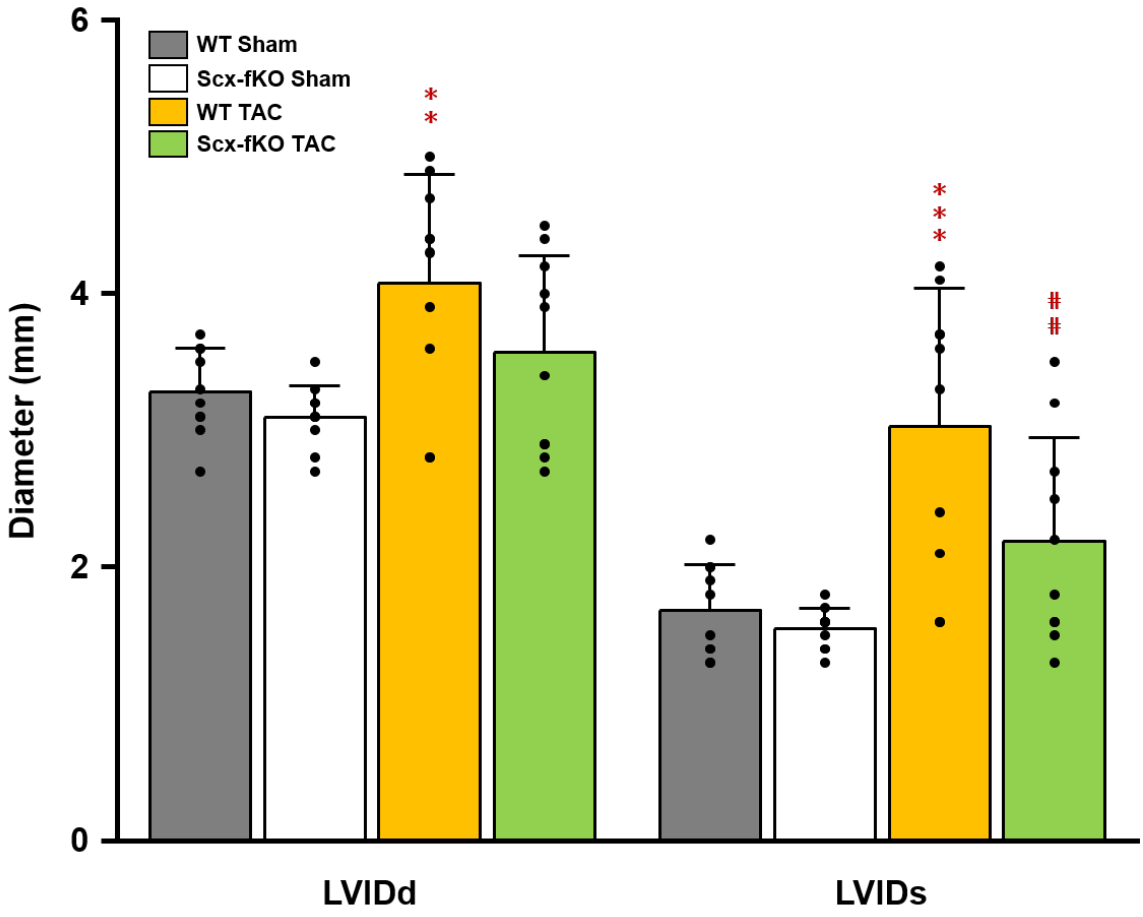

Figure 20: Scleraxis gene deletion improves cardiac dimensions in pressure-overloaded myocardium.

Cardiac dimension parameter LVIDs showed significant improvement in Scx-fKO TAC animals compared to WT TAC 8 weeks after pressure overload, with WT sham as a control. While LVIDd showed trend towards improvement in Scx-fKO TAC animals than WT TAC but not significantly different at this time point; n=10, two-way ANOVA, mean ± standard deviation; ***p<0.001, **p<0.01 vs WT sham; ##p<0.01, vs WT TAC.

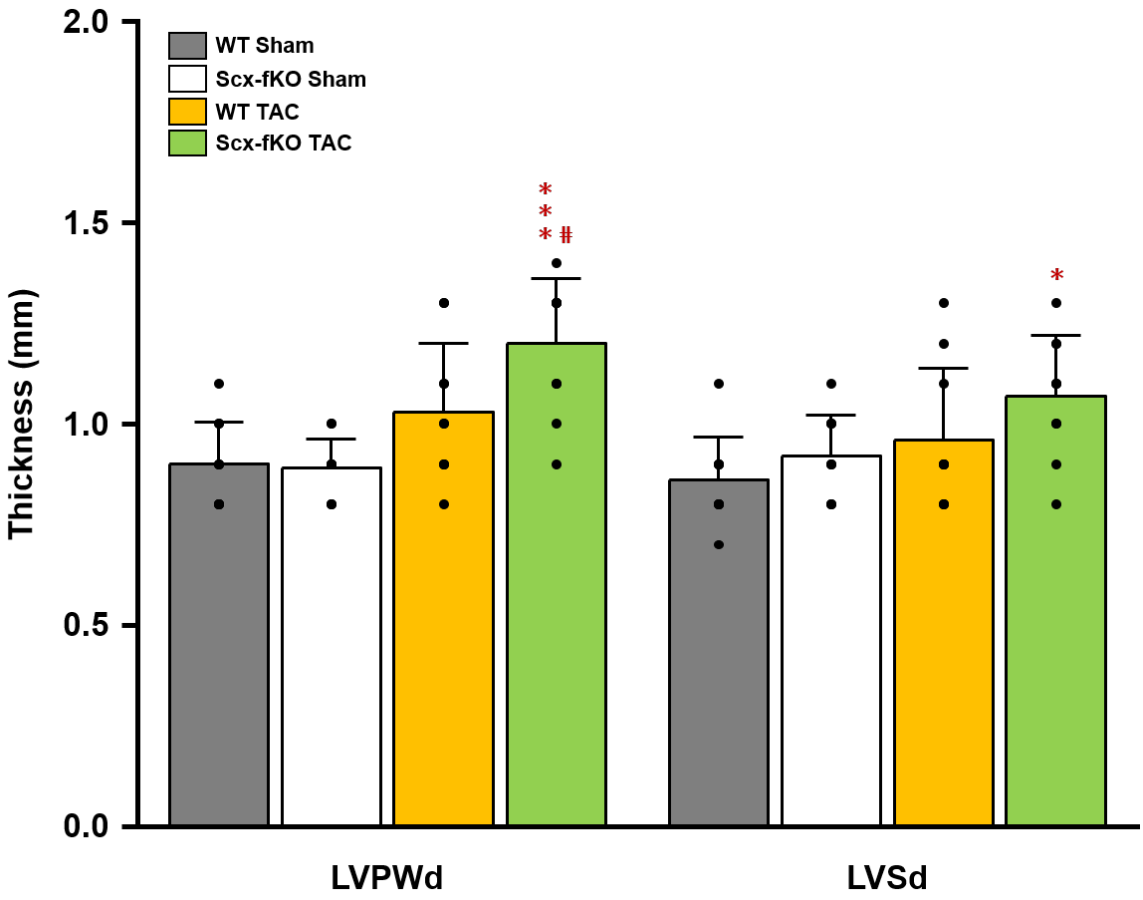

Figure 21: Scleraxis gene deletion increases myocardial wall thickness in pressure-overloaded myocardium.

Cardiac functional measurements obtained using echocardiography showed an increase in LVPWd of Scx-fKO TAC animals after 8 weeks of pressure overload compared to WT TAC animals, with WT sham controls. In the case of LVSd no difference was noted between Scx-fKO TAC, WT TAC, and WT sham; n=10, two-way ANOVA, mean ± standard deviation; ***p<0.001, *p<0.05 vs WT sham; #p<0.05 vs WT TAC.

1.3: Role of scleraxis in the reversal of pre-existing pressure-overload-induced cardiac fibrosis

1.3.1: Study design

Initially, scleraxis-floxed Tcf21-iCre animals underwent 4 weeks of either sham or TAC surgery at 8 weeks of age to develop cardiac fibrosis. After 4 weeks of sham or TAC surgery, animals were gavaged with either tamoxifen for scleraxis gene deletion

(Scx-fKO) or corn oil to leave the scleraxis gene intact (WT) once a day for 5 days. A total of 40 animals were used in this study, and each group consists of 10 animals. Cardiac function was assessed using echocardiography 1 day before TAC (Baseline), 1 day before scleraxis gene deletion (Midpoint) and 1 day before animal sacrifice (Endpoint). Animals were sacrificed after 8 weeks of sham or TAC surgery (Fig. 22).

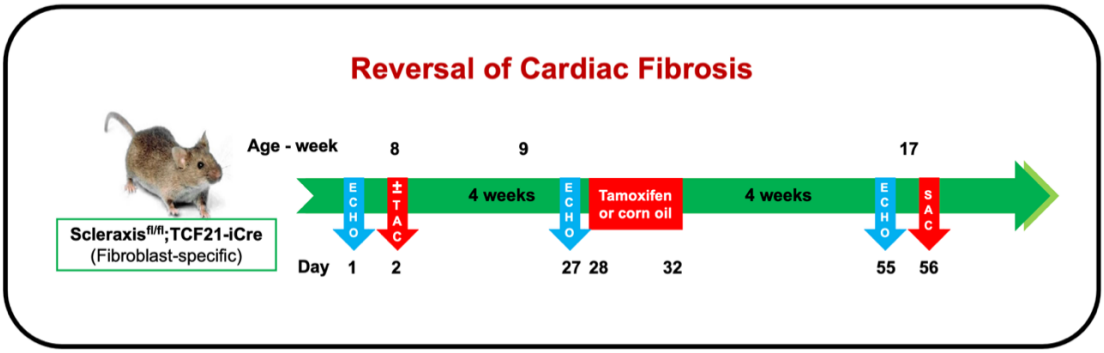

Figure 22: Experimental design for reversal of pressure-overload-induced cardiac fibrosis.

This schematic representation of the study design includes the intervention of sham or TAC surgery to develop cardiac fibrosis. Then, 4 weeks later, animals either underwent scleraxis gene deletion or were left intact for another 4 weeks, followed by cardiac functional measurement using echocardiography.

1.3.2: Scleraxis gene deletion does not reverse pre-established pressure-overload-mediated cardiac hypertrophy

Both WT and Scx-fKO TAC animals with pre-established pressure overload developed similar degrees of cardiac hypertrophy, with no significant differences observed in HW/BW, HW/Tibia, or LW/BW (Fig. 23). Scleraxis gene deletion in a pre-existing pressure-overload condition, therefore, does not interfere with cardiac hypertrophy.

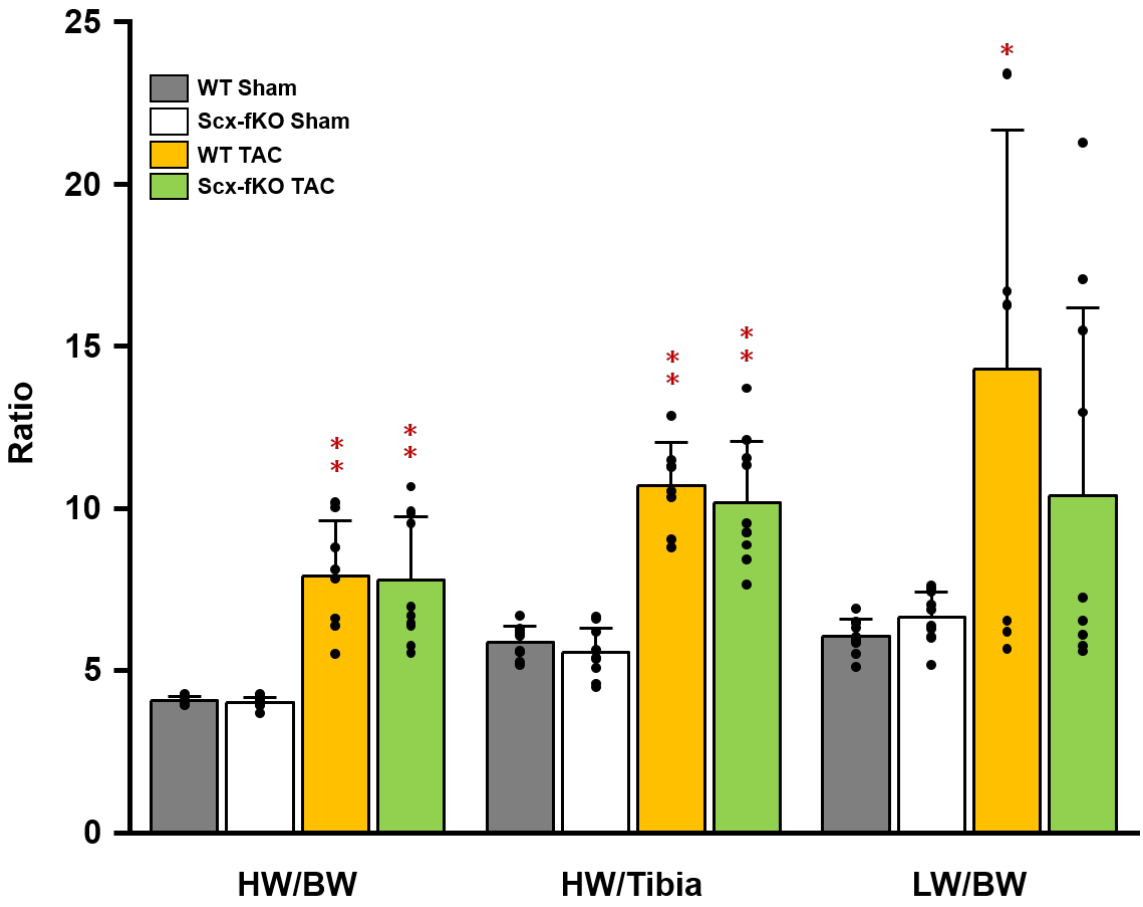

Figure 23: Scleraxis deletion does not interfere with cardiac hypertrophy in pre-established pressure overload.

After 8 weeks of pressure overload, there was no difference in the degree of cardiac hypertrophy between Scx-fKO TAC and WT TAC animals; WT sham served as control. Data represented HW/BW, HW/Tibia, and LW/BW; n=10, two-way ANOVA, mean ± standard deviation; **p<0.01, *p ≤ 0.05 vs WT sham.

3.3: Scleraxis gene deletion reduces myocardial fibrosis in pre-established pressure-overloaded myocardium

Histopathological sections of WT TAC hearts stained with trichrome or PSR showed a dramatic increase in fibrosis after 8 weeks of pressure overload, compared to WT sham hearts. On the other hand, Scx-fKO TAC hearts showed a drastic reduction in fibrosis compared to WT TAC animals even in the case of a pre-established fibrotic

condition (Fig. 24A). The fibrotic areas were quantified using ImageJ (Fig. 24B). Thus, scleraxis gene deletion can limit cardiac fibrosis even after 4 weeks of pre-established pressure overload.

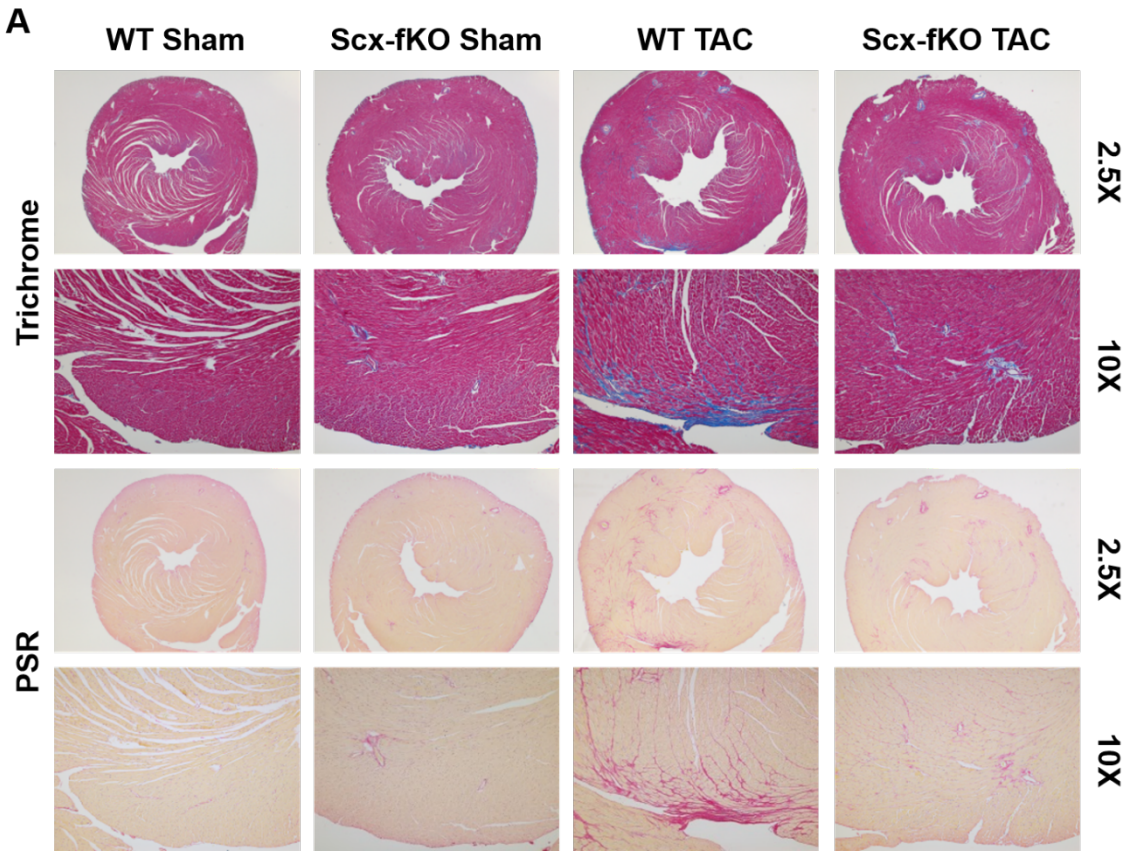

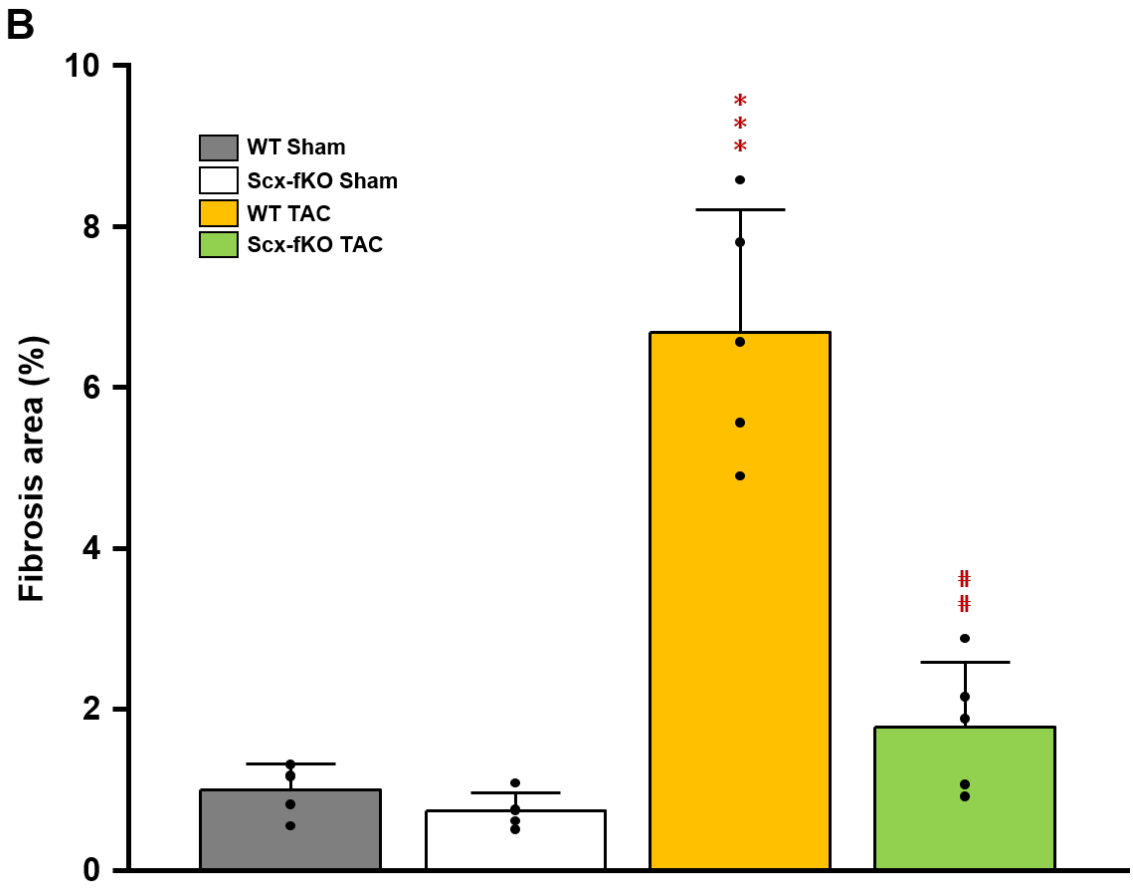

Figure 24: Histopathological staining and quantification of pre-established pressure-overloaded hearts.

Cardiac tissue sections were stained for fibrosis using trichrome (blue) and PSR (red). After 8 weeks of pressure overload, staining revealed enhanced fibrosis inside WT TAC myocardium compared to WT sham, whereas scleraxis gene deletion attenuated fibrosis (**A**). Quantification of fibrosis area in trichrome- or PSR-stained histopathological sections was performed using ImageJ (**B**); n=5, two-way ANOVA, mean ± standard deviation; ***p<0.001 vs WT sham; ##p<0.01 vs WT TAC.

1.3.4: Scleraxis gene deletion attenuates cardiac fibrosis responsive protein expression in pre-established pressure-overloaded myocardium

Western blots revealed that the expression pattern of fibrotic-responsive genes, such as collagen, EDA-Fn, and periostin, was elevated in WT TAC hearts after 8 weeks of pressure overload, but reduced in Scx-fKO TAC hearts even in a pre-existing pressure-

overload condition (Fig. 25). Therefore, removal of the scleraxis gene is sufficient to attenuate matrix proteins responsible for cardiac fibrosis, even in conditions of pre-existing pressure overload.

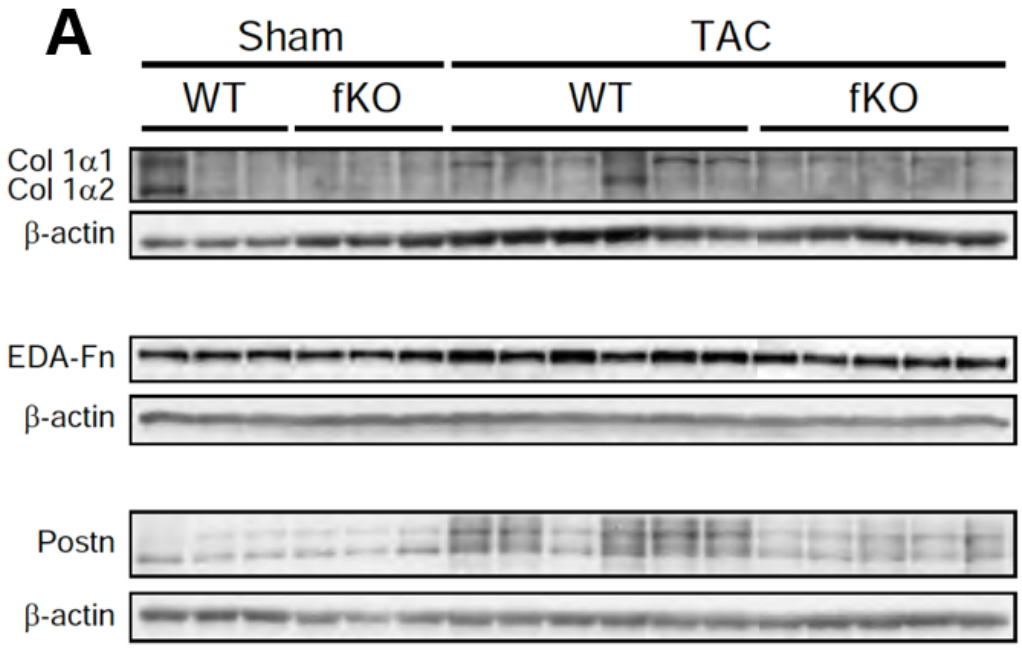

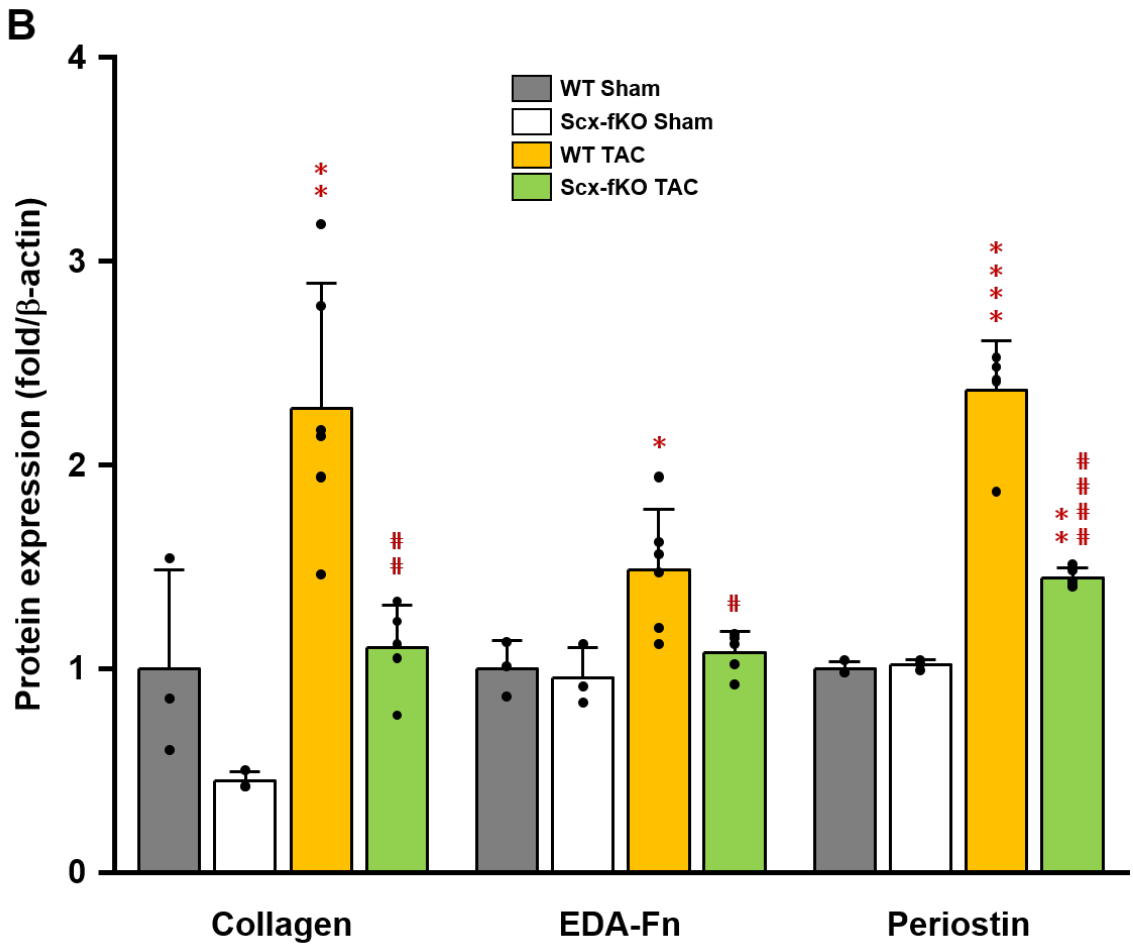

Figure 25: Scleraxis deletion down-regulates fibrotic protein expression in pre-established pressure-overloaded myocardium.

In pre-established pressure-overloaded hearts, scleraxis gene deletion drastically reduces cardiac fibro-responsive genes such as type I collagen, EDA-Fn, and periostin protein expression compared to WT TAC; WT sham served as a control (**A**), and quantification was performed using ImageJ (**B**); n=3-6, two-way ANOVA, mean ± standard deviation; **p≤ 0.01, *p ≤ 0.05 vs WT sham; ####p ≤ 0.0001, ##p ≤ 0.01, #p ≤ 0.05 vs WT TAC.

1.3.5: Scleraxis gene deletion limits periostin-positive cells in pre-established pressure-overloaded myocardium

Periostin is a marker protein for cardiac myofibroblasts [83, 204]. Histopathological sections of pre-established pressure-overloaded hearts were stained for periostin. WT TAC hearts showed a dramatic increase in periostin-positive cell numbers,

whereas scleraxis gene deletion reduced the number of periostin-positive cells (Fig. 26A). Periostin-positive cells numbers were quantified (Fig. 26B). Thus, myofibroblast populations are reduced due to scleraxis gene deletion in pre-established pressure-overloaded myocardium.

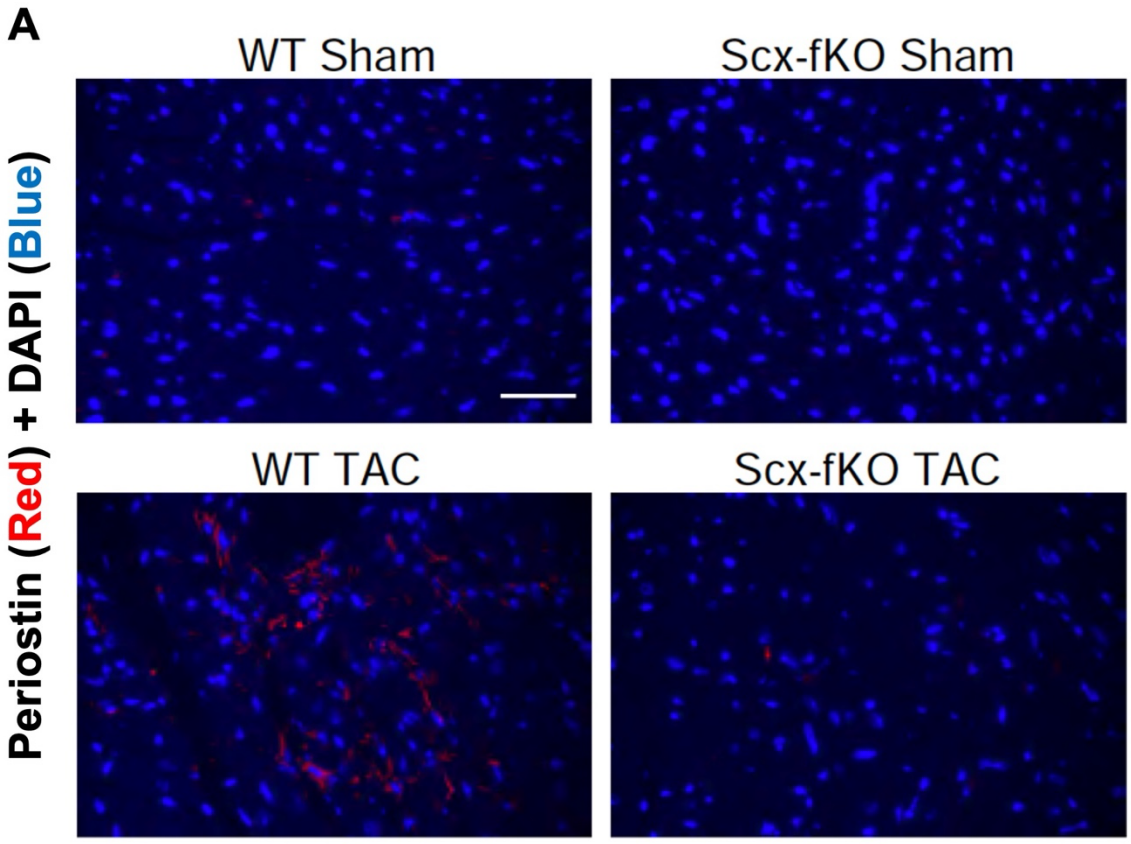

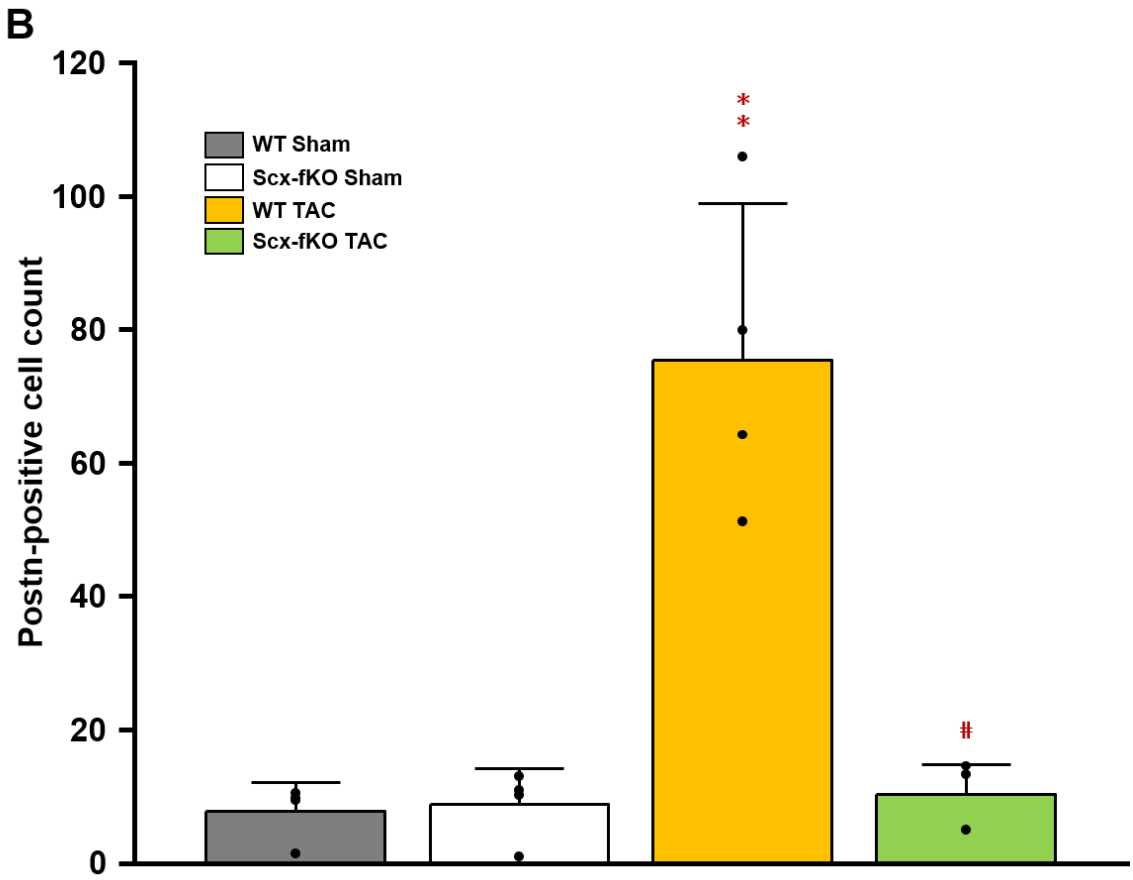

Figure 26: Immuno-labelling and quantification of periostin-positive cells in pre-established pressure-overloaded myocardium.

Pre-established pressure-overloaded hearts were stained with periostin (red) and DAPI (blue) **(A)**. Scx-fKO TAC hearts showed a significant reduction in periostin-positive cells compared to WT TAC; WT sham served as a control **(B)**; n=4, two-way ANOVA, mean ± standard deviation; **p ≤ 0.01 vs WT sham; #p ≤ 0.05 vs WT TAC.

1.3.6: Scleraxis gene deletion enhances cardiac function in pre-established pressure-overloaded myocardium.

Echocardiographic measurements 4 weeks after pressure overload or sham surgery (Midpoint), but prior to scleraxis deletion, showed that systolic functional parameters LVEF and FS deteriorated in pressure-overloaded animals. After scleraxis deletion and 4 more weeks of pressure overload (Endpoint), WT TAC animals showed a further decline in LVEF and FS, whereas scleraxis-deleted TAC hearts showed preserved

systolic function (Fig. 27A, B). Similarly, both diastolic parameters E and A had declined in TAC compared to WT sham animals at the Midpoint. WT TAC animals displayed a further drop in diastolic function from Midpoint to Endpoint, but notably, Scx-fKO TAC animals displayed functional rescue in both E and A at the Endpoint. At this time, only early filling E showed a significant difference compared to WT TAC; but late filing showed a trend toward rescue in function (Fig. 28A, B).

Additionally, there were no significant differences in E/A between WT TAC and Scx-fKO TAC animals at both the Midpoint and Endpoint. These values suggested that WT TAC animals underwent pseudo-normalization of the E/A ratio (Fig. 28C). These combined results strongly indicate that scleraxis gene deletion helps to preserve both systolic and diastolic function in pre-established pressure-overload-induced fibrosis.

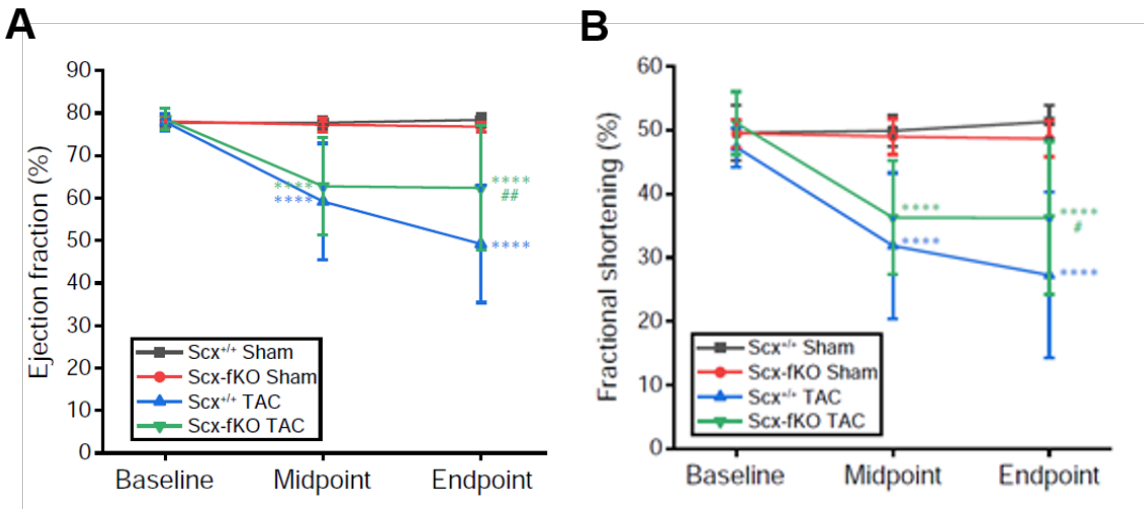

Figure 27: Scleraxis deletion preserves systolic function in pre-existing pressure-overloaded animals.

Echocardiographic functional measurements showed that systolic parameters LV ejection fraction (**A**) and fractional shortening (**B**) were preserved from the Midpoint (time of Scx deletion) to the Endpoint in Scx-fKO TAC, while WT TAC continued to decline; WT sham animals served as a control; n=8-11, two-way ANOVA, mean ± standard deviation; ****$p \leq 0.0001$ vs WT sham; ##$p \leq 0.01$, #$p \leq 0.05$ vs WT TAC.

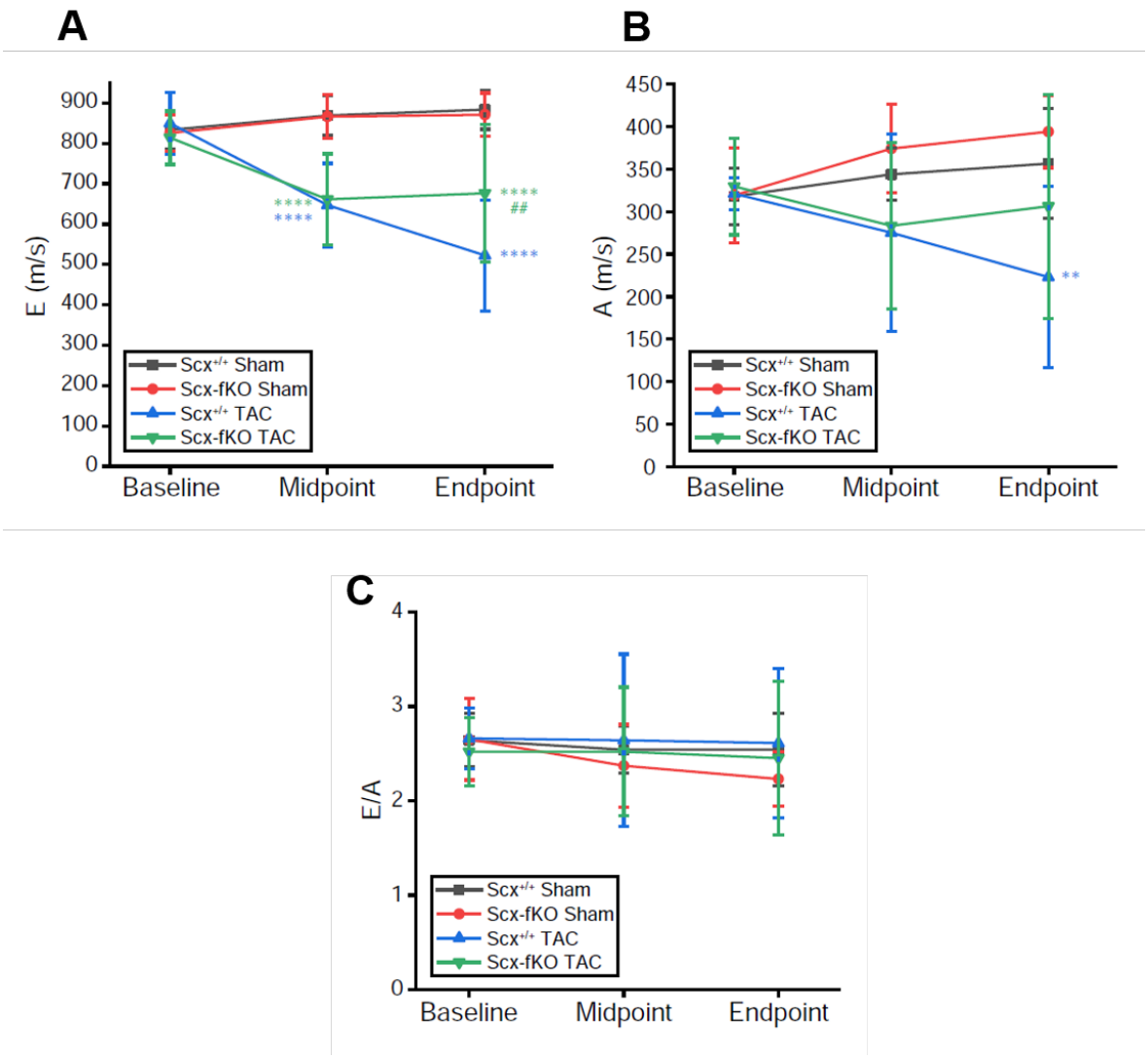

Figure 28: Scleraxis deletion rescues diastolic function in pre-existing pressure-overloaded animals.

Diastolic parameters E (**A**) and A (**B**) showed improvement from the Midpoint (time of scleraxis gene deletion) to the Endpoint in Scx-fKO TAC, while in WT TAC they continued to decline; WT sham animals served as a control. No significant differences were noted in the E/A ratio between all groups (**C**); n=8-11, two-way ANOVA, mean ± standard deviation; ****p ≤ 0.0001, **p ≤ 0.01 vs WT sham; ##p ≤ 0.01 vs WT TAC.

1.3.7: Scleraxis gene deletion does not affect cardiac morphological parameters in pre-established pressure-overloaded myocardium

Cardiac structural parameters LVIDd and LVIDs showed a trend toward improvement in Scx-fKO TAC animals at the Endpoint; however, this improvement was not significant compared to WT TAC animals (Fig. 29A, B). Similarly, cardiac thickness parameters LVPWd and LVSd showed no difference between WT TAC and Scx-fKO TAC animals at the Endpoint (Fig. 30A, B). Overall, these results suggest that in a pre-established pressure-overload condition, scleraxis gene deletion only marginally improves cardiac morphological parameters.

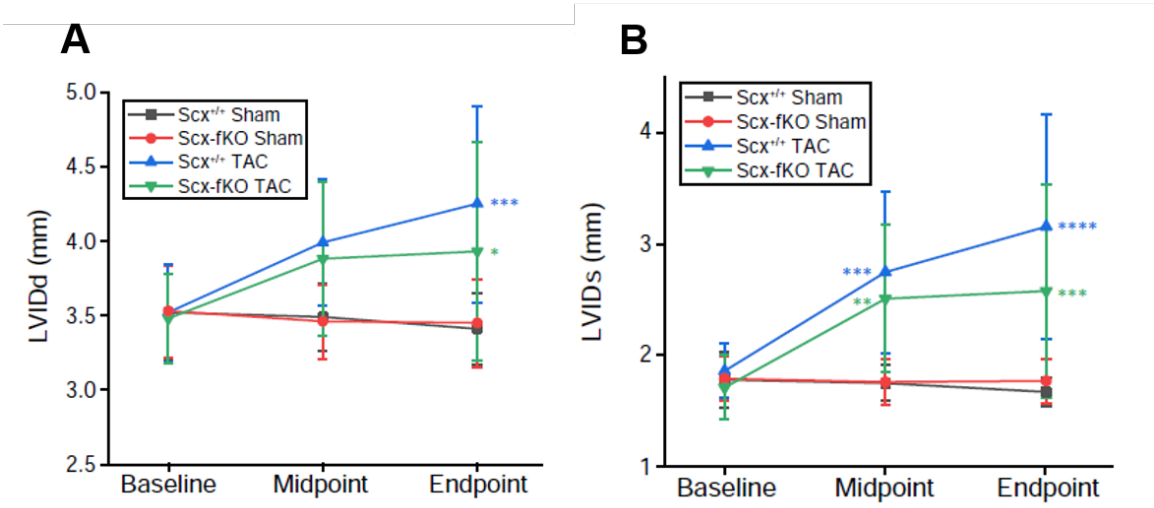

Figure 29: Scleraxis gene deletion does not significantly improve cardiac dimensions in pre-established pressure-overloaded myocardium.

In Scx-fKO TAC animals, cardiac dimensions LVIDd (**A**) and LVIDs (**B**) showed a trend toward improvement compared to WT TAC animals, but this trend was not significant; n=8-11, two-way ANOVA, mean ± standard deviation; ****p<0.0001, ***p<0.001, **p<0.01, *p<0.05 vs WT sham.

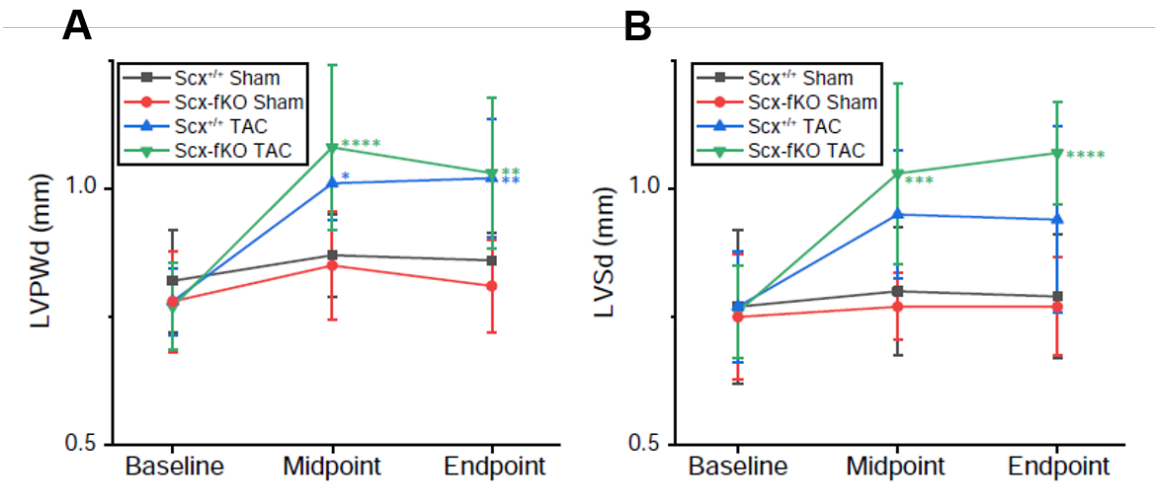

Figure 30: Scleraxis gene deletion has no impact on myocardial wall thickness in pressure-overloaded myocardium.

Echocardiographic measurements displayed a marginal increase in LVPWd (**A**) and LVSd (**B**) in Scx-fKO TAC compared to WT TAC animals, but no significant differences were noted in LVSd or LVPWd between Scx-fKO TAC and WT TAC; WT sham animals served as a control; n=8-11, two-way ANOVA, mean ± standard deviation; *p<0.05, **p<0.01, ****p<0.0001, ***p<0.001 vs WT sham.

1.4: Effect of scleraxis gene deletion in pre-existing long-term pressure-overloaded myocardium

1.4.1: Study design

Pressure overload (TAC) surgeries were performed to induce cardiac fibrosis in scleraxis-floxed Tcf21-iCre mice at 8 weeks of age. Four weeks later, TAC animals underwent gavage, with either tamoxifen for scleraxis gene deletion (Scx-fKO) or corn oil to leave the scleraxis gene intact (WT), once daily for 5 days. Each group consisted of n=11-12 animals. Cardiac function was assessed using echocardiography 1 day before TAC (Baseline), 1 day before scleraxis gene deletion (Midpoint-4wk), 1 day before 8 weeks post-TAC (Midpoint-8wk), 1 day before 10 weeks post-TAC (Midpoint-10wk), and 1 day before 12 weeks post-TAC (Endpoint). Animals were sacrificed 12 weeks after surgery (Fig. 31).

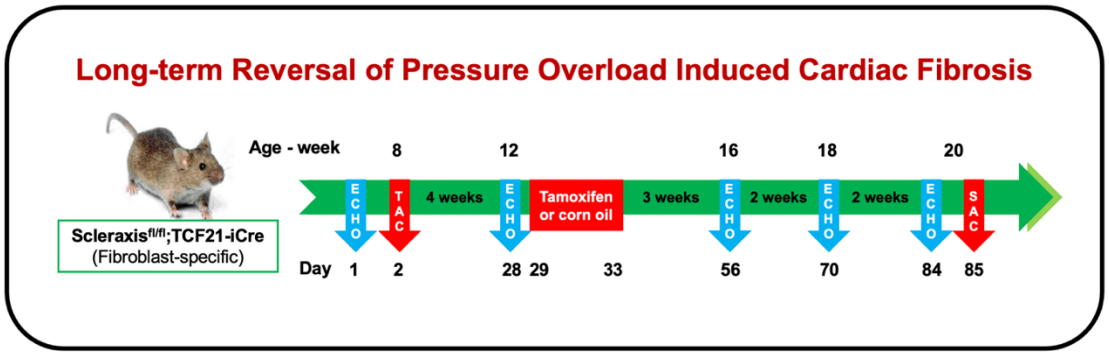

Figure 31: Experimental design for long-term reversal of pressure-overload-induced cardiac fibrosis.

Comprehensive study design details about pressure-overload surgery and scleraxis gene deletion. This long-term study design consists of 12 weeks of pressure overload in all animals. Groups underwent scleraxis gene deletion (Scx-fKO) or were left intact (WT) 4 weeks post- pressure-overload surgery (TAC). Cardiac functions were measured throughout using echocardiography.

1.4.2: Scleraxis gene deletion does not impact pre-established long-term pressure-overload-induced cardiac hypertrophy

After 12 weeks of pressure overload, both WT TAC and Scx-fKO TAC animals developed cardiac hypertrophy, and no significant differences were noted between them based on HW/BW, HW/Tibia, or LW/BW measurements (Fig. 32). These results indicate that scleraxis gene deletion in pre-existing pressure-overload condition does not impact cardiac hypertrophy.

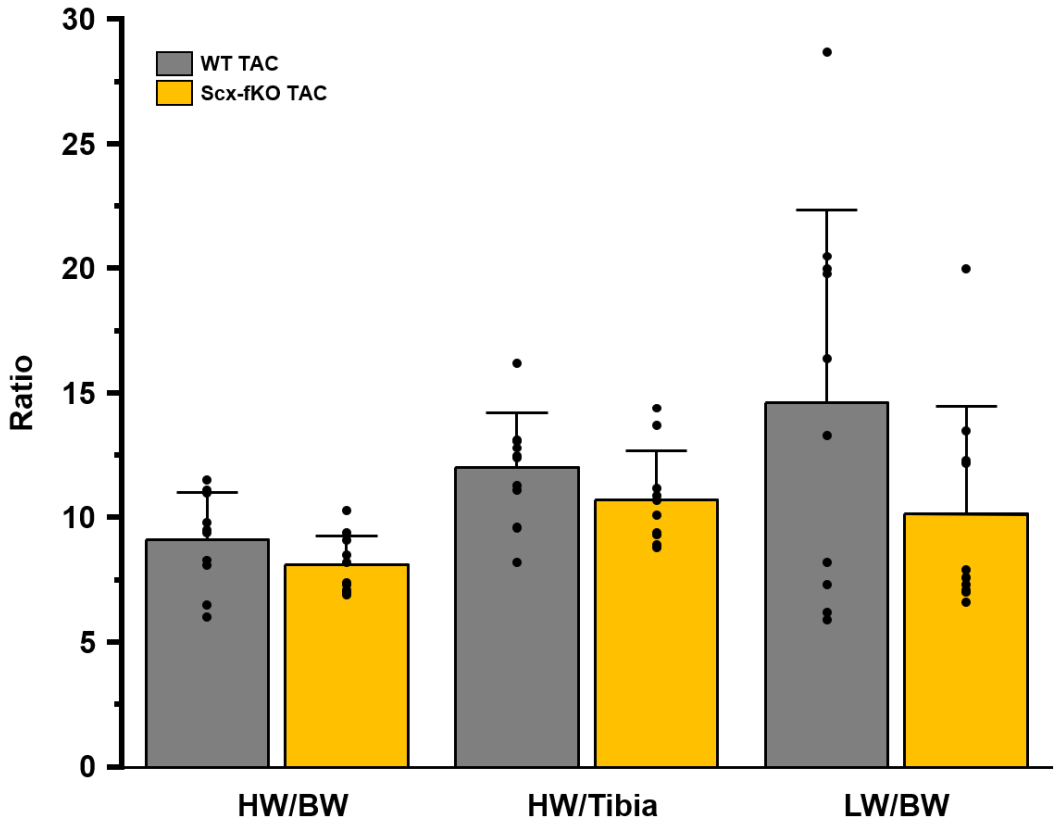

Figure 32: Scleraxis deletion does not impact cardiac hypertrophy in pre-established long-term pressure overload.

Hypertrophy developed 12 weeks after pressure overload, but there were no differences between Scx-fKO TAC and WT TAC animals. Data represented as HW/BW, HW/Tibia, and LW/BW; n=11-12, two-tailed unpaired t-test, mean ± standard deviation; *p<0.05 vs WT sham.

1.4.3: Scleraxis gene-deleted animals displayed a better survival rate in long-term pre-existing pressure overload

Reports from other groups that assessed the length of survival after pressure overload in C57BL/6J mice showed 40% of the animals died within 4 weeks of TAC, and 100% mortality was observed by 5 months compared to sham-operated animals [328]. Another study reported that the median survival rate of WT animals was 35 days following TAC [326]. In our current study, survival rate analysis revealed that WT TAC animals began to die after 7 weeks of pressure overload, and by 12 weeks, one-third of

the animals had died. In contrast, Scx-fKO TAC animals had a remarkable 100% survival rate. Intriguingly, all the Scx-fKO TAC animals survived even in the case of a pre-existing pressure-overload condition (Fig. 33).

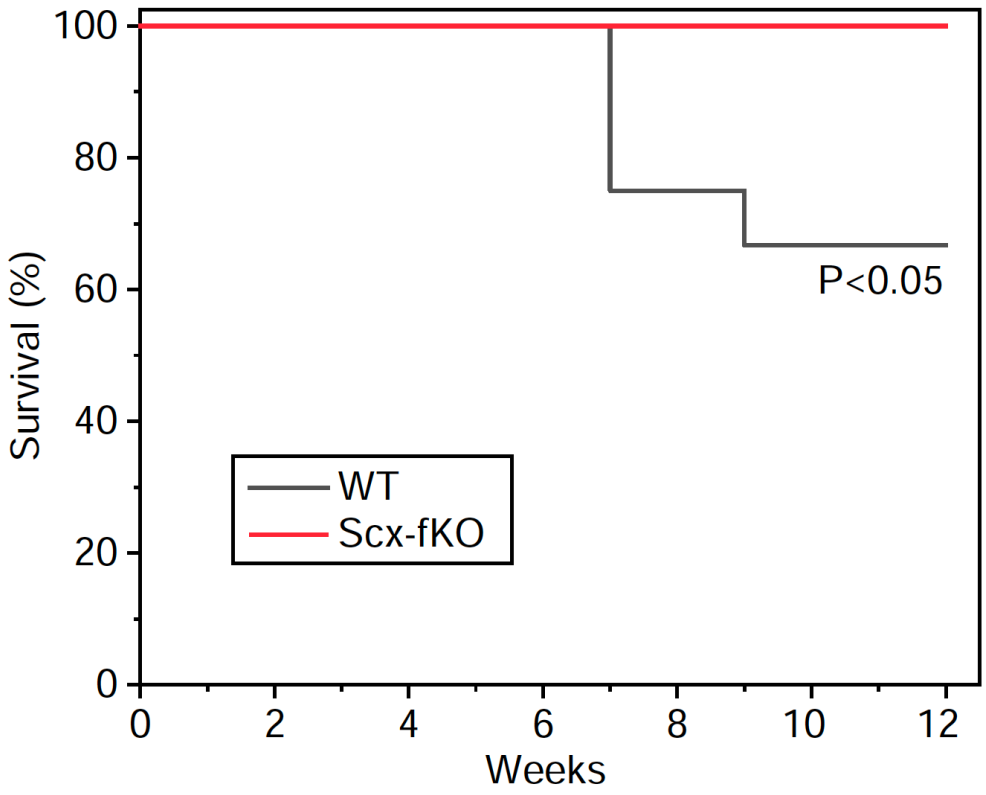

Figure 33: Scleraxis gene deletion reduces the mortality rate in pre-established long-term pressure overload.

In pre-established pressure overload, scleraxis gene-deleted animals showed better survival rates than WT TAC animals, even after 12 weeks; n=11-12, Log-rank (Mantel-Cox) test; *p<0.05 vs WT TAC.

1.4.4: Scleraxis gene-deleted animals displayed improved systolic function in long-term pre-existing pressure overload

In the case of long-term pre-existing pressure-overloaded myocardium, Scx-fKO animals exhibited better LVEF than WT TAC animals after 12 weeks. Scx-fKO TAC animals also showed improved FS after 12 weeks, but this was not statistically significant

compared to WT TAC animals (Fig. 34). Altogether, scleraxis gene deletion improves systolic function after 12 weeks of pre-existing pressure overload in animals.

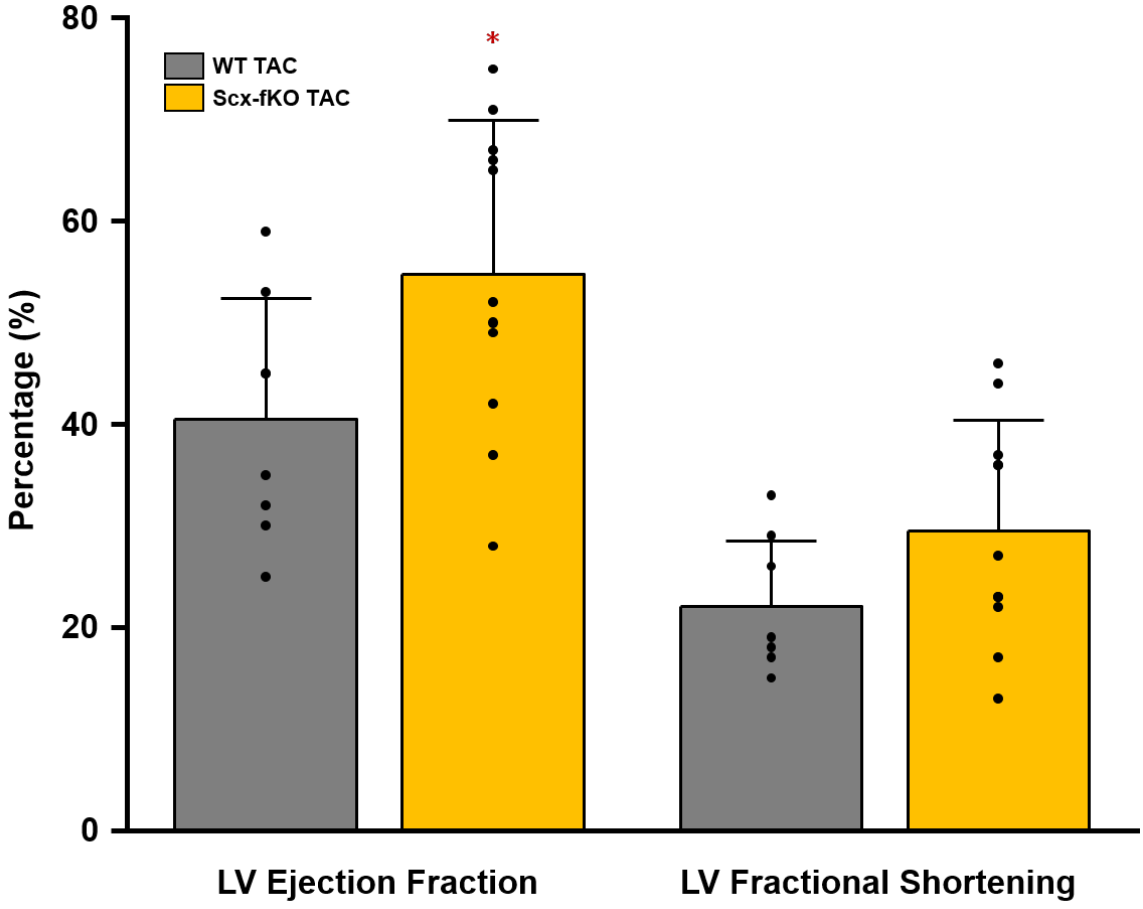

Figure 34: Scleraxis gene deletion improves systolic function in long-term pre-established pressure-overloaded myocardium.
Echocardiography reveals scleraxis gene-deleted animals had improved systolic parameters, LV ejection fraction and fractional shortening, compared to WT TAC animals; n=8-11, two-tailed unpaired t-test, mean ± standard deviation; *$p \leq 0.05$ vs WT TAC.

1.4.5: Scleraxis gene deletion fails to improve cardiac morphology in long-term pre-existing pressure-overloaded myocardium

After 12 weeks of pressure overload, cardiac dimensional parameters LVIDd and LVIDs were not significantly different between Scx-fKO and WT TAC hearts (Fig. 35A).

Likewise, cardiac thickness parameters such as LVPWd and LVSd were similarly increased in Scx-fKO TAC and WT TAC hearts (Fig. 35B). These results indicate that scleraxis gene deletion does not affect cardiac morphological parameters in pre-existing long-term pressure overload.

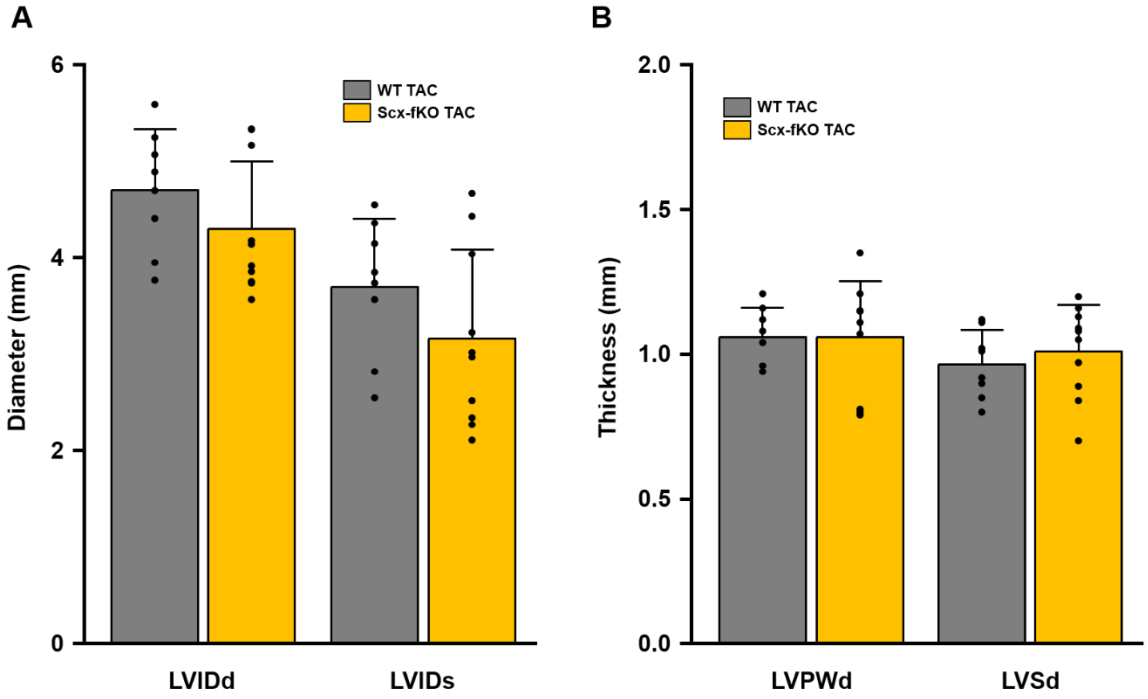

Figure 35: Scleraxis gene deletion does not improve cardiac morphology in long-term pre-established pressure-overloaded myocardium.

Echocardiography showed no difference in cardiac dimensions LVIDd and LVIDs **(A)** or cardiac thickness parameters LVPWd and LVSd **(B)** after scleraxis gene deletion in TAC compared to WT TAC animals; n=8-11, two-tailed unpaired t-test, mean ± standard deviation; *p ≤ 0.05 vs WT TAC.

2: Scleraxis transcriptionally regulates matrix proteins periostin and MMP2

2.1: Transcriptional regulation of periostin gene expression in cardiac myofibroblasts by scleraxis

2.1.1: Periostin and scleraxis are expressed in parallel in cardiac myofibroblasts

Scleraxis has previously been shown to be progressively up-regulated during the activation of cardiac fibroblasts to become myofibroblasts, while periostin is highly expressed in myofibroblasts but not in fibroblasts [164]. Scleraxis also directly transactivates several fibrosis-associated genes in cardiac fibroblasts and myofibroblasts, including Col-1α2, α-SMA, fibronectin, and MMP2 [165, 288, 317]. We thus confirmed that both scleraxis and periostin are significantly up-regulated in cardiac myofibroblasts as compared to fibroblasts (Fig. 36A). TGFβ1 is a potent cytokine that drives the activation and conversion of fibroblasts to myofibroblasts [329]. Treatment of P1 activated cardiac fibroblasts with TGFβ1 significantly induced mRNA expression of both scleraxis and periostin (Fig. 36B), and induced the secretion of periostin protein to the cell culture medium (Fig. 36C). Scleraxis and periostin expression are thus similarly increased as fibroblasts become myofibroblasts, and following TGFβ1 stimulation.

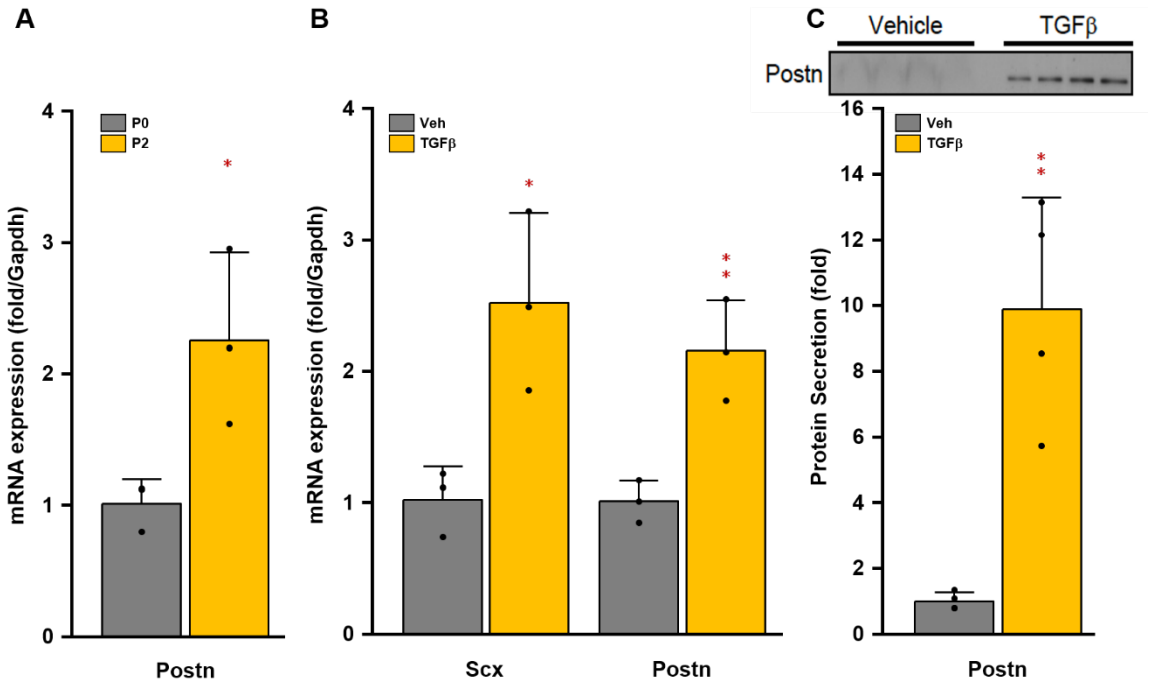

Figure 36: Scleraxis and periostin are expressed in parallel in cardiac fibroblasts and myofibroblasts.

(A) Conversion of primary adult rat cardiac fibroblasts (P0; within 6 h of initial plating) to myofibroblasts (P2; passaged twice) increases both scleraxis (Scx) and periostin (Postn) mRNA expression; n=3, two-tailed unpaired t-test, mean ± standard deviation; *p<0.05 vs. P0. Samples are normalized to Gapdh and P0 cells. Treatment of activated adult rat cardiac fibroblasts (P1; passaged once) with 10 ng/ml TGFβ1 for 24 h to induce conversion to myofibroblasts up-regulates expression of scleraxis and periostin mRNA **(B)** and periostin protein secretion to the cell medium **(C)**; n=3 **(B)** or n=4 **(C)**; two-tailed unpaired t-test, mean ± standard deviation; *p<0.05 vs. vehicle.

2.1.2: Scleraxis induces periostin expression in cardiac fibroblasts

Given the parallel changes in scleraxis and periostin expression noted above, we investigated whether scleraxis may specifically regulate periostin expression using a gain-of-function approach. Scleraxis was overexpressed in activated adult primary rat P1 fibroblasts using adenoviral-mediated gene delivery for 48 h, resulting in a ~5-fold induction of scleraxis mRNA (Fig. 37A), similar to the level of pathologic induction of scleraxis expression in the cardiac post-infarction scar [164]. Scleraxis significantly

increased periostin mRNA expression nearly 20-fold compared to adenovirus GFP control (AdGFP) (Fig. 37A). Intracellular periostin protein expression was also induced significantly by scleraxis (Fig. 37B). Since periostin is primarily exported to the ECM, we assessed periostin secretion following scleraxis overexpression. Secreted periostin was nearly undetectable in control (AdGFP) cells, and was dramatically increased by scleraxis (Fig. 37C). Scleraxis is thus sufficient to increase periostin expression and secretion in activated cardiac fibroblasts.

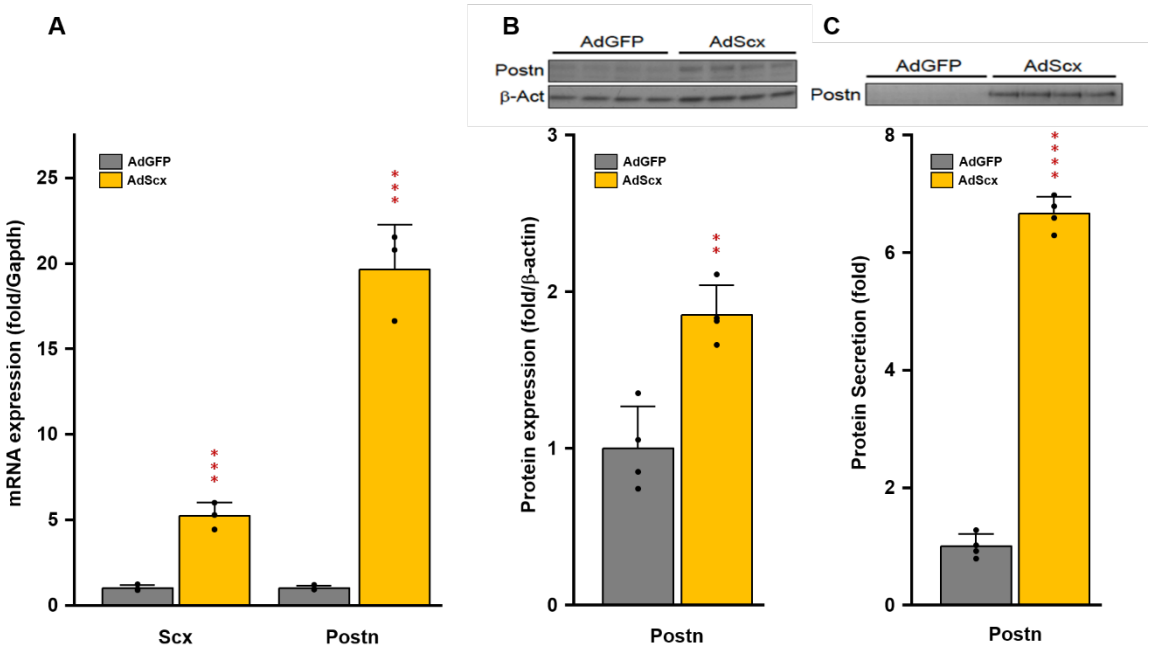

Figure 37: Scleraxis induces periostin expression in cardiac fibroblasts. Adenovirus-mediated overexpression of scleraxis (AdScx, 48 h, 10 MOI) in activated P1 rat cardiac fibroblasts increases mRNA expression of periostin compared to GFP control (AdGFP) at both the mRNA **(A)** and protein **(B)** level. For secretory periostin expression, conditioned medium was collected from P1 rat cardiac fibroblasts treated with AdScx or AdGFP for 24 h, 10 MOI **(C)**. n=3 **(A)** or n=4 **(B)** and **(C)**, two-tailed unpaired t-test, mean ± standard deviation; *p<0.05 vs. AdGFP. Results were normalized to Gapdh **(A)** or β-actin **(B)** and to AdGFP.

2.1.3: Transactivation of the human periostin promoter by scleraxis

As a member of the basic helix-loop-helix superfamily of transcription factors, scleraxis can directly transactivate target gene promoters by binding to E-box consensus binding sites with sequence CA*NN*TG, where *N* is any nucleotide [285]. While scleraxis was able to potently induce periostin expression (Fig. 38), it was unclear whether this effect was via direct transcriptional regulation or via an intermediary factor. For example, we have shown that scleraxis directly up-regulates Twist1 in epithelial cells, and Twist1 is one of the few transcription factors known to transactivate the periostin promoter [205, 278]. We thus assessed the ability of scleraxis to transactivate the human proximal periostin gene promoter.

Examination of the human periostin promoter, spanning from -886 to +93 bp relative to the transcription start site, revealed 4 putative E-boxes to which scleraxis may bind (Fig. 38A). Luciferase assays conducted in NIH3T3 fibroblasts revealed that scleraxis significantly transactivated the periostin promoter (Fig. 38B). A shorter promoter construct, spanning -504 to +93 bp and excluding the 2 most distal E-boxes, was transactivated by scleraxis to a virtually identical degree as the longer promoter construct (Fig. 38B), suggesting that E-boxes E3 and E4 are dispensable for scleraxis-mediated transactivation, thus further analysis focused on the short promoter construct.

The 2 E-boxes E1 and E2 located in the short periostin promoter are separated by only 2 nucleotides. To determine their relative importance in scleraxis-mediated promoter transactivation, these sites were sequentially mutated to abrogate scleraxis binding. Site-specific mutation of E2 reduced promoter transactivation by scleraxis by approximately 50% compared to the intact promoter (Fig. 38C). Mutation of both E2 and E1 together further reduced transactivation by more than 90% compared to the intact promoter, marking a further significant reduction compared to mutation of E2 alone (Fig. 38C) and demonstrating the critical importance of both E-boxes in scleraxis-mediated transactivation of the human periostin promoter.

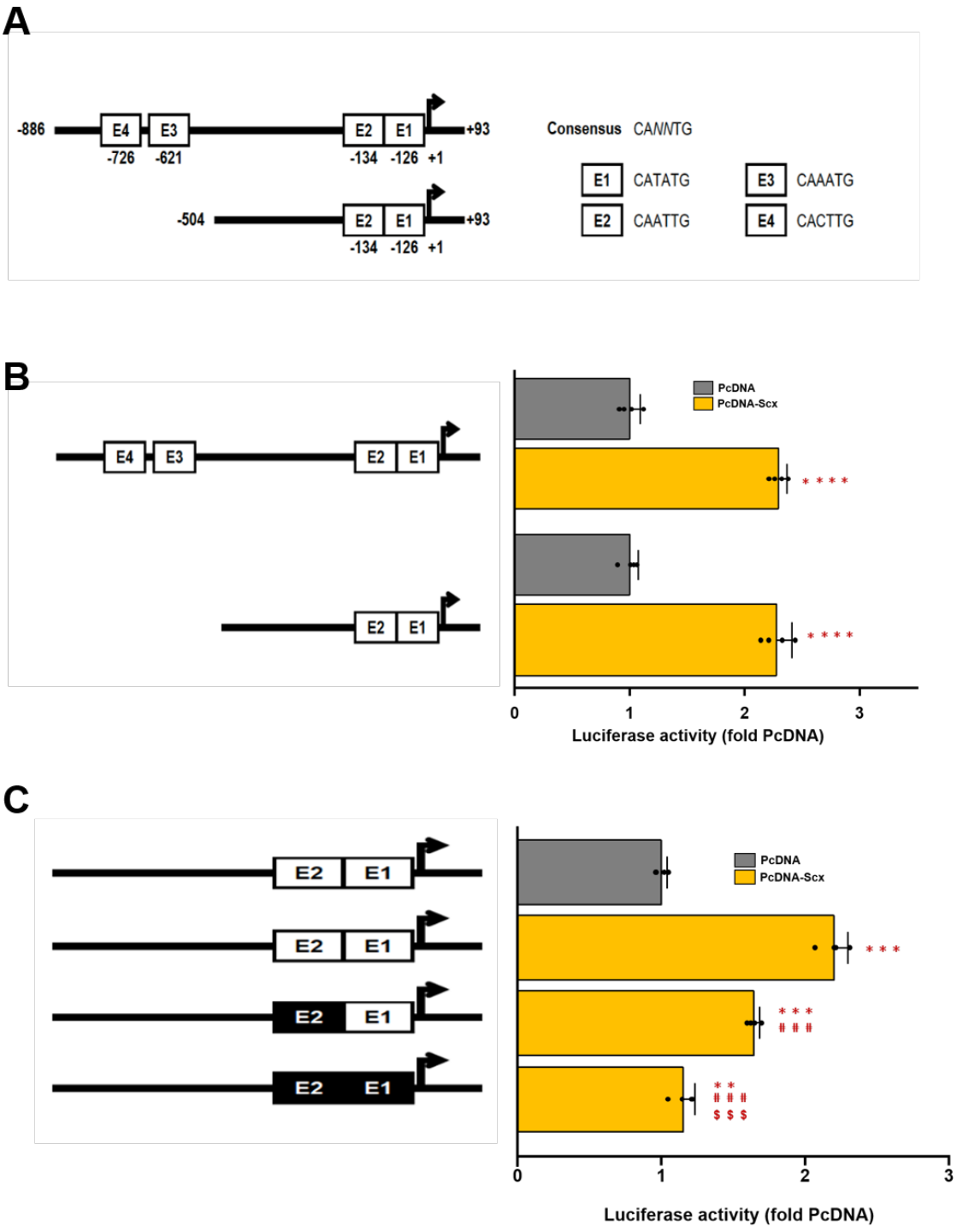

Figure 38: Transactivation of the human periostin promoter by scleraxis.

(A) Short (597 bp) or long (979 bp) regions of the human proximal periostin (POSTN) promoter, containing 2 or 4 putative E-boxes respectively, were cloned into pGL4.10. **(B)** Constructs were transfected into NIH3T3 fibroblasts with a scleraxis expression vector

(pcDNA-Scx) or empty vector control (pcDNA) with normalization to co-transfected Renilla luciferase pRL. After 24 h, cells were lysed, and luciferase assays were performed. Short and long POSTN promoters were similarly transactivated by Scx; n=4, two-tailed unpaired t-test, mean ± standard deviation; ****p<0.0001 vs pcDNA. **(C)** Site-directed mutagenesis of E2 alone, or E1 and E2 together (black boxes), attenuated scleraxis-induced POSTN promoter transactivation in a stepwise fashion; n=4, one-way ANOVA, mean ± standard deviation; **p<0.01, ***p<0.001 vs. pcDNA; $^{###}$p<0.001 vs. pcDNA-Scx+intact promoter; $^{\$\$\$}$p<0.001 vs. pcDNA-Scx+E2 mutant.

2.1.4: Validation of scleraxis interaction with periostin promoter E-boxes

To confirm specific binding of scleraxis to E-boxes E1 and E2, we performed electrophoretic mobility shift assays using oligonucleotides encompassing both sites. Incubation of scleraxis-enriched nuclear extracts with biotin-labelled oligonucleotides spanning E1 and E2 resulted in a clear shifted complex indicative of specific binding of scleraxis to this site (Fig. 39A left side, lane S). This complex was not observed when competed by “cold” unlabelled oligonucleotides (lane cold competition (CC) and was super-shifted to a higher molecular weight in the presence of a scleraxis-specific antibody but not non-specific IgG antibody (lanes Scx and IgG), confirming the presence of scleraxis in the complex. Mutation of E1 and E2 to abrogate scleraxis binding attenuated both the shifted and super-shifted complex formation (Fig. 39A right side). Collectively, these results support the luciferase assay results and demonstrate that scleraxis transactivates the periostin promoter via specific binding at E1 and E2.

TGFβ_1/Smad signalling up-regulates scleraxis, which in turn promotes increased binding to target gene promoters [165]. We assessed scleraxis interaction with the human periostin promoter in isolated human cardiac myofibroblasts by ChIP assay, as well as the impact of treatment of these cells with TGFβ1. Given the close proximity of E1 and E2, ChIP cannot delineate specific binding to either site individually but can provide a readout of scleraxis interaction with the region overall. In vehicle-treated cells, scleraxis was not enriched at the periostin promoter compared to controls (Fig. 39B). In sharp contrast, TGFβ1 treatment induced a dramatic and significant enrichment of scleraxis at

the periostin promoter, suggesting a potential novel mechanism for scleraxis-mediated periostin up-regulation in response to profibrotic TGFβ1.

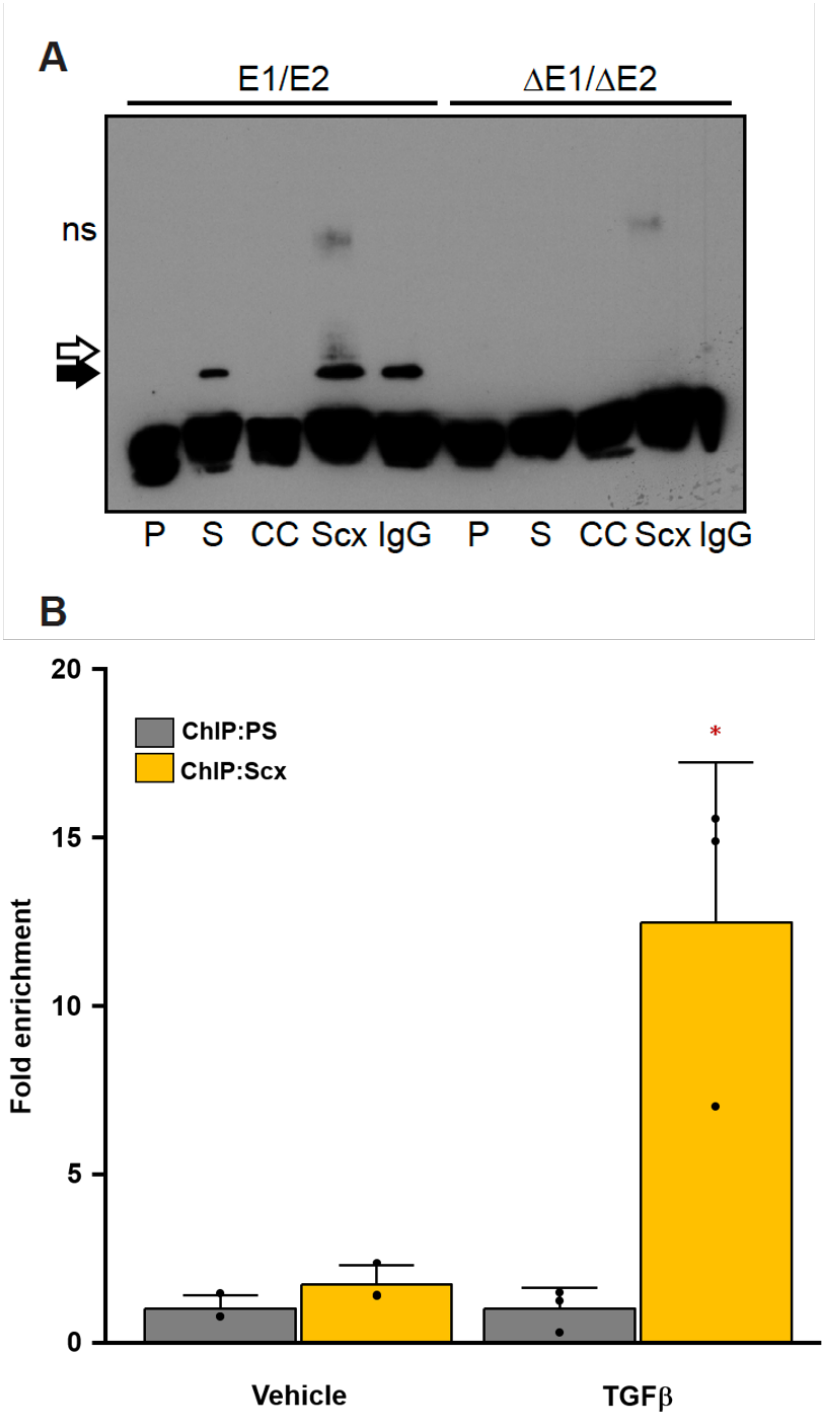

Figure 39: Scleraxis binds to E-boxes E1 and E2 of the human periostin promoter.

(**A**) Scleraxis-enriched HEK293 nuclear extracts were incubated with biotin-labelled DNA oligonucleotide probes containing the periostin promoter E-boxes E1 and E2, or oligonucleotides with mutated E-boxes (ΔE1/ΔE2). Lanes represent free probe (P), scleraxis nuclear extract (S), cold competition (CC), and complex incubation with anti-scleraxis (Scx) or non-specific (IgG) antibodies. The solid arrow depicts the shifted protein-oligonucleotide complex; the hollow arrow depicts the super-shifted protein-oligonucleotide-antibody complex. ns, non-specific complex. (**B**) Human cardiac myofibroblasts were treated with vehicle or TGFβ1 (10 ng/ml) for 24 h followed by ChIP using anti-scleraxis antibody (Scx) or pre-immune serum (PS). qPCR was used to amplify the E1/E2-containing region of the periostin promoter. Genomic DNA was used as a positive input control. Results represent n=3 independent experiments, and were normalized to PS and input; two-tailed unpaired t-test, mean ± standard deviation; *$p<0.05$ vs. PS.

2.1.5: TGFβ1-mediated periostin expression requires scleraxis

Previous data from our laboratory have revealed that scleraxis is an essential and integral regulator of TGFβ1-mediated fibrotic signalling mechanisms in cardiac fibroblasts and myofibroblasts. For example, scleraxis knockdown in primary cardiac myofibroblasts completely attenuates TGFβ1-induced cell contraction [288]. To determine if a similar requirement for scleraxis exists in TGFβ1-mediated periostin up-regulation, we employed a loss-of-function approach via experiments in activated cardiac fibroblasts isolated from WT or scleraxis knockout (KO) mice. WT or KO cells were treated with vehicle, or with TGFβ1 to induce periostin expression. While TGFβ1 induced a 4-fold up-regulation of periostin in WT cells, KO cells exhibited a significant baseline decrease in periostin mRNA expression in vehicle-treated cells, and a complete failure to up-regulate periostin in response to TGFβ1 (Fig. 40A). Similarly, periostin secretion was very low in vehicle-treated WT cells and increased nearly 20-fold after TGFβ1 treatment (Fig. 40B). In contrast, KO cells lost the ability to increase periostin secretion in response to TGFβ1. Together, these results reveal a critical and absolute requirement for scleraxis in TGFβ1-mediated periostin expression.

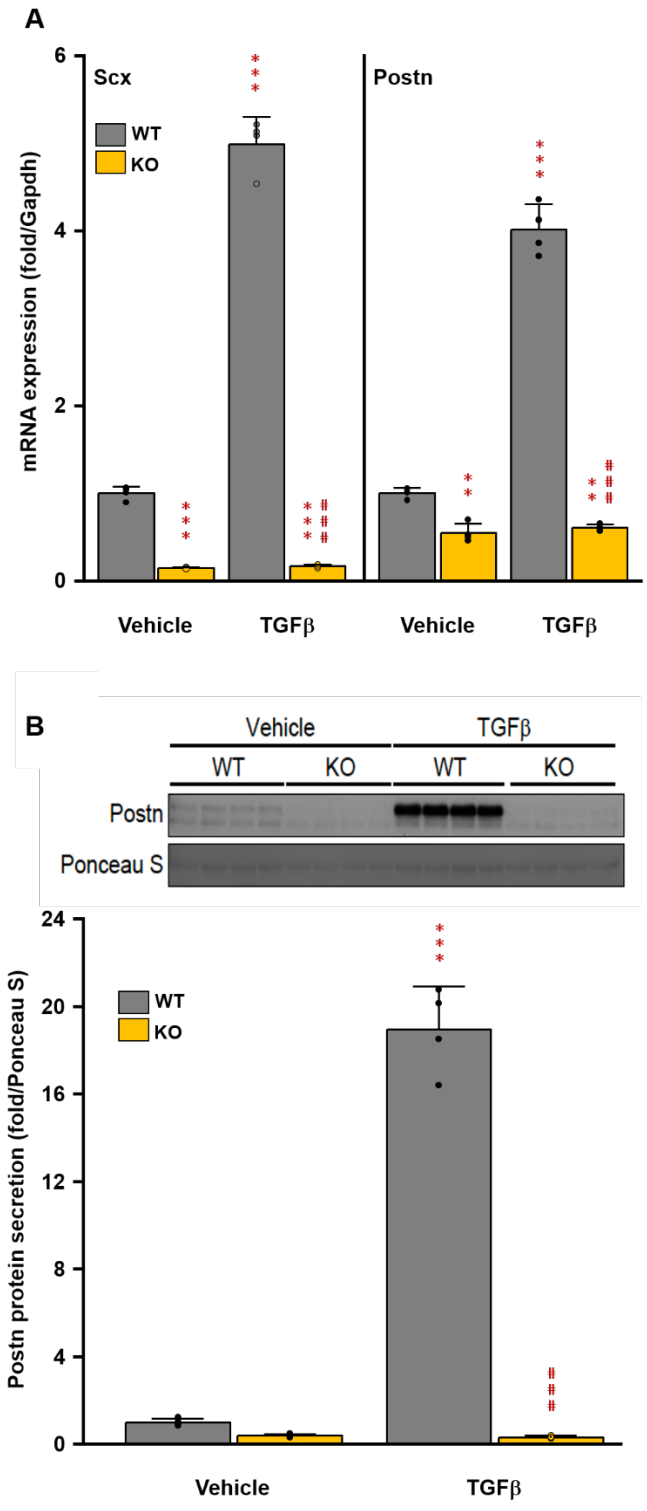

Figure 40: Scleraxis is required for TGFβ1-induced periostin expression.

(A) Activated primary mouse P1 cardiac fibroblasts were isolated from WT or scleraxis knockout (KO) hearts and treated with TGFβ1 (10 ng/ml) or vehicle. TGFβ1 induced

scleraxis and periostin expression in WT but not KO cardiac fibroblasts. **(B)** Conditioned medium from WT or scleraxis KO cardiac fibroblasts treated with TGFβ1 (10 ng/ml) or vehicle was analyzed by western blot for periostin protein secretion, with results normalized to WT+vehicle and to Ponceau S-stained membranes. TGFβ1 induces periostin secretion in WT but not scleraxis KO cardiac fibroblasts; n=4 for (**A**) and (**B**); two-way ANOVA, mean ± standard deviation; ***$p<0.001$ vs. WT+vehicle; $^{###}p<0.001$ vs. WT+TGFβ1.

2.1.6: Rescue of scleraxis expression restores periostin protein secretion

Scleraxis KO cells failed to up-regulate periostin expression in response to TGFβ1 (Fig. 40), however, it is unclear if this is due to a permanent loss in the ability of KO cells to produce periostin. We therefore restored scleraxis expression in KO cells by adenoviral gene delivery. Scleraxis overexpression in WT activated cardiac fibroblasts induced a significant ~11-fold increase in periostin protein secretion (Fig. 41). While scleraxis overexpression in KO cells was less potent in inducing periostin secretion than in WT cells, KO cells nonetheless exhibited a significant ~5-fold up-regulation compared to GFP-overexpressing cells. These results demonstrate that, while periostin induction by scleraxis is blunted in KO cells, these cells retain the ability to produce periostin when scleraxis expression is rescued. We previously observed a similar regulatory scheme governing MMP2 protein expression, suggesting a common mechanism of scleraxis activity across target genes [323].

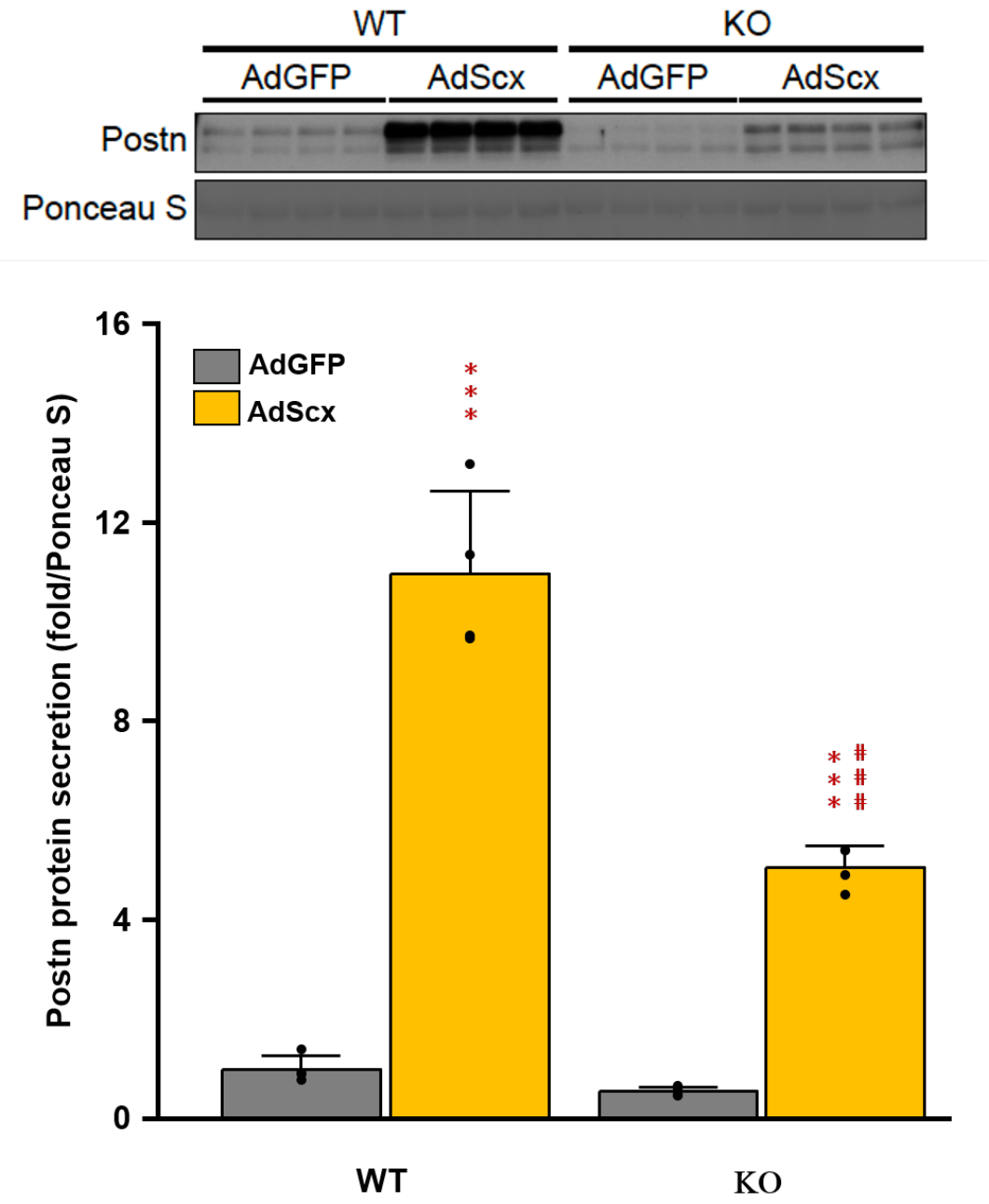

Figure 41: Rescue of scleraxis expression in scleraxis knockout cardiac fibroblasts is sufficient to restore periostin protein secretion.

Adenovirus-mediated overexpression of scleraxis (AdScx, 48 h, 10 MOI) increased periostin secretion in both WT and KO mouse activated cardiac fibroblasts; n=4; two-way ANOVA, mean ± standard deviation; ***p<0.001 vs. corresponding AdGFP sample; ###p<0.001 vs. WT+AdScx.

2.2: Regulation of cardiac fibroblast MMP2 gene expression by scleraxis[3]

2.2.1: Scleraxis governs MMP2 expression

Previous data from our laboratory showed that the bHLH family member scleraxis regulates fibrosis-associated proteins including Col-1α2, α-SMA, and EDA-Fn in cardiac myofibroblasts, and that MMP2 expression tracked closely with scleraxis expression [165, 288, 317]. We therefore performed gain- and loss-of-function studies to elucidate the role of scleraxis in regulating MMP2 expression. Overexpression of scleraxis in NIH3T3 fibroblasts resulted in a 2-fold induction of MMP2 mRNA expression (Fig. 42A), an increase that was mirrored at the protein level (Fig. 42B). To confirm these results in primary cells, we employed adenovirus-mediated scleraxis gene delivery to infect adult rat cardiac P1 myofibroblasts at high efficiency. P1 myofibroblasts are derived from fibroblasts that have been passaged once to induce their conversion toward the myofibroblast phenotype—they express elevated levels of ECM proteins but unlike myofibroblasts, they are not contractile [288]. Poised between the fibroblast and full myofibroblast phenotype, these cells are uniquely useful for the examination of pro- and antifibrotic mechanisms. In agreement with our previously published data, as well as our present results in NIH3T3 fibroblasts, scleraxis induced the up-regulation of MMP2 mRNA and protein by approximately 2–2.5 fold (Fig. 42C, D) [288]. High-efficiency knockdown of scleraxis expression in rat cardiac myofibroblasts was attained using adenoviral delivery of shRNA. Loss of scleraxis (AdshScx) almost completely abolished MMP2 protein expression (Fig. 42E). Together, these results demonstrate that scleraxis potently controls MMP2 expression in both immortalized NIH3T3 fibroblasts and in primary cardiac myofibroblasts.

---

[3] Reprinted from Raghu S. Nagalingam, Hamza A. Safi, Danah S. Al-Hattab, Rushita A. Bagchi, Natalie M. Landry, Ian M.C. Dixon, Jeffrey T. Wigle, Michael P. Czubryt, Regulation of cardiac fibroblast MMP2 gene expression by scleraxis, Journal of Molecular and Cellular Cardiology. 120: 64-73 © 2018, with permission from Elsevier. https://www.jmcc-online.com/article/S0022-2828(18)30151-2/fulltext

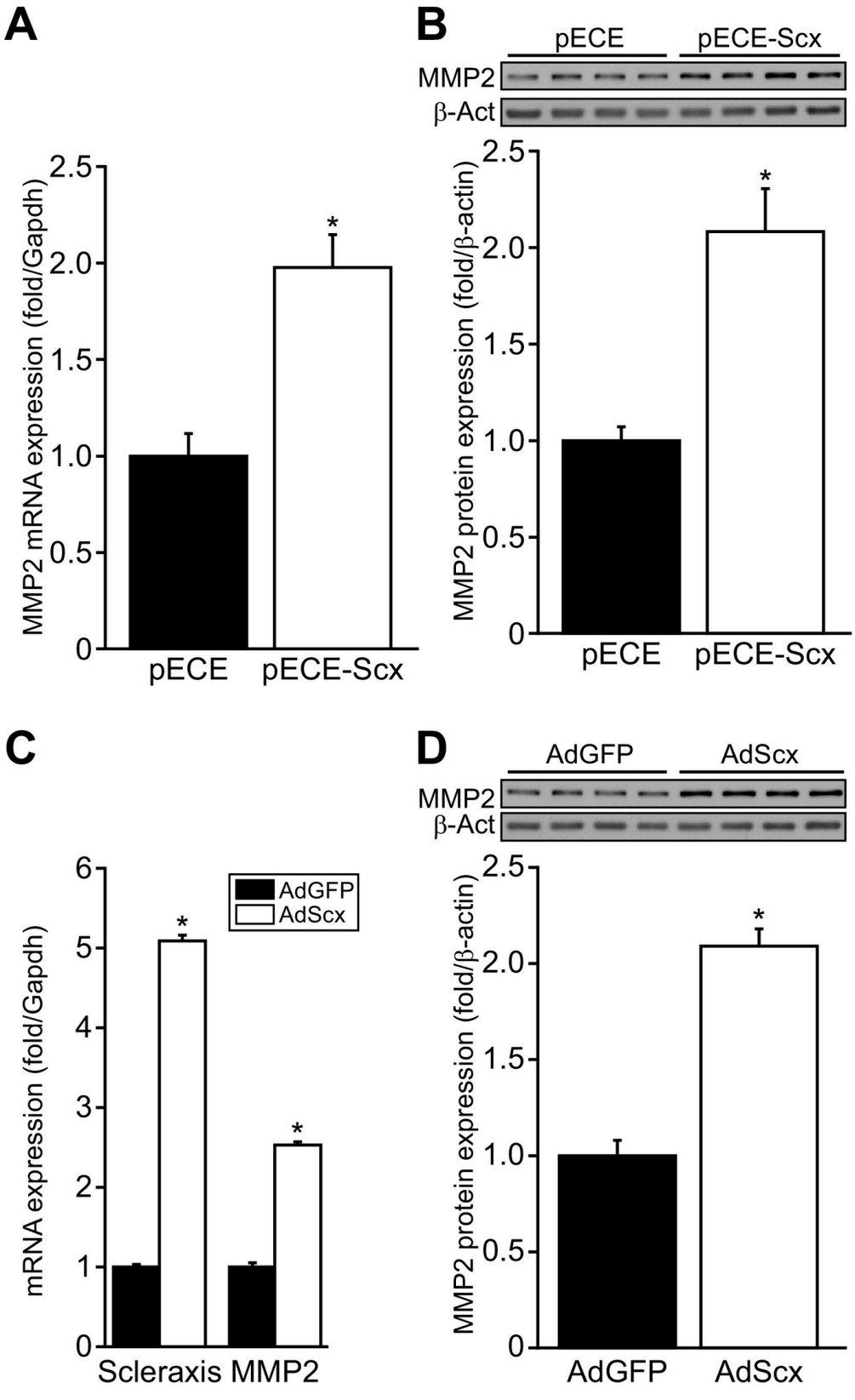
A
MMP2 mRNA expression (fold/Gapdh)
2.5
2.0
1.5
1.0
0.5
0
*
pECE
pECE-Scx
B
pECE
pECE-Scx
MMP2
β-Act
MMP2 protein expression (fold/β-actin)
2.5
2.0
1.5
1.0
0.5
0
*
pECE
pECE-Scx
C
mRNA expression (fold/Gapdh)
6
5
4
3
2
1
0
AdGFP
AdScx
*
*
Scleraxis
MMP2
D
AdGFP
AdScx
MMP2
β-Act
MMP2 protein expression (fold/β-actin)
2.5
2.0
1.5
1.0
0.5
0
*
AdGFP
AdScx

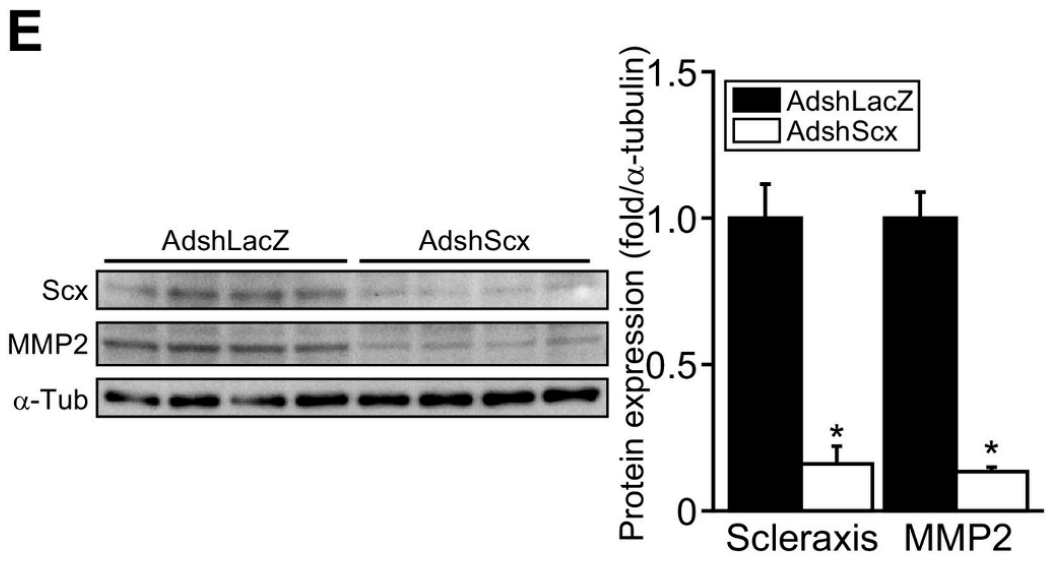

Figure 42: Regulation of MMP2 expression by scleraxis.

(A) NIH3T3 fibroblasts were transfected with scleraxis (pECE-Scx) or empty control (pECE) vectors for 48 h and total RNA assayed by qPCR. Overexpression of scleraxis significantly increased MMP2 mRNA levels in NIH3T3 fibroblasts; n=3, *p<0.05 vs. pECE. **(B)** Total protein was isolated from NIH3T3 fibroblasts transfected as in panel **(A)** and subjected to western blotting. Scleraxis overexpression doubled MMP2 protein expression; n=4, *p<0.05 vs. pECE. **(C)** Scleraxis was overexpressed in adult rat cardiac P1 myofibroblasts via adenovirus-mediated gene delivery (AdScx; 48 h treatment, 10 MOI); GFP was used as a negative control (AdGFP). AdScx significantly increased mRNA expression of both scleraxis and MMP2 compared to AdGFP; n=4, *p<0.05 vs. AdGFP. **(D)** Cells treated as in panel **(C)** were assessed for MMP2 protein expression by western blot. Scleraxis significantly up-regulated MMP2 protein expression in cardiac P1 myofibroblasts; n=4, *p<0.05 vs. AdGFP. **(E)** Adenovirus-mediated knockdown of scleraxis using targeted shRNA (AdshScx; 72 h treatment, 200 MOI) was performed in rat cardiac P1 myofibroblasts. Scleraxis knockdown strongly attenuated protein expression of scleraxis and MMP2 protein compared to control shRNA targeting LacZ (AdshLacZ); n=4, *p<0.05 vs. AdshLacZ. For all panels, results are normalized to controls.

2.2.2: Scleraxis transactivates the MMP2 gene promoter

Scleraxis belongs to the bHLH transcription factor family, whose members regulate gene transcription by specifically binding to E-box consensus sequences (CA*NN*TG) present in target gene promoters. *In silico* analysis of the human proximal 1.6 kb MMP2 promoter revealed the presence of 6 putative E-boxes (Fig. 43A), providing a potential mechanism for direct transcriptional control of MMP2 gene expression by scleraxis. To examine this possibility, we performed luciferase assays in NIH3T3 fibroblasts. Co-transfection of a luciferase reporter construct containing the human MMP2 proximal promoter with a scleraxis expression vector resulted in an increase in luciferase activity by greater than 2-fold compared to an empty vector control (Fig. 43B), indicating that scleraxis is capable of transactivating the MMP2 promoter. To query the significance of the individual E-box motifs in scleraxis-mediated MMP2 expression, we introduced various combinations of site-specific mutations of the 6 putative scleraxis-binding sites (Fig 43B, black boxes). Notably and surprisingly, only mutation of E-box 6 (E6) resulted in a loss of scleraxis-induced luciferase activity (Fig. 43B). Mutating the E6 site in combination with other E-box mutations had no further effect compared to mutating the E6 site alone. No other single E-box mutation or combination of mutations tested, including a combined E1 to E4 mutation, mimicked the effect of the E6 mutation alone. To confirm the necessity of E6 in scleraxis-mediated transactivation of the MMP2 promoter, we generated a reporter construct in which the promoter was truncated immediately 5' to E6. Similar to the full-length promoter, reporter activity was significantly induced by scleraxis (Fig. 43C). Mutation of E6 in this truncated promoter to attenuate binding by scleraxis eliminated activation by scleraxis.

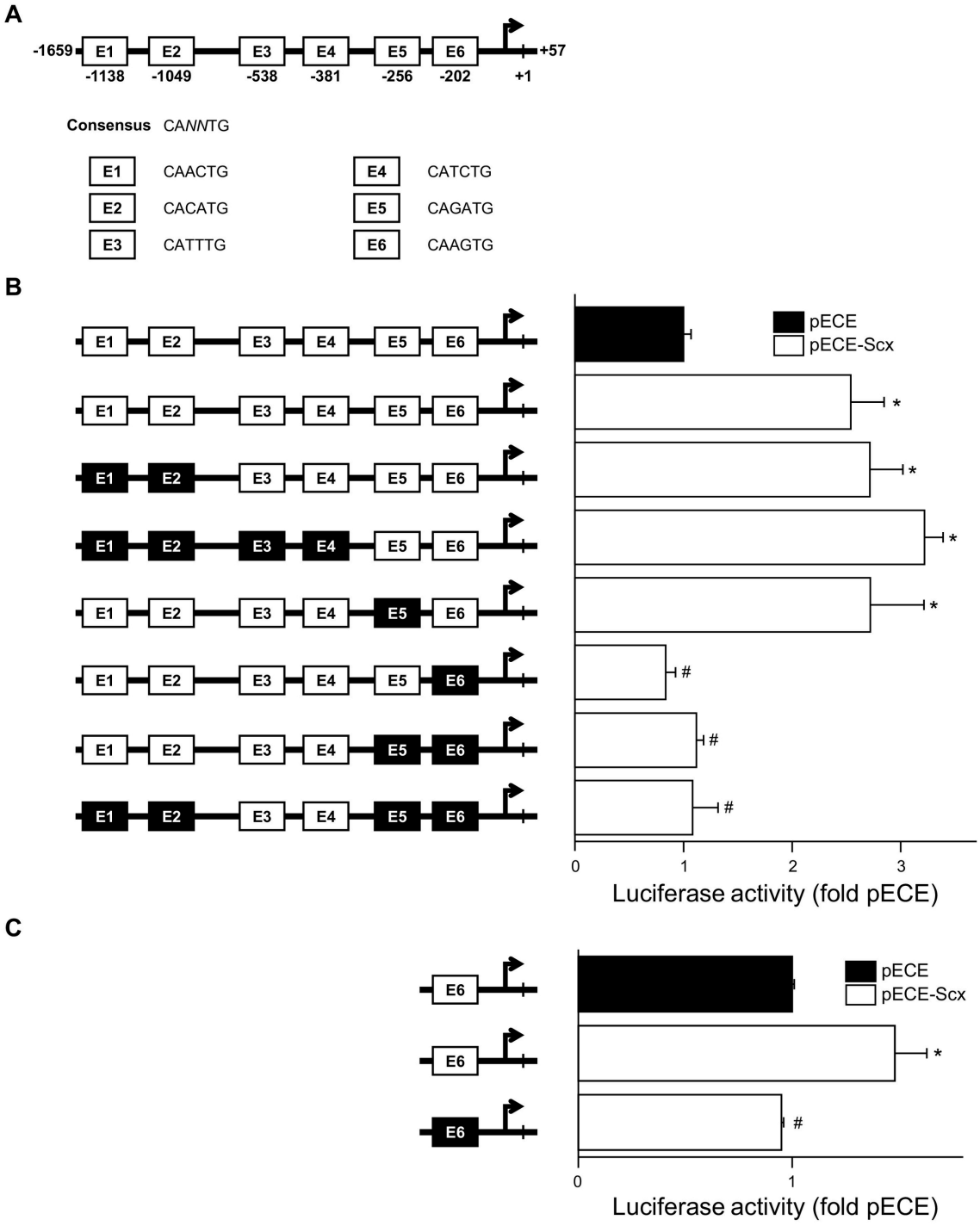

Figure 43: Transactivation of the MMP2 promoter by scleraxis.

(A) The human MMP2 proximal gene promoter is depicted with putative scleraxis-binding E-box sites (white boxes denoted E1 to E6) shown schematically. Numbers denote nucleotide coordinates relative to the transcription start site at +1. Individual E-

box sequences are shown. **(B)** Luciferase reporter assays were performed to assess transactivation of the MMP2 gene promoter by scleraxis (pECE-Scx) compared to empty vector control (pECE), with results normalized to pRL transfection control and pECE; mutation of different E-boxes (black boxes; individually or in combinations) was performed by site-specific mutagenesis. Only mutation of E-box 6 (E6) attenuated promoter transactivation by scleraxis; n=4, *p<0.05 vs. pECE; #p<0.05 vs. pECE-Scx+intact MMP2 promoter. **(C)** A reporter construct truncated immediately 5' to E6 was transfected with scleraxis or empty vector control, with results normalized to pRL and pECE. The truncated promoter containing E6 was transactivated by scleraxis, and this induction was lost following mutation of E6 (black box); n=3, *p<0.05 vs. pECE; #p<0.05 vs. pECE-Scx+ E6-intact truncated MMP2 promoter.

2.2.3: Validation of scleraxis binding to the MMP2 proximal promoter

To confirm the physiological interaction of scleraxis with the MMP2 promoter, we performed a ChIP assay in human adult cardiac myofibroblasts. Since our luciferase assays indicated that scleraxis binds only to E6, we employed primers encompassing the E5-E6 region of the MMP2 proximal promoter, since these 2 E-boxes are located very closely to one another (Fig. 44A). Scleraxis antibody-mediated genomic DNA pulldown resulted in a significantly greater qPCR amplification of this region compared to pulldown by PS control (Fig. 44A). Scleraxis is thus bound preferentially to this region in human cardiac myofibroblasts; however, given the limitations in ChIP resolution, we cannot determine the precise site to which scleraxis binds using this method alone.

To address this shortcoming, we performed an electrophoretic mobility shift assay using biotin-labelled oligonucleotides corresponding to E6, or to a mutant E6 (mE6) in which the E-box is altered to prevent scleraxis binding. We observed the presence of a shifted protein-oligonucleotide complex in the presence of scleraxis-containing nuclear lysates, but not in control (scleraxis-negative) lysates (Fig. 44B). This complex was attenuated in the presence of cold, unlabelled oligonucleotides, and was super-shifted in the presence of anti-scleraxis antibodies. Mutation of the E-box (mE6) prevented the formation of the protein-oligonucleotide complex. We also incubated E5 oligonucleotide

probes with scleraxis-enriched nuclear extracts but observed no complex formation (data not shown). These results are in agreement with our luciferase assay data indicating that scleraxis regulates MMP2 promoter transactivation via interaction with E6 but not E5 (Fig. 44B).

Transcriptionally active chromatin is associated with acetylation of histone 3 lysine 9 (H3K9-Ac), thus we assessed the effect of scleraxis on H3K9-Ac within the proximal MMP2 promoter using quantitative ChIP. Overexpression of scleraxis in human cardiac myofibroblasts resulted in enrichment of H3K9-Ac at the E5-E6 region of the MMP2 proximal promoter compared to GFP-transfected controls (Fig. 44C). Scleraxis thus acts in part by inducing epigenetic alterations associated with active chromatin.

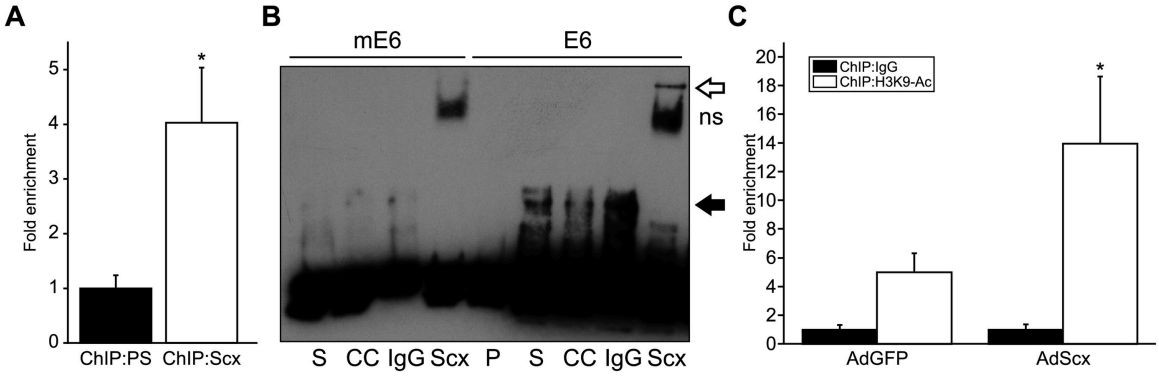

Figure 44: Validation of scleraxis binding to the MMP2 proximal promoter. **(A)** Chromatin immunoprecipitation was performed in human cardiac myofibroblasts using an anti-scleraxis antibody (Scx) or pre-immune serum (PS), and the MMP2 proximal promoter region encompassing E5 and E6 amplified by qPCR. Amplification of this region was significantly enriched using the anti-scleraxis antibody compared to PS; n=3, *p<0.05 vs. PS. **(B)** Electrophoretic mobility shift assay was performed using biotin-labelled oligonucleotides encompassing E6, with or without mutation to prevent scleraxis binding (mE6). Incubation of labelled oligo probe with scleraxis (S) produced a shifted complex (solid arrow), which was not seen with probe alone (P). Complex intensity was reduced by cold competition (CC) with unlabelled probe. Incubation of oligo-protein complexes with anti-scleraxis antibody (Scx) produced a super-shift (open arrow), which was not seen with non-specific antibody (IgG). Complexes were not

obtained with mE6 probe. ns, non-specific band. **(C)** Human cardiac myofibroblasts were infected for 24 h with AdGFP or AdScx, then subjected to chromatin immunoprecipitation with anti-acetylated histone 3 lysine 9 (H3K9-Ac) antibodies, or with non-specific IgG controls. The MMP2 proximal promoter encompassing E5 and E6 was then amplified by qPCR. Scleraxis induced a significant increase in enrichment of H3K9-Ac at the MMP2 promoter compared to GFP; n=3, *p<0.05 vs AdGFP.

2.2.4: Scleraxis knockout animals show reduced expression of MMP2

To determine the importance of scleraxis in mediating MMP2 expression in vivo, we analyzed primary cardiac P1 myofibroblasts derived from WT or scleraxis KO mice. Myofibroblasts from KO mice exhibited dramatically reduced MMP2 mRNA expression compared to cells from WT animals (Fig. 45A). To confirm this result, we examined MMP2 protein expression via immunofluorescence of cardiac P1 myofibroblasts derived from WT or scleraxis KO mice. We noted a decrease in both the overall number of labelled cells as well as the intensity per cell (Fig. 45B), confirming our mRNA analysis. We also analyzed cardiac protein lysates from scleraxis KO and WT mice; MMP2 protein expression was significantly reduced in KO heart samples (Fig. 45C). These results also confirm our previously reported findings, and in addition, demonstrate that scleraxis is required for normal levels of MMP2 expression *in vivo* [288].

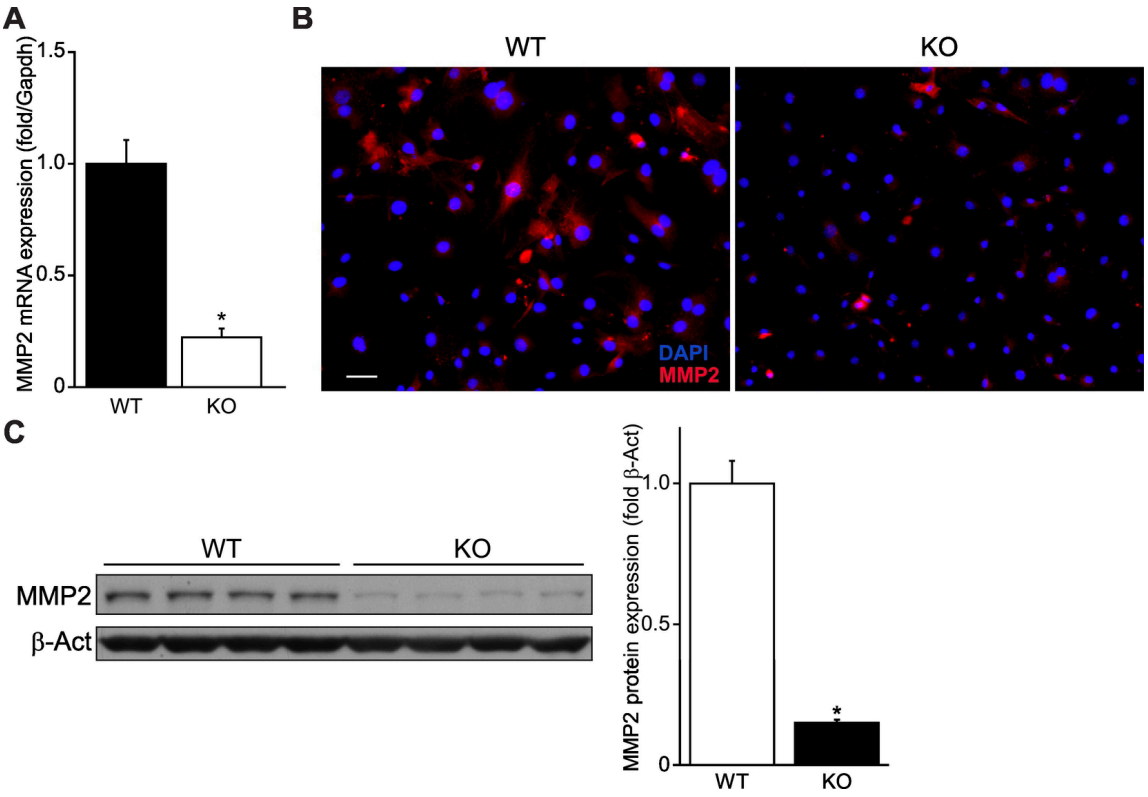

Figure 45: Loss of MMP2 expression in scleraxis knockout animals.

(A) Cardiac P1 myofibroblasts isolated from WT or scleraxis knockout (KO) mice were assessed for MMP2 mRNA expression by qPCR, with results normalized to WT. MMP2 mRNA expression was significantly decreased in KO cardiac P1 myofibroblasts compared to WT; n=3, *p<0.05 vs. WT. **(B)** Immunofluorescence labelling of MMP2 was reduced in cardiac P1 myofibroblasts from KO mice compared to WT mice (red, MMP2; blue, DAPI). Scale bar, 50μm. **(C)** Protein lysates from hearts of WT or scleraxis KO mice were analyzed by western blot for MMP2 expression, with results normalized to β-actin (β-Act). MMP2 protein expression was greatly reduced in KO hearts compared to WT hearts; n=3, *p<0.05 vs. WT.

2.2.5: Rescue of MMP2 expression in scleraxis null cardiac fibroblasts

It is possible that scleraxis loss results in MMP2 down-regulation through a mechanism not directly related to the loss of scleraxis itself. To test this possibility, we rescued scleraxis expression in scleraxis KO cardiac P1 myofibroblasts, or overexpressed scleraxis in WT cardiac P1 myofibroblasts, using adenovirus-mediated gene delivery.

Scleraxis overexpression in WT cells significantly up-regulated MMP2 mRNA expression compared to AdGFP control (Fig. 46A). Scleraxis KO cells showed a significant loss of MMP2 mRNA expression, and this loss was rescued by scleraxis overexpression, although total MMP2 mRNA expression failed to match that induced by scleraxis overexpression in WT cells. This result suggests the possibility of a gene dosage effect, i.e., that net MMP2 expression directly correlates with the level of scleraxis expression.

Using immunofluorescent staining, we observed a similar effect on MMP2 protein expression: scleraxis KO cells exhibited reduced MMP2 staining compared to WT, and fewer cells stained positive for MMP2. Overexpression of scleraxis strongly up-regulated MMP2 expression, although KO cells still attained a lower level of MMP2 expression compared to WT cells in which scleraxis was overexpressed (Fig. 46B). Together, these results suggest that loss of MMP2 expression is a direct result of scleraxis loss, and show that overexpression of scleraxis is sufficient to restore MMP2 expression in KO cells to greater than WT levels. Again, the results suggest that a gene dosage effect exists, whereby MMP2 levels track closely with overall scleraxis levels.

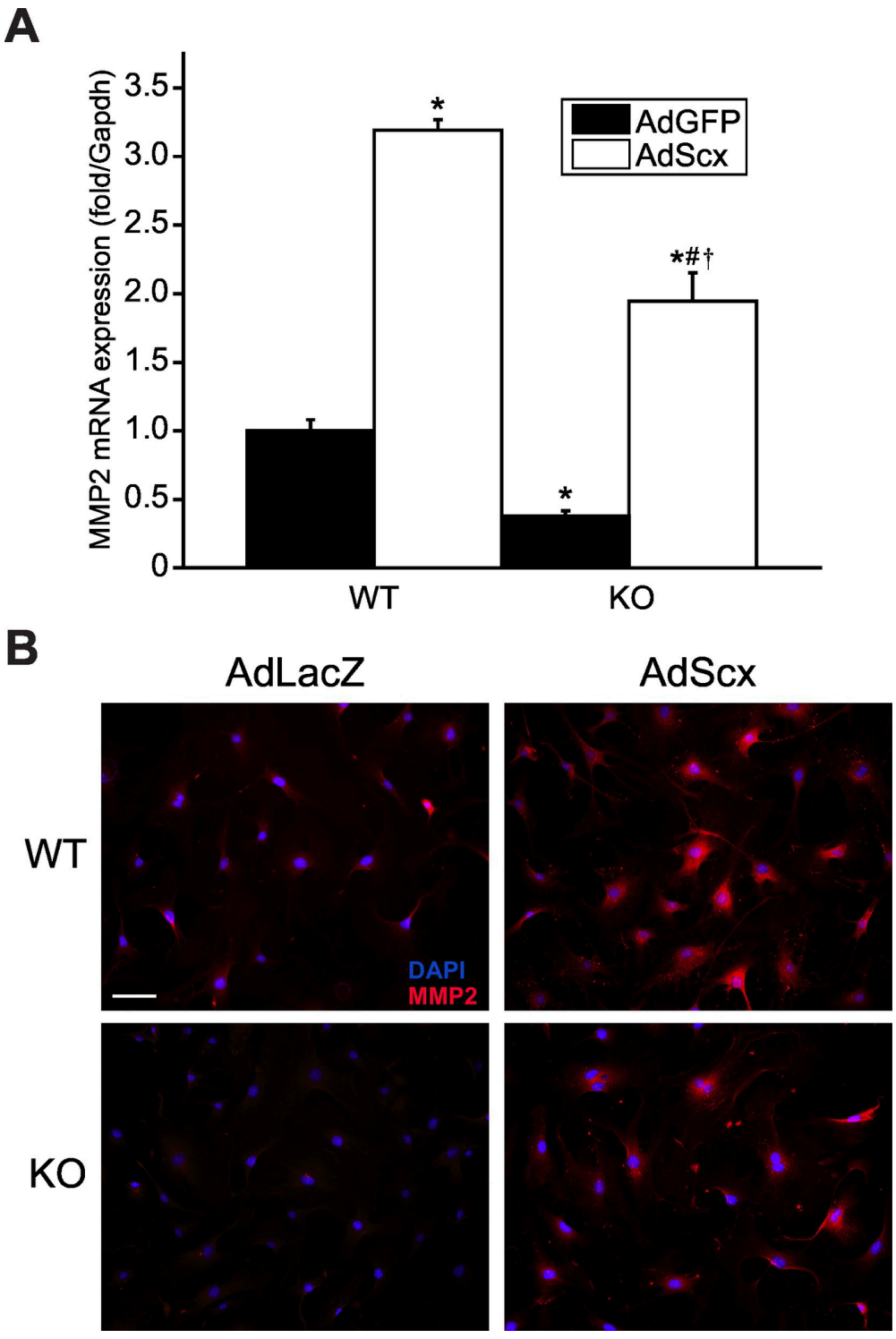

Figure 46: Restoration of MMP2 expression in scleraxis null cardiac fibroblasts by scleraxis overexpression.

(A) Cardiac P1 myofibroblasts isolated from WT or scleraxis knockout (KO) mice were transduced with adenoviruses encoding scleraxis (AdScx) or GFP control (AdGFP) for 48 h at 10 MOI, then assessed for MMP2 mRNA expression by qPCR, with results normalized to WT+AdGFP. AdScx up-regulated MMP2 expression in both WT and KO cardiac P1 myofibroblasts, although to a lesser degree in KO cells than in WT; n=3, *p<0.05 vs. WT+AdGFP; #p<0.05 vs. KO+AdGFP; †p<0.05 vs. WT+AdScx. **(B)** WT or KO cardiac P1 myofibroblasts were treated as in panel **(A)**, and MMP2 was visualized by immunofluorescence. MMP2 protein expression reflected changes in MMP2 mRNA in response to scleraxis knockout with or without scleraxis overexpression (red, MMP2; blue, DAPI). Scale bar, 75 μm.

2.2.6: An obligatory role for scleraxis in TGFβ1-mediated MMP2 expression

Several studies have reported that the potent profibrotic factor TGFβ1 increases MMP2 expression in various types of fibroblasts [330-333]. Similarly, we have reported that TGFβ1 regulates scleraxis expression and that the profibrotic effects of TGFβ1 are dependent upon the presence of scleraxis [164, 165, 288]. We thus sought to determine whether the up-regulation of MMP2 by TGFβ1 is dependent upon scleraxis. We first confirmed that TGFβ1 induces protein expression of both scleraxis and MMP2 in NIH3T3 fibroblasts, up-regulating scleraxis by ~3.5 fold and MMP2 by ~2.5 fold (Fig. 47A).

To test the relationship between TGFβ1, scleraxis, and MMP2, we treated adult rat primary cardiac P1 myofibroblasts with TGFβ1, with or without scleraxis knockdown. As observed earlier, scleraxis knockdown significantly reduced MMP2 expression by ~40% (Fig. 47B). Intriguingly, while TGFβ1 more than doubled MMP2 expression in the presence of scleraxis, this up-regulation was completely abolished by scleraxis knockdown, suggesting that scleraxis is necessary for the actions of TGFβ1. To confirm this result, we treated adult primary cardiac P1 myofibroblasts derived from either WT or scleraxis KO mice with TGFβ1. As in our scleraxis knockdown experiment, TGFβ1 failed to induce MMP2 expression in KO cells, but significantly up-regulated MMP2 expression in WT cells (Fig. 47C). Transfection of WT cells with the truncated E6-

containing MMP2 promoter luciferase reporter, followed by treatment with TGFβ1, resulted in significant activation of the reporter (Fig. 47D). In contrast, TGFβ1 was unable to activate the reporter in KO cells. These results are in agreement with what we have observed for other gene targets of scleraxis and TGFβ1, including Col-1α2 and EDA-Fn, as well as TGFβ1-induced myofibroblast contraction, which is lost in the absence of scleraxis, demonstrating consistently that the downstream effects of TGFβ1 are dependent upon scleraxis (Fig. 47E) [288, 317].

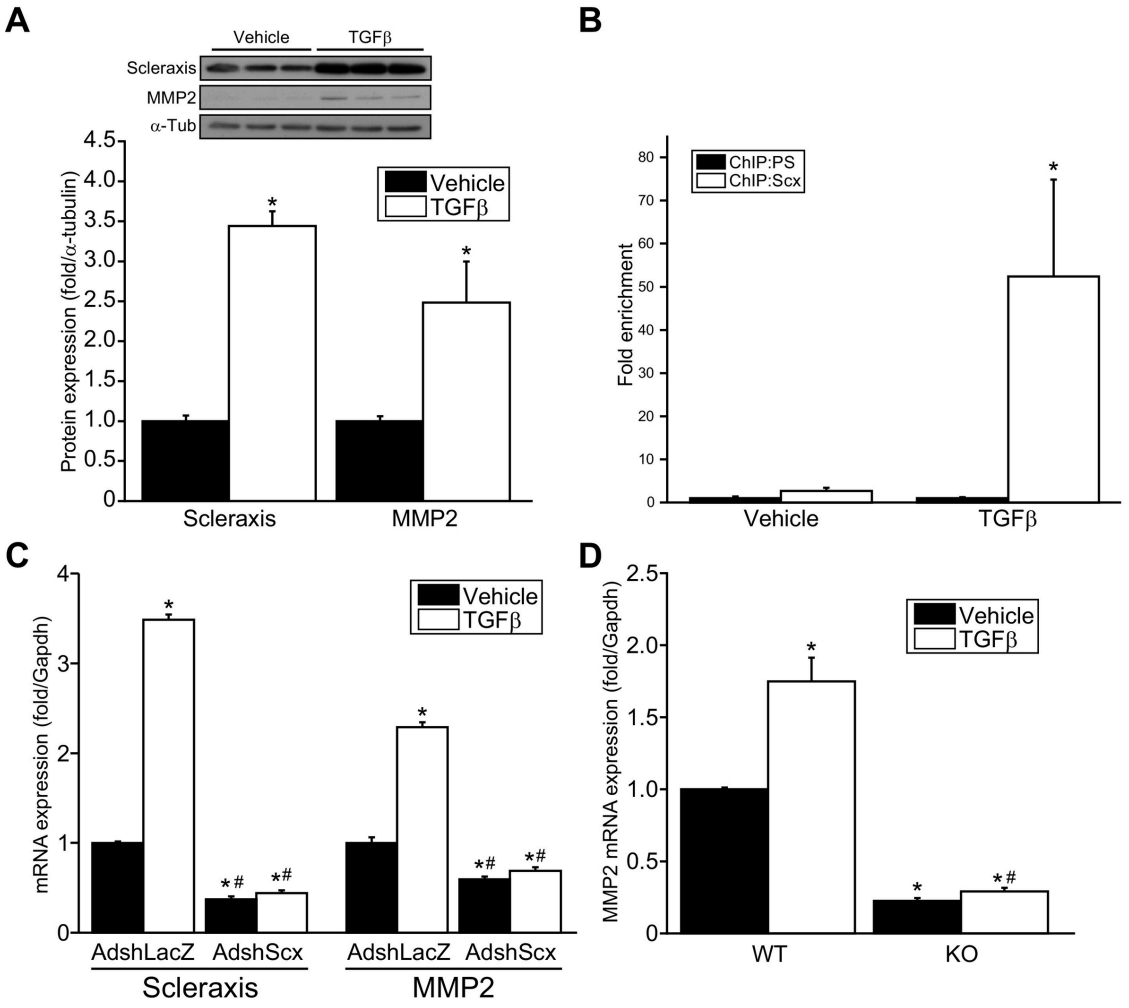

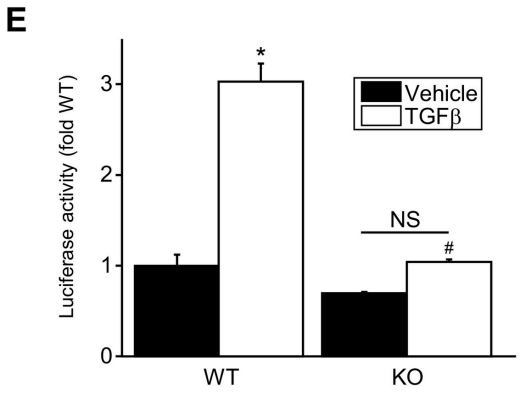

Figure 47: Scleraxis is required for TGFβ1-mediated MMP2 expression.

(A) NIH3T3 fibroblasts were treated with vehicle or TGFβ1 (10 ng/ml) for 24 h. Both scleraxis and MMP2 protein expression were up-regulated by TGFβ1 compared to vehicle as assessed by western blot, with results normalized to vehicle-treated samples; n=3, *p<0.05 vs. vehicle. **(B)** Human cardiac myofibroblasts were treated with TGFβ (10 ng/ml) or vehicle control for 24 h, then subjected to ChIP assay using scleraxis-specific antibodies or pre-immune serum (PS). The MMP2 proximal promoter encompassing E5 and E6 was then amplified by qPCR. TGFβ induced a significant increase in enrichment of scleraxis at the MMP2 promoter compared to vehicle; n=3, *p<0.05 vs vehicle. **(C)** Rat cardiac P1 myofibroblasts were subjected to adenovirus-mediated knockdown of scleraxis using targeted shRNA (AdshScx; 48 h, 200 MOI), or received control adenovirus (AdshLacZ), then were treated with TGFβ1 (10 ng/ml, 24 h) or vehicle. AdshScx strongly attenuated mRNA expression of both scleraxis and MMP2 compared to AdshLacZ as determined by qPCR. While TGFβ1 significantly up-regulated MMP2 mRNA expression in the presence of scleraxis, this effect was completely lost after knockdown; n=4, *p<0.05 vs. AdshLacZ+vehicle; #p<0.05 vs. AdshLacZ+TGFβ1. Results were normalized to AdshLacZ+vehicle samples. **(D)** Cardiac P1 myofibroblasts from WT or scleraxis KO mice were treated with TGFβ1 (10 ng/ml, 24 h) or vehicle, and MMP2 mRNA expression was determined by qPCR, with normalization to WT+vehicle. TGFβ1 induced MMP2 mRNA expression in cells derived from WT but not KO mice; n=3, *p<0.05 vs WT+vehicle; #p<0.05 vs. WT+ TGFβ1. **(E)** Cardiac P1 myofibroblasts from WT or scleraxis KO mice were transfected with the truncated E6-containing MMP2

promoter reporter for 24 hours, then treated with TGFβ1 (10 ng/ml, 24 h) or vehicle and luciferase activity assayed and normalized to WT vehicle-treated cells. TGFβ1 activated the MMP2 promoter in cells derived from WT but not KO mice; n=4, *$p<0.05$ vs WT+vehicle; #$p<0.05$ vs. WT+ TGFβ1. NS, not significant.

CHAPTER V: DISCUSSION

Aim 1: Scleraxis regulates pressure-overload-induced cardiac fibrosis

Therapeutic approaches to treat cardiac fibrosis in humans are severely limited; currently, there are no drugs available to treat fibrosis-associated pathologies. Effective druggable therapeutic targets and extended survival-related preclinical studies are inadequate. Furthermore, the transcriptional control of this process is poorly understood.

Persistent stress in the pressure-overloaded myocardium activates TGFβ-Smad signalling, leading to fibroblast-to-myofibroblast activationexcessive collagen and ECM synthesis [334-336]; This remodelling process results in a reduction of LVEF along with a change in LVEDV and LVESV, resulting in eventual heart failure [335-338]. Fibroblast activation and conversion to myofibroblasts are required for fibrosis to occur; therefore, timely intervention to block the myofibroblast numbers inside the myocardium would avoid adverse clinical outcomes.

Previous studies from our laboratory reported that germline scleraxis-null animals exhibited a reduction in cardiac ECM components as compared to age-matched control littermates. The reduced matrix contents—because of the impairment in epithelial-to-mesenchymal transition—led to a 50% loss of cardiac fibroblasts in the adult heart [288]. furthermore, the remaining fibroblasts failed to convert to myofibroblasts even when subjected to mechanical stretch [300]. Thus, developing conditional knockout of scleraxis will help address scleraxis-mediated impacts on myofibroblast-related preclinical pathologies *in vivo*.

In the current study, we demonstrate that scleraxis expression is up-regulated in murine pressure-overloaded myocardium (Fig. 10) and plays a crucial role in promoting cardiac fibrosis. Conditional knockout of scleraxis in cardiac fibroblasts prevents and reverses myofibroblast activation and fibrosis, thereby improving cardiac function in murine pressure-overloaded hearts (Figs 16 and 26). Additionally, conditional knockout of scleraxis results in a better survival rate than WT animals, even after 12 weeks of pre-existing pressure overload (Fig. 33). Most importantly, periostin, a known biological

marker for myofibroblasts, drives the cardiac fibrotic response to stress or injury and requires the presence of scleraxis to maintain its expression inside the pressure-overloaded myocardium.

Activation of fibroblasts to myofibroblasts is highly elevated in pressure-overloaded hearts and promotes collagen synthesis and profibrotic gene expression of periostin and EDA-Fn, thereby leading to fibrosis and cardiac dysfunction [211]. In our present study, 8 weeks of pressure overload in WT animals resulted in an increased expression of collagen, EDA-Fn, and periostin (Figs 14 and 15). For the first time, conditional loss of scleraxis expression before pressure overload in the murine myocardium significantly reduced the expression of the following profibrotic genes: collagen, periostin, and EDA-Fn (Figs 14 and 15). This reduction was concurrent with the attenuation of cardiac fibrosis inside the Scx-fKO TAC myocardium (Figs 13A and 13B). These results suggest that scleraxis is essential for the expression of profibrotic genes responsible for cardiac fibrosis in pressure-overloaded animals.

Transcription factors are crucial in regulating the collagen gene expression responsible for cardiac fibrosis [339]. In isolated cardiac myofibroblasts, scleraxis and Smad-3 synergistically regulate Col-1α2 gene expression in cardiac myofibroblasts [165]; also, scleraxis is necessary for the recruitment of Smad-3 to the Col-1α2 promoter at the chromatin level [288]. However, the role of scleraxis in regulating the Col-1α2 promoter in pressure-overloaded myocardium or in failing hearts is unknown. In our study, 8 weeks of pressure overload in WT TAC myocardium showed increased RNA Pol II-bound periostin and Col-1α2 promoter at the chromatin level compared to WT sham animals. Surprisingly, Scx-fKO TAC animals showed a reduction in RNA Pol II-bound periostin and Col-1α2 promoter at the chromatin level (Fig. 17). These results shed light on how profibrotic genes are tightly regulated by scleraxis and their importance in transcription complex recruitment to the target gene promoter at the chromatin level during pressure overload.

Chronic stress in pressure-overloaded myocardium reduces WT animals' systolic and diastolic functions [326, 340]. Our study showed a similar reduction in systolic

functional parameters such as LVEF and FS after 8 weeks of TAC in WT animals, whereas, in Scx-fKO TAC animals, these parameters were improved (Fig. 18). At the same time, the diastolic functional parameter E/A was not altered (Fig. 19B); however, E and A filling velocities were drastically reduced in WT TAC animals but not in Scx-fKO TAC animals (Fig. 19A). Based on this data, we believe that WT TAC animals underwent pseudo-normalization of diastolic function. Cardiac structural parameters LVIDd and LVIDs were significantly altered in WT TAC animals but not in Scx-fKO TAC animals after 8 weeks of pressure overload. (Fig. 20). These functional improvements were achieved in Scx-fKO TAC animals parallel with a reduction in cardiac fibrosis even after 8 weeks of pressure overload due to prior loss of scleraxis in cardiac fibroblasts.

From a clinical perspective, patients with DCM presenting with mid-wall fibrosis showed an 18-fold increased mortality rate compared to DCM patients without mid-wall fibrosis [46]. The severity of cardiac pathogenesis, in the cases of DCM, ICM, and MI, was determined based on its association with cardiac fibrosis. Most of the patients who presented clinically with heart failure also presented with cardiac fibrosis. To determine the therapeutic potential of scleraxis in pre-existing fibrotic conditions, we knocked out the scleraxis gene 4 weeks after pressure overload and followed the animals for another 4 weeks. The loss of scleraxis gene in a pre-existing pressure-overload condition resulted in a remarkable reduction in the profibrotic genes, collagen, EDA-Fn and periostin (Fig. 25), concomitant with attenuation of cardiac fibrosis in histopathological sections of Scx-fKO TAC animals compared to WT TAC animals (Figs 24A and 24B). Furthermore, 4 weeks of pressure overload worsened both systolic and diastolic parameters. However, the same animals that underwent scleraxis gene deletion after 4 weeks avoided further systolic and diastolic functional decline when compared to scleraxis-intact animals (Figs 27A, 27B, 28A, and 28B). As before, no differences were noted in the E/A ratio between WT TAC and Scx-fKO TAC animals (Fig. 28C); however, scleraxis deletion in pre-existing pressure overload resulted in improved filing velocities of E and A compared to scleraxis-intact animals (Figs 28A and 28B). These results indicate that scleraxis removal

in pre-existing pressure-overload conditions can help avoid adverse remodelling and functional deterioration.

Periostin expression is highly elevated after myocardial injury [202, 211], pressure overload [211, 341] and failing hearts [204] and is also used as a marker for myofibroblasts, linked to cardiac fibrosis [83, 204, 325, 342]. Periostin promotes fibroblasts derived from the dermis of hypertrophic scars to become myofibroblasts [343]. Similarly, periostin is also involved in the wound healing process. In skin wound healing, Postn−/− animals show reduced wound closure because of reduced myofibroblast populations within the granulation tissue [344]. This evidence supports how periostin influences the myofibroblast population after injury. In the current study, immunolabelling of periostin-positive cells and protein expression in WT TAC myocardium indicates a significant surge in myofibroblast population after 8 weeks of pressure overload compared to WT sham. On the other hand, regardless of the timing of scleraxis deletion (i.e., before or after the establishment of pressure overload), Scx-fKO TAC hearts revealed a dramatic reduction in periostin-positive cells and protein expression (Figs 16A, 16B, 26A, and 26B). Thus, scleraxis deficiency results in reduced periostin expression which leads to a decrease in the myocardium's myofibroblast population. Eventually, loss of the myofibroblasts results in a significant attenuation of profibrotic gene expression responsible for cardiac fibrosis in Scx-fKO TAC animals, even in existing pressure overload.

Further, we wanted to investigate the survival rate of animals during an extended period of scleraxis gene knockout and pre-existing pressure overload, and whether scleraxis gene deletion could preserve functional phenotype from 8 to 12 weeks without any further deterioration. Our study determined that WT TAC animals started to die 7 weeks after TAC surgery and that by the end of 12 weeks, nearly 33% of animals were lost. Remarkably, Scx-fKO TAC animals showed a 100% survival rate after 12 weeks with pre-existing pressure overload (Fig. 33). Regarding systolic function, the Scx-fKO TAC animals showed better LVEFs than WT TAC animals even after 12 weeks of pressure overload (Fig. 34). Our proof-of-concept study reveals that targeting fibrosis alone can significantly improve cardiac function and survival. Scleraxis plays a crucial

role in pressure overload-associated cardiac fibrosis, and timely knockdown of scleraxis could eliminate the myofibroblast population by directly targeting periostin expression at the transcriptional level. Thus, scleraxis may be a potent antifibrotic target for patients with pre-existing heart failure to improve overall health and patient care management (Fig. 48).

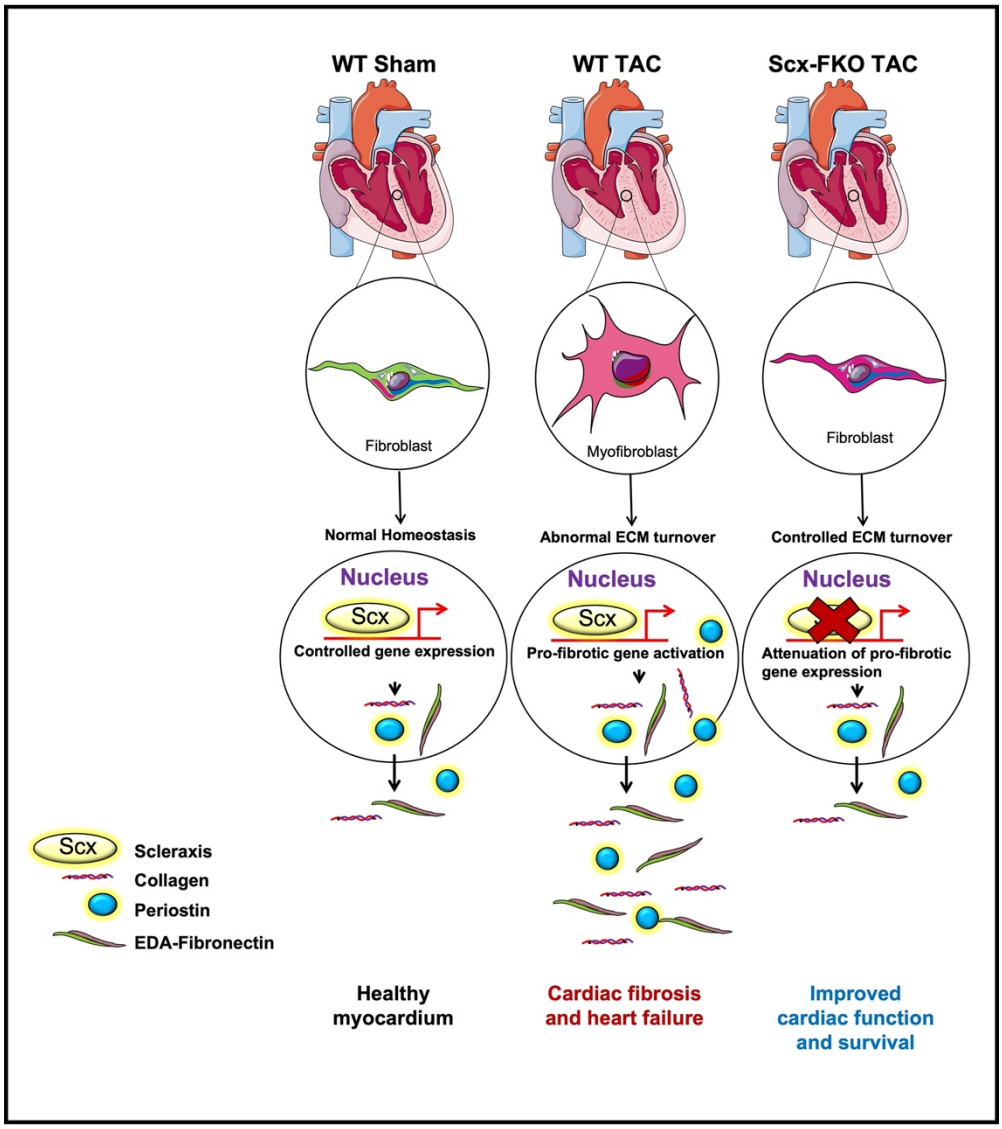

Figure 48: Role of scleraxis in the pressure-overloaded myocardium.
This schematic representation details scleraxis function in normal and pathological conditions. Scleraxis transcriptionally controls ECM gene expression to maintain cardiac matrix homeostasis, whereas, during pathological remodelling, scleraxis promotes

profibrotic gene expression responsible for cardiac fibrosis and heart failure. Furthermore, scleraxis gene deletion limited myofibroblast activation and attenuated cardiac fibrosis inside pressure-overloaded myocardium. Most importantly, scleraxis gene deletion improves survival rate compared to control animals. These heart, fibroblast and myofibroblast images were adopted from the Smart Medical Servier Art and copyright obtained from Creative Commons Attribution 3.0 Unported License. https://smart.servier.com/

Aim 2: Scleraxis transcriptionally regulates matrix proteins periostin and MMP2

Cardiac ECM remodelling plays a vital role in the preservation of myocardial function after acute myocardial injury. Several key players are involved in this early adaptation process, in which fibroblast activation and conversion to myofibroblasts play an essential role in infarct scar formation. The molecular mechanisms responsible for fibroblast activation and adverse remodelling related to fibrosis are not fully characterized. Identification of these mechanisms continues to be a critical goal in the field, as cardiac fibrosis remains without direct treatment options despite its significant impact on patient morbidity and mortality.

Previously, our lab demonstrated that scleraxis could transcriptionally regulate a variety of fibrosis-associated genes like Col-1α2, α-SMA, and fibronectin via direct binding to E-boxes in target gene promoters [165, 288, 317]. Our current pressure-overload study revealed a parallel elevation of scleraxis and periostin expression after 4 weeks of TAC (Fig. 10), whereas periostin expression is attenuated in scleraxis conditional knockout pressure-overloaded hearts leading to a reduction in cardiac fibrosis (Figs 14 and 15). Previous work from our lab showed that MMP2 expression increased with scleraxis overexpression and decreased in scleraxis-null (KO) mice [288]. These results suggest that periostin and MMP2 may be a direct gene target of the transcription factor scleraxis.

Our current study results demonstrate that scleraxis overexpression is sufficient to promote both mRNA and protein expression of periostin and MMP2 in cardiac

myofibroblasts (Figs 37A, 37B, 37C, 42A, 42B, 42C, and 42D). Furthermore, we now report a novel transcriptional regulatory mechanism, in which scleraxis directly binds to specific E-boxes present in the proximal gene promoters of human periostin and MMP2, and transcriptionally controls their gene expression (Figs 38 and 43). These promoter bindings are validated by luciferase, electrophoretic mobility shift, and ChIP assays (Figs 38B, 38C, 39A, 39B, 43B, 43C, 44A, and 44B). These results suggest that scleraxis plays a central role in regulating multiple target genes responsible for cardiac ECM remodelling.

TGFβ is a potent profibrotic signalling mediator that promotes the fibroblast-to-myofibroblast activation involved in pathological remodelling. Previous studies from our lab reported that scleraxis is sufficient and necessary for converting cardiac fibroblasts to myofibroblasts and is a critical effector of TGFβ1/Smad signalling [164, 330]. In the current study, we report that TGFβ1 treatment of primary cardiac myofibroblasts showed elevated scleraxis, periostin, and MMP-2 expression. However, scleraxis-null (KO) primary cardiac myofibroblasts failed to respond to TGFβ1-mediated induction of periostin and MMP-2 expression (Figs 40A, 40B, and 47E). These results combined with our previous studies find that scleraxis is essential for TGFβ1-mediated regulation of periostin and MMP-2 expression in cardiac myofibroblasts.

Additionally, primary scleraxis-null (KO) cardiac fibroblasts showed a drastic reduction of periostin and MMP-2 expression. Replenishing scleraxis expression via adenoviral-mediated overexpression in scleraxis-null primary cardiac fibroblasts resulted in increased expression of periostin and MMP-2 (Figs 41, 46A, and 46B). These results cement our previous claims that scleraxis is necessary and sufficient to drive the target genes.

Myocardial fibrosis is an effect of mechanical stress or infarction, but the molecular mechanism behind this remodelling process is poorly characterized. In the course of cardiac wound healing, there is a significant overlap between scleraxis, periostin, and MMP-2 expression patterns, roles in tissue repair and fibrosis, and effects of gain or loss of function. The current pressure-overload study provides a detailed

mechanistic role for scleraxis in fibrotic myocardium; here, scleraxis acts as a core regulator of the periostin-mediated myofibroblast population contributing to cardiac fibrosis. We believe that the early part of tissue injury requires scleraxis for scar formation and tissue repair, while targeting scleraxis at later stages will prevent cardiac fibrosis. Thus, timely intervention against scleraxis using pharmaceuticals will open new opportunities for cardiac remodelling and tissue repair.

CHAPTER VI: CONCLUSION

According to the results from our current study, we conclude that:

Aim 1: Scleraxis regulates pressure-overload-induced cardiac fibrosis

- Scleraxis and periostin expression were elevated in pressure-overloaded myocardium after 4 weeks.

Scleraxis gene deletion prior to 8 weeks of pressure overload:

- Does not affect cardiac hypertrophy but attenuates cardiac fibrosis.
- Reduces the periostin-positive myofibroblast population.
- Improves cardiac systolic and diastolic function.

Scleraxis gene deletion after 4 weeks of pressure overload:

- Does not affect cardiac hypertrophy but reduces cardiac interstitial fibrosis.
- Limits the periostin-positive myofibroblast population in pre-existing pressure-overloaded myocardium.
- Preserves cardiac systolic and diastolic function.

Scleraxis gene deletion in long-term pre-existing pressure overload:

- Results in improved survival rate compared with control animals.
- Improves cardiac systolic function.

Aim 2: Scleraxis transcriptionally regulates matrix proteins periostin and MMP2

- Scleraxis transactivates human periostin and MMP-2 gene promoters by directly binding to the E-boxes present in the proximal promoter.

- Scleraxis-null primary cardiac fibroblasts fail to respond to TGFβ1-mediated induction of periostin and MMP-2 expression.

- Rescuing scleraxis expression in scleraxis-null primary cardiac fibroblasts restores periostin and MMP-2 expression.

CHAPTER VII: STUDY LIMITATIONS AND FUTURE DIRECTIONS

The current study provides a deeper insight into scleraxis-dependent profibrotic gene activation and cardiac fibrosis in pressure-overloaded myocardium, and demonstrates pathways for cardiac functional benefits. Additionally, it describes scleraxis-mediated direct transactivation of periostin and MMP2 promoters in cardiac myofibroblasts. Overall, scleraxis plays a central role in regulating pressure overload-induced cardiac fibrosis. Although our study is foundationally solid and produced a wealth of evidence to support our hypothesis, there are limitations with our study. These limitations can be addressed by future studies in our lab.

First, in the pressure-overloaded myocardium with set endpoints of 4, 8, and 12 weeks after TAC, we missed the peak expression of several matrix proteins and profibrotic signalling proteins like α-SMA, MMPs, TIMPs, TGFβ-1, and Smads in the myocardial tissues. In future studies, we would set up earlier endpoints such as 1 and 2 weeks after TAC.

Second, when we gavaged the animals orally for 5 days (either with tamoxifen or corn oil to delete the scleraxis gene), we lost several small animals prior to the Endpoint due to tracheal inflammation. To avoid this complication in future animal studies, we would feed them instead with a tamoxifen chow diet.

Third, the most critical study limitation was that the Tcf21-iCre-based gene deletion cassette did not contain fluorescent tags, which made it difficult to trace the target gene-deleted cells. Because there are no specific markers available to tag cardiac fibroblasts, previously used marker proteins were also expressed in other neighbouring cells. Currently, Tcf21-iCre -R26R^{YFP} or Tcf21-iCre -R26R^{tdTomato} mouse lines are available on the market, and they can be crossed with Scxfl/fl mouse to get fluorescent-tagged deletion cassettes. Scleraxis gene deletion will enable the fluorescent marker proteins to help trace the cells. These mouse lines can be added to future studies.

Future directions of the study

Study direction 1: Wound healing is a crucial process that determines the integrity and function of tissue after injury. Cardiac fibrosis is evident in tissues when improper or prolonged wound healing has occurred. For example, during skin wound healing after scar formation, myofibroblasts are removed from the injury area by apoptosis, regression of scar and recellularization with newer cells, which completes the wound healing process and prevents fibrosis at the injury site. However, cardiac wound healing is more complicated, because of terminally differentiated cardiomyocytes, which cannot repopulate at the injury area, myofibroblasts evade the apoptosis and stay near the injury site longer than expected, which eventually leads to chronic inflammation and myocardial fibrosis. Thus, myofibroblast removal is essential after wound healing to avoid adverse outcomes.

In our current pressure-overload study, we noticed cell death in scleraxis gene-deleted pressure-overloaded animals but not in WT TAC animals (Fig. 49). We believe that these dead cells are cardiac myofibroblasts due to a reduction in periostin-positive cells along with fibrosis attenuation and an improvement in cardiac function. Although we were not able to verify that the dead cells were myofibroblasts (due to lack of specific marker proteins), this could be addressed in the future by counter-staining cardiomyocytes with cardiac troponin I. Previously our lab reported that scleraxis-null cardiac fibroblasts failed to respond to the stretch-mediated myofibroblast activation. It is now clear that the activated myofibroblasts require scleraxis to stay alive, while lack of scleraxis promotes the myofibroblasts to undergo apoptosis. Our results are preliminary and require further studies to determine the nature of the scleraxis-mediated myofibroblast regulation.

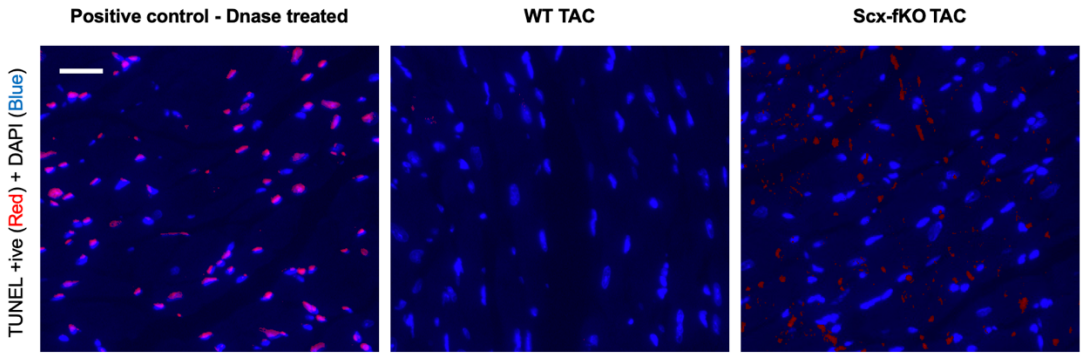

Figure 49: Scleraxis gene deletion promotes myofibroblast apoptosis in pressure-overloaded myocardium.

Cardiac cells that underwent pressure overload for 8 weeks were stained with TUNEL (red) and DAPI (blue), and showed increased myofibroblast cell death by apoptosis in Scx-fKO compared to WT; n=1.

Study direction 2: To investigate the potential impacts of scleraxis gene deletion after MI. Based on our previous studies as well as our current pressure-overload study, scleraxis expression is essential in defining the myofibroblast phenotype, which can help stabilize the myocardium after acute MI. Scleraxis gene deletion prior to MI could detrimentally affect the acute scar formation after injury, possibly leading to cardiac rapture. Thus, studying scleraxis gene deletion after scar formation (3, 4, 6, and 8 weeks post-MI) may elucidate cardiac functional benefits of this approach and whether fibrosis-associated adverse outcomes can be avoided.

Study direction 3: For an effective wound healing process in preclinical or *in vivo* animal models, the timely intervention of scleraxis is essential to avoid pathological remodelling. X-ray crystallographic determination of scleraxis protein structure will provide a better insight into high throughput screening for drugs or small molecules. Once viable target molecules are found, it can be helpful in the anti-fibrotic treatment in small animal models after injury.

REFERENCES

1. Weber, K.T., *Cardiac interstitium in health and disease: the fibrillar collagen network.* J Am Coll Cardiol, 1989. **13**(7): p. 1637-52.
2. Janicki, J.S., et al., *Ventricular remodeling in heart failure: the role of myocardial collagen.* Adv Exp Med Biol, 1995. **382**: p. 239-45.
3. Francis Stuart, S.D., et al., *The crossroads of inflammation, fibrosis, and arrhythmia following myocardial infarction.* J Mol Cell Cardiol, 2016. **91**: p. 114-22.
4. Li, F., et al., *Diffuse myocardial fibrosis and the prognosis of heart failure with reduced ejection fraction in Chinese patients: a cohort study.* Int J Cardiovasc Imaging, 2020. **36**(4): p. 671-689.
5. Echegaray, K., et al., *Role of Myocardial Collagen in Severe Aortic Stenosis With Preserved Ejection Fraction and Symptoms of Heart Failure.* Rev Esp Cardiol (Engl Ed), 2017. **70**(10): p. 832-840.
6. Paulus, W.J. and C. Tschope, *A novel paradigm for heart failure with preserved ejection fraction: comorbidities drive myocardial dysfunction and remodeling through coronary microvascular endothelial inflammation.* J Am Coll Cardiol, 2013. **62**(4): p. 263-71.
7. Martos, R., et al., *Diastolic heart failure: evidence of increased myocardial collagen turnover linked to diastolic dysfunction.* Circulation, 2007. **115**(7): p. 888-95.
8. Sweeney, M., B. Corden, and S.A. Cook, *Targeting cardiac fibrosis in heart failure with preserved ejection fraction: mirage or miracle?* EMBO Mol Med, 2020. **12**(10): p. e10865.
9. Gulati, A., et al., *Association of fibrosis with mortality and sudden cardiac death in patients with nonischemic dilated cardiomyopathy.* JAMA, 2013. **309**(9): p. 896-908.
10. Weber, K.T. and C.G. Brilla, *Pathological hypertrophy and cardiac interstitium. Fibrosis and renin-angiotensin-aldosterone system.* Circulation, 1991. **83**(6): p. 1849-65.
11. Dang, S., et al., *Blockade of beta-adrenergic signaling suppresses inflammasome and alleviates cardiac fibrosis.* Ann Transl Med, 2020. **8**(4): p. 127.
12. Weber, K.T., et al., *Collagen remodeling of the pressure-overloaded, hypertrophied nonhuman primate myocardium.* Circ Res, 1988. **62**(4): p. 757-65.
13. Tanaka, M., et al., *Quantitative analysis of myocardial fibrosis in normals, hypertensive hearts, and hypertrophic cardiomyopathy.* Br Heart J, 1986. **55**(6): p. 575-81.
14. Boudina, S. and E.D. Abel, *Diabetic cardiomyopathy revisited.* Circulation, 2007. **115**(25): p. 3213-23.
15. Weber, K.T. and C.G. Brilla, *Factors associated with reactive and reparative fibrosis of the myocardium.* Basic Res Cardiol, 1992. **87 Suppl 1**: p. 291-301.
16. Brooks, A., et al., *Interstitial fibrosis in the dilated non-ischaemic myocardium.* Heart, 2003. **89**(10): p. 1255-6.

17. Treibel, T.A., et al., *Reappraising myocardial fibrosis in severe aortic stenosis: an invasive and non-invasive study in 133 patients.* Eur Heart J, 2018. **39**(8): p. 699-709.
18. Edwards, N.C., et al., *Quantification of left ventricular interstitial fibrosis in asymptomatic chronic primary degenerative mitral regurgitation.* Circ Cardiovasc Imaging, 2014. **7**(6): p. 946-53.
19. Shinde, A.V. and N.G. Frangogiannis, *Fibroblasts in myocardial infarction: a role in inflammation and repair.* J Mol Cell Cardiol, 2014. **70**: p. 74-82.
20. van den Borne, S.W., et al., *Myocardial remodeling after infarction: the role of myofibroblasts.* Nat Rev Cardiol, 2010. **7**(1): p. 30-7.
21. Lopez, B., et al., *Identification of a potential cardiac antifibrotic mechanism of torasemide in patients with chronic heart failure.* J Am Coll Cardiol, 2007. **50**(9): p. 859-67.
22. Querejeta, R., et al., *Serum carboxy-terminal propeptide of procollagen type I is a marker of myocardial fibrosis in hypertensive heart disease.* Circulation, 2000. **101**(14): p. 1729-35.
23. Lijnen, P.J., et al., *Serum collagen markers and heart failure.* Cardiovasc Hematol Disord Drug Targets, 2012. **12**(1): p. 51-5.
24. Lin, Y.H., et al., *The relationship between serum galectin-3 and serum markers of cardiac extracellular matrix turnover in heart failure patients.* Clin Chim Acta, 2009. **409**(1-2): p. 96-9.
25. Lopez-Andres, N., et al., *Association of galectin-3 and fibrosis markers with long-term cardiovascular outcomes in patients with heart failure, left ventricular dysfunction, and dyssynchrony: insights from the CARE-HF (Cardiac Resynchronization in Heart Failure) trial.* Eur J Heart Fail, 2012. **14**(1): p. 74-81.
26. Lombardi, R., et al., *Myocardial collagen turnover in hypertrophic cardiomyopathy.* Circulation, 2003. **108**(12): p. 1455-60.
27. Zhu, A., et al., *Scleraxis as a prognostic marker of myocardial fibrosis in hypertrophic cardiomyopathy (SPARC) study.* Can J Physiol Pharmacol, 2020. **98**(7): p. 459-465.
28. Picard, F., et al., *Increased cardiac mRNA expression of matrix metalloproteinase-1 (MMP-1) and its inhibitor (TIMP-1) in DCM patients.* Clin Res Cardiol, 2006. **95**(5): p. 261-9.
29. Chi, H., et al., *Circulating Connective Tissue Growth Factor Is Associated with Diastolic Dysfunction in Patients with Diastolic Heart Failure.* Cardiology, 2019. **143**(3-4): p. 77-84.
30. Segiet, O.A., et al., *Role of interleukins in heart failure with reduced ejection fraction.* Anatol J Cardiol, 2019. **22**(6): p. 287-299.
31. Laviades, C., et al., *Abnormalities of the extracellular degradation of collagen type I in essential hypertension.* Circulation, 1998. **98**(6): p. 535-40.
32. Zervoudaki, A., et al., *Plasma levels of active extracellular matrix metalloproteinases 2 and 9 in patients with essential hypertension before and after antihypertensive treatment.* J Hum Hypertens, 2003. **17**(2): p. 119-24.
33. Compton, G., et al., *Echocardiography as a Screening Test for Myocardial Scarring in Children with Hypertrophic Cardiomyopathy.* Int J Pediatr, 2016. **2016**: p. 1980636.

34. Kobayashi, T., et al., *Association between septal strain rate and histopathology in symptomatic hypertrophic cardiomyopathy patients undergoing septal myectomy.* Am Heart J, 2013. **166**(3): p. 503-11.
35. Fabiani, I., et al., *Micro-RNA-21 (biomarker) and global longitudinal strain (functional marker) in detection of myocardial fibrotic burden in severe aortic valve stenosis: a pilot study.* J Transl Med, 2016. **14**(1): p. 248.
36. Cordero-Reyes, A.M., et al., *Molecular and cellular correlates of cardiac function in end-stage DCM: a study using speckle tracking echocardiography.* JACC Cardiovasc Imaging, 2014. **7**(5): p. 441-52.
37. Witjas-Paalberends, E.R., *Familial hypertrophic cardiomyopathy: an energetic story about cellular remodeling and sarcomere function.* 2014.
38. Moon, J.C., et al., *Myocardial T1 mapping and extracellular volume quantification: a Society for Cardiovascular Magnetic Resonance (SCMR) and CMR Working Group of the European Society of Cardiology consensus statement.* J Cardiovasc Magn Reson, 2013. **15**: p. 92.
39. Messroghli, D.R., et al., *Modified Look-Locker inversion recovery (MOLLI) for high-resolution T1 mapping of the heart.* Magn Reson Med, 2004. **52**(1): p. 141-6.
40. Piechnik, S.K., et al., *Shortened Modified Look-Locker Inversion recovery (ShMOLLI) for clinical myocardial T1-mapping at 1.5 and 3 T within a 9 heartbeat breathhold.* J Cardiovasc Magn Reson, 2010. **12**: p. 69.
41. Wu, E., et al., *Infarct size by contrast enhanced cardiac magnetic resonance is a stronger predictor of outcomes than left ventricular ejection fraction or end-systolic volume index: prospective cohort study.* Heart, 2008. **94**(6): p. 730-6.
42. Roes, S.D., et al., *Comparison of myocardial infarct size assessed with contrast-enhanced magnetic resonance imaging and left ventricular function and volumes to predict mortality in patients with healed myocardial infarction.* Am J Cardiol, 2007. **100**(6): p. 930-6.
43. Mascherbauer, J., et al., *Cardiac magnetic resonance postcontrast T1 time is associated with outcome in patients with heart failure and preserved ejection fraction.* Circ Cardiovasc Imaging, 2013. **6**(6): p. 1056-65.
44. Kuruvilla, S., et al., *Increased extracellular volume and altered mechanics are associated with LVH in hypertensive heart disease, not hypertension alone.* JACC Cardiovasc Imaging, 2015. **8**(2): p. 172-80.
45. Moon, J.C., et al., *The histologic basis of late gadolinium enhancement cardiovascular magnetic resonance in hypertrophic cardiomyopathy.* J Am Coll Cardiol, 2004. **43**(12): p. 2260-4.
46. Leyva, F., et al., *Left ventricular midwall fibrosis as a predictor of mortality and morbidity after cardiac resynchronization therapy in patients with nonischemic cardiomyopathy.* J Am Coll Cardiol, 2012. **60**(17): p. 1659-67.
47. Yu, C.M., et al., *Effects of combination of angiotensin-converting enzyme inhibitor and angiotensin receptor antagonist on inflammatory cellular infiltration and myocardial interstitial fibrosis after acute myocardial infarction.* J Am Coll Cardiol, 2001. **38**(4): p. 1207-15.
48. Sodhi, S.S., et al., *Effects of eplerenone on markers of myocardial fibrosis, 6-minute walk distance, and quality of life in adults with tetralogy of Fallot and*

complete transposition of the great arteries. Proc (Bayl Univ Med Cent), 2018. **31**(1): p. 12-19.
49. Shao, P.P., et al., *Eplerenone Reverses Cardiac Fibrosis via the Suppression of Tregs by Inhibition of Kv1.3 Channel.* Front Physiol, 2018. **9**: p. 899.
50. King, T.E., Jr., et al., *A phase 3 trial of pirfenidone in patients with idiopathic pulmonary fibrosis.* N Engl J Med, 2014. **370**(22): p. 2083-92.
51. Richeldi, L., et al., *Design of the INPULSIS trials: two phase 3 trials of nintedanib in patients with idiopathic pulmonary fibrosis.* Respir Med, 2014. **108**(7): p. 1023-30.
52. Noth, I., et al., *Cardiovascular safety of nintedanib in subgroups by cardiovascular risk at baseline in the TOMORROW and INPULSIS trials.* Eur Respir J, 2019. **54**(3).
53. Lee, K.W., et al., *Pirfenidone prevents the development of a vulnerable substrate for atrial fibrillation in a canine model of heart failure.* Circulation, 2006. **114**(16): p. 1703-12.
54. Yamazaki, T., et al., *The antifibrotic agent pirfenidone inhibits angiotensin II-induced cardiac hypertrophy in mice.* Hypertens Res, 2012. **35**(1): p. 34-40.
55. Shi, Q., et al., *In vitro effects of pirfenidone on cardiac fibroblasts: proliferation, myofibroblast differentiation, migration and cytokine secretion.* PLoS One, 2011. **6**(11): p. e28134.
56. Xiao, H., et al., *Metformin attenuates cardiac fibrosis by inhibiting the TGFbeta1-Smad3 signalling pathway.* Cardiovasc Res, 2010. **87**(3): p. 504-13.
57. Rangarajan, S., et al., *Metformin reverses established lung fibrosis in a bleomycin model.* Nat Med, 2018. **24**(8): p. 1121-1127.
58. Ma, Z.G., et al., *Piperine Attenuates Pathological Cardiac Fibrosis Via PPAR-gamma/AKT Pathways.* EBioMedicine, 2017. **18**: p. 179-187.
59. Wei, W.Y., et al., *Pioglitazone Alleviates Cardiac Fibrosis and Inhibits Endothelial to Mesenchymal Transition Induced by Pressure Overload.* Cell Physiol Biochem, 2018. **45**(1): p. 26-36.
60. de Jong, S., et al., *Fibrosis and cardiac arrhythmias.* J Cardiovasc Pharmacol, 2011. **57**(6): p. 630-8.
61. Disertori, M., M. Mase, and F. Ravelli, *Myocardial fibrosis predicts ventricular tachyarrhythmias.* Trends Cardiovasc Med, 2017. **27**(5): p. 363-372.
62. Ciulla, M., et al., *Echocardiographic patterns of myocardial fibrosis in hypertensive patients: endomyocardial biopsy versus ultrasonic tissue characterization.* J Am Soc Echocardiogr, 1997. **10**(6): p. 657-64.
63. Burke, A.P., et al., *Effect of hypertension and cardiac hypertrophy on coronary artery morphology in sudden cardiac death.* Circulation, 1996. **94**(12): p. 3138-45.
64. Brilla, C.G., R.C. Funck, and H. Rupp, *Lisinopril-mediated regression of myocardial fibrosis in patients with hypertensive heart disease.* Circulation, 2000. **102**(12): p. 1388-93.
65. Burlew, B.S. and K.T. Weber, *Cardiac fibrosis as a cause of diastolic dysfunction.* Herz, 2002. **27**(2): p. 92-8.
66. Burlew, B.S. and K.T. Weber, *Connective tissue and the heart. Functional significance and regulatory mechanisms.* Cardiol Clin, 2000. **18**(3): p. 435-42.

67. Schwartzkopff, B., et al., *Structural and functional alterations of the intramyocardial coronary arterioles in patients with arterial hypertension.* Circulation, 1993. **88**(3): p. 993-1003.
68. Villarreal, F.J. and W.H. Dillmann, *Cardiac hypertrophy-induced changes in mRNA levels for TGF-beta 1, fibronectin, and collagen.* Am J Physiol, 1992. **262**(6 Pt 2): p. H1861-6.
69. Takahashi, N., et al., *Hypertrophic stimuli induce transforming growth factor-beta 1 expression in rat ventricular myocytes.* J Clin Invest, 1994. **94**(4): p. 1470-6.
70. Porreca, E., et al., *Increased transforming growth factor-beta production and gene expression by peripheral blood monocytes of hypertensive patients.* Hypertension, 1997. **30**(1 Pt 1): p. 134-9.
71. Brilla, C.G., et al., *Collagen metabolism in cultured adult rat cardiac fibroblasts: response to angiotensin II and aldosterone.* J Mol Cell Cardiol, 1994. **26**(7): p. 809-20.
72. Hayakawa, Y., et al., *High salt intake damages the heart through activation of cardiac (pro) renin receptors even at an early stage of hypertension.* PLoS One, 2015. **10**(3): p. e0120453.
73. Zannad, F., et al., *Limitation of excessive extracellular matrix turnover may contribute to survival benefit of spironolactone therapy in patients with congestive heart failure: insights from the randomized aldactone evaluation study (RALES). Rales Investigators.* Circulation, 2000. **102**(22): p. 2700-6.
74. Lopez, B., et al., *Usefulness of serum carboxy-terminal propeptide of procollagen type I in assessment of the cardioreparative ability of antihypertensive treatment in hypertensive patients.* Circulation, 2001. **104**(3): p. 286-91.
75. Diez, J., et al., *Losartan-dependent regression of myocardial fibrosis is associated with reduction of left ventricular chamber stiffness in hypertensive patients.* Circulation, 2002. **105**(21): p. 2512-7.
76. Wu, L.M., et al., *Fibrosis quantification in Hypertensive Heart Disease with LVH and Non-LVH: Findings from T1 mapping and Contrast-free Cardiac Diffusion-weighted imaging.* Sci Rep, 2017. **7**(1): p. 559.
77. Treibel, T.A., et al., *Extracellular volume quantification in isolated hypertension - changes at the detectable limits?* J Cardiovasc Magn Reson, 2015. **17**: p. 74.
78. Brilla, C.G., J.S. Janicki, and K.T. Weber, *Impaired diastolic function and coronary reserve in genetic hypertension. Role of interstitial fibrosis and medial thickening of intramyocardial coronary arteries.* Circ Res, 1991. **69**(1): p. 107-15.
79. Brilla, C.G., L. Matsubara, and K.T. Weber, *Advanced hypertensive heart disease in spontaneously hypertensive rats. Lisinopril-mediated regression of myocardial fibrosis.* Hypertension, 1996. **28**(2): p. 269-75.
80. Schmieder, R.E., P. Martus, and A. Klingbeil, *Reversal of left ventricular hypertrophy in essential hypertension. A meta-analysis of randomized double-blind studies.* JAMA, 1996. **275**(19): p. 1507-13.
81. Pitt, B., et al., *Effects of eplerenone, enalapril, and eplerenone/enalapril in patients with essential hypertension and left ventricular hypertrophy: the 4E-left ventricular hypertrophy study.* Circulation, 2003. **108**(15): p. 1831-8.

82. de Boer, R.A., et al., *Towards better definition, quantification and treatment of fibrosis in heart failure. A scientific roadmap by the Committee of Translational Research of the Heart Failure Association (HFA) of the European Society of Cardiology.* Eur J Heart Fail, 2019. **21**(3): p. 272-285.
83. Kanisicak, O., et al., *Genetic lineage tracing defines myofibroblast origin and function in the injured heart.* Nat Commun, 2016. **7**: p. 12260.
84. Gladka, M.M., et al., *Single-Cell Sequencing of the Healthy and Diseased Heart Reveals Cytoskeleton-Associated Protein 4 as a New Modulator of Fibroblasts Activation.* Circulation, 2018. **138**(2): p. 166-180.
85. Schafer, S., et al., *IL-11 is a crucial determinant of cardiovascular fibrosis.* Nature, 2017. **552**(7683): p. 110-115.
86. Soliman, H. and F.M.V. Rossi, *Cardiac fibroblast diversity in health and disease.* Matrix Biol, 2020. **91-92**: p. 75-91.
87. Tallquist, M.D., *Cardiac Fibroblast Diversity.* Annu Rev Physiol, 2020. **82**: p. 63-78.
88. Fu, X., et al., *Specialized fibroblast differentiated states underlie scar formation in the infarcted mouse heart.* J Clin Invest, 2018. **128**(5): p. 2127-2143.
89. Hinz, B. and D. Lagares, *Evasion of apoptosis by myofibroblasts: a hallmark of fibrotic diseases.* Nat Rev Rheumatol, 2020. **16**(1): p. 11-31.
90. Czubryt, M.P., *Common threads in cardiac fibrosis, infarct scar formation, and wound healing.* Fibrogenesis Tissue Repair, 2012. **5**(1): p. 19.
91. Sutton, M.G. and N. Sharpe, *Left ventricular remodeling after myocardial infarction: pathophysiology and therapy.* Circulation, 2000. **101**(25): p. 2981-8.
92. Bacmeister, L., et al., *Inflammation and fibrosis in murine models of heart failure.* Basic Res Cardiol, 2019. **114**(3): p. 19.
93. Frangogiannis, N.G., *The inflammatory response in myocardial injury, repair, and remodelling.* Nat Rev Cardiol, 2014. **11**(5): p. 255-65.
94. Dobaczewski, M., C. Gonzalez-Quesada, and N.G. Frangogiannis, *The extracellular matrix as a modulator of the inflammatory and reparative response following myocardial infarction.* J Mol Cell Cardiol, 2010. **48**(3): p. 504-11.
95. Barallobre-Barreiro, J., et al., *Proteomics analysis of cardiac extracellular matrix remodeling in a porcine model of ischemia/reperfusion injury.* Circulation, 2012. **125**(6): p. 789-802.
96. Heino, J., *The collagen receptor integrins have distinct ligand recognition and signaling functions.* Matrix Biol, 2000. **19**(4): p. 319-23.
97. Amin, P., M. Singh, and K. Singh, *beta-Adrenergic Receptor-Stimulated Cardiac Myocyte Apoptosis: Role of beta1 Integrins.* J Signal Transduct, 2011. **2011**: p. 179057.
98. Rosamond, W., et al., *Heart disease and stroke statistics--2008 update: a report from the American Heart Association Statistics Committee and Stroke Statistics Subcommittee.* Circulation, 2008. **117**(4): p. e25-146.
99. Pfeffer, M.A. and J.M. Pfeffer, *Ventricular enlargement and reduced survival after myocardial infarction.* Circulation, 1987. **75**(5 Pt 2): p. IV93-7.
100. Pfeffer, M.A., et al., *Survival after an experimental myocardial infarction: beneficial effects of long-term therapy with captopril.* Circulation, 1985. **72**(2): p. 406-12.

101. Ibanez, B., et al., *2017 ESC Guidelines for the management of acute myocardial infarction in patients presenting with ST-segment elevation: The Task Force for the management of acute myocardial infarction in patients presenting with ST-segment elevation of the European Society of Cardiology (ESC).* Eur Heart J, 2018. **39**(2): p. 119-177.
102. Pfeffer, M.A., et al., *Effect of captopril on mortality and morbidity in patients with left ventricular dysfunction after myocardial infarction. Results of the survival and ventricular enlargement trial. The SAVE Investigators.* N Engl J Med, 1992. **327**(10): p. 669-77.
103. Levine, G.N., et al., *2015 ACC/AHA/SCAI Focused Update on Primary Percutaneous Coronary Intervention for Patients With ST-Elevation Myocardial Infarction: An Update of the 2011 ACCF/AHA/SCAI Guideline for Percutaneous Coronary Intervention and the 2013 ACCF/AHA Guideline for the Management of ST-Elevation Myocardial Infarction.* J Am Coll Cardiol, 2016. **67**(10): p. 1235-1250.
104. Aronow, W.S., et al., *Prognosis of congestive heart failure in patients aged > or = 62 years with unoperated severe valvular aortic stenosis.* Am J Cardiol, 1993. **72**(11): p. 846-8.
105. Aronow, W.S., et al., *Prognosis of patients with heart failure and unoperated severe aortic valvular regurgitation and relation to ejection fraction.* Am J Cardiol, 1994. **74**(3): p. 286-8.
106. Joint Task Force on the Management of Valvular Heart Disease of the European Society of, C., et al., *Guidelines on the management of valvular heart disease (version 2012).* Eur Heart J, 2012. **33**(19): p. 2451-96.
107. Kitkungvan, D., et al., *Myocardial Fibrosis in Patients With Primary Mitral Regurgitation With and Without Prolapse.* J Am Coll Cardiol, 2018. **72**(8): p. 823-834.
108. Bui, A.H., et al., *Diffuse myocardial fibrosis in patients with mitral valve prolapse and ventricular arrhythmia.* Heart, 2017. **103**(3): p. 204-209.
109. Constant Dit Beaufils, A.L., et al., *Replacement Myocardial Fibrosis in Patients With Mitral Valve Prolapse: Relation to Mitral Regurgitation, Ventricular Remodeling, and Arrhythmia.* Circulation, 2021. **143**(18): p. 1763-1774.
110. Basso, C., et al., *Arrhythmic Mitral Valve Prolapse and Sudden Cardiac Death.* Circulation, 2015. **132**(7): p. 556-66.
111. Han, Y., et al., *Cardiovascular magnetic resonance characterization of mitral valve prolapse.* JACC Cardiovasc Imaging, 2008. **1**(3): p. 294-303.
112. Vohra, J., et al., *Malignant ventricular arrhythmias in patients with mitral valve prolapse and mild mitral regurgitation.* Pacing Clin Electrophysiol, 1993. **16**(3 Pt 1): p. 387-93.
113. Farb, A., et al., *Comparison of cardiac findings in patients with mitral valve prolapse who die suddenly to those who have congestive heart failure from mitral regurgitation and to those with fatal noncardiac conditions.* Am J Cardiol, 1992. **70**(2): p. 234-9.
114. Duren, D.R., A.E. Becker, and A.J. Dunning, *Long-term follow-up of idiopathic mitral valve prolapse in 300 patients: a prospective study.* J Am Coll Cardiol, 1988. **11**(1): p. 42-7.

115. Sriram, C.S., et al., *Malignant bileaflet mitral valve prolapse syndrome in patients with otherwise idiopathic out-of-hospital cardiac arrest.* J Am Coll Cardiol, 2013. **62**(3): p. 222-230.
116. Nishimura, R.A., et al., *2017 AHA/ACC Focused Update of the 2014 AHA/ACC Guideline for the Management of Patients With Valvular Heart Disease: A Report of the American College of Cardiology/American Heart Association Task Force on Clinical Practice Guidelines.* Circulation, 2017. **135**(25): p. e1159-e1195.
117. Dweck, M.R., N.A. Boon, and D.E. Newby, *Calcific aortic stenosis: a disease of the valve and the myocardium.* J Am Coll Cardiol, 2012. **60**(19): p. 1854-63.
118. Liu, A.C., V.R. Joag, and A.I. Gotlieb, *The emerging role of valve interstitial cell phenotypes in regulating heart valve pathobiology.* Am J Pathol, 2007. **171**(5): p. 1407-18.
119. O'Brien, K.D., et al., *Association of angiotensin-converting enzyme with low-density lipoprotein in aortic valvular lesions and in human plasma.* Circulation, 2002. **106**(17): p. 2224-30.
120. Sainger, R., et al., *Human myxomatous mitral valve prolapse: role of bone morphogenetic protein 4 in valvular interstitial cell activation.* J Cell Physiol, 2012. **227**(6): p. 2595-604.
121. Bonow, R.O., et al., *2008 Focused update incorporated into the ACC/AHA 2006 guidelines for the management of patients with valvular heart disease: a report of the American College of Cardiology/American Heart Association Task Force on Practice Guidelines (Writing Committee to Revise the 1998 Guidelines for the Management of Patients With Valvular Heart Disease): endorsed by the Society of Cardiovascular Anesthesiologists, Society for Cardiovascular Angiography and Interventions, and Society of Thoracic Surgeons.* Circulation, 2008. **118**(15): p. e523-661.
122. Hein, S., et al., *Progression from compensated hypertrophy to failure in the pressure-overloaded human heart: structural deterioration and compensatory mechanisms.* Circulation, 2003. **107**(7): p. 984-91.
123. Krayenbuehl, H.P., et al., *Left ventricular myocardial structure in aortic valve disease before, intermediate, and late after aortic valve replacement.* Circulation, 1989. **79**(4): p. 744-55.
124. Weidemann, F., et al., *Impact of myocardial fibrosis in patients with symptomatic severe aortic stenosis.* Circulation, 2009. **120**(7): p. 577-84.
125. Azevedo, C.F., et al., *Prognostic significance of myocardial fibrosis quantification by histopathology and magnetic resonance imaging in patients with severe aortic valve disease.* J Am Coll Cardiol, 2010. **56**(4): p. 278-87.
126. Ng, C.M., et al., *TGF-beta-dependent pathogenesis of mitral valve prolapse in a mouse model of Marfan syndrome.* J Clin Invest, 2004. **114**(11): p. 1586-92.
127. Bing, R., et al., *Imaging and Impact of Myocardial Fibrosis in Aortic Stenosis.* JACC Cardiovasc Imaging, 2019. **12**(2): p. 283-296.
128. Regan, T.J., et al., *Evidence for cardiomyopathy in familial diabetes mellitus.* J Clin Invest, 1977. **60**(4): p. 884-99.
129. Kwong, R.Y., et al., *Incidence and prognostic implication of unrecognized myocardial scar characterized by cardiac magnetic resonance in diabetic patients*

without clinical evidence of myocardial infarction. Circulation, 2008. **118**(10): p. 1011-20.
130. Turkbey, E.B., et al., *Myocardial structure, function, and scar in patients with type 1 diabetes mellitus.* Circulation, 2011. **124**(16): p. 1737-46.
131. Wong, T.C., et al., *Myocardial extracellular volume fraction quantified by cardiovascular magnetic resonance is increased in diabetes and associated with mortality and incident heart failure admission.* Eur Heart J, 2014. **35**(10): p. 657-64.
132. Shamhart, P.E., et al., *Hyperglycemia enhances function and differentiation of adult rat cardiac fibroblasts.* Can J Physiol Pharmacol, 2014. **92**(7): p. 598-604.
133. Aguilar, H., et al., *Role for high-glucose-induced protein O-GlcNAcylation in stimulating cardiac fibroblast collagen synthesis.* Am J Physiol Cell Physiol, 2014. **306**(9): p. C794-804.
134. Huynh, K., et al., *Cardiac-specific IGF-1 receptor transgenic expression protects against cardiac fibrosis and diastolic dysfunction in a mouse model of diabetic cardiomyopathy.* Diabetes, 2010. **59**(6): p. 1512-20.
135. Ares-Carrasco, S., et al., *Myocardial fibrosis and apoptosis, but not inflammation, are present in long-term experimental diabetes.* Am J Physiol Heart Circ Physiol, 2009. **297**(6): p. H2109-19.
136. Li, J., et al., *Deficiency of rac1 blocks NADPH oxidase activation, inhibits endoplasmic reticulum stress, and reduces myocardial remodeling in a mouse model of type 1 diabetes.* Diabetes, 2010. **59**(8): p. 2033-42.
137. Hao, P.P., et al., *Angiotensin-(1-7) treatment mitigates right ventricular fibrosis as a distinctive feature of diabetic cardiomyopathy.* Am J Physiol Heart Circ Physiol, 2015. **308**(9): p. H1007-19.
138. Pupo, A.A., et al., *Department of Medicina, Faculdade de Medicina da Universidade de Sao Paulo, Brazil.* Diabetes, 1976. **25**(3): p. 161-6.
139. Haider, B., et al., *Influence of diabetes on the myocardium and coronary arteries of rhesus monkey fed an atherogenic diet.* Circ Res, 1981. **49**(6): p. 1278-88.
140. Zaman, A.K., et al., *Salutary effects of attenuation of angiotensin II on coronary perivascular fibrosis associated with insulin resistance and obesity.* J Mol Cell Cardiol, 2004. **37**(2): p. 525-35.
141. Khaidar, A., et al., *L-arginine reduces heart collagen accumulation in the diabetic db/db mouse.* Circulation, 1994. **90**(1): p. 479-83.
142. Gonzalez-Quesada, C., et al., *Thrombospondin-1 induction in the diabetic myocardium stabilizes the cardiac matrix in addition to promoting vascular rarefaction through angiopoietin-2 upregulation.* Circ Res, 2013. **113**(12): p. 1331-44.
143. Biernacka, A., et al., *Smad3 Signaling Promotes Fibrosis While Preserving Cardiac and Aortic Geometry in Obese Diabetic Mice.* Circ Heart Fail, 2015. **8**(4): p. 788-98.
144. Huynh, K., et al., *Coenzyme Q10 attenuates diastolic dysfunction, cardiomyocyte hypertrophy and cardiac fibrosis in the db/db mouse model of type 2 diabetes.* Diabetologia, 2012. **55**(5): p. 1544-53.
145. Segura, A.M., O.H. Frazier, and L.M. Buja, *Fibrosis and heart failure.* Heart Fail Rev, 2014. **19**(2): p. 173-85.

146. Fan, D., E.E. Creemers, and Z. Kassiri, *Matrix as an interstitial transport system.* Circ Res, 2014. **114**(5): p. 889-902.
147. Hynes, R.O., *The extracellular matrix: not just pretty fibrils.* Science, 2009. **326**(5957): p. 1216-9.
148. Jourdan-Lesaux, C., J. Zhang, and M.L. Lindsey, *Extracellular matrix roles during cardiac repair.* Life Sci, 2010. **87**(13-14): p. 391-400.
149. Colige, A., et al., *Cloning and characterization of ADAMTS-14, a novel ADAMTS displaying high homology with ADAMTS-2 and ADAMTS-3.* J Biol Chem, 2002. **277**(8): p. 5756-66.
150. Kessler, E., et al., *Bone morphogenetic protein-1: the type I procollagen C-proteinase.* Science, 1996. **271**(5247): p. 360-2.
151. Weber, K.T., *Monitoring tissue repair and fibrosis from a distance.* Circulation, 1997. **96**(8): p. 2488-92.
152. Lopez, B., et al., *Circulating Biomarkers of Myocardial Fibrosis: The Need for a Reappraisal.* J Am Coll Cardiol, 2015. **65**(22): p. 2449-56.
153. Cicoira, M., et al., *Independent and additional prognostic value of aminoterminal propeptide of type III procollagen circulating levels in patients with chronic heart failure.* J Card Fail, 2004. **10**(5): p. 403-11.
154. Eghbali, M., et al., *Collagen chain mRNAs in isolated heart cells from young and adult rats.* J Mol Cell Cardiol, 1988. **20**(3): p. 267-76.
155. Leask, A., *Getting to the heart of the matter: new insights into cardiac fibrosis.* Circ Res, 2015. **116**(7): p. 1269-76.
156. Kupfahl, C., et al., *Angiotensin II directly increases transforming growth factor beta1 and osteopontin and indirectly affects collagen mRNA expression in the human heart.* Cardiovasc Res, 2000. **46**(3): p. 463-75.
157. Eghbali, M., et al., *Cardiac fibroblasts are predisposed to convert into myocyte phenotype: specific effect of transforming growth factor beta.* Proc Natl Acad Sci U S A, 1991. **88**(3): p. 795-9.
158. Butt, R.P., G.J. Laurent, and J.E. Bishop, *Collagen production and replication by cardiac fibroblasts is enhanced in response to diverse classes of growth factors.* Eur J Cell Biol, 1995. **68**(3): p. 330-5.
159. Guarda, E., et al., *Effects of endothelins on collagen turnover in cardiac fibroblasts.* Cardiovasc Res, 1993. **27**(12): p. 2130-4.
160. Rizvi, M.A., et al., *The effects of endothelin-1 on collagen type I and type III synthesis in cultured porcine coronary artery vascular smooth muscle cells.* J Mol Cell Cardiol, 1996. **28**(2): p. 243-52.
161. Wang, B., et al., *Decreased Smad 7 expression contributes to cardiac fibrosis in the infarcted rat heart.* Am J Physiol Heart Circ Physiol, 2002. **282**(5): p. H1685-96.
162. Gao, X., et al., *Angiotensin II increases collagen I expression via transforming growth factor-beta1 and extracellular signal-regulated kinase in cardiac fibroblasts.* Eur J Pharmacol, 2009. **606**(1-3): p. 115-20.
163. Ma, F., et al., *Macrophage-stimulated cardiac fibroblast production of IL-6 is essential for TGF beta/Smad activation and cardiac fibrosis induced by angiotensin II.* PLoS One, 2012. **7**(5): p. e35144.

164. Espira, L., et al., *The basic helix-loop-helix transcription factor scleraxis regulates fibroblast collagen synthesis.* J Mol Cell Cardiol, 2009. **47**(2): p. 188-95.
165. Bagchi, R.A. and M.P. Czubryt, *Synergistic roles of scleraxis and Smads in the regulation of collagen 1alpha2 gene expression.* Biochim Biophys Acta, 2012. **1823**(10): p. 1936-44.
166. Thiele, B.J., et al., *RNA-binding proteins heterogeneous nuclear ribonucleoprotein A1, E1, and K are involved in post-transcriptional control of collagen I and III synthesis.* Circ Res, 2004. **95**(11): p. 1058-66.
167. Fraccarollo, D., et al., *Collagen accumulation after myocardial infarction: effects of ETA receptor blockade and implications for early remodeling.* Cardiovasc Res, 2002. **54**(3): p. 559-67.
168. Jugdutt, B.I. and R.W. Amy, *Healing after myocardial infarction in the dog: changes in infarct hydroxyproline and topography.* J Am Coll Cardiol, 1986. **7**(1): p. 91-102.
169. Querejeta, R., et al., *Increased collagen type I synthesis in patients with heart failure of hypertensive origin: relation to myocardial fibrosis.* Circulation, 2004. **110**(10): p. 1263-8.
170. Yamamoto, K., et al., *ACE inhibitor and angiotensin II type 1 receptor blocker differently regulate ventricular fibrosis in hypertensive diastolic heart failure.* J Hypertens, 2005. **23**(2): p. 393-400.
171. Ahumada, G.G., et al., *Cardiac fibronectin: developmental distribution and quantitative comparison of possible sites of synthesis.* J Mol Cell Cardiol, 1981. **13**(7): p. 667-78.
172. Johnson, C.M. and S.C. Helgeson, *Fibronectin biosynthesis and cell-surface expression by cardiac and non-cardiac endothelial cells.* Am J Pathol, 1993. **142**(5): p. 1401-8.
173. Stenman, S. and A. Vaheri, *Distribution of a major connective tissue protein, fibronectin, in normal human tissues.* J Exp Med, 1978. **147**(4): p. 1054-64.
174. George, E.L., et al., *Defects in mesoderm, neural tube and vascular development in mouse embryos lacking fibronectin.* Development, 1993. **119**(4): p. 1079-91.
175. Hynes, R., *Molecular biology of fibronectin.* Annu Rev Cell Biol, 1985. **1**: p. 67-90.
176. Li, L., Q. Zhao, and W. Kong, *Extracellular matrix remodeling and cardiac fibrosis.* Matrix Biol, 2018. **68-69**: p. 490-506.
177. Arslan, F., et al., *Lack of fibronectin-EDA promotes survival and prevents adverse remodeling and heart function deterioration after myocardial infarction.* Circ Res, 2011. **108**(5): p. 582-92.
178. Serini, G., et al., *The fibronectin domain ED-A is crucial for myofibroblastic phenotype induction by transforming growth factor-beta1.* J Cell Biol, 1998. **142**(3): p. 873-81.
179. Ammarguellat, F.Z., et al., *Fibrosis, matrix metalloproteinases, and inflammation in the heart of DOCA-salt hypertensive rats: role of ET(A) receptors.* Hypertension, 2002. **39**(2 Pt 2): p. 679-84.
180. Gabbiani, G., *The myofibroblast in wound healing and fibrocontractive diseases.* J Pathol, 2003. **200**(4): p. 500-3.

181. Valiente-Alandi, I., et al., *Inhibiting Fibronectin Attenuates Fibrosis and Improves Cardiac Function in a Model of Heart Failure.* Circulation, 2018. **138**(12): p. 1236-1252.
182. van Dijk, A., et al., *Accumulation of fibronectin in the heart after myocardial infarction: a putative stimulator of adhesion and proliferation of adipose-derived stem cells.* Cell Tissue Res, 2008. **332**(2): p. 289-98.
183. Heling, A., et al., *Increased expression of cytoskeletal, linkage, and extracellular proteins in failing human myocardium.* Circ Res, 2000. **86**(8): p. 846-53.
184. Magnusson, M.K. and D.F. Mosher, *Fibronectin: structure, assembly, and cardiovascular implications.* Arterioscler Thromb Vasc Biol, 1998. **18**(9): p. 1363-70.
185. van Keulen, J.K., et al., *Levels of extra domain A containing fibronectin in human atherosclerotic plaques are associated with a stable plaque phenotype.* Atherosclerosis, 2007. **195**(1): p. e83-91.
186. Samuel, J.L., et al., *Accumulation of fetal fibronectin mRNAs during the development of rat cardiac hypertrophy induced by pressure overload.* J Clin Invest, 1991. **88**(5): p. 1737-46.
187. Konstandin, M.H., et al., *Fibronectin contributes to pathological cardiac hypertrophy but not physiological growth.* Basic Res Cardiol, 2013. **108**(5): p. 375.
188. Pulakazhi Venu, V.K., et al., *Fibronectin extra domain A stabilises atherosclerotic plaques in apolipoprotein E and in LDL-receptor-deficient mice.* Thromb Haemost, 2015. **114**(1): p. 186-97.
189. Doddapattar, P., et al., *Differential Roles of Endothelial Cell-Derived and Smooth Muscle Cell-Derived Fibronectin Containing Extra Domain A in Early and Late Atherosclerosis.* Arterioscler Thromb Vasc Biol, 2020. **40**(7): p. 1738-1747.
190. Ulrich, M.M., et al., *Increased expression of fibronectin isoforms after myocardial infarction in rats.* J Mol Cell Cardiol, 1997. **29**(9): p. 2533-43.
191. Knowlton, A.A., et al., *Rapid expression of fibronectin in the rabbit heart after myocardial infarction with and without reperfusion.* J Clin Invest, 1992. **89**(4): p. 1060-8.
192. Willems, I.E., J.W. Arends, and M.J. Daemen, *Tenascin and fibronectin expression in healing human myocardial scars.* J Pathol, 1996. **179**(3): p. 321-5.
193. Kruzynska-Frejtag, A., et al., *Periostin (an osteoblast-specific factor) is expressed within the embryonic mouse heart during valve formation.* Mech Dev, 2001. **103**(1-2): p. 183-8.
194. Tkatchenko, T.V., et al., *Lack of periostin leads to suppression of Notch1 signaling and calcific aortic valve disease.* Physiol Genomics, 2009. **39**(3): p. 160-8.
195. Norris, R.A., et al., *Periostin regulates collagen fibrillogenesis and the biomechanical properties of connective tissues.* J Cell Biochem, 2007. **101**(3): p. 695-711.
196. Chamberlain, C.S., et al., *Temporal healing in rat achilles tendon: ultrasound correlations.* Ann Biomed Eng, 2013. **41**(3): p. 477-87.
197. Gumina, S., et al., *The attempt of spontaneous repair of rotator cuff tear: The role of periostin.* J Orthop, 2019. **16**(5): p. 400-404.

198. Sugiura, T., et al., *Expression and characterization of murine osteoblast-specific factor 2 (OSF-2) in a baculovirus expression system.* Protein Expr Purif, 1995. **6**(3): p. 305-11.
199. Kii, I., et al., *Periostin is an extracellular matrix protein required for eruption of incisors in mice.* Biochem Biophys Res Commun, 2006. **342**(3): p. 766-72.
200. Takayama, G., et al., *Periostin: a novel component of subepithelial fibrosis of bronchial asthma downstream of IL-4 and IL-13 signals.* J Allergy Clin Immunol, 2006. **118**(1): p. 98-104.
201. Maruhashi, T., et al., *Interaction between periostin and BMP-1 promotes proteolytic activation of lysyl oxidase.* J Biol Chem, 2010. **285**(17): p. 13294-303.
202. Shimazaki, M., et al., *Periostin is essential for cardiac healing after acute myocardial infarction.* J Exp Med, 2008. **205**(2): p. 295-303.
203. Piras, B.A., et al., *Systemic injection of AAV9 carrying a periostin promoter targets gene expression to a myofibroblast-like lineage in mouse hearts after reperfused myocardial infarction.* Gene Ther, 2016. **23**(5): p. 469-78.
204. Zhao, S., et al., *Periostin expression is upregulated and associated with myocardial fibrosis in human failing hearts.* J Cardiol, 2014. **63**(5): p. 373-8.
205. Oshima, A., et al., *A novel mechanism for the regulation of osteoblast differentiation: transcription of periostin, a member of the fasciclin I family, is regulated by the bHLH transcription factor, twist.* J Cell Biochem, 2002. **86**(4): p. 792-804.
206. Amara, S., et al., *Synergistic effect of pro-inflammatory TNFalpha and IL-17 in periostin mediated collagen deposition: potential role in liver fibrosis.* Mol Immunol, 2015. **64**(1): p. 26-35.
207. Prakoura, N., et al., *NFkappaB-Induced Periostin Activates Integrin-beta3 Signaling to Promote Renal Injury in GN.* J Am Soc Nephrol, 2017. **28**(5): p. 1475-1490.
208. Snider, P., et al., *Periostin is required for maturation and extracellular matrix stabilization of noncardiomyocyte lineages of the heart.* Circ Res, 2008. **102**(7): p. 752-60.
209. Rios, H., et al., *periostin null mice exhibit dwarfism, incisor enamel defects, and an early-onset periodontal disease-like phenotype.* Mol Cell Biol, 2005. **25**(24): p. 11131-44.
210. Li, Q., X. Liu, and J. Wei, *Ageing related periostin expression increase from cardiac fibroblasts promotes cardiomyocytes senescent.* Biochem Biophys Res Commun, 2014. **452**(3): p. 497-502.
211. Oka, T., et al., *Genetic manipulation of periostin expression reveals a role in cardiac hypertrophy and ventricular remodeling.* Circ Res, 2007. **101**(3): p. 313-21.
212. Iekushi, K., et al., *Novel mechanisms of valsartan on the treatment of acute myocardial infarction through inhibition of the antiadhesion molecule periostin.* Hypertension, 2007. **49**(6): p. 1409-14.
213. Katsuragi, N., et al., *Periostin as a novel factor responsible for ventricular dilation.* Circulation, 2004. **110**(13): p. 1806-13.
214. Guan, J., et al., *Elevated expression of periostin in diabetic cardiomyopathy and the effect of valsartan.* BMC Cardiovasc Disord, 2015. **15**: p. 90.

215. Li, L., et al., *Angiotensin II increases periostin expression via Ras/p38 MAPK/CREB and ERK1/2/TGF-beta1 pathways in cardiac fibroblasts.* Cardiovasc Res, 2011. **91**(1): p. 80-9.
216. Wu, H., et al., *Periostin expression induced by oxidative stress contributes to myocardial fibrosis in a rat model of high salt-induced hypertension.* Mol Med Rep, 2016. **14**(1): p. 776-82.
217. Gupta, S., et al., *Postmortem cardiac tissue maintains gene expression profile even after late harvesting.* BMC Genomics, 2012. **13**: p. 26.
218. Rios, H.F., et al., *Periostin is essential for the integrity and function of the periodontal ligament during occlusal loading in mice.* J Periodontol, 2008. **79**(8): p. 1480-90.
219. Kim, J.H., et al., *Dynamic Mechanical and Nanofibrous Topological Combinatory Cues Designed for Periodontal Ligament Engineering.* PLoS One, 2016. **11**(3): p. e0149967.
220. Stansfield, W.E., et al., *Periostin is a novel factor in cardiac remodeling after experimental and clinical unloading of the failing heart.* Ann Thorac Surg, 2009. **88**(6): p. 1916-21.
221. Birkedal-Hansen, H., et al., *Matrix metalloproteinases: a review.* Crit Rev Oral Biol Med, 1993. **4**(2): p. 197-250.
222. Agewall, S., *Matrix metalloproteinases and cardiovascular disease.* Eur Heart J, 2006. **27**(2): p. 121-2.
223. Liu, P., M. Sun, and S. Sader, *Matrix metalloproteinases in cardiovascular disease.* Can J Cardiol, 2006. **22 Suppl B**: p. 25B-30B.
224. Lindsey, M.L., *MMP induction and inhibition in myocardial infarction.* Heart Fail Rev, 2004. **9**(1): p. 7-19.
225. Raffetto, J.D. and R.A. Khalil, *Matrix metalloproteinases and their inhibitors in vascular remodeling and vascular disease.* Biochem Pharmacol, 2008. **75**(2): p. 346-59.
226. Visse, R. and H. Nagase, *Matrix metalloproteinases and tissue inhibitors of metalloproteinases: structure, function, and biochemistry.* Circ Res, 2003. **92**(8): p. 827-39.
227. Spinale, F.G., *Myocardial matrix remodeling and the matrix metalloproteinases: influence on cardiac form and function.* Physiol Rev, 2007. **87**(4): p. 1285-342.
228. Mann, D.L. and F.G. Spinale, *Activation of matrix metalloproteinases in the failing human heart: breaking the tie that binds.* Circulation, 1998. **98**(17): p. 1699-702.
229. Bergman, M.R., et al., *A functional activating protein 1 (AP-1) site regulates matrix metalloproteinase 2 (MMP-2) transcription by cardiac cells through interactions with JunB-Fra1 and JunB-FosB heterodimers.* Biochem J, 2003. **369**(Pt 3): p. 485-96.
230. Brown, R.D., et al., *Cytokines regulate matrix metalloproteinases and migration in cardiac fibroblasts.* Biochem Biophys Res Commun, 2007. **362**(1): p. 200-205.
231. Guo, X.G., et al., *Imidaprilat inhibits matrix metalloproteinase-2 activity in human cardiac fibroblasts induced by interleukin-1beta via NO-dependent pathway.* Int J Cardiol, 2008. **126**(3): p. 414-20.

232. Husse, B., et al., *Cyclical mechanical stretch modulates expression of collagen I and collagen III by PKC and tyrosine kinase in cardiac fibroblasts.* Am J Physiol Regul Integr Comp Physiol, 2007. **293**(5): p. R1898-907.
233. Makino, N., et al., *Peroxisome proliferator-activated receptor-gamma ligands attenuate brain natriuretic peptide production and affect remodeling in cardiac fibroblasts in reoxygenation after hypoxia.* Cell Biochem Biophys, 2006. **44**(1): p. 65-71.
234. Stawowy, P., et al., *Regulation of matrix metalloproteinase MT1-MMP/MMP-2 in cardiac fibroblasts by TGF-beta1 involves furin-convertase.* Cardiovasc Res, 2004. **63**(1): p. 87-97.
235. Siwik, D.A., P.J. Pagano, and W.S. Colucci, *Oxidative stress regulates collagen synthesis and matrix metalloproteinase activity in cardiac fibroblasts.* Am J Physiol Cell Physiol, 2001. **280**(1): p. C53-60.
236. Siwik, D.A., D.L. Chang, and W.S. Colucci, *Interleukin-1beta and tumor necrosis factor-alpha decrease collagen synthesis and increase matrix metalloproteinase activity in cardiac fibroblasts in vitro.* Circ Res, 2000. **86**(12): p. 1259-65.
237. Tsuruda, T., et al., *Brain natriuretic Peptide is produced in cardiac fibroblasts and induces matrix metalloproteinases.* Circ Res, 2002. **91**(12): p. 1127-34.
238. Porter, K.E., et al., *Tumor necrosis factor alpha induces human atrial myofibroblast proliferation, invasion and MMP-9 secretion: inhibition by simvastatin.* Cardiovasc Res, 2004. **64**(3): p. 507-15.
239. Tyagi, S.C., S. Kumar, and G. Glover, *Induction of tissue inhibitor and matrix metalloproteinase by serum in human heart-derived fibroblast and endomyocardial endothelial cells.* J Cell Biochem, 1995. **58**(3): p. 360-71.
240. Heymans, S., et al., *Increased cardiac expression of tissue inhibitor of metalloproteinase-1 and tissue inhibitor of metalloproteinase-2 is related to cardiac fibrosis and dysfunction in the chronic pressure-overloaded human heart.* Circulation, 2005. **112**(8): p. 1136-44.
241. Tyagi, S.C., et al., *Co-expression of tissue inhibitor and matrix metalloproteinase in myocardium.* J Mol Cell Cardiol, 1995. **27**(10): p. 2177-89.
242. Tyagi, S.C., et al., *Matrix metalloproteinase activity expression in infarcted, noninfarcted and dilated cardiomyopathic human hearts.* Mol Cell Biochem, 1996. **155**(1): p. 13-21.
243. Li, Y.Y., et al., *Differential expression of tissue inhibitors of metalloproteinases in the failing human heart.* Circulation, 1998. **98**(17): p. 1728-34.
244. Thomas, C.V., et al., *Increased matrix metalloproteinase activity and selective upregulation in LV myocardium from patients with end-stage dilated cardiomyopathy.* Circulation, 1998. **97**(17): p. 1708-15.
245. Yu, Q. and I. Stamenkovic, *Cell surface-localized matrix metalloproteinase-9 proteolytically activates TGF-beta and promotes tumor invasion and angiogenesis.* Genes Dev, 2000. **14**(2): p. 163-76.
246. Hirohata, S., et al., *Time dependent alterations of serum matrix metalloproteinase-1 and metalloproteinase-1 tissue inhibitor after successful reperfusion of acute myocardial infarction.* Heart, 1997. **78**(3): p. 278-84.

247. Fertin, M., et al., *Serum MMP-8: a novel indicator of left ventricular remodeling and cardiac outcome in patients after acute myocardial infarction.* PLoS One, 2013. **8**(8): p. e71280.
248. Blankenberg, S., et al., *Plasma concentrations and genetic variation of matrix metalloproteinase 9 and prognosis of patients with cardiovascular disease.* Circulation, 2003. **107**(12): p. 1579-85.
249. Darby, I.A., et al., *Fibroblasts and myofibroblasts in wound healing.* Clin Cosmet Investig Dermatol, 2014. **7**: p. 301-11.
250. Ma, Y., et al., *Cardiac Fibroblast Activation Post-Myocardial Infarction: Current Knowledge Gaps.* Trends Pharmacol Sci, 2017. **38**(5): p. 448-458.
251. Roche, P.L., et al., *Intracellular signaling of cardiac fibroblasts.* Compr Physiol, 2015. **5**(2): p. 721-60.
252. Willems, I.E., et al., *The alpha-smooth muscle actin-positive cells in healing human myocardial scars.* Am J Pathol, 1994. **145**(4): p. 868-75.
253. Ruiz-Villalba, A., et al., *Interacting resident epicardium-derived fibroblasts and recruited bone marrow cells form myocardial infarction scar.* J Am Coll Cardiol, 2015. **65**(19): p. 2057-66.
254. Hermans, K.C., E.P. Daskalopoulos, and W.M. Blankesteijn, *The Janus face of myofibroblasts in the remodeling heart.* J Mol Cell Cardiol, 2016. **91**: p. 35-41.
255. Tomasek, J.J., et al., *Myofibroblasts and mechano-regulation of connective tissue remodelling.* Nat Rev Mol Cell Biol, 2002. **3**(5): p. 349-63.
256. Nanthakumar, C.B., et al., *Dissecting fibrosis: therapeutic insights from the small-molecule toolbox.* Nat Rev Drug Discov, 2015. **14**(10): p. 693-720.
257. Roche, P. and M. Czubryt, *Current and Future Strategies for the Diagnosis and Treatment of Cardiac Fibrosis.* 2015: p. 181-217.
258. Chang, H.Y., et al., *Diversity, topographic differentiation, and positional memory in human fibroblasts.* Proc Natl Acad Sci U S A, 2002. **99**(20): p. 12877-82.
259. Jelaska, A., D. Strehlow, and J.H. Korn, *Fibroblast heterogeneity in physiological conditions and fibrotic disease.* Springer Semin Immunopathol, 1999. **21**(4): p. 385-95.
260. Driskell, R.R. and F.M. Watt, *Understanding fibroblast heterogeneity in the skin.* Trends Cell Biol, 2015. **25**(2): p. 92-9.
261. Driskell, R.R., et al., *Distinct fibroblast lineages determine dermal architecture in skin development and repair.* Nature, 2013. **504**(7479): p. 277-281.
262. Lie-Venema, H., et al., *Origin, fate, and function of epicardium-derived cells (EPDCs) in normal and abnormal cardiac development.* ScientificWorldJournal, 2007. **7**: p. 1777-98.
263. Snider, P., et al., *Origin of cardiac fibroblasts and the role of periostin.* Circ Res, 2009. **105**(10): p. 934-47.
264. Eisenberg, L.M. and R.R. Markwald, *Molecular regulation of atrioventricular valvuloseptal morphogenesis.* Circ Res, 1995. **77**(1): p. 1-6.
265. de Lange, F.J., et al., *Lineage and morphogenetic analysis of the cardiac valves.* Circ Res, 2004. **95**(6): p. 645-54.
266. Burstein, B., et al., *Differential behaviors of atrial versus ventricular fibroblasts: a potential role for platelet-derived growth factor in atrial-ventricular remodeling differences.* Circulation, 2008. **117**(13): p. 1630-41.

267. Ivey, M.J. and M.D. Tallquist, *Defining the Cardiac Fibroblast.* Circ J, 2016. **80**(11): p. 2269-2276.
268. Kong, P., et al., *Lack of specificity of fibroblast-specific protein 1 in cardiac remodeling and fibrosis.* Am J Physiol Heart Circ Physiol, 2013. **305**(9): p. H1363-72.
269. Li, D., et al., *Targeting activated hepatic stellate cells (aHSCs) for liver fibrosis imaging.* EJNMMI Res, 2015. **5**(1): p. 71.
270. Gabbiani, G., G.B. Ryan, and G. Majne, *Presence of modified fibroblasts in granulation tissue and their possible role in wound contraction.* Experientia, 1971. **27**(5): p. 549-50.
271. Li, B. and J.H. Wang, *Fibroblasts and myofibroblasts in wound healing: force generation and measurement.* J Tissue Viability, 2011. **20**(4): p. 108-20.
272. Lerman, O.Z., et al., *Cellular dysfunction in the diabetic fibroblast: impairment in migration, vascular endothelial growth factor production, and response to hypoxia.* Am J Pathol, 2003. **162**(1): p. 303-12.
273. Sarrazy, V., et al., *Mechanisms of pathological scarring: role of myofibroblasts and current developments.* Wound Repair Regen, 2011. **19 Suppl 1**: p. s10-5.
274. Endo, J., et al., *Bone marrow derived cells are involved in the pathogenesis of cardiac hypertrophy in response to pressure overload.* Circulation, 2007. **116**(10): p. 1176-84.
275. Zeisberg, E.M., et al., *Endothelial-to-mesenchymal transition contributes to cardiac fibrosis.* Nat Med, 2007. **13**(8): p. 952-61.
276. Liu, Y., et al., *Snail1 is involved in de novo cardiac fibrosis after myocardial infarction in mice.* Acta Biochim Biophys Sin (Shanghai), 2012. **44**(11): p. 902-10.
277. Kramann, R., et al., *Perivascular Gli1+ progenitors are key contributors to injury-induced organ fibrosis.* Cell Stem Cell, 2015. **16**(1): p. 51-66.
278. Al-Hattab, D.S., et al., *Scleraxis regulates Twist1 and Snai1 expression in the epithelial-to-mesenchymal transition.* Am J Physiol Heart Circ Physiol, 2018. **315**(3): p. H658-H668.
279. Ali, S.R., et al., *Developmental heterogeneity of cardiac fibroblasts does not predict pathological proliferation and activation.* Circ Res, 2014. **115**(7): p. 625-35.
280. Dostal, D.E. and K.M. Baker, *Angiotensin and endothelin: messengers that couple ventricular stretch to the Na+/H+ exchanger and cardiac hypertrophy.* Circ Res, 1998. **83**(8): p. 870-3.
281. Lijnen, P.J., V.V. Petrov, and R.H. Fagard, *Angiotensin II-induced stimulation of collagen secretion and production in cardiac fibroblasts is mediated via angiotensin II subtype 1 receptors.* J Renin Angiotensin Aldosterone Syst, 2001. **2**(2): p. 117-22.
282. Turner, N.A. and K.E. Porter, *Function and fate of myofibroblasts after myocardial infarction.* Fibrogenesis Tissue Repair, 2013. **6**(1): p. 5.
283. Levay, A.K., et al., *Scleraxis is required for cell lineage differentiation and extracellular matrix remodeling during murine heart valve formation in vivo.* Circ Res, 2008. **103**(9): p. 948-56.

284. Murchison, N.D., et al., *Regulation of tendon differentiation by scleraxis distinguishes force-transmitting tendons from muscle-anchoring tendons.* Development, 2007. **134**(14): p. 2697-708.
285. Cserjesi, P., et al., *Scleraxis: a basic helix-loop-helix protein that prefigures skeletal formation during mouse embryogenesis.* Development, 1995. **121**(4): p. 1099-110.
286. Muir, T., et al., *Integration of CREB and bHLH transcriptional signaling pathways through direct heterodimerization of the proteins: role in muscle and testis development.* Mol Reprod Dev, 2008. **75**(11): p. 1637-52.
287. Berthet, E., et al., *Smad3 binds Scleraxis and Mohawk and regulates tendon matrix organization.* J Orthop Res, 2013. **31**(9): p. 1475-83.
288. Bagchi, R.A., et al., *The transcription factor scleraxis is a critical regulator of cardiac fibroblast phenotype.* BMC Biol, 2016. **14**: p. 21.
289. Schweitzer, R., et al., *Analysis of the tendon cell fate using Scleraxis, a specific marker for tendons and ligaments.* Development, 2001. **128**(19): p. 3855-66.
290. Asou, Y., et al., *Coordinated expression of scleraxis and Sox9 genes during embryonic development of tendons and cartilage.* J Orthop Res, 2002. **20**(4): p. 827-33.
291. Bavin, E.P., et al., *Scleraxis Is Essential for Tendon Differentiation by Equine Embryonic Stem Cells and in Equine Fetal Tenocytes.* Stem Cells Dev, 2017. **26**(6): p. 441-450.
292. Dyment, N.A., et al., *The paratenon contributes to scleraxis-expressing cells during patellar tendon healing.* PLoS One, 2013. **8**(3): p. e59944.
293. Chen, X., et al., *Scleraxis-overexpressed human embryonic stem cell–derived mesenchymal stem cells for tendon tissue engineering with knitted silk-collagen scaffold.* Tissue Engineering Part A, 2014. **20**(11-12): p. 1583-1592.
294. Hsieh, C.F., et al., *Scaffold-free Scleraxis-programmed tendon progenitors aid in significantly enhanced repair of full-size Achilles tendon rupture.* Nanomedicine (Lond), 2016. **11**(9): p. 1153-67.
295. Kalluri, R. and E.G. Neilson, *Epithelial-mesenchymal transition and its implications for fibrosis.* J Clin Invest, 2003. **112**(12): p. 1776-84.
296. Kovacic, J.C., et al., *Epithelial-to-mesenchymal and endothelial-to-mesenchymal transition: from cardiovascular development to disease.* Circulation, 2012. **125**(14): p. 1795-808.
297. Acharya, A., et al., *The bHLH transcription factor Tcf21 is required for lineage-specific EMT of cardiac fibroblast progenitors.* Development, 2012. **139**(12): p. 2139-49.
298. Killian, M.L. and S. Thomopoulos, *Scleraxis is required for the development of a functional tendon enthesis.* FASEB J, 2016. **30**(1): p. 301-11.
299. Alberton, P., et al., *Conversion of human bone marrow-derived mesenchymal stem cells into tendon progenitor cells by ectopic expression of scleraxis.* Stem Cells Dev, 2012. **21**(6): p. 846-58.
300. Roche, P.L., et al., *Role of scleraxis in mechanical stretch-mediated regulation of cardiac myofibroblast phenotype.* Am J Physiol Cell Physiol, 2016. **311**(2): p. C297-307.

301. Wilson-Rawls, J., J.M. Rhee, and A. Rawls, *Paraxis is a basic helix-loop-helix protein that positively regulates transcription through binding to specific E-box elements.* J Biol Chem, 2004. **279**(36): p. 37685-92.
302. Bhandari, R.K., et al., *SRY induced TCF21 genome-wide targets and cascade of bHLH factors during Sertoli cell differentiation and male sex determination in rats.* Biology of reproduction, 2012. **87**(6): p. 131, 1-14.
303. Chen, W., et al., *Dexamethasone inhibits the differentiation of rat tendon stem cells into tenocytes by targeting the scleraxis gene.* J Steroid Biochem Mol Biol, 2015. **152**: p. 16-24.
304. Spang, C., J. Chen, and L.J. Backman, *The tenocyte phenotype of human primary tendon cells in vitro is reduced by glucocorticoids.* BMC Musculoskelet Disord, 2016. **17**(1): p. 467.
305. Spang, C., et al., *Glutamate signaling through the NMDA receptor reduces the expression of scleraxis in plantaris tendon derived cells.* BMC Musculoskelet Disord, 2017. **18**(1): p. 218.
306. Ghebes, C.A., et al., *Muscle-Secreted Factors Improve Anterior Cruciate Ligament Graft Healing: An In Vitro and In Vivo Analysis.* Tissue Eng Part A, 2018. **24**(3-4): p. 322-334.
307. Le, W. and J. Yao, *The effect of myostatin (GDF-8) on proliferation and tenocyte differentiation of rat bone marrow-derived mesenchymal stem cells.* The Journal of Hand Surgery (Asian-Pacific Volume), 2017. **22**(02): p. 200-207.
308. Uemura, K., et al., *Myostatin promotes tenogenic differentiation of C2C12 myoblast cells through Smad3.* FEBS Open Bio, 2017. **7**(4): p. 522-532.
309. Zeglinski, M.R., et al., *TGFbeta1 regulates Scleraxis expression in primary cardiac myofibroblasts by a Smad-independent mechanism.* Am J Physiol Heart Circ Physiol, 2016. **310**(2): p. H239-49.
310. Lohberger, B., et al., *Impact of cyclic mechanical stimulation on the expression of extracellular matrix proteins in human primary rotator cuff fibroblasts.* Knee Surg Sports Traumatol Arthrosc, 2016. **24**(12): p. 3884-3891.
311. Liu, Y., et al., *Cystic fibrosis transmembrane conductance regulator mediates tenogenic differentiation of tendon-derived stem cells and tendon repair: accelerating tendon injury healing by intervening in its downstream signaling.* FASEB J, 2017. **31**(9): p. 3800-3815.
312. Bagchi, R.A., et al., *Regulation of scleraxis transcriptional activity by serine phosphorylation.* J Mol Cell Cardiol, 2016. **92**: p. 140-8.
313. Barnette, D.N., et al., *Tgfbeta-Smad and MAPK signaling mediate scleraxis and proteoglycan expression in heart valves.* J Mol Cell Cardiol, 2013. **65**: p. 137-46.
314. Busch, F., et al., *Resveratrol modulates interleukin-1beta-induced phosphatidylinositol 3-kinase and nuclear factor kappaB signaling pathways in human tenocytes.* J Biol Chem, 2012. **287**(45): p. 38050-63.
315. Li, Y., et al., *The Role of Scleraxis in Fate Determination of Mesenchymal Stem Cells for Tenocyte Differentiation.* Sci Rep, 2015. **5**: p. 13149.
316. Lejard, V., et al., *Scleraxis and NFATc regulate the expression of the pro-alpha1(I) collagen gene in tendon fibroblasts.* J Biol Chem, 2007. **282**(24): p. 17665-75.

317. Bagchi, R.A., et al., *Regulation of fibronectin gene expression in cardiac fibroblasts by scleraxis.* Cell Tissue Res, 2016. **366**(2): p. 381-391.
318. Abe, H., et al., *Scleraxis modulates bone morphogenetic protein 4 (BMP4)-Smad1 protein-smooth muscle alpha-actin (SMA) signal transduction in diabetic nephropathy.* J Biol Chem, 2012. **287**(24): p. 20430-42.
319. Liu, Y., et al., *Overexpression of a single helix-loop-helix-type transcription factor, scleraxis, enhances aggrecan gene expression in osteoblastic osteosarcoma ROS17/2.8 cells.* J Biol Chem, 1997. **272**(47): p. 29880-5.
320. Pryce, B.A., et al., *Generation of transgenic tendon reporters, ScxGFP and ScxAP, using regulatory elements of the scleraxis gene.* Dev Dyn, 2007. **236**(6): p. 1677-82.
321. Patten, R.D. and M.R. Hall-Porter, *Small animal models of heart failure: development of novel therapies, past and present.* Circ Heart Fail, 2009. **2**(2): p. 138-44.
322. Richards, D.A., et al., *Distinct Phenotypes Induced by Three Degrees of Transverse Aortic Constriction in Mice.* Sci Rep, 2019. **9**(1): p. 5844.
323. Nagalingam, R.S., et al., *Regulation of cardiac fibroblast MMP2 gene expression by scleraxis.* J Mol Cell Cardiol, 2018. **120**: p. 64-73.
324. Hittel, D.S., et al., *Increased secretion and expression of myostatin in skeletal muscle from extremely obese women.* Diabetes, 2009. **58**(1): p. 30-8.
325. Dixon, I.M.C., N.M. Landry, and S.G. Rattan, *Periostin Reexpression in Heart Disease Contributes to Cardiac Interstitial Remodeling by Supporting the Cardiac Myofibroblast Phenotype.* Adv Exp Med Biol, 2019. **1132**: p. 35-41.
326. Sung, M.M., et al., *Resveratrol treatment of mice with pressure-overload-induced heart failure improves diastolic function and cardiac energy metabolism.* Circ Heart Fail, 2015. **8**(1): p. 128-37.
327. Zhang, Y., et al., *Baicalin Attenuates Cardiac Dysfunction and Myocardial Remodeling in a Chronic Pressure-Overload Mice Model.* Cell Physiol Biochem, 2017. **41**(3): p. 849-864.
328. Furihata, T., et al., *The experimental model of transition from compensated cardiac hypertrophy to failure created by transverse aortic constriction in mice.* Int J Cardiol Heart Vasc, 2016. **11**: p. 24-28.
329. Vivar, R., et al., *FoxO1 mediates TGF-beta1-dependent cardiac myofibroblast differentiation.* Biochim Biophys Acta, 2016. **1863**(1): p. 128-38.
330. Overall, C.M., J.L. Wrana, and J. Sodek, *Transcriptional and post-transcriptional regulation of 72-kDa gelatinase/type IV collagenase by transforming growth factor-beta 1 in human fibroblasts. Comparisons with collagenase and tissue inhibitor of matrix metalloproteinase gene expression.* J Biol Chem, 1991. **266**(21): p. 14064-71.
331. Philips, N., T. Keller, and S. Gonzalez, *TGF beta-like regulation of matrix metalloproteinases by anti-transforming growth factor-beta, and anti-transforming growth factor-beta 1 antibodies in dermal fibroblasts: Implications for wound healing.* Wound Repair Regen, 2004. **12**(1): p. 53-9.
332. Howard, E.W., et al., *MMP-2 expression by fibroblasts is suppressed by the myofibroblast phenotype.* Exp Cell Res, 2012. **318**(13): p. 1542-53.

333. Liu, Y., et al., *TGF-beta1 promotes scar fibroblasts proliferation and transdifferentiation via up-regulating MicroRNA-21.* Sci Rep, 2016. **6**: p. 32231.
334. Khalil, H., et al., *Fibroblast-specific TGF-beta-Smad2/3 signaling underlies cardiac fibrosis.* J Clin Invest, 2017. **127**(10): p. 3770-3783.
335. Russo, I., et al., *Protective Effects of Activated Myofibroblasts in the Pressure-Overloaded Myocardium Are Mediated Through Smad-Dependent Activation of a Matrix-Preserving Program.* Circ Res, 2019. **124**(8): p. 1214-1227.
336. Huo, Q., et al., *Acetazolamide attenuates cardiac fibrosis induced by aortic constriction through inhibiting transforming growth factor-beta1/Smad2 signaling pathway in mice.* Exp Ther Med, 2019. **17**(3): p. 2317-2321.
337. Boulaksil, M., et al., *Longitudinal arrhythmogenic remodelling in a mouse model of longstanding pressure overload.* Neth Heart J, 2010. **18**(10): p. 509-15.
338. Shinde, A.V., et al., *Tissue transglutaminase induction in the pressure-overloaded myocardium regulates matrix remodelling.* Cardiovasc Res, 2017. **113**(8): p. 892-905.
339. Roche, P. and M.P. Czubryt, *Transcriptional control of collagen I gene expression.* Cardiovasc Hematol Disord Drug Targets, 2014. **14**(2): p. 107-20.
340. De Acetis, M., et al., *Cardiac overexpression of melusin protects from dilated cardiomyopathy due to long-standing pressure overload.* Circ Res, 2005. **96**(10): p. 1087-94.
341. Wang, D., et al., *Effects of pressure overload on extracellular matrix expression in the heart of the atrial natriuretic peptide-null mouse.* Hypertension, 2003. **42**(1): p. 88-95.
342. Tarbit, E., et al., *Biomarkers for the identification of cardiac fibroblast and myofibroblast cells.* Heart Fail Rev, 2019. **24**(1): p. 1-15.
343. Crawford, J., et al., *Periostin induces fibroblast proliferation and myofibroblast persistence in hypertrophic scarring.* Exp Dermatol, 2015. **24**(2): p. 120-6.
344. Elliott, C.G., et al., *Periostin modulates myofibroblast differentiation during full-thickness cutaneous wound repair.* J Cell Sci, 2012. **125**(Pt 1): p. 121-32.